

ELECTRICAL MACHINE BEARING FAULTS: STATISTICAL ANALYSIS AND DIAGNOSTICS

A THESIS

***Submitted in partial fulfilment of the
requirements for the award of the degree***

of

DOCTOR OF PHILOSOPHY

in

ELECTRICAL ENGINEERING

by

KHWAJA HINA AHMAD



**DEPARTMENT OF ELECTRICAL ENGINEERING
INDIAN INSTITUTE OF TECHNOLOGY ROORKEE
ROORKEE-247 667 (INDIA)**

DECEMBER, 2010

©INDIAN INSTITUTE OF TECHNOLOGY ROORKEE, ROORKEE - 2010
ALL RIGHTS RESERVED



INDIAN INSTITUTE OF TECHNOLOGY ROORKEE ROORKEE

CANDIDATE'S DECLARATION

I hereby certify that the work which is being presented in the thesis entitled **ELECTRICAL MACHINE BEARING FAULTS: STATISTICAL ANALYSIS AND DIAGNOSTICS** in partial fulfilment of the requirements for the award of the Degree of Doctor of Philosophy and submitted in the Department of Electrical Engineering of the Indian Institute of Technology Roorkee, Roorkee is an authentic record of my own work carried out during a period from January 2004 to December 2010 under the supervision of Dr. S. P. Gupta and Dr. Vinod Kumar, Professors, Department of Electrical Engineering, Indian Institute of Technology Roorkee, Roorkee.

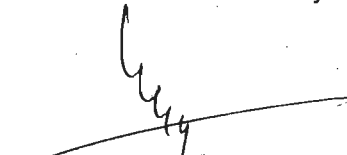
The matter presented in this thesis has not been submitted by me for the award of any other degree of this or any other Institute.


H. Ahmad

(KHWAJA HINA AHMAD)

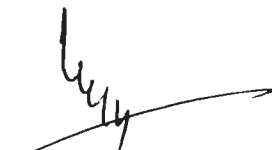
This is to certify that the above statement made by the candidate is correct to the best of our knowledge.

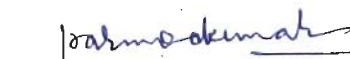
Date: December 31, 2010


(Dr. Vinod Kumar)
Supervisor


(Dr. S. P. Gupta)
Supervisor

The Ph.D. Viva-Voce Examination of **Ms. Khwaja Hina Ahmad**, Research Scholar, has been held on30.6.2011.....


S. P. Gupta
Signature of Supervisor(s)


30.6.2011
Signature of External Examiner

DEDICATION

This piece of work is dedicated to my father Late Mr Khwaja Safi Ahmad who dreamt and wished my PhD in IITR. To my mother Mrs. Meher Jabin Khwaja, a strong pillar, who laid my foundations, and finally to my brother Khwaja Talha Tul Faiyaz and sister Mrs. Saeeda Ahmad who made me believe in my potentials and thus resulting in giving my best in this research work.

ABSTRACT

The present research work is focussed to detect bearing faults in electrical machines at the incipient stage through analysis of the monitoring data. Analysis is done on the vibration signal which is acquired using the accelerometer. Investigations of bearing faults are carried out on the basis of statistical analysis of vibration signal in time domain.

The basic vibration data is obtained on a 7.5kW, 3-phase, 415Volts, 50Hz, 7.5kW, 15A, 1440 rpm cage Induction motor. A DC generator, directly coupled to the motor, is used for loading. The vibration signal is picked up by placing the vibration transducer, which is of piezo-electric type (PU-601R) on the bearing cap of the load-end bearing. For signal conditioning, a machine analyzer MK-500 is employed, the output of which is an analog signal which is converted in digital form by NI-6024E card. The data is acquired in the PC using the LabVIEW software and stored in Excel file. The statistical analysis to determine time domain features is done in EXCEL.

The vibration signal in terms of acceleration is obtained for a given bearing while the motor is running on selected loading condition. In each run 50,000 data sample points are obtained at a sampling frequency of 1280Hz. For ensuring consistency a number of runs are taken for each operating condition.

The bearings used in the experimentation have been obtained directly from the manufacturer - National Engineering Industries Limited, Jaipur, India. A set of healthy bearings (NBC 6308) and bearings having a small point fault in (a) outer race and (b) inner race, supplied by the manufacturer, have been employed in the present work.

In machine condition monitoring, time domain analysis is used for studying the time waveform of the vibration signal. To enhance feature extraction, different time domain techniques are used. For a time domain signal, the characteristic features are: peak value, RMS value, crest factor, standard deviation, kurtosis, geometric mean and skewness. Upon onset of a fault, the variation in the values of these characteristic features is examined for diagnosis purpose.

The present research work implements the statistical method which can be categorized firstly, into statistical parameters which are: the mean, standard error, median, mode standard deviation, sample variance, kurtosis, skewness, range, minimum, maximum and confidence interval and secondly, the statistical

inference, namely the probability density function (PDF) and cumulative distribution function(CDF).

Statistical Analysis is broadly classified into two major components namely

- 1) Statistical parameters which includes the
 - a) Measure of Central Tendency-(MCT): mean, median and mode
 - b) Measure of Variability-(MV): range, variance, standard deviation and standard error
 - c) Measure of Dispersion-(MD): kurtosis and skewness
- 2) Statistical Inferences which includes the
 - a) Probability Density Function (PDF) or Gaussian distribution
 - b) Cumulative Distribution Function (CDF)

The statistical parameters are calculated using 50000 data point in EXCEL. To determine the Gaussian distribution, the 50000 vibration data points are broken down by Sturge's formula into 17 classes.

The FFT is also calculated and plotted to determine the bearing fault frequencies, present in the spectra. This was done for healthy (fault free) bearing, outer race fault and inner race faults. Further, for each of the cases, four load conditions were investigated namely the no load, slight load, half load and three quarter load.

In present work some of the findings are:

- 1) For the statistical parameters the measure of variability is found to show a marked change both in the case of occurrence of a fault as well as when the load is gradually increased. On the other hand no significant change is seen in the measure of central tendency and measure of dispersion for an incipient fault.
- 2) As the fault progresses the pdf spreads and the amplitude dips. This indicates that the vibration levels have increased as also the range in both the pdf and cdf.
- 3) The vibration signal at incipient stage of fault remains Gaussian.

ACKNOWLEDGEMENT

I wish to acknowledge that Prof. S. P. Gupta and Prof. Vinod Kumar, Department of Electrical Engineering, I.I.T. Roorkee, Roorkee, opened my gates of knowledge, carefully carved and polished this work to its destination, with their invaluable guidance, their patience and foresightedness, their nurturing me in these past years, their sincere advice and encouragement throughout the completion of this research work, which makes me feel highly privileged to have worked under them during the course of this research work.

Their encouraging support, discussion, suggestions and thorough involvement yielded this contribution of the research work in the field of FDEM. The preparation of the manuscript, numerous discussions, criticism on particular techniques are some of the facts that I gratefully acknowledge. I sincerely appreciate their pronounced individualities, patience, humanistic and warm personal approach, which has given me strength to carry out this research work smoothly. I humbly acknowledge my gurus for a lifetime's gratitude.

My heartily gratitude to Prof. S. C. Saxena, Prof. M. K. Vasantha, Dr. Indra Gupta, Prof. H. K. Verma, of the Department of Electrical Engineering, IIT Roorkee, and Prof. S. C. Jain, Department of Mechanical Engineering, IIT Roorkee, whose humanistic and warm personal approach always helped me from beginning to the end of my work. My thanks are also due to Prof. Tanuja Chandra, Department of Mathematics, IIT Roorkee, who helped me when I needed to understand a particular technique.

I thank Prof. S. P. Gupta, Prof. Vinod Kumar and Prof. N. P. Padhy, who imparted knowledge through lectures, presentation and workshops which benefited me in a tremendous way. I also thank Prof. Pramod Aggarwal, Dr. S. P. Singh, Prof. S. P. Srivastava and Shri. Y. P. Singh for their teaching through the lab assignments.

I thank the Librarian Mr. Yogendra Singh and Ms. Nisha who helped me with the required research material, and all the members of the central library, IITR, one of the richest den of information during my education tenure. I would also like to include in my list, the staff of our departmental Library.

I express my deep sense of gratitude to Dr Harsh of SSPL, Ministry of Defence, Prof. Surendra Prasad, Director IIT Delhi, Prof. K.M. Mittal, Prof. G. Yadava, Prof. S.S. Islam, Dr. Tripathi, Prof. R. Moinuddin, Prof. M. Alam, Prof. M. R. Khan, Dr. Rifaqat Ali - all of Jamia Millia Islamia University, Delhi who always boosted my confidence levels, and reminded me to fulfill my parents dream.

I am indebted to all my B.Tech Lecturers from ATBU, Bauchi state of Nigeria, Prof. Aliyu and Prof. M.L. Audu who always encouraged me for higher goals.

I wish to portray my regards to my medical doctors Dr Suman Kirti and Dr. Mishra both of Holy Family Hospital, Delhi who made me understand the desire for our country to progress.

I convey special thanks to Mr Reddy, Mr Shailendra, Mr Deepak who eliminated my computer related problems in a jiffy. I would also like to thank Ms.Anita for always encouraging me and the lab staff Mr. Nafees Ahmad, Mr. Tula Ram, Mr. Ameer Ahmad, Mr. M. P.Tewari, Mr. Rajendra Singh, Mr.Shadiram and Mr. Satpal Singh, who helped me in the experimental work.

I will never forget my good friends from B. Tech, M. Tech, Ph.D. and my colleagues whose positive attitude and cooperation always encouraged me to accomplish my research work. I also would like to include Raja, Manish and Neha who contributed immensely in this work. I owe to all the known authorities both educational and industries who replied to my emails and cleared the intricacies in this thesis. I am indebted to my brother whose knowledge also had its own role in the completion of my work.

I gratefully acknowledge the moral support and encouragement of my family, and I would like to quote a saying of my parents saying which I had heard in my yester years which says;

“To Discover Deeper Oceans you must leave the sight of the shore”

Above all I would like to thank my creator ALLAH for

“He taught man by the pen and He taught man what he knows not”

(KHWAJA HINA AHMAD)

CONTENTS

| | |
|--|------|
| Title | |
| Copyright | |
| Dedication | |
| Candidate's Declaration | |
| Abstract | i |
| Acknowledgement | iii |
| Contents | v |
| List of Acronyms | vii |
| List of Symbols | viii |
| List of Figures | ix |
| List of Tables | xii |
| | |
| 1 Introduction | |
| 1.1 Introduction | 1 |
| 1.2 Need for Fault Diagnosis | 4 |
| 1.3 Review of Published work | 7 |
| 1.3.1 Vibration Monitoring | 8 |
| 1.3.2 Current Monitoring | 27 |
| 1.3.3 Vibration and Current Monitoring | 35 |
| 1.3.4 Speed Monitoring | 36 |
| 1.3.5 Voltage Monitoring | 37 |
| 1.3.6 Sound Monitoring | 37 |
| 1.3.7 Oil Monitoring | 38 |
| 1.4 Scope of Present Work | 38 |
| 1.5 Organization of the Thesis | 38 |
| | |
| 2 Data Acquisition | |
| 2.1 Introduction | 41 |
| 2.2 DAQ Components | 49 |
| 2.3 Transducers in DAQ | 51 |
| 2.3.1 Accelerometer | 51 |
| 2.3.2 Current Clamps | 54 |
| 2.3.3 Potential Transducers | 55 |
| 2.3.4 Speed | 55 |
| 2.4 Signal Conditioning Unit | 55 |
| 2.4.1 MK-500 | 57 |
| 2.4.2 BNC-2120 | 58 |
| 2.4.3 NI-6024E | 58 |
| 2.5 PC LabVIEW Program | 59 |
| 2.5.1 Data Acquisition Block | 60 |
| 2.5.2 Output Generation | 63 |
| 2.2.3 Excel Sheet Creation Block | 65 |
| 2.6 Final Diagram of the DAQ system used | 66 |
| 2.7 Conclusions | 67 |
| | |
| 3 Analysis Techniques | |
| 3.1 Introduction | 71 |
| 3.2 Drawback from Literature Review Techniques | 71 |

| | | |
|----------|--|-----|
| 3.2.1 | Time Domain Technique | 72 |
| 3.2.2 | Statistical Technique | 72 |
| 3.2.3 | FFT Technique | 75 |
| 3.2.4 | STFT Technique | 76 |
| 3.2.5 | Wavelet Transform Technique | 77 |
| 3.2.6 | Artificial Neural Network Technique | 80 |
| 3.2.7 | Fuzzy Technique | 82 |
| 3.2.8 | Acoustic Emission Technique | 82 |
| 3.2.9 | Independent Component Analysis | 83 |
| 3.2.10 | Other Techniques | 84 |
| 3.3 | Parameters for FDEM | 87 |
| 3.4 | Importance of Vibration Parameters | 88 |
| 3.4.1 | Deterministic Vibration | 88 |
| 3.4.2 | Random or Stochastic Vibration | 88 |
| 3.4.3 | Choice of using Acceleration | 88 |
| 3.4 | Analysis Techniques in Present Work | 89 |
| 3.5 | Conclusions | 99 |
| 4 | Behaviour of the Vibration Data | |
| 4.1 | Introduction | 101 |
| 4.2 | Chitest for Behaviour Analysis of Data | 101 |
| 4.3 | Advantages of Chitest | 103 |
| 4.4 | Applications of chi square distribution | 103 |
| 4.5 | Conditions of the validity of chitest | 104 |
| 4.6 | Final Steps for chitest | 105 |
| 4.7 | Guideline for a chitest | 106 |
| 4.8 | Results and Discussions | 107 |
| 4.9 | Conclusions | 114 |
| 5 | A Statistical Approach for Fault Diagnosis in Electrical Machines | |
| 5.1 | Introduction | 117 |
| 5.2 | Analysis of the Data Acquired | 119 |
| 5.3 | Statistical Parameters | 121 |
| 5.4 | Statistical Inferences | 123 |
| 5.4.1 | Probabilty Density Function | 123 |
| 5.4.2 | Cumulative Distribution Function | 126 |
| 5.5 | Frequency Domain Signals | 127 |
| 5.6 | An Overview of Healthy, Outer and Inner race Fault | 132 |
| 5.7 | Repeated Runs showing the Statistical Parameters | 133 |
| 5.8 | Important Observations made in this study | 134 |
| 6 | Experiment Investigations on Outer Race Fault | |
| 6.1 | Introduction | 135 |
| 6.2 | Analysis of the Data Acquired | 137 |
| 6.2.1 | Time Domain Signal | 138 |
| 6.2.2 | Statistical Parameters | 139 |
| 6.3 | Statistical Inferences | 143 |
| 6.3.1 | Probabilty Density Function and Results | 143 |
| 6.3.2 | Cumulative Distribution Function and Results | 145 |
| 6.4 | Frequency Domain Representation | 148 |
| 6.5 | Discussion | 150 |
| 6.6 | Trend of ORF with Load Variations | 154 |

| | | |
|----------|--|-----|
| 6.7 | Conclusion | 156 |
| 7 | Experiment Investigation on Inner Race Fault of Ball Bearings of Electrical Machines using Statistical Analysis | |
| 7.1 | Introduction | 159 |
| 7.2 | Time Domain Representation of the Acquired Data | 162 |
| 7.3 | Statistical Analysis of the Acquired Data | 164 |
| | 7.3.1 Statistical Parameter | 164 |
| | 7.3.2 Statistical Inferences | 167 |
| 7.4 | Frequency Domain Representation | 172 |
| | 7.3.1 Probabilty Density Function and Results | 178 |
| | 7.3.2 Cumulative Distribution Function and Results | 178 |
| 7.6 | Trend of IRF with Load Variations | 178 |
| 7.7 | Conclusion | 180 |
| 8 | Conclusions | |
| 8.1 | Introduction | 183 |
| 8.2 | Overview of Results and conclusion | 184 |
| 8.3 | A Comparison of all the Statistical Parameters and Reference to Fault Free ORF and IRF | 185 |
| 8.4 | Positive Points Achieved in this thesis | 185 |
| 8.5 | Scope of future work | 186 |
| | Bibliography | 189 |
| | Published Paper/Communicated Paper | 201 |
| | Appendix-A1 | 203 |
| | Appendix-A2 | 204 |
| | Appendix-A3 | 205 |
| | Appendix-A4 | 207 |
| | Appendix-A5 | 211 |

List of Acronyms

| Name of Acronym | Meaning of Acronym |
|------------------------|--|
| <i>AE</i> | Acoustic Emission |
| <i>AI</i> | Artificial Intelligence |
| <i>ANN</i> | Artificial Neural Network |
| <i>AR</i> | Auto Regressive |
| <i>BCF</i> | Bearing Characteristic Frequency |
| <i>BNC</i> | Bayonet Neil Concelman or Bayonet Net Connector |
| <i>CDF</i> | Cumulative Distribution Function |
| <i>DLI</i> | Delivering Machine Intelligence |
| <i>DSP</i> | Digital Signal Processing |
| <i>DWPA</i> | Discrete Wavelet Packet |
| <i>ED</i> | Envelope Detection |
| <i>EPRI</i> | Electric Power Research Institute |
| <i>FDEM</i> | Faults Diagnostics of Electrical Machines |
| <i>FFT</i> | Fast Fourier Transforms |
| <i>FT</i> | Fourier Transform |
| <i>GP</i> | Genetic Programming |
| <i>HFRT</i> | High Frequency Resonance Technique |
| <i>HMM</i> | Hidden Markov Modeling |
| <i>HOS</i> | Higher Order Statistics |
| <i>HPF</i> | High Pass Filter |
| <i>HWT</i> | Harmonic Wavelet |
| <i>IEEE</i> | Institute of Electrical and Electronic Engineers |
| <i>IRF</i> | Inner Race Fault |
| <i>LDA</i> | Linear Discriminant Analysis |
| <i>LPF</i> | Low Pass Filter |
| <i>NBC</i> | National Bearing Corporation |
| <i>NEI</i> | National Engineering Industries |
| <i>NI</i> | National Instrument |
| <i>NTN</i> | New Technology Network |
| <i>ORF</i> | Outer Race Fault |
| <i>PC</i> | Personal Computer |
| <i>PDF</i> | Probability Density Function |
| <i>PDMA</i> | Product Development and Management Association |
| <i>PSD</i> | Power Spectral Density |
| <i>REB</i> | Rolling Element Bearing |
| <i>SANC</i> | Self Adaptive Noise Cancellation |
| <i>SK</i> | Spectral Kurtosis |
| <i>SKF</i> | Svenska Kullager Fabriken |
| <i>STFT</i> | Short Time Fourier Transforms |
| <i>VI</i> | Virtual Instrumentation |
| <i>WA</i> | Wavelet Analysis |
| <i>WPT</i> | Wavelet Packet |
| <i>WT</i> | Wavelet Transform |

List of Symbols

| Symbols | Meaning of the Symbol |
|----------------------|--|
| α | Significance level |
| χ | Chi values |
| β and θ | Contact angle |
| σ or s | Standard deviation |
| μ | Mean of the distribution |
| b | Ball diameter |
| d | Ball pitch diameter |
| Df or DOF | Degree of freedom |
| e | Constant =2.7183 |
| e_i | Expected value |
| $F(X)$ | Cumulative Distribution Function |
| $f(x)$ | Probability Density Function |
| f_{bd} | Ball defect characteristic frequency |
| f_{in} | Inner race defect characteristic frequency |
| f_i | Observed value |
| f_o | Outer race defect characteristic frequency |
| f_r | Rotational frequency |
| f_{td} | Train defect characteristic frequency |
| g | Measure of acceleration $1g=9.8m/sec^2$ |
| k | Width of the window |
| n | Each discrete value of a sample |
| W | Window function |
| x | Acceleration g values |
| z | Normally distributed population |
| π | Constant =3.1416 |

Figures Chapter 1

| | Pages | |
|-----|--|---|
| 1.1 | Growing expectations of maintenance over 60 years | 3 |
| 1.2 | Changing maintenance techniques over 60 years | 3 |
| 1.3 | Distribution of faults (EPRI 1982) | 5 |
| 1.4 | Distribution of Failures among failed components for electrical machines working in petrochemical industry | 5 |
| 1.5 | Plot showing a spread of this study | 8 |

Chapter 2

| | | |
|------|--|----|
| 2.1 | View of cage induction motor | 41 |
| 2.2 | Induction motor component failing rate versus survey | 42 |
| 2.3 | Five basic types of bearings: tapered, needle, ball, spherical and cylindrical. Each is named for the type of rolling element it employs | 48 |
| 2.4 | Flow diagram of the DAQ for FDEM | 50 |
| 2.5 | Depicts the Transducers and experiment setup used in this work | 51 |
| 2.6 | Main measurement considered for vibration monitoring | 53 |
| 2.7 | A piezoelectric accelerometer | 54 |
| 2.8 | Signal processing | 56 |
| 2.9 | Signal conditioning unit | 57 |
| 2.10 | Labview PC program for DAQ | 60 |
| 2.11 | Final Diagram | 66 |
| 2.12 | Condition Monitoring methodology at a glance | 68 |

Chapter 3

| | | |
|-----|--|-----|
| 3.1 | Basic Analysis tool for FDEM | 89 |
| 3.2 | Classification of statistical Parameters | 91 |
| 3.3 | Two Skewed distribution curves | 94 |
| 3.4 | Classification of statistical Inference | 95 |
| 3.5 | Relationship showing the PDF and CDF | 97 |
| 3.6 | Flow Diagram on Analysis Techniques used in this research work | 100 |

Chapter 4

| | | |
|------|--|-----|
| 4.1 | Need for a validation test for a Vibration Signal | 102 |
| 4.2 | Critical values for 95% confident interval | 103 |
| 4.3 | Chi square distribution for different dof. | 106 |
| 4.4 | observed and expected frequency for no load vibration for healthy bearing | 108 |
| 4.5 | Observed and expected frequency for slight load vibration for healthy bearing | 108 |
| 4.6 | Observed and expected frequency for half load vibration for healthy bearing | 109 |
| 4.7 | Observed and expected frequency for three quarter load vibration for healthy bearing | 109 |
| 4.8 | Observed and expected frequency for no load vibration for ORF | 110 |
| 4.9 | Observed and expected frequency for slight load vibration for ORF | 111 |
| 4.10 | Observed and expected frequency for half load vibration for ORF | 111 |

| | | |
|------------------|---|-----|
| 4.11 | Observed and expected frequency for three quarter load vibration for ORF | 112 |
| 4.12 | Observed and expected frequency for no load vibration for IRF | 112 |
| 4.13 | Observed and expected frequency for slight load vibration for IRF | 113 |
| 4.14 | Observed and expected frequency for half load vibration for IRF | 113 |
| 4.15 | Observed and expected frequency for three quarter load vibration for IRF | 114 |
| Chapter 5 | | |
| 5.1 | Vibration signal for a healthy bearing | 120 |
| 5.2 | Vibration signal for a outer race fault | 120 |
| 5.3 | Vibration signal for a inner race fault | 120 |
| 5.4 | A 3-D plot showing the behaviour of the statistical parameters in the three cases | 123 |
| 5.5 | Probability density function of a healthy bearing data | 124 |
| 5.6 | Probability density function of an outer race fault | 125 |
| 5.7 | Probability density function of an inner race fault | 125 |
| 5.8 | Cumulative distribution function of a healthy bearing | 126 |
| 5.9 | Cumulative distribution function of an outer race fault | 126 |
| 5.10 | Cumulative distribution function of an inner race fault | 127 |
| 5.11 | Frequency spectrum of a healthy machine | 128 |
| 5.12 | Frequency spectrum of an outer race fault | 129 |
| 5.13 | Frequency spectrum of an inner race fault | 129 |
| 5.14 | A comparative PDF diagram showing the Healthy (Fault Free), ORF and IRF | 132 |
| 5.15 | A comparative CDF diagram showing the Healthy (Fault Free), ORF and IRF | 133 |
| Chapter 6 | | |
| 6.0 | Flow diagram to detect ORF at different load conditions | 137 |
| 6.1 | Vibration signal for outer race fault at no load | 138 |
| 6.2 | Vibration signal for outer race fault at slight load | 138 |
| 6.3 | Vibration signal for outer race fault at half load | 139 |
| 6.4 | Vibration signal for outer race fault at three quarter load | 139 |
| 6.5 | A 3-D plot showing the behaviour of statistical parameters at four load condition for Healthy Machine | 142 |
| 6.6 | A 3-D plot showing the behaviour of statistical parameters at four load condition for ORF | 142 |
| 6.7 | The probability density function for no load condition for outer race fault | 144 |
| 6.8 | The probability density function for slight load condition for outer race fault | 144 |
| 6.9 | The probability density function for half load condition for outer race fault | 144 |
| 6.10 | The probability density function for three quarter load condition for outer race fault | 145 |
| 6.11 | The cumulative distribution function for no load condition for outer race fault | 146 |
| 6.12 | The cumulative distribution function for slight load condition for outer race fault. | 146 |
| 6.13 | The cumulative distribution function for half load condition for outer race fault | 147 |
| 6.14 | The cumulative distribution function for three quarter load condition for outer race fault. | 147 |
| 6.15 | The FFT for no load condition for outer race fault | 148 |

| | | |
|------|---|-----|
| 6.16 | The FFT for slight load condition for outer race fault | 149 |
| 6.17 | The FFT for half load condition for outer race fault | 149 |
| 6.18 | The FFT for three quarter load condition for outer race fault | 149 |
| 6.19 | PDF of Healthy at four load condition | 154 |
| 6.20 | PDF of Outer race fault at four load condition | 155 |
| 6.21 | CDF of Healthy at four load condition | 155 |
| 6.22 | CDF of Outer race fault at four load condition | 155 |

Chapter 7

| | | |
|------|---|-----|
| 7.1 | Percentage of occurrence of faults found in bearings | 160 |
| 7.2 | Vibration signal for inner race fault at no load | 162 |
| 7.3 | Vibration signal for inner race fault at slight load | 163 |
| 7.4 | Vibration signal for inner race fault at half load | 163 |
| 7.5 | Vibration signal for inner race fault at three quarter load | 163 |
| 7.6 | A 3-D plot showing the behaviour of statistical parameters at four load condition for Healthy Machine | 166 |
| 7.7 | A 3-D plot showing the behaviour of statistical parameters at four load conditions for inner race fault | 166 |
| 7.8 | The probability density function for no load condition for inner race fault. | 168 |
| 7.9 | The probability density function for slight load condition for inner race fault | 168 |
| 7.10 | The probability density function for half load condition for inner race fault | 168 |
| 7.11 | The probability density function for three quarter load condition for inner race fault | 169 |
| 7.12 | The cumulative distribution function for no load condition for inner race fault | 170 |
| 7.13 | The cumulative distribution function for slight load condition for inner race fault | 171 |
| 7.14 | The cumulative distribution function for half load condition for inner race fault | 171 |
| 7.15 | The cumulative distribution function for three quarter load condition for inner race fault | 171 |
| 7.16 | The FFT for no load condition for inner race fault | 173 |
| 7.17 | The FFT for slight load condition for inner race fault | 173 |
| 7.18 | The FFT for slight load condition for inner race fault | 174 |
| 7.19 | The FFT for three quarter load condition for inner race fault | 174 |
| 7.20 | PDF of Healthy at four load condition | 179 |
| 7.21 | PDF of Inner race fault at four load condition | 179 |
| 7.22 | CDF of Healthy at four load condition | 179 |
| 7.23 | CDF of Inner race fault at four load condition | 180 |

List of Tables

| Tables | Chapter 1 | Pages |
|---------------|--|--------------|
| 1.1 | The power of predictive Maintenance | 6 |
| 1.2 | The Literature Survey | 7 |
| | Chapter 2 | |
| 2.1 | Specification of an induction motor used in the Experiment | 41 |
| 2.2 | Settings of the MK-500 | 58 |
| | Chapter 3 | |
| 3.1 | Formula as well as calculated frequencies of the bearing defects | 99 |
| | Chapter 4 | |
| 4.1 | The chi square values | 107 |
| | Chapter 5 | |
| 5.1 | A comparative study of the statistical values obtained for a bearing under the condition (a) healthy, (b) outer race faults, and (c) inner race faults | 121 |
| 5.2 | A comparative study of the calculated and the practical value magnitudes of the FFT spectra for the three cases. | 128 |
| 5.3 | Shows seven repeated runs of the machine for half load outer race fault | 133 |
| | Chapter 6 | |
| 6.1 | Statistical Parameters for four load conditions for a Healthy Machine (Fault Free) | 140 |
| 6.2 | Statistical Parameters for four load conditions for an outer race fault | 141 |
| 6.3 | The practical value of magnitudes of PDF obtained for four different load conditions | 145 |
| 6.4 | The practical value of magnitudes of the peaks obtained for four different load conditions | 150 |
| 6.5 | Measure of Central tendency (MCT) | 151 |
| 6.6 | Measure of variability (MV) | 151 |
| 6.7 | Measure of dispersion (MD) | 152 |
| | Chapter 7 | |
| 7.1 | Statistical Parameters for four load conditions for a Healthy Machine (Fault Free) | 164 |
| 7.2 | Statistical Parameter for four load condition for an inner race fault | 165 |
| 7.3 | The practical value of magnitudes of the maximum value of PDF obtained for four different load conditions for inner race fault | 169 |
| 7.4 | The practical value of magnitudes of the peaks obtained for four different load conditions | 175 |
| 7.5 | Measure of Central tendency (MCT) | 175 |
| 7.7 | Comparison of MD | 177 |

Introduction

A status review of condition monitoring and fault diagnostics of rotating electrical machines is presented in this chapter.

1.1 Introduction

Condition monitoring of electrical machines is essentially a field of technical activity in which selected physical parameters, associated with machinery operation, are observed for the purpose of determining whether machine condition is normal or abnormal. Induction machines have widespread application and can be found in the aerospace, railway, metro, steel, shipping, paper mill and space industries etc. Each of these industries requires an accurate, precise, cost effective method of detecting faults in the machine at a very early stage so that it can be saved from major failure.

Terms such as diagnosis, prognosis, proactive and preventive maintenance are employed which give an insight to the nature of monitoring. Faults can be defined into three categories a) incipient stage, b) advanced stage and c) a final breakdown which leads to a catastrophic failure. By and large incipient fault detection is the objective of modern monitoring tools. The present work focuses and contributes to further development in this field.

All rotating electrical machines constitute of a stator, rotor and bearings. Bearing manufacturer such as NBC, NTN, SKF, Emersons and research bodies namely IEEE, EPRI, DLI, PDMA, and the Research papers indicate that the bearings are the most common component to fail. It is reported that 40% to 50% bearings face the brunt because of the continuous wear and tear. Furthermore, studies indicate that bearing faults in the inner race has the highest tendency of around 64%, followed by outer race with 18% and 18% by other components. The onset of a fault is a chain reaction. If not detected, it will gradually end up in a catastrophic failure. Failures pass through an incipient phase, even if they do so quickly.

Three common methods of approach to achieve condition monitoring are:

- i) Breakdown Maintenance-which implies that if the machine breaks, fix it. This method is commonly employed for non critical plant.
- ii) Planned Predictive Maintenance-Periodically scheduled tests, examinations and replacements are carried out to reduce the possibility of unforeseen defects and downtime.
- iii) Predictive Maintenance-Employs a number of methods of testing a machine operating condition, enabling trending of fault levels and hence rates of deterioration. This predictive maintenance may than be used to govern any further maintenance action.

Figure 1.1 and 1.2 show how development of maintenance techniques has evolved over a 60 years span. Initially, when the industries were not highly mechanized, the prevention of equipment failure was not a high priority. Skills of condition monitoring was an unknown subject. The second generation led to increased mechanization and hence the concept of preventive maintenance led to maintenance planning and control systems. Thus, the cost of maintenance also started to rise sharply relative to other operating costs. More and more failures have safety and environmental consequence and hence in the third generation the need for reliability, availability, accuracy and safety became an integral part of the industry. This explains the need and the importance of effective condition monitoring of electrical machines, employing modern tools of knowledge.

Traditional methods of monitoring include, hearing the sound and noise, seeing anything unusual, smelling, and observing a rise in temperature and increase in vibration. These concepts were replaced by the transducers and the decision making was transferred to the sensitive signal processing techniques. The monitoring of machine vibration has been used as a versatile maintenance tool for both planned and predictive maintenance. The present work exploits the concept of predictive maintenance to detect bearing faults using techniques of observing the pattern of, statistical parameters desired from vibration signal obtained from the machine while in operation. The focus has been on the identification of incipient point faults in inner and outer races of the load end bearings. The findings are based on extensive experimentation.

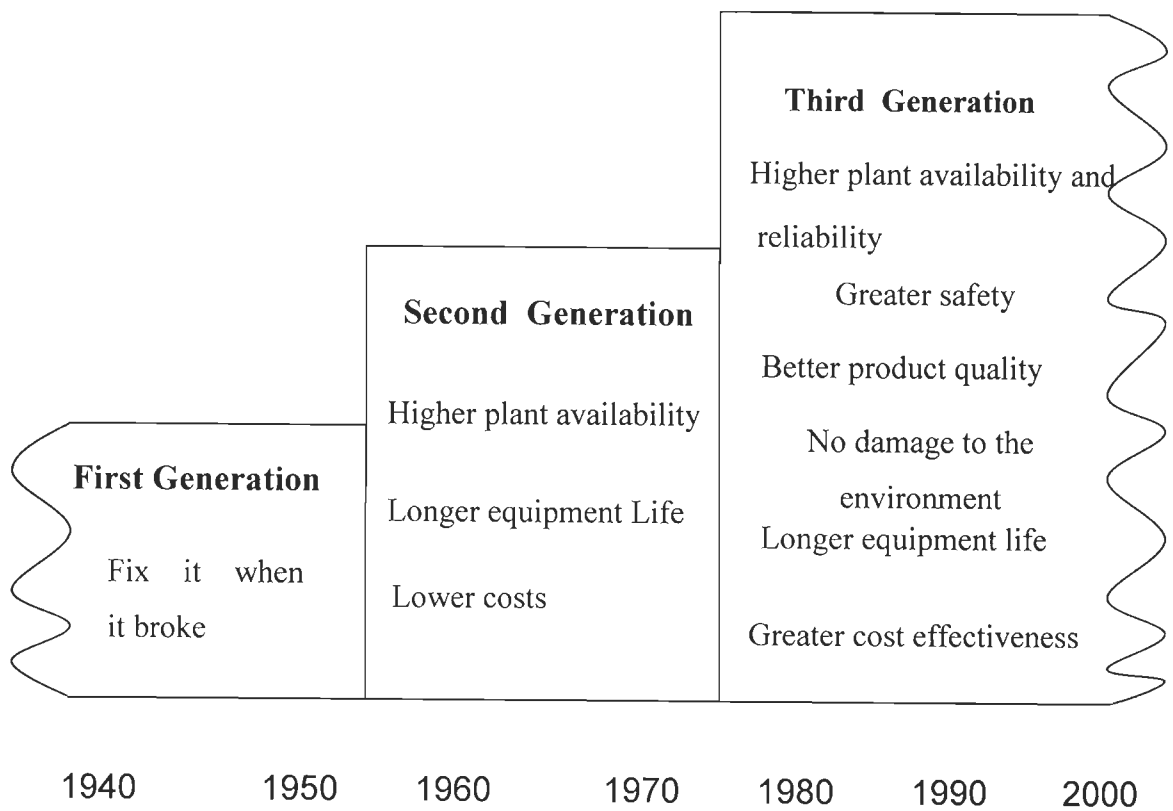


Figure 1.1: Growing expectations of maintenance over 60 years

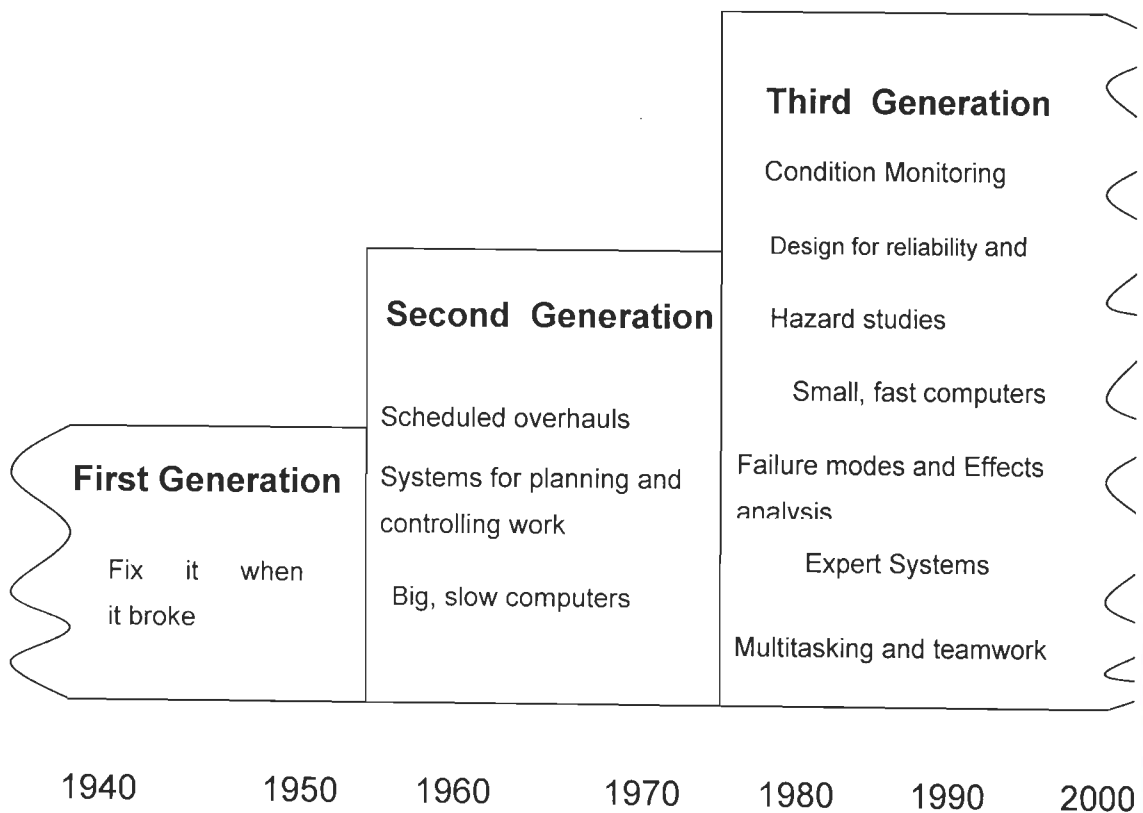


Figure 1.2: Changing maintenance techniques over 60 years

1.2 **Need for Fault Diagnosis:** An effective predictive monitoring

- i) reduces in lost production
- ii) reduces cost of maintenance
- iii) less likelihood of secondary damage
- iv) reduces inventory
- v) extends the life of plant items and
- vi) improves product quality

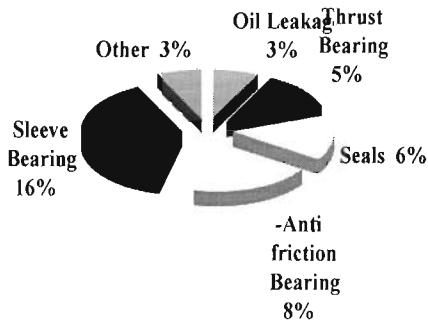
The causes of failure of electrical machines in a very broad sense can be termed as

- a) design deficiencies
- b) material deficiencies
- c) processing deficiencies
- d) improper assembly practices
- e) improper service conditions
- f) inappropriate maintenance
- g) excessive demands

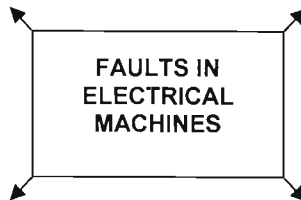
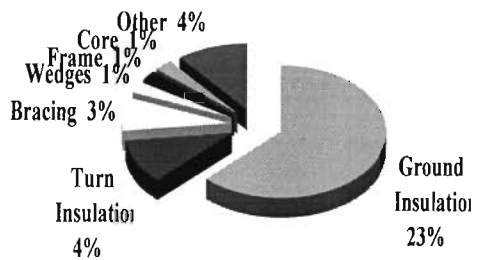
Almost, in all industries, machine failure is evident and this reality has to be faced and tackled to increase efficiency, accuracy and precision. Hence, condition monitoring is the answer to attain and achieve this goal. Machinery failures has been quoted in the Lloyd's register as a big problem in shipping industry. The derailment of trains caused by wheel bearing faults is a significant issue in the rails transport industry. A considerable number of derailment and train stoppage annually around the world are due to actual and potential overheated bearings. Trains often consist of about 300 wheels containing 2400 bearings. The failure of just one bearing poses a significant risk.

M. D.Negrea [95] in his thesis quotes that Thorsen and Dalva shows the distribution of failures among failed components of electrical machines working in the petrochemical industry and is intended to highlight the failure distribution among failed components in 483 high voltage induction machine. Such motors very often operate in extreme condition within offshore activities.

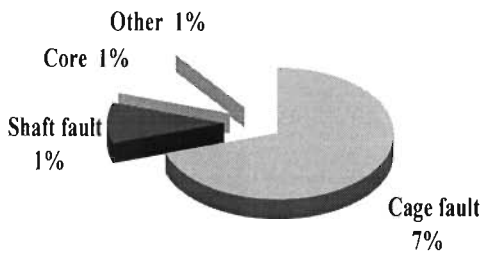
Bearing related faults (41% of the total faults)



Stator related faults (37% of the total faults)



Rotor related faults(10% of the total faults)



Other faults (12% of the total faults)

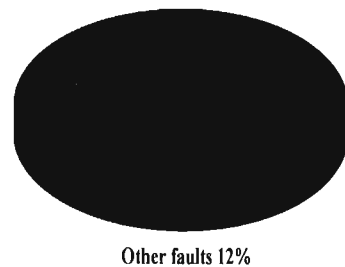


Figure 1.3 Distribution of faults (EPRI 1982)

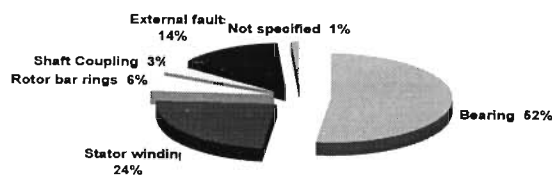


Figure 1.4 Distribution of failed components for electrical machines working in the petrochemical industry (Thorsen and Dalva 1999).

B.K.N. Rao [16] sums up the power of predictive maintenance in a Tabular manner given by (Works Management Boardroom Report, into late 902, July91)

Table 1.1: The power of predictive Maintenance (courtesy of B.K.N.Rao [16])

| Industry | Application | Savings due to predictive maintenance |
|---------------|-------------------------|--|
| Defence | Navy | The Canadian Navy estimate average savings of \$2m/annum through the use of PM across its fleet of destroyers |
| Metals | Aluminium Mill | ALCOA saved \$1.1m in1992 in motor repairs alone |
| Metals | Steel Works | Armco Steel saves some \$ 12 m/annum through PM |
| Metals | Steel Mill | Unplanned repair of a failed 1000hp motor bearing cost \$79k before PM; planned repair of same motor after PM identified potential bearing failure :\$1.6k |
| Petrochemical | Oil Production | Introduction of PM reduced gas turbine compressor maintenance outages by 20% and eliminated the associated lost production cost of 1100 barrels of crude oil per hour |
| Petrochemical | Oil refinery | An oil refinery produced nearly \$ 1m/year saving by reducing maintenance costs by 29% on 100 major and 3900 minor machines |
| Power | Co-generation | On average, maintenance of co-generation plant costs \$7/hp;one western Texas facility reduced theirs to \$ 3.5/hp through PM |
| Power | Nuclear | Following installation of PM in 1985,a nuclear power plant estimated 1 st year savings were \$2m,2 nd year savings were \$3.5m |
| Power | Utilities | An electric power research Institute study compared the actual costs of maintenance in N. America utilities :run to failure, \$18/hp;periodic, \$13/hp;predictive,\$9/hp |
| Pulp & Paper | Paper & Board Converter | Company specialising in high –value coating of plastic film and paper saved \$40k within three months of installing PM |
| Pulp & Paper | Paper & Board Mill | Georgia Pacific Paper saved \$ 72K on one machine outage when PM detected a pump problem |

From Table 1.1, it can be seen that faults diagnostic can be applied to a vast area of application and new emerging trends and technology. Hence, the need of condition monitoring is an ultimate solution to avoid failures from these quotes it is evident that in all rotating machines the bearing is the root culprit whose proper functioning determines the longevity of the machine. Thus, this research work

considers that bearings are the heart of the machine and the machine is the heart of the industry and hence focuses on capturing, analysing the faults in bearings.

1.3 Review of Published Work

This Review of published work involves the meticulous study of unravelling the mystery of which technique will be suitable for our study of bearings. A tabular arrangement shows a glimpse of the research papers which are categorized according to the parameter under consideration and the number of papers consulted according to our aim.

Table 1.2: The Literature Survey.

| Fault Detection Methods | Number of papers in this survey |
|--------------------------------|--|
| Vibration | 86 |
| Current | 46 |
| Voltage | 3 |
| Speed | 3 |
| Sound | 2 |
| Temperature | 1 |
| Oil | 1 |
| Others | 11 |
| Induction Machine | 5 |
| Review Paper | 9 |
| Bibliography | 1 |

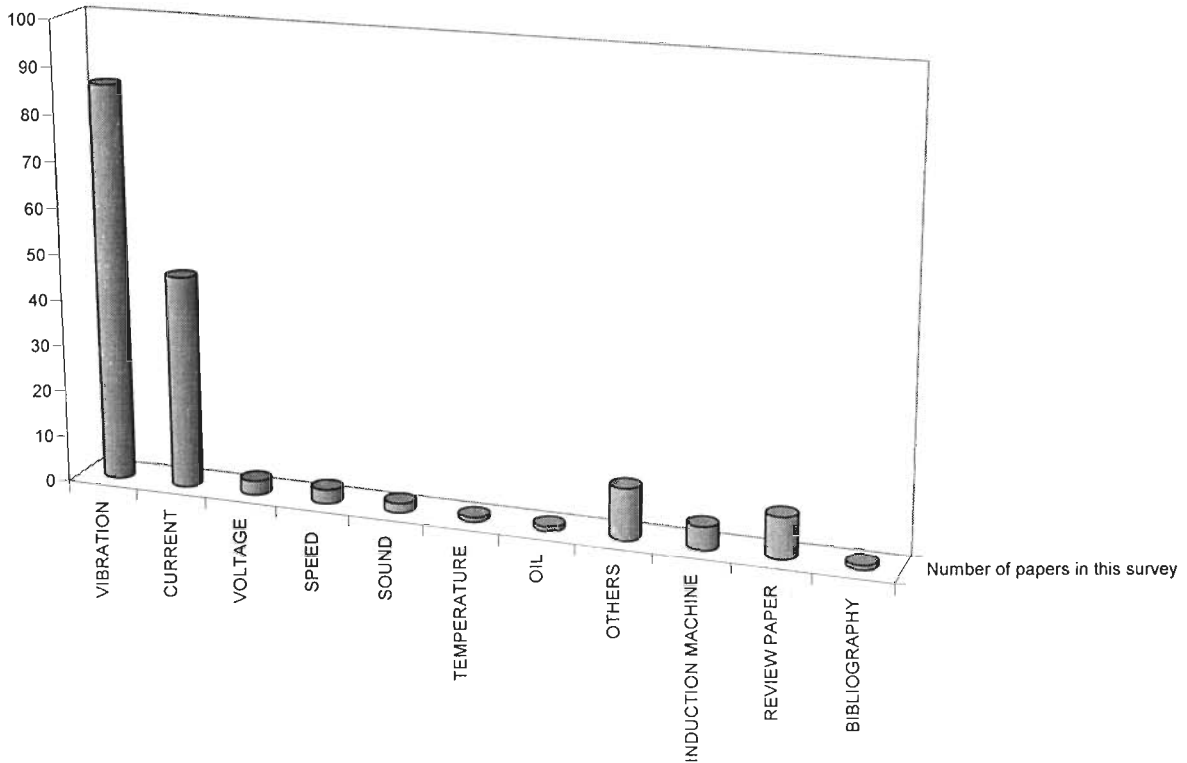


Figure 1.5 Plot showing a spread of this study.

The above plots and graph show that vibration is the most popular parameter in condition monitoring followed by current and the rest of the parameters are least approached. Much exploration has yet to be done with voltage, speed, sound, temperature and oil. The survey categorizes itself as in Table 1.2 and it unfolds as follows:

1.3.1 Vibration Monitoring: The vibration parameter has drawn significant interest by both researchers and manufacturers of machine analyzer. This thesis focuses on vibration based monitoring. In digital signal processing, signals can be divided into random and deterministic signals, random signals carry a lot of information which when analyzed and deciphered produce the components of interest.

A. Choudhary and N.Tandon [2] investigate, a theoretical model that has been developed to obtain the vibration response due to a localized defect in various bearing elements in a rotor-bearing system under radial load conditions and conclude that variation in load and speed indicate that better agreement between theoretical and experimental results can be obtained if the pulse area does not vary with load and is inversely proportional to the speed.

A. M. Al-Ghamd and David Mba [3] give an experimental investigation on the application of the Acoustic Emission (AE) technique for identifying the presence and size of a defect on a radially loaded bearing and discusses the source of AE for seeded defects which is attributed to material protrusions above the surface roughness of the outer race. This was established, as the smooth defect could not be distinguished from the no-defect condition. Furthermore, their work presents two important features; firstly, AE was more sensitive than vibration to variation in defect size, and secondly, that no further analysis of the AE response was required in relating the defect source to the AE response, which was not the case for vibration signatures.

A. Murray and J. Penman [4] describe the vibration data from an induction machine is employed to investigate higher order properties associated with electrical machine faults and concludes that when implemented in conjunction with an Artificial Neural Network ANN diagnostic system, it has been shown that Higher Order System HOS can improve recognition performance.

A.J. Hoffman and N.T. van der Merwe [7] demonstrate that the presence of a bearing defect makes it impossible to determine the degree of imbalance based on a single vibration feature, e.g. the peak at rotational frequency. In such a case, it is necessary to employ diagnostic techniques that are suited to the parallel processing of multiple features. Neural networks are the best known technique to approach such a problem and conclude that it was demonstrated that incomplete training sets will lead to faulty diagnostic decisions.

A. Siddique et al. [9] reviews prominent electrical faults in case of induction motors, especially stator faults, has been presented here giving the state of art trends in the detection and diagnosis of these faults. More accurate and efficient modelling and simulation techniques of stator faults are taken into consideration.

B. Liu, et al. [10] reveal a new approach to the detection of localized defects in rolling element bearings is proposed. It employs matching pursuit with time –frequency atoms to analyze bearing vibration and extract vibration signatures, it further concludes that since the signature obtained this way contained less unrelated components to the defects than traditional band pass filtering, thus it had a higher signal to noise ratio and gave more explicit information for the failure detection.

Bo Li, et al. [11] present an approach for motor rolling bearing fault diagnosis using neural networks and time/frequency-domain bearing vibration analysis. Vibration simulation

is used to assist in the design of various motor rolling bearing fault diagnosis strategies and concludes that results show that neural networks can be effectively used in the diagnosis of various motor bearing faults through appropriate measurement and interpretation.

Bo Li, et al. [12] present an approach of using neural networks to detect common bearing defects from motor vibration data and suggests in the future research, that by additionally incorporating the time domain signal, specifically the presence of peak amplitudes, the severity of the defect should be ascertainable. Eventually, this hybrid frequency and time-domain approach should give further insight into the presence and severity of motor bearing faults. This information will be highly useful for the maintenance of rotating machinery in industrial applications.

B. Samanta, et al. [13] propose a procedure is presented for fault diagnosis of rolling element bearings through Artificial Neural Network (ANN). The characteristic features of time-domain vibration signals of the rotating machinery with normal and defective bearings have been used as inputs to the ANN consisting of input, hidden and output layers, and concludes that the ANN-based approach has its inherent shortcomings, that the ANN needs to be trained for each machine condition: normal and defective with different fault types and severity levels. Another limitation of the ANN-based approach is that the numerical values and the ANN structure would not probably be optimal for another machine.

B.T. Holm-Hansen, et al. [14] deal with an analysis of the vibrational behavior of a deep groove ball bearing with a structurally integrated force sensor and suggests in its future work, that focus on developing advanced and efficient signal processing techniques using wavelet transformation and neural-fuzzy networks to relate signal features to specific bearing faults.

B.T. Holm-Hansen, et al. [15] present a new, structural dynamics based wavelet transformation technique for bearing defect detection. Specifically, a customized wavelet was developed analytically, using the scaling function derived from the actual impulse response of a ball bearing and future research is being continued to further investigate the sensitivity and robustness of the presented wavelet customization technique for the condition monitoring of other types of machine structures and systems.

C. K. Mechefske, et al. [18] present an effective procedure for vibration condition monitoring of low speed ($< \sim 100$ RPM) rolling element bearings is described by using parametric models to generate frequency spectra. Successful fault detection and diagnosis can

be achieved from considerably shorter signal lengths than when using conventional procedures and in their discussion highlights that techniques, based largely on the FFT frequency spectra generated from vibration signals, do not effectively accomplish these tasks when applied to low speed rotating machinery. Finally, the concluding comments say that the AR model based procedure has been shown to accomplish this task and the future work will evaluate the procedure when using signals that represent gradual deterioration in bearings.

C. Li, et al. [19] propose a WPT-RST based fault diagnosis approach for bearing fault. The experiments have demonstrated that this approach can successfully diagnose the bearing condition and the accuracy is nearly the same as BP network. A better discretization of attribute may get better accuracy. The method based on WPT-RST offered an alternative approach for the fault detection of bearing. Further more, it attains nearly the same accuracy, compared with Artificial Neural Network.

C.J. Li, et al. [20] have established the utility of advanced signal processing and pattern recognition to investigate the Acoustic Emission (AE) of bearings, the linear discriminant functions have been established to detect defects on the outer race of the roller bearings and further suggest that AE is found to be a better signal than vibration when the transducers have to be remotely placed from the bearing.

C. T. Kowalski, et al. [23] deal with diagnosis problems of the induction motors in the case of rotor, stator and rolling bearing faults. Two kinds of neural networks (NN) were proposed for diagnostic purposes: multilayer perceptron networks and self organizing Kohonen networks, but concludes, that results of experimental tests show that neural networks can be effectively used for the recognition of stator, rotor, rolling bearings and supply asymmetry faults by appropriate measurements and interpretation of FFT analysis of current and vibration spectra.

C. Wang, et al. [24] discuss the modelling of vibration behaviour of a 2.2 kW induction motor. By comparing the calculated natural frequencies and the mode shapes with the results obtained from experimental modal testing, the effects of the teeth of the stator, windings, outer casing, slots, end-shields and support on the overall vibration behaviour are analyzed. It is concluded that despite these simplifications, results obtained under these conditions are within 10% of the values determined from the experimental testing.

The simulated bearing fault signals were used to investigate the efficient application of Self-Adaptive Noise Cancellation (SANC) in conjunction with envelope analysis in order

to remove discrete frequency masking signals by D. Ho, et al. [25]. The subsequent envelope analysis can then be performed by using the Hilbert transform technique or band-pass rectification, but concludes, that techniques such as SANC can be used to remove discrete frequency noise from the signal before performing envelope analysis. Since this requires real-valued signals as inputs, band-pass rectification is a faster way of performing envelope analysis than the Hilbert transform technique. However, band-pass rectification will also need the extra zero padding used for analysing the squared envelope in order to move the pseudo-sum frequencies outside the frequency range of interest and thus time records will have double the number of samples.

D. Stegemann, et al. [26] categorize modern techniques into *a*) statistical time values (e.g. standard deviation, crest factor, kurtosis-factor, form-factor) to describe the vibrational signals in general, *b*) spectral functions (auto/cross-power-spectral-density, transfer function, coherence) to determine the frequency components and phase-relation of the excitation sources for source localization and *c*) cepstral values (cepstrum, coherence) to quantify periodical information of spectral and coherence data, and finally concludes, that the prove and applicability and reliability of the vibration monitoring system for failure root cause analysis and process optimization is dependent on certain operation condition.

D.Chanda,et al. [27] present an application of wavelet multiresolution analysis MRA theory for the location of lightning strike has been proposed. The property of multiresolution in time and frequency provided by wavelets allows an accurate time resolution while retaining information about higher order harmonics. This property has been used to extract the characteristic features leading to determination of surge location.

D.Dyer, et al. [28] present a method based on statistical parameter kurtosis, that remains constant for an undamaged bearing irrespective of load and speed, yet changes with damage is presented. The extent of damage can be assessed from the distribution of this statistical parameter in selected frequency ranges, and further summarize that the technique is applicable to all types of rolling element bearings but faced problems in interpreting the results from split bearings and from those in close proximity to cavitation.

F. K. Choy, et al.[33] present results from an experimental rotor-bearing test rig with quantified damage induced in the supporting rolling element bearings. Both good and damaged radial and tapered ball bearings are used and the use of the modified Poincare map, based on the relative carrier speed, can provide an effective way for identification and

quantification of bearing damage in rolling element bearings. Finally, in the conclusion it mentions that for ball element failure, if the damage location did not make contact with the inner/outer races during the sampling time window, the damage cannot be detected in the frequency spectrum on any type of time window analysis. The use of the modified Poincare map with vibration data for over 2000 revolutions can assure the contact of the damaged area and eliminate the problem.

F. Wan, et al. [34] present the vibration of a cracked rotor sliding bearing system with rotor–stator rubbing is investigated using Harmonic Wavelet Transform (HWT). Three non-linear factors, non-linear oil film forces, rotor–stator rubbing and the presence of crack, are taken into account, and concludes firstly, that HWT may be a feasible and efficient technique to analyze a multi-non-linear factors rotor. Secondly, the effect of the bearings oil film force on system is significant and should be considered adequately. Thirdly, the effect of multi-non-linear factors is coupling and must be considered simultaneously. It is necessary to consider each vital factor and set up a reasonable non-linear dynamic model. Then, detection and diagnosis of rotor bearing system can be performed accurately.

G.G. Yen, et al. [37] investigate the feasibility of applying the WPT to the classification of vibration signals. Using the WPT, a rich collection of time-frequency characteristics in a signal can be obtained and examined for classification purposes, and conclude, that although the wavelet packet node energy provided us with a multiresolution view of a signal, it simultaneously introduced a higher dimension space, compared to the original time-domain signal. To reduce the dimensionality, it was shown that LDA had some practical problems when the feature dimension was relatively high, compared to the number of collected samples, since it involved calculation of the inverse of the covariance matrix.

G. Goddu, et al. [38] propose the frequency spectrum of the bearing vibration signal is analyzed using a fuzzy logic fault diagnosis methodology, and suggest, future research should extend it by incorporation of intelligent membership function optimization, as well as, employing the method on a real data set.

G.Betta, et al. [41] describe in detail the approach followed to built up fault and unfault, models together with the chosen hardware and software solutions. A DSP-based architecture for vibration analysis is described. It allows machine monitoring to be carried out on-line, with a consequent increase in the system and in environmental safety, and suggests,

the emulation based method used to estimate vibration signal in the faulty condition proves to be very effective, and can be easily extended to numerous application fields.

G.K. Singh, et al. [42] present signals obtained from monitoring system have been processed using Wavelet Transform (WT) with suitably modified algorithms to extract detailed information for induction machine fault diagnosis. The results of this investigation depict that the application of WT for processing and analysis of the vibration signal to different frequency regions in time domain, improves the extraction of the information, and concludes, that WT can be used effectively to specify one-machine fault at a time, while it cannot treat multiple faults simultaneously. However, the use of wavelet and FT together, can provide an effective tool for extracting important information about the machine's condition.

G.K. Singh, et al. [43] assess and compare the effectiveness and reliability of different vibration analysis techniques, for fault detection and diagnostics, in cam mechanisms used in high performance automatic packaging machines, and concludes, that common techniques used to analyze casing vibration such as amplitude probability density and, above all, power spectra density are quite effective for health assessment, but are unable to give diagnostic information. Moreover, time domain analyses of the casing vibration do not give definite diagnostic information either. On the other hand, the use of time frequency analysis method is well suited.

H. Ocak and K.A. Loparo [46] introduce a new bearing fault detection and diagnosis scheme based on Hidden Markov Modeling (HMM) of vibration signals. The technique allow for online detection of faults by monitoring the probabilities of the pre-trained HMM for the normal case. It also allows for the diagnosis of the fault by the HMM that gives the highest probability.

A new scheme is proposed by H. Ocak and K.A. Loparo [47], HMM models were trained to represent various bearing conditions. These models were then used to detect both single and multiple bearing faults based on the model probabilities, and concludes, that the method has been extended to address the problem of bearing prognostics.

H. Ocak and K.A. Loparo [48] present two separate algorithms, for estimating the running speed and the bearing key frequencies of an induction motor using vibration data, and conclude, that the magnitude of the peak increases as the fault diameter increases. Thus, the severity of the fault can be assessed by tracking the magnitude of the defect frequency in the demodulated spectrum. This only applies in the early stages of a fault. In more advanced

stages of bearing failure, the magnitudes of the spectrum at the defect frequencies often reduce to normal like levels.

H. Yang, et al [52] presents an application of this new basis pursuit method, in the extraction of features from signals collected from faulty rolling element bearings with inner race and outer race faults. Results obtained using this new technique were compared with Discrete Wavelet Packet Analysis (DWPA) and the Matching Pursuit Technique, and concludes, that the limitation of basis pursuit is that, its computation, tends to take longer in comparison with DWPA and matching pursuit, using the same length of data. However, this disadvantage is offset by the fact that basis pursuit can use shorter data lengths than the other techniques.

H. Zhengjia, et al. [53] apply the signal decomposition via wavelet transform and wavelet packet, provide an effective approach of multiresolution analysis. The decomposed signals are independent due to the orthogonality of the wavelet functions. There is no redundant information in the decomposed frequency bands, which are independent. Multiresolution signal decomposition, in tandem, with autoregressive spectrum, energy monitoring, fractal dimension analysis, etc., can provide desirable results from the independent frequency bands.

I.E. Alguindigue, et al. [54] propose a vibration monitoring methodology for rolling element bearings (REB) based on neural network technology. This technology provide an attractive complement to traditional vibration analysis because of the potential of neural networks, to operate in real-time mode, and to handle data that may be distorted or noisy, and conclude, that neural networks can provide a methodology for improving the analysis of spectra for vibration analysis, and may provide a viable complement to PSD analysis for monitoring and diagnostics of vibrating components.

J P Dron, et al. [57] present parametric spectrum analysis using high resolution technique for setting up a conditional maintenance program via vibration analysis, and mention that the results show, that parametric methods are particularly worthwhile in the early detection of component defects, especially, when two characteristic frequencies are close to one another. However, the complexity of these techniques necessitates many precautions when they are implemented; consequently, they should not replace conventional methods, but supplement them.

J. Antoni and R.B. Randall [58] show how the Spectral Kurtosis SK can be efficiently used in the vibration-based condition monitoring of rotating machines, and concludes that SK offers the rather unique opportunity to find out which frequency band should be processed and further refutes the common belief that envelope analysis must rely on expertise.

This paper describes a tool based on discriminative energy functions which reveal discriminative frequency-domain regions, where failures can be identified by J. Ilonen, et al. [59]. The tool was applied to induction motor bearing fault detection and succeeded in finding characteristic frequencies, which allow accurate detection of bearing faults, and concludes, that the method also lacks generality due to its Gaussianity assumption, but it still succeeds in many practical situations. The Gaussianity limitation can be overcome by the proposed extensions using Gaussian mixture models, and the Kullback–Leibler divergence. These improvements will be studied in the future versions of the tool.

J. Pineyro, et al. [61] deal with the application of advanced spectral method aimed to be used for detection and diagnosis of localized defects in rolling element bearings. Second order power spectral density, proves to be useful as a tool for peak identification and an aid to classical linear spectra. One of the main drawback is the amount of memory needed during data processing. Wavelet techniques based on the Haar transform, prove to be useful in short transient detection, because after an appropriate filtering process it is possible to eliminate noise and periodic signals. The spectra of this denoised signal retain the main characteristic of frequency peaks in the spectra. On the other hand, this technique has failed in the detection of transients, using acoustic emission sensors.

This paper is to identify single-point defects in rolling element bearings by J. R. Stack , et al. [62]. An Amplitude Modulation (AM) detector is developed to identify these interactions, and detect the bearing fault, while it is still in an incipient stage of development, and concludes that the AM detector is computed from the machine vibration and its interpretation, which only requires knowledge of the bearings characteristic fault frequencies. This method does not require training from various faulted bearings, nor does it require baseline data from the machine being monitored.

J. R. Stack , et al. [63] develop a fault-signature model and a fault-detection scheme for using machine vibration to detect inner-race defects. This scheme examines machine-vibration spectra for peaks with phase-coupled sidebands, occurring at a spacing predicted by the model and discusses in the experimental results that a major difficulty in evaluating the

proficiency of this type of bearing-condition-monitoring scheme is that it is difficult to quantify how challenging it should be to detect a given artificially seeded defect.

J. R. Stack, et al. [67] investigate the effects of a variable machine speed on machine vibration and the implication for bearing fault detection, and verifies that a variable machine speed can directly and nonlinearly alter the level of machine vibration. This is due to differences in mechanical damping and resonance at various machine speeds, and conclude that when comparing vibration data to baseline values in variable speed applications, all measurements must be obtained at the same machine speed to provide a valid comparison. In addition to checking machine vibration against thresholds, the vibration should also be trended over time. This data should be periodically inspected for trends of gradual increase and abrupt decrease.

J. Shiroishi, et al. [68] investigate defect detection methodologies for rolling element bearings through vibration analysis. Specifically, the utility of a new signal processing scheme combining the High Frequency Resonance Technique (HFRT) and Adaptive Line Enhancer (ALE) is investigated, and conclude, that results from this study show that increasing RPM tends to decrease sensitivity to defects.

Jing Lin, et al. [69] propose a denoising method based on wavelet analysis is applied to feature extraction for mechanical vibration signals, and conclude, that Donoho's "soft-thresholding denoising" method does not behave well in these two applications. Therefore, this denoising method based on Morlet wavelet has more advantages than Donoho's & soft-thresholding denoising" method in feature extraction, from these impulse signals. It is a stronger tool for feature extraction and mechanical fault diagnosis.

K Mori, et al. [74] propose the Discrete Wavelet Transform (DWT) is applied to vibration signals to predict the occurrence of 'spalling' in ball bearings. The DWT yield information on both the time and frequency characteristics of the input signals, and is particularly helpful in detecting subtle time localized changes, and conclude, that the DWT of the vibration signals is a sensitive index of the impulsive responses. The values of the wavelet coefficients during these impulsive responses, increase, as the occurrence of 'spalling' comes near. Prediction of 'spalling' is possible by monitoring the trend of the wavelet coefficient maximum values.

L. M. Rogers, [81] describes a methodology for the reliable detection of incipient damage due to fatigue, fretting and false brinelling in large, heavily loaded, rolling element

bearings, such as, found in pedestal slewing cranes and ship azi-pod propulsors. It has been found that combining acoustic emission source location, and spectrum analysis of the associated time-domain signatures, has produced a powerful diagnostic tool, for the detection of micro-damage to the various working faces of the bearing, under variable speed and loading conditions, before any metal loss is evident in the bearing lubricant, and conclude that whereas in the past, bearing condition diagnostic systems using accelerometer have fully met the needs of industry, the trend towards increasing power, complexity and tolerance of modern machinery, requires improved detectability of incipient damage mechanisms, so to avoid the serious consequences of an in-service failure. It has been shown in this paper, that by combining acoustic emission source location with signal envelope spectrum analysis, it is possible to identify different wear processes occurring at different times in different parts of complex machinery. The method has provided reliable information on the condition of the main bearings of marine propulsion engines, before microscopic loss of metal from the rolling contact faces of the bearing is detectable in the lubricant.

M.Bodruzzaman, et al [83] mention that when the frequencies of interest are closely spaced, the Fourier Transform spectrum analysis fails to resolve these frequencies and hence High resolution frequency estimation approach such as Forward –Backward Linear Prediction (FBLP) method is adopted to identify all the prominent frequencies in a certain bandwidth.

M.E.H.Benbouzid, et al [84] find the frequency signature of some asymmetrical motor faults are well identified using the FFT, leading to a better interpretation of the motor current spectra, and conclude that the stator current high resolution spectral analysis, proposed as a medium for induction motor fault detection, has definite advantages over the traditionally, used FFT spectral analysis.

M.E.H. Benbouzid [85] describe a method for simulating signal, and modeling the various stages of incipient failure. Statistical and spectral analysis is used to describe the fault development, and conclude that these results suggest that kurtosis will be a very useful monitoring parameter in situations where pulses contribute significantly to the signal level.

M. Kalkat, et al. [88] illustrate the effectiveness of the artificial NN predictor for vibration analysis of a rotor-bearing system and discusses the experimental results, that the hidden neuron size plays an important role during the training of the network. When size of the neuron was increased, the training time of the network increased.

M. F. White [89] develops a neural network-based incipient fault detector for small and medium size induction motors. The neural network-based incipient fault detector avoids the problems associated with traditional incipient fault detection schemes, by employing more readily available information such as rotor speed and stator current.

M. Bai, et al [93] focus on the development of an intelligent diagnostic system for rotating machinery. The system is composed of a signal processing module and a state inference module. In the signal processing module, the Recursive Least Square (RLS) algorithm and the Kalman filter are exploited to extract the order amplitudes of vibration signals, followed by fault classification using the fuzzy state inference module signals. In addition, more sophisticated methods in the areas of speech and pattern recognition are being sought, in an attempt to enhance the feature extraction and intelligent inference.

A neural network simulator built for prediction of faults in rotating machinery is discussed by N.S. Vyas, and D. Satishkumar, [98] . A back propagation learning algorithm and a multi-layer network have been employed, and conclude, that it has been found that the testing success in addition to the input and hidden layer architecture is crucially dependent on the two training parameters, namely the learning rate coefficient and the momentum. These parameters do not show a linear pattern of behavior and their role needs to be investigated further.

P.Chen, et al [100] propose a fault diagnosis method for plant machinery in an unsteady operating condition using Instantaneous Power Spectrum (IPS) and Genetic Programming (GP). IPS is used to extract feature frequencies of each machine state from measured vibration signals, for distinguishing faults by relative crossing information. GP can sensitively reflect the characteristics of signals for precise diagnosis.

P. D. McFadden and J. D. Smith, [101] develop a model to describe the vibration produced by a single point defect on the inner race of a rolling element bearing under constant radial load and conclude that it is hoped, that this improved understanding, will provide the first step in the development of improved methods of condition monitoring, of rolling element bearings, by vibration analysis.

P. D. McFadden and J. D. Smith, [102] build a model for the high-frequency vibration, produced by a single point defect on the inner race of a rolling element bearing, under radial load, is extended to describe the vibration produced by multiple point defects, and conclude that the frequencies of component from defects are independent of position. The

phase angles of these components are related to the position of the defect, and the frequency of the component.

P.Forster and C.L.Nikias [103] find a new array processing method for bearing estimation, based on the cross bispectrum of the array output data, and conclude that when additive noise, is spatially correlated Gaussian, the bispectrum based method can yield better bearing estimates than the stochastic maximum likelihood, with known cross spectral matrix, provided, the source skewness is large enough.

P. K. Dunn [104] suggests that three tools cover the areas of the central limit theorem, the normal approximation to the binomial, and the bivariate normal distribution.

Conditional time-frequency moments are discussed and applied to the Westland helicopter test data by P. Loughlin and F. Cakrak, [105]. The conditional moments, used have a simple physical interpretation, namely, they are the mean, median and mode frequencies at a given time, and the spread about the mean frequency at a given time (the 'instantaneous spectral bandwidth'). They characterize the faults well, and can differentiate between different fault classes. Finally, it conclude that these statistics can be computed in real time, distinguishes between different fault conditions, and provide a clear physical description of the process. Consequently, they are simple and effective features for on-line monitoring and diagnosis of developing faults, and they contribute to our understanding of transient development and propagation.

P. V. Goode and M.Chow, [106] present a neuro fuzzy system in this paper to perform bearing and insulation wear fault detection, in single phase induction motors. The neural fuzzy system can provide quantitative descriptions of the motor faults under different operating conditions, as well as, qualitative heuristic explanation of these operating condition, and the fault detection procedures through fuzzy rules and membership functions.

P. Vlok, et al.[107] illustrate how statistical Residual Life Estimates (RLE) of bearings can be used to justify maintenance practices, and conclude that while using RLE as a benchmarking tool one should introduce procedures of monitoring process changes that could impact additionally measured covariates. In this case similar behaviour was observed related to greasing change for all the bearings used for analysis.

P.W, Tse, et al. [108] propose the WA and the FFT with ED method in finding the bearing outer-race fault. However, to diagnose the faults of inner-race and roller, the tool of

WA is found to be easier for the machine operator to interpret the analyzed results, and conclude that WA does provide good resolution in frequency at the low frequency range, and fine resolution in time at the high frequency range. Such a multiresolution capability is essential for vibration-based machine fault diagnosis.

An innovative wavelet called exact wavelet analysis has been designed to enhance the robustness of vibration-based machine fault diagnosis by P.W, Tse, et al. [109]. It concludes that this technique is particularly suitable for detecting randomly occurring faults.

Q. Sun, et al [112] present a methodology for machinery fault diagnosis through pattern recognition technique was developed. The proposed technique contains effective feature extraction, good learning ability, reliable feature fusion, and a simple classification algorithm, and finally, conclude that future development of the technique will be directed towards the ability to estimate the remaining life of mechanical components.

R.A. Gupta, et al [113] suggest that the rotor position angle can be estimated by using the unique relationship between flux linkage and phase current in term of fuzzy rule base. Both simulation and experiment results on a DSP based real time drive are presented to show the effectiveness of this scheme.

R.B.W. Heng, and M.J.M. Nor, [114] present a study on the application of sound pressure and vibration signals to detect the presence of defects in a rolling element bearing, using a statistical analysis method. The well established statistical parameter such as the crest factor and the distribution of moments, including kurtosis and skew, are utilized in the study, and conclude that the first study reveals, that the statistical parameters calculated from the results are affected by the shaft speed. This is contrary to the findings of other researchers. Secondly, it highlights, that this study also reveal that there are no significant advantages in using the beta function statistical parameters, compared to using kurtosis and crest factor, for detecting and identifying defects in rolling element bearings.

The modeling is done using full covariance Gaussian Mixture Models of time domain signatures by R. J. Povinelli, et al. [115]. In contrast with current and previous work in signal classification, that is typically focused on either linear systems analysis using frequency content, or simple nonlinear machine learning models, such as, artificial neural networks, and conclude that three separate data sets are used for validation, including motor current simulations, electrocardiogram recordings, and speech waveforms. The results show that the

proposed method is robust across these diverse domains, significantly outperforming the time delay neural network used as a baseline.

R. Yacamini and S. C. Chang, [121] examine how the noise and vibration level of machines is affected by increased levels of distortion, and also how the vibration is affected by machine loading. The method described will apply to a wide range of machine applications, and conclude that there is a significant difference in the vibration levels measured (and calculated) on machines which are working on full load, compared to unloaded machines. It is therefore important that the type of testing of motors be carried out with loaded machines. It is also obvious that any family of machines will give a different noise level, depending on how hard they are being driven.

R. Yan, and R. X. Gao, [122] present a machine health evaluation technique using the Lempel-Ziv complexity as a numerical measure, but conclude that research is being continued to analyze vibration signals from different defect locations, and on different types of bearings, to systematically validate the utility of this technique.

R. Yan, and R. X. Gao, [123] present a new approach based on the Approximate Entropy (ApEn), which is a statistical measure that quantifies the regularity of a time series, such as vibration signals measured from an electrical motor or a rolling bearing, but conclude that research is being continued to analyse vibration signals from different types of defects and on different types of bearings, to further validate the broad applicability of this technique, for machine system health monitoring and diagnosis.

R.B. Randall, [124] compares the original Short Time Fourier Transform (STFT) with wavelet analysis for the time/frequency decomposition, and for determining the optimum combination of centre frequency and bandwidth for maximizing the Spectral Kurtosis (SK). The paper also describes how the SK can be enhanced by “prewhitening” the signal using an Auto Regressive (AR) model, thus, revealing an incipient fault at a much earlier stage, and conclude that the original definition of the SK uses the STFT for the time/frequency decomposition, but the paper also discusses the use of wavelets as an alternative, also for the equivalent of the kurtogram.

S.S. Murthy et al. [125] suggest from various experiment conducted that virtual instrumentation has wider applications in condition monitoring, effect of unbalances, thermal effects, noise and vibration, energy audit/conservation, Direct torque control, Field oriented control and transient and dynamic studies.

S.A. Ansari and R. Baig [126] present a fast-response PC-based vibration analyzer which has been developed, for fault detection and preventive maintenance of process machinery. The analyzer acquires multiple vibration signals with high resolution, and computes frequency spectra, root mean square amplitude, and other peak parameters of interest, and further discusses, that the probable cause of excessive vibration is the bearing defect, since the bearing noise gives rise to a wide range of vibration frequencies-each bearing component velocity producing individual characteristic frequency.

S.A. McInerny, and Y.Dai,[127] propose a laboratory module on fault detection in rolling element bearings. It states that after reviewing the basic operation of rolling element bearings and the characteristics of idealized bearing fault vibration signatures, the shortcomings of conventional spectral analysis were illustrated with a synthetic signal generated in MATLAB. The basis and effectiveness of envelope analysis for bearing fault analysis were then examined.

S.A.S. Al Kazzaz and G.K. Singh [128] suggest that signals obtained from the monitoring system are treated with different processing techniques with suitably modified algorithms to extract detailed information for machine health diagnosis.

S.A.S. Al Kazzaz [129] propose in his research work an intelligent diagnostic and monitoring system based on fast and efficient methods for induction machine health monitoring. The Neural Network algorithm was designed such that the input of the module is the wavelet decomposition of different machine conditions.

S. Nandi, et al. [134] mention that almost 40-50% of all motor failures are bearing related, very little has been reported in literature regarding bearing related fault detection. Bearing faults might manifest themselves as rotor asymmetry faults, which are usually covered under the category of eccentricity related faults. Otherwise, the ball bearing related defects can be categorized as outer bearing race defect, inner bearing race defect, ball defect and train defect and the vibration frequencies to detect these faults are given by the bearing characteristic frequency.

S. Prabhakar, et al. [136] present bearing race faults that have been detected by using Discrete Wavelet Transform (DWT). Vibration signals from ball bearings having single and multiple point defects on inner race, outer race and the combination faults have been considered for analysis. The impulses in vibration signals due to bearing faults are prominent in wavelet decompositions, but in the results and discussion, it pinpoints that kurtosis values

increase as the bearing defects increase, i.e., $(\text{kurtosis})_{\text{good}} < (\text{kurtosis})_{\text{single defect}} < (\text{kurtosis})_{\text{two defects}}$. However, with these values, one cannot pinpoint the location of the defect in the bearing.

S.Seker, and E. Ayaz,[137] deal with the statistical behavior of vibration test data acquired from seven accelerated aging processes undertaken for a three-phase, 5 HP, squirrel-cage induction motor is examined. It is found, that statistical examination of vibration measurements related to each aging cycle has a Gaussian distribution. The second moment, also termed “standard deviation,” appears to be the most dominant parameter employed throughout the analysis.

S. Thanagasundram and F.S. Schlindwein [138] investigate the vibration characteristics of a ‘Roots and Claws’ based dry vacuum pump under different operating conditions was conducted. An Autoregressive (AR)-based condition monitoring algorithm was developed and tested on both a fault-free and a pump with an implanted ceramic bearing with an inner race defect at the High Vacuum (HV) end, and conclude that the results obtained with the AR method for fault classification purposes were conclusive, showing that the system is able to identify and classify defective bearings for a set of used experimental data.

S. Kumaraswamy, [139] an attempt has been made to study the vibration level of various machine tools to explore the possibility of establishing the standard vibration level. It states that till today no vibration standards are available for determining the acceptable vibration level for specific machine tools.

The feature extraction is divided into two parts by S.Wadhvani [140]. The first feature extraction process uses the RMS, Peak, Crest Factor, Skewness and Kurtosis and the frequency domain analysis is computed. In the second part the wavelet transforms are used additionally the complexity measures were also calculated and finally the knowledge base was used to identify the vibration signal.

T.Williams, et al. [143] involve running new undamaged ball and roller bearings through to failure. Traditional vibration metrics such as: root mean square, peak value, kurtosis and crest factor are recorded through the test duration, from accelerometers and acoustic emission sensors, and concludes, that the new system is capable of providing ‘real’ crack information. It is believed that the research is the first one to combine multiple sensors to monitor bearing condition without an artificially induced crack.

T. Zhang, et al. [144] analyze the fault mechanism and vibration characteristics of typical faults of rolling bearings. In order to increase the Signal Noise Ratio, an approach to extract fault features from their vibrations, with envelope analysis and orthogonal decomposition of wavelet is presented, where envelope analysis is used as the pre-processing of the decomposition, and concludes, that the proposed method can be used to pick up other kinds of fault characteristics besides rolling bearing.

T.W.S Chow and G. Fei, [145] introduce bispectrum analysis for three-phase induction machine, faults identification and condition monitoring, and concludes, that results indicated bispectrum magnitude of the dominant component, caused by the machine rotation, increased with the increase in the level of asymmetrical fault. But the bispectrum magnitudes of harmonic components were diminished due to the decrease in m.m.f when the level of the asymmetrical fault increased.

T W. S. Chow and H.Tan, [146] suggest two different state-of-the-art HOS-based methods, namely, a nonparametric phase-analysis approach, and a parametric linear or nonlinear modeling approach for machine fault diagnostic analysis, and conclude that although the order-recursive linear identification approach, does not require the model order to be known *a priori*, it provides less accurate approximation to the measured vibration signals compared with the approach of quadratic nonlinear modeling.

T W. S. Chow and S.Hai, [147] propose a wavelets-transform based technique is used to design specified narrow filter banks. This enables effective machine fault diagnostic analysis, to be performed in the frequency domain. Gaussian-enveloped, oscillation-type wavelet, is employed, and concludes, that as a family of wavelet functions is created with the same shape as the mother wavelet, a Gaussian-enveloped oscillation wavelet is employed in this paper because of its versatility in allowing the parameters of the filter banks to be selected.

U.Chong, et al.[148] introduce a sound detection system which is used to detect unusual sounds and relay the sound information of the operating machine's status to the plant operators, and concludes, the need of an additional monitoring system with neural network using the digital image processing to improve the safety of the plant system.

W.J.Wang and P.D.McFadden, [150] examine the application of the spectrogram to the calculation of the time frequency distribution, of a gear vibration signal is examined, and concludes, that the spectrogram has advantages over the Wigner –Ville distribution (WVD),

for the analysis of the vibration signals, and further states, that the spectrogram gives a clear one- to- one time frequency distribution of the energy in the signal due to the damage, and also provides a high sensitivity to changes of short duration in the signal.

W.J.Wang, et al, [151] report on the application of nonlinear dynamics and higher-order spectra, with particular regard to the correlation dimension and bispectra in rotating machinery fault identification, and concludes, that although the methods of correlation dimension are valuable in the understanding of nonlinear systems, they do not present detailed information about nonlinear mode coupling on a frequency by frequency basis. Such frequency domain information is necessary in order to classify different faults. Moreover, the Gaussian noise contained in the signals can be suppressed in the bispectra. Therefore, a combination of correlation dimension and higher-order spectra offers a good description of a nonlinear system.

W.J.Wang, et al, [152] find a new approach is proposed to determine the gear run-out. Moreover, gear tooth damage detection is conducted using the beta kurtosis and the continuous wavelet transform, based on the overall residual signal. The beta kurtosis of original signal average is also shown here to be useful in detecting excessive gear run-out. Test results from printing presses demonstrated the viability of the proposed methods, and conclude that more tests are currently being conducted to apply the proposed techniques to other machines where the rotation synchronization on different stages is required.

W.J.Wang, et al, [153] develop a new neuro-fuzzy diagnostic system is developed, whereby the strengths of three robust signal processing techniques are integrated. The adopted techniques are: the continuous wavelet transforms (amplitude) and beta kurtosis based on the overall residual signal, and the phase modulation by employing the signal average, and conclude that research is underway to develop a neuro-fuzzy prognostic system to verify the diagnostic results, and to adaptively update its knowledge (rule) base, to further improve the reliability of this diagnostic system.

W.Reimche, et al. [154] suggest basics of comprehensive vibration analysis based on an aimed instrumentation of the unit to be supervised and the state of art in monitoring using statistical time values for general signal description and threshold comparison, envelope analysis and spectrum, phase and correlation analysis of multi sensor arrangements are approached. Hints are also given to data reduction using cepstral and coherence analysis in

combination with the extraction of machine or fault specific characteristic patterns as input values of vector or neural classification.

X.Lou, and K.A.Loparo, [156] deal with a new scheme for the diagnosis of localised defects in ball bearings, based on the wavelet transform and neuro-fuzzy classification, and conclude that using the wavelet transform together with fuzzy logic to quantify the degree of severity of an incipient fault, is a promising technique for prognostics. Further investigations should be conducted on optimal wavelet decomposition in the sense of best performance in incipient fault detection, isolation and severity monitoring. A more challenging task is to explore identifying simultaneous multiple faults through the smart use of time-scale analysis and other techniques, in systems science and engineering.

Y.Choi and Y.Kim, [157] address the way in which we can find the faults for periodic pulse signals. Specifically, we have an interest in the case that it is embedded in noise. How well we can detect the fault signal in noise directly determines the quality of fault diagnosis of rotating machines. We propose a signal processing method to detect fault signals in noisy environments. The proposed method is ‘minimum variance cepstrum’ because it minimizes the variance of the signal power in its cepstrum representation, and discusses in the results, that the proposed signal processing method is able to detect a periodic pulse signal as early as possible. It is independent of the level of noise as the theory proved and also as the experiment demonstrated.

Z. Chen, et al. [158] propose the evolutionary strategy for classification problems which includes GKMT and HENN, and conclude that the comparison of the performance of the HENN and the BP algorithm shows, that HENN is superior to the BP algorithm.

Z.K. Peng, et al. [159] present a review about the application of the wavelet in machine fault diagnostics, including the following main aspects: the time–frequency analysis of signals, the fault feature extraction, the singularity detection for signals, the denoising and extraction of the weak signals, the compression of vibration signals and the system identification, and concludes, that some problems occurred in the use of the wavelet to fault diagnostics.

1.3.2 Current Monitoring: another very important parameter for fault diagnosis on which the researchers are focusing is the current. This becomes vital when vibration parameter is inaccessible from the electrical machine one such example is as in oil rigs where the machine might be immersed in deep waters. Notwithstanding, each parameter has its own merits and

demerits but many researchers have made this as their tool for monitoring. The survey is as follows:

A. Barbour, and W. T. Thomson, [1] apply finite element analysis to predict the frequency components in the current signal which are a function of air gap eccentricity in a 3-phase squirrel cage induction motor but concludes that research is continuing to improve the accuracy of predictions and to consider the influence of different slot designs.

A. Sedighi, et al. [5] suggest a novel method for High Impedance Fault (HIF) detection based on pattern recognition systems is presented that uses that uses combination of wavelet transform and statistical technique as a fault detector but in the results and discussion it is mentioned that because of practical limitations, a larger set of data for HIF tests could not be obtained from the real network.

A. Stavrou, et al. [6] describe, the stator winding itself is used as the sensor for the detection of abnormalities in the stator winding and concludes that it was apparent that some of the specified frequency components were redundant, but whether or not this would be the case for other machines and for the same harmonics requires further investigation.

A.Siddiqui, et al. [8] explore the radial basis function based ANN for the identification of various external faults on a three-phase induction motor. The simulated fault data has been used for training and testing/validation. The instantaneous values of all the three phase currents and voltages have been used for training of the ANN.

B. Raison, et al. [17] present two Motor Current Signature Analysis (MCSA) methods dedicated to the fault detection in the mechanical part of an induction drive: bearing damage, eccentricity and rotor unbalance. The method employed cepstrum and parcels summation was used for bearing monitoring but concludes that the last method seems to be very promising and the signal transformations before parcels summation and the algorithm in itself must be carefully detailed and explored.

F. Briz, et al. [29] describe, fault diagnostics for induction machines using an injected high-frequency carrier signal is presented and analyzed and concludes that while broken rotor bar detection has been shown to be viable with a machine having semi-open rotor slots, the rotor-fault-related component in the negative-sequence, carrier-signal current spectrum was found to be too small for the case of closed-rotor-slot machines to allow reliable rotor fault detection.

F. Filippetti, et al. [32] propose a neural network that can substitute in a more effective way the faulted machine models used to formalize the knowledge base of the diagnostic system when inputs and outputs are suitably chosen and mentions that this procedure substitutes the statement of a trigger threshold, required by the diagnostic procedure based on the machine models.

F.F. Costa, et al. [35] propose to replace the analog notch filter by a Digital/Analog cancelling technique, based on recursive discrete Fourier transform and this reduces the fundamental 60 Hz amplitude before the A/D conversion, leaving only the sidebands in the captured current signal. Broken cage bars were considered, and further conclude that the operation of acquiring and suppressing fundamental component of the signal must be performed in real time via the recursive algorithm.

G. Dalpiaz and A. Rivola [36], review the progress since its inception made in electrical drive condition monitoring and diagnostic research and development. Attempts are made to highlight the current and future issues involved for the development of automatic diagnostic process technology, and concludes, that it is observed that the methods presently being used for condition monitoring of induction machines are either insensitive for incipient faults or do not consider real industrial situations.

G. H. Müller, and C. F. Landy, [39], present a mathematical model showing that interbar currents interact with stator flux to produce a force in the axial direction. The measurements also show that these components are load dependent and conclude that the significance of this method is that it is based on the presence of interbar currents, where the existing vibration methods used today are based on the magnetic disturbance around the broken rotor bar.

H. Henao, et al. [45] suggest that it is proved that a simple external stray flux sensor is more efficient than the classical stator current signature analysis, to detect inter-turn short circuit in three-phase induction machines, and concludes, that this detection technique is more reliable than the MCSA, especially when the number of shorted turns is small, compared to the total number of turns in a phase winding.

H. Guldemir, [50] present the machine with offset (eccentric) rotor has been studied. This study has proved that some of the components in the line current spectrum of an induction motor are a function of eccentricity. The magnitudes of these components increase

when the level of eccentricity increases. These harmonics are used to monitor the eccentricity of the motor.

H.Nejjari, and M. E.H. Benbouzid, [51] propose methodology based on the so-called Park's vector approach. In fact, stator current Park's vector patterns are first learned, using ANN's, and then used to discern between "healthy" and "faulty" induction motors, and concludes, that it was tested on both classical and decentralized approaches.

J. L. Kohler, et al. [60] address the level of turn-to-turn insulation deterioration that can be resolved using an online monitoring technique, based upon an effective negative-sequence impedance detector. The detection of turn-to-turn defects is especially important because they are believed to represent the beginning stage of most motor winding failures, and concludes, that a fault in the presence of the supply unbalance can cause the detector to change unpredictably at very low levels of deterioration, because the effect of the fault, combined with the supply unbalance may initially cause the motor currents to become more balanced.

J. R. Stack, et al. [64] introduce the notion of categorizing bearing faults as either single-point defects or generalized roughness, and in the conclusion suggests, generalized roughness faults produce unpredictable (and often broadband) changes in the machine vibration and stator current.

J. R. Stack, et al. [66], propose a method for detecting developing bearing faults via stator current. The filtered stator current is used to train an autoregressive signal model. This model is first trained while the bearings are healthy, and a baseline spectrum is computed. As bearing health degrades, the modeled spectrum deviates from its baseline value; the mean spectral deviation is then used as the fault index and in the results discusses that as the load level of the machine increases, the magnitude of the fundamental and its harmonics increase drastically. However, the magnitudes of the various bearing fault signatures do not change significantly with load. This phenomenon adds difficulty to the process of current-based bearing condition monitoring. Since the harmonics of the fundamental are the largest components in the stator current spectrum (assuming the fundamental itself is removed before sampling), these components will fully span the dynamic range of the hardware used for sampling. As the difference between the magnitude of these components and the magnitude of the bearing fault signatures becomes larger, the bearing fault signatures are effectively pushed closer to the noise floor in the sampled signal.

J.Zarei, and J.Poshtan, [70] suggest that induction motor vibrations, caused by bearing defects, result in the modulation of the stator current. In this research, bearing defect is detected using the stator current analysis via Meyer wavelet, in the wavelet packet structure, with energy comparison as the fault index. The advantage of this method is in the detection of incipient faults, and concludes, that the frequency bands in defect detection are more tolerant due to the fact, that the actual bearing-defect induced vibration frequency, may vary slightly from the predicted values due to slippage that occurs within bearing.

K. Kim, and A. G. Parlos, [73] deal with the motor current predictor for a wide range of healthy operating conditions. The resulting motor current residuals are nonstationary, and a wavelet packet decomposition algorithm is used to separate the different harmonics, and to compute the fault indicators.

K.Siwiek, et al. [76] present an automatic system for diagnosis of the parametric fault of the individual elements of the electrical circuit, on the basis of external measurements of the voltage and current in this circuit, and concludes, that once the network was trained, the recognition of fault is done immediately, irrespective of the size of the circuit. Thus, the solution is suited for the real time applications of fault location.

L. E. Atlas, et al. [77] present applications of Time Frequency TF analysis to several important manufacturing and machine monitoring tasks, to show the value of these forms of digital signal processing, applied to manufacturing, and concludes, that the results presented in this paper suggests that advanced TF analysis will prove valuable when applied to monitoring of many other manufacturing and machine processes.

L.Eren, and M.J. Devaney, [78] propose that the stator current is analyzed via wavelet packet decomposition to detect bearing defects and concludes that the use of such bands in defect detection is more tolerant of the fact that the actual bearing-defect induced vibration frequencies may vary slightly from the predicted values due to slippage that occurs within the bearing.

L.Eren et al [79], study Radial Basis Function Neural Networks are used to improve the bearing fault detection procedure, and concludes, that the line current data provides and yields a useful predictive maintenance diagnostic when analyzed by the discrete wavelet packet transform.

L.Eren et al [80] present the starting current transient of an induction motor via DWT to detect bearing faults. The frequency sub bands for bearing pre-fault and post-fault conditions are compared to identify the effects of bearing/machine resonant frequencies as the motor starts, but concludes, that this monitoring, on each start ,is achieved in a non invasive manner.

M. E. H. Benbouzid, et al. [86] address the application of motor current spectral analysis for the detection and localization of abnormal electrical and mechanical conditions that indicate, or may lead to, a failure of induction motors, and concludes, that Extensive experimental studies are necessary to fully assess usefulness of the proposed technique, for the preventive maintenance diagnostics and failure prevention, in drive systems with induction motors.

M. E. H. Benbouzid, and G. B. Kliman, [87] deal with a comparison of signal processing-based techniques for the detection of broken bars and bearing deterioration in induction motors. Features of these techniques which are relevant to fault detection are presented. These features are then analyzed and compared to deduce the most appropriate technique for induction motor rotor fault detection. From these discussions, it appears that, for the most difficult cases, time-frequency and time-scale transformations, such as wavelets, provide a more optimal tool for the detection and the diagnosis of faulty induction motor rotors. On the one hand, they remedy the main drawbacks of motor current signal processing techniques for fault detection (i.e., nonstationarity). On the other hand, these techniques exhibit some interesting application advantages, such as for coal crushers, where speed varies rapidly and for deteriorated bearings where speed and signatures may vary in an unpredictable manner.

M.Haji, and H.A. Toliyat, [90] suggest a pattern recognition technique based on Bayes minimum error classifier, is developed, to detect broken rotor bar faults in induction motors at the steady state and concludes that without loss of generality, the algorithm can be revised to include other faults such as eccentricity and phase unbalance. Also, if appropriate features are derived, this method can be applied for fault classification in other electric machines like DC machines.

M.J. Devaney, and L. Eren, [91] find a proactive approach to mitigating uncertainty is needed. This approach starts with acknowledging uncertainty's existence, and then identifying its possible causes so that the mitigation strategy can be designed. Different

techniques are discussed in this paper, and summarizes, that monitoring the induced current frequencies to detect the characteristic bearing failure, involves suppressing the more dominant power system harmonics and then analyzing the remaining current spectrum. WPD provides a means to assess this spectrum, which is less sensitive than the FT to variations in the motor speed, which may result from changes in mechanical load or line voltage. A radial basis neural network then provides an effective means of detecting two common sources of bearing failure.

M. Xu, and T. Alford, [92] propose the induction motor operating principles and motor current measurement, are described. The characteristics of two types of induction motor problems, namely broken rotor bars and air-gap eccentricity, in the measured spectral data are discussed, and one of the conclusions is that the broken rotor bar problem was not evident in the vibration measurement but consistently showed up in the current spectrum. This is not uncommon in detecting rotor problems, because, the damping and other effects exist in the signal transmission path for motor vibration measurement.

M. Bliddt, et al. [94] suggest a new fault model that has been proposed which considers fault-related air gap length variations and changes in the load torque. New, more complete expressions for the frequency content of the stator current are obtained for the three major fault types.

M. Fenger, and W.T. Thomson, [96] demonstrate through case histories, how current signature analysis can reliably diagnose rotor winding problems in induction motors, and concludes, that reliable detection of broken rotor bars, can also involve the correct identification of current components due to mechanical components in the drive system.

P.Pillay, and Z.Xu, [111] develop a Labview implementation of motor current signature analysis. A key feature is the method to demodulate the fundamental component, so that the components of interest can be detected with greater ease. While the technique can be applied to a range of problems associated with condition monitoring, particular attention was paid to the detection of the speed signal for closing the speed loop.

R.M. Tallam, et al. [116] propose an on-line training algorithm for Neural Network (NN) based fault detection schemes, but conclude that the COT algorithm is a viable solution for real-time implementation of any NN-based fault detection scheme. However, continual training, results in an inability to detect a fault that develops very slowly compared to the time between weight updates. Further work is in progress to overcome this drawback.

R.M. Tallam, et al. [117] present neural network scheme for turn fault detection in line-connected induction machines is extended to inverter-fed machines, with special emphasis on closed-loop drives, and conclude that experimental results showed that the scheme is insensitive to arbitrary supply voltage variations and non-idealities in the machine or instrumentation.

R.M. Tallam, et al. [118] present a feed-forward neural network, which learns the model of a healthy machine, has been used in conjunction with a Self-organizing Feature Map (SOFM), to visually display the condition of the monitored machine, and concludes, that experimental results have been provided to show that this method is not sensitive to unbalanced supply voltages or asymmetries in the machine and instrumentation.

R.R.Schoen, et al. [119] present a method for online detection of incipient induction motor failures, which requires no user interpretation of the motor current signature, even in the presence of unknown load and line conditions, and concludes, that the combination of rule based frequency filter and a neural network, maximizes the systems ability to detect the small spectral changes produced by incipient fault conditions.

R.R.Schoen, et al. [120] address the application of motor current spectral analysis for the detection of rolling element bearing damage in induction machines. This paper takes the initial step of investigating the efficacy of current monitoring for bearing fault detection, by correlating the relationship between vibration and current frequencies, caused by incipient bearing failures, but concludes, that the test results clearly illustrate that the stator current signature can be used to identify the presence of bearing fault.

S. M. A. Cruz, et al. [130] describe the use of multiple reference frames for the diagnosis of stator, rotor, and eccentricity faults, in line-fed and Direct Torque Controlled (DTC), inverter-fed induction motors, but concludes, that the proposed method avoids the burden of computation of FFT's, which require intensive computation resources and long sampling periods, necessary to obtain a good spectral resolution.

S. Nandi, et al. [131] propose a detailed simulation results on mixed eccentricity faults are presented. The simulation results show all the low and high frequency harmonics expected to be present in a mixed eccentric machine, but concludes, that the effects of saturation and slot effects on eccentricity related current harmonic components, are yet to be studied.

S. Nandi, et al. [133] present a brief review of bearing, stator, rotor and eccentricity related faults and their diagnosis have been presented in this paper. It is clear from various literatures that non-invasive motor current signature analysis (MCSA) is by far the most preferred technique to diagnose fault. However, theoretical analysis and modelling of machine faults are indeed necessary to distinguish the relevant frequency components from the others that may be present due to time harmonics, machine saturation, etc. Other techniques for fault detection such as axial flux based measurements, vibration analysis, etc. have also been discussed. A section on automated fault detection has also been included.

S.Han, et al. [135], suggest the proposed method utilizes ICA estimation of unifying structure, which includes mutual information and time structure. If the signals have no time correlation, their complexity may be achieved by their entropies, and concludes, that the results provide more accurate defect analysis with noisy corrupted data, over conventional ICA, is a feasible approach for extraction of a machine signal from noisy measurements.

T.Han, et al. [142] propose an on-line fault diagnosis system for induction motors through the combination of Discrete Wavelet Transform (DWT), feature extraction, Genetic Algorithm (GA) and Artificial Neural Network (ANN) techniques, and concludes, that the disadvantage of DWT, which results in feature dimension increasing, can be overcome by feature selection using GA. Also the difficulty of neural network parameter setting has been solved through GA optimization.

V.K.Sharma et al. [149] investigate by modelling and simulation technique for fault tolerant behaviour of SRM, based on current and position dependent nonlinear flux linkage. It was applied to both fault and abnormal conditions.

W.T.Thomson, and R.J.Gilmore, [155] present the fundamentals on MCSA plus data interpretation, and the presentation of industrial histories, and concludes, with the advantages of using MCSA as a tool for assessing the operational condition of three phase induction motor.

1.3.3 Vibration and Current Monitoring: the need to know what parameter should one chooses led to the compare and contrast study of two parameters vibration and sound. The survey is as follows:

C. M. Riley, et al. [21] present an initial study into the relationship between vibration and current harmonics of electric motors, including the effect of externally induced

vibrations. The RMS vibration sum and the RMS current sum were found to have a fairly monotonic relationship at a given frequency, and are tightly correlated. This high correlation implies that the current spectrum can be used to evaluate motor vibration.

C. M. Riley, et al. [22] propose a method for sensorless online vibration monitoring of induction machines based on the relationship between the current harmonics in the machine and their related vibration harmonics, and concludes, that vibration information can be gained in a sensorless fashion by utilizing the nearly linear relation between a particular vibration spectral component and its corresponding current harmonics.

G.S. Maruthi, and K.P. Vittal, [44] suggest two methods of fault diagnosis vibration analysis and current signature analysis, have been analyzed on their ability to detect induction motor operation abnormalities, and concludes, that the detection of electrical abnormalities through vibration analysis is more beneficial when compared to MCSA, as it is non electrical contact type measurement.

J. R. Stack, et al. [65] develop a method that employs an externally applied shaft current to initiate and progress a bearing fault in an accelerated time frame, and concludes, that In machines operated at load levels greater than 50%, the increase in vibration is not monotonic, and the transition from incipient to advanced fault stage is not always easy to predict.

P.J. McCully, and C.F. Landy, [110] show that significant interbar currents reduce the unbalance brought about by a broken rotor bar, and thus, why it is necessary to focus attention elsewhere in the current spectrum to diagnose a broken bar. This paper also explains the technique of monitoring the vibration spectrum, and the effect of interbar currents which produce tell-tale components in the vibration spectrum, and concludes, that at present, development of the software program is ongoing, to produce a tool for analysing both current and vibration spectra, in the quest for conclusive proof of the condition of rotor bars in induction motors.

1.3.4 Speed Monitoring: studies suggest that any disturbance in a machine leads to change in speeds and eventually in wind power generation the harmonics present a bitter reality that are not only random in nature but also erratic. Thus introducing speed monitoring and survey is as follows:

F. Filippetti, et al. [31] present a new and simple procedure based on a model which includes the speed ripple effect is developed. This procedure leads to a new diagnostic index, independent of the machine operating condition and inertia value, that allows the implementation of the diagnostic system with a minimum configuration intelligence, and concludes, that an experimental proof of the improvement in the fault diagnosis and of the independence of the sum of the current components on inertia are given.

I. S. Cade, et al. [55] proposes a method of online fault identification in rotor/magnetic bearing systems is presented using wavelet analysis, and concludes, that Consideration of sudden rotor unbalance indicates that in a synchronously rotating reference frame, wavelet coefficients will only be nonzero during the transient response. In the case of rotor/bearing contact, it has been shown that nonzero coefficients will also be present only during the transient response. However, in the contact case this is argued to be independent of the reference frame.

1.3.5 Voltage Monitoring: this parameter is another approach found in fault diagnosis. In the field of condition monitoring it is not a famous parameter for detecting fault. Moreover, very few papers address this issue. The survey is as given;

F. C. Trutt, et al. [30] present a theoretical and experimental analysis of a voltage mismatch technique that may be used in operating situations to monitor the health of induction motor windings, and concludes, that both voltage mismatch parameters are seen to predict deterioration independent of whether this deterioration acts to create more balance or to create more unbalance in the motor. Future research should include more extensive experimental testing on a variety of induction motor systems, in order to provide additional verification of the proposed monitoring scheme.

S. Nandi, and H. A. Toliyat, [132] the method proposed in this paper monitors certain rotor-slot-related harmonics at the terminal voltage of the machine, once it is switched off, but concludes, that Unlike negative-sequence current or impedance measurements, this technique is insensitive to supply voltage unbalance. The faulty phase can be detected, too. The very nature of the test also suggests that the supply harmonics have little influence on detectability.

1.3.6 Sound Monitoring: this has a lot of dimensions for condition monitoring and might hold a lot of answers to the questions faced by researchers. This parameter is mainly exploited in the aerospace industry.

K. Shibata, et al. [75] describe a Symmetrised Dot Pattern (SDP) method, which visualises sound signals in a diagrammatic representation. Using SDP to visualize sound signals measured for fans, it was possible to distinguish differences between normal and faulty bearings, and concludes, that SDP method is effective to detect the abnormality on bearings through visualization of sound signals, when the measured sound pressure level is higher than the background noise. Therefore, maintenance personnel can distinguish easily between the normal and abnormal state on motor bearings.

1.3.7 Oil Monitoring: the world of tribology contributes that development in faults changes the properties of the lubricant in terms of viscosity and the rest but one study show that this does not offer much promise.

J D Turner, and L Austin, [56] report a study in which changes to the dielectric and magnetic properties of the oil are assessed as methods of measuring the degradation of lubricating oil, and mentions that The magnetic characteristics of lubricating oil (i.e. its magnetic permeability) do change as the oil degrades, but the measurements were poorly correlated with viscosity, and do not seem to offer much promise as the basis of an oil monitoring system.

1.4 Scope of Present Work

This research work focuses on detection of incipient fault in motor running under rated supply condition at selected loading. The bearing faults related to outer and inner race are considered for demonstration of the approach. The statistical parameters are derived from the time domain vibration signal to examine their behaviour for fault diagnosis. These investigations are done in laboratory on a 7.5kW cage induction motor.

1.5 Organization of the Thesis

This thesis organization is as shown below

Chapter 1 Introduction

A status review of condition monitoring and fault diagnostics of rotating electrical machines is presented in this chapter and also provides an intensive literature review.

Chapter 2 Data Acquisition

It describes the experimental set up used in present work including introduction to DAQ, Transducers in DAQ, Processing of the signal, LabVIEW program used for the analysis.

Chapter 3 Analysis Techniques

It discusses the different analysis techniques used in FDEM. It suggests and explains the choice of analysis technique proposed in this thesis. Statistical Analysis in tandem with time domain vibration signal becomes a powerful toll for FDEM.

Chapter 4 Behaviour of Vibration Data

This chapter, introduces chitest as a validation test of vibration signal, states the advantages and its application. Further gives the conditions of validity of chitest, defines goodness to fit, final steps of chitest is given, the guidelines to calculate chitest. Last but not the least the results and Discussions are stated.

Chapter 5 A Statistical Approach for Fault Diagnosis in Electrical Machines

In this chapter, a healthy machine, outer race fault and inner race fault were considered and their comparisons were done for half full load conditions. The analysis technique used are; statistical parameters and statistical inference.

Chapter 6 Experimental Investigations on Outer Race Fault

This chapter focuses on outer race fault under four load conditions that is no load, slight load, half load and $\frac{3}{4}$ loads. It specifically identifies the condition at an incipient stage and categorically gives an increase in the peaks of FFT as load increases and a decrease in peaks of the PDF was observed and CDF indicating a wider spread implying increased dispersions. A validity test was executed showing Gaussian distribution.

Chapter 7 Experimental Investigations on Inner Race Fault

This chapter deals with the inner race fault which is a 64% contributor of faults amongst all the bearing faults that exists. This fault was specifically pinpointed under four load conditions and different analysis techniques were

applied to detect the existence of this fault. It is one of the most difficult faults to detect at an incipient stage since it is deep rooted and it hides behind the spectra. This chapter gives an insight how to classify the inner race fault using the statistical parameter and inference and eventually validating with the results with a non parametric test.

Chapter 8 Conclusions

This chapter highlights the objective, aim achieved and suggests the positive points conquered in this field, suggestions are given as to an insight of the futuristic approach to FDEM.

Data Acquisition

This chapter describes the experimental set up used in the present work including introduction to DAQ, Transducer in DAQ, Processing of the signal, LabVIEW program used for the analysis.

2.1 Introduction

The faults in induction machines broadly take place in the rotor, stator, bearings and other components. A typical induction machine is shown in Figure 2.1:

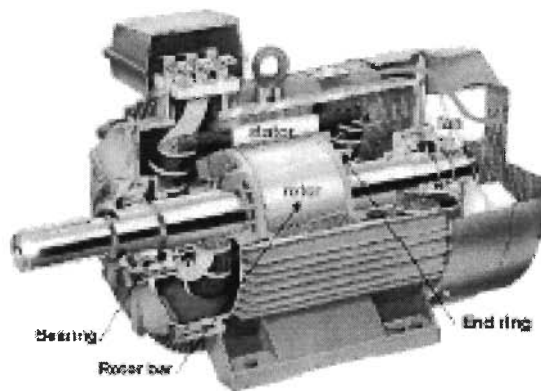


Figure 2.1 View of cage induction motor

The rating of the induction motor employed in the research work is given in Table 2.1 as shown below. This induction motor is considered as the prime mover coupled to a DC generator for loading.

Table 2.1: Specification of the induction motor used in the Experiment

| Rating and Specification of Induction Motor |
|---|
| 3-phase , 415 Volts, 50Hz, 7.5 kW, 15 A, 1440 rpm |
| Type: TEFC, Frame: 132m, Insulation class B, Efficiency: 85%. |

Chapter 1 mentions, that bearing is the greatest contributor and has 40% of faults compared to the rest of the components. Furthermore, the study by IEEE and EPRI indicate that bearings are the culprit that bears the brunt. According to the nature and severity of fault that erupts in a bearing either it damages the unit or further transmits to other parts causing multiple failure. A study shows the graph of bearings taking the maximum brunt.

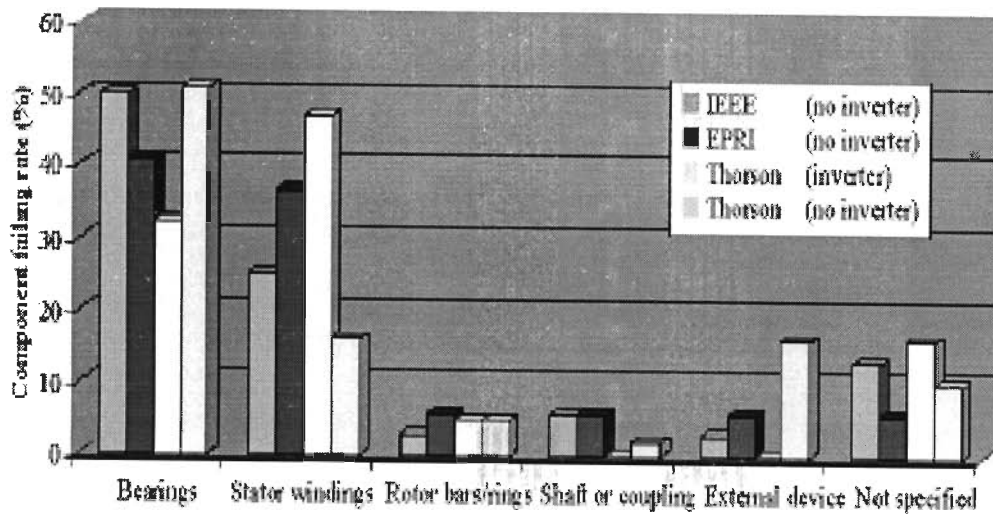


Figure 2.2 Induction motor component failing rate [courtesy MEH Benbouzid]

Bearing are of different makes, brands and kinds but the basic structure and the behavioural pattern remains the same. Many causes are attributed to bearing failure as mentioned by the manufacturer’s of bearings (that is Emersons) and is given below:

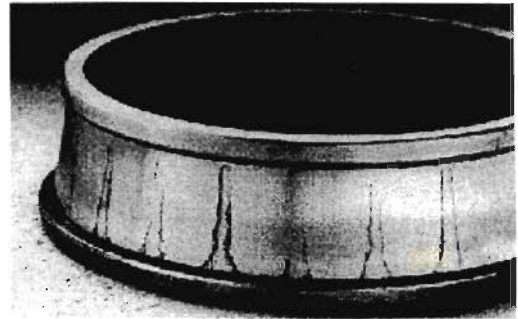
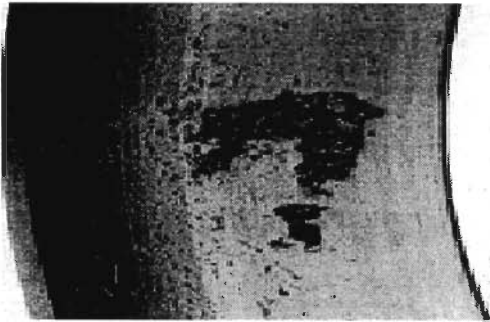
Contamination

Contamination is one of the leading causes of premature bearing failure. Symptoms of contamination are dents or scratches embedded in the bearing raceways and balls/rollers, resulting in undue bearing vibration and wear. Contaminants may include airborne dust, dirt or any abrasive substance that gets into the bearing. Principal sources are dirty tools, contaminated work areas, dirty hands and foreign matter in lubricant or cleaning solutions.

Corrosion

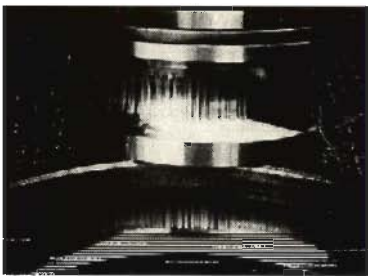
Corrosion results from the chemical attack on bearing materials by hostile fluids or atmospheres. Symptoms include red/brown areas on rolling elements, raceways, or cages.

Corrosion usually results in increased vibration followed by wear, with subsequent increase in radial clearance or loss of preload.



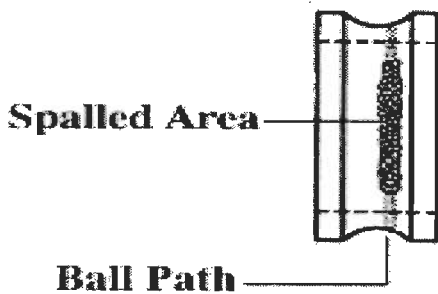
Electrical Fluting

Electrical Fluting occurs when a current is passed through the bearing, instead of to a grounded source. Frequently seen in electric motors Can be eliminated by ceramic-coating the OD of the bearing.



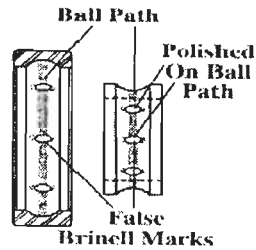
Excess Load

Excessive load normally causes premature bearing failure. Symptoms are the same as normal fatigue, although showing heavier ball wear paths, greater evidence of overheating, and a more widespread and deeper spalling (fatigue area).



False Brinelling

Occurs when there is small relative motion between the balls/rollers and raceways during non-rotation times. Characterized by elliptical wear marks in the axial direction at each ball/roller position. When the bearing isn't turning, an oil film cannot be formed to prevent raceway wear. Wear marks are perpendicular to the line of motion, normally well-defined, and sometimes surrounded by debris.

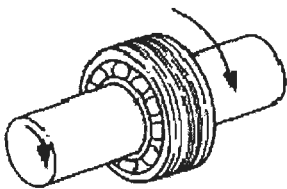


Install Damage

Occurs when a sharp impact is applied incorrectly to a bearing during mounting or dismounting.

Loose Fit

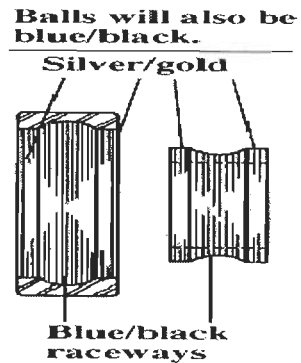
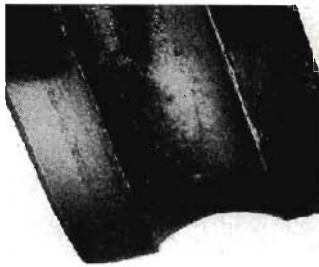
It is caused by relative motion between mating parts which, in turn, causes fretting. Fretting occurs when fine metal particles oxidize, leaving a distinctive brown color. This normally occurs through outer ring slippage in the housing due to improper fits. Outer ring slippage caused by improper housing fits. Discoloration and scoring will appear on the outside of the outer ring.



Lubrication

Symptoms include discolored (blue/brown) raceways and balls/rollers. Restricted lubricant flow or excessive temperatures that degrade the lubricant's properties typically

cause failures. Lubricant failure will lead to excessive wear, overheating and subsequent bearing failure.

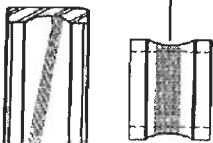


Misalignment

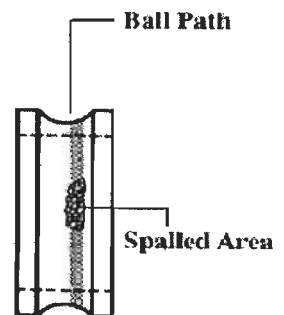
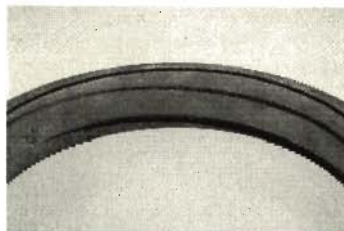
Misalignment failure can be detected on the raceway of the non-rotating ring by a rolling element wear path that is not parallel to the raceway edges. Excess misalignment can cause abnormal temperature rise and/or heavy wear in the cage pockets. The most prevalent causes of misalignment are:

- bent shafts
- burrs or dirt on the shaft or housing shoulders
- shaft threads not square with the shaft seats
- locking nuts with faces that are not square to the thread axis

Wide ball path on inner raceway.



Nonparallel ball path on outer raceway.



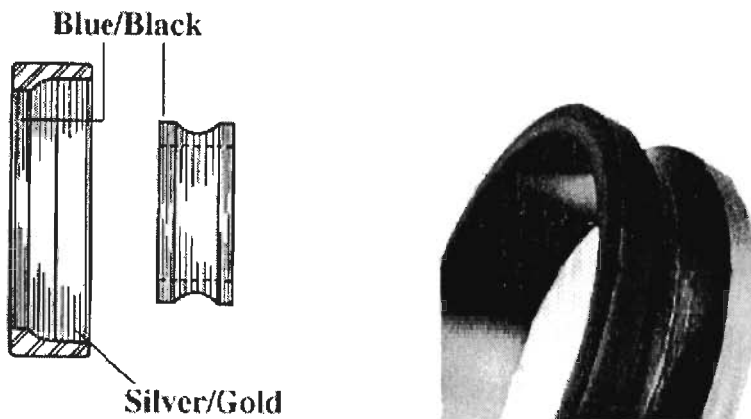
Normal Fatigue Failure

Normal fatigue failure is characterized by "spalling", or a fracture of the running surface and subsequent removal of small, discrete particles of material. Spalling can occur on balls, rollers or raceways, and is always accompanied by a marked increase in vibration.

Moderately spalled areas indicate that the bearing has reached the end of its useful life.

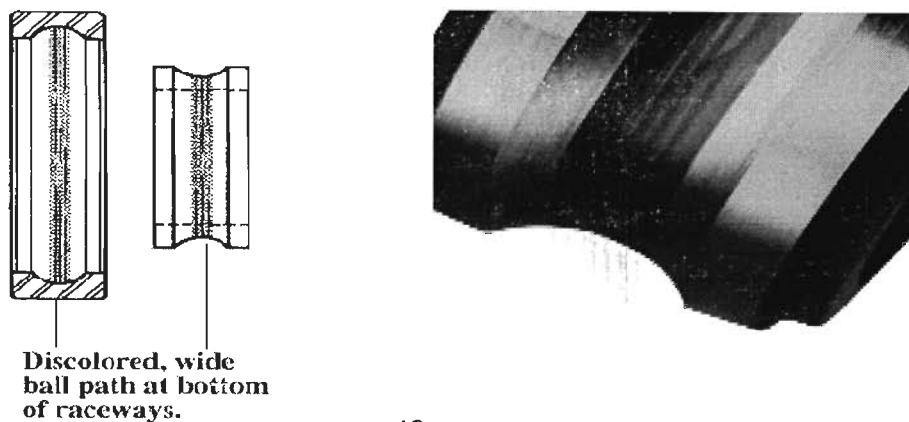
Overheating Failures

Symptoms of overheating are the discoloration of the rings, balls/rollers and cages from gold to blue. Temperatures in excess of 400 degrees C. Extreme cases result in deformation of balls/rollers and rings. Primary indications are blue/black and silver/gold discoloration, and balls/rollers will usually be blue/black.



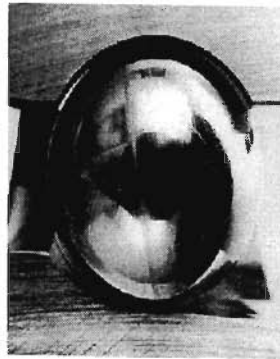
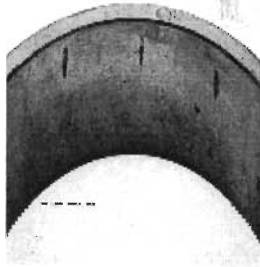
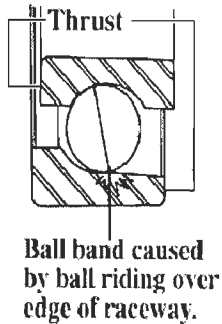
Preload Failures

Preload is indicated by heavy rolling element wear paths in the bottom of the raceway around the entire circumference of the inner and outer ring. If interference fits exceed the internal radial clearance, the rolling elements become preloaded. If clearance is lost in a bearing, it results in rapid temperature rises accompanied by high torque. Continued operation can lead to rapid wear and fatigue.



Reverse Loading

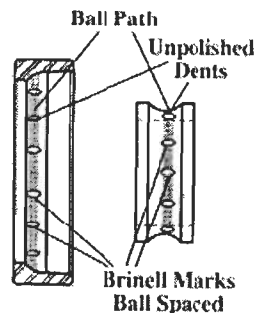
Occurs when loads shift direction in bearings that can only take axial loads in one direction (angular contact ball bearings). When loaded in the opposite direction, the elliptical contact area on the outer ring is truncated by the low shoulder on that side of the outer ring. The balls will show a band caused by the ball riding over the edge of the raceway. Failure mode is very similar to that of heavy interface (tight) fits. A thrust load applied to the wrong bearing face results in a wear band on the balls.



True Brinelling

True Brinelling occurs when loads exceed the elastic limit of the ring material.

Brinell marks are indentations at ball/roller frequency caused by any static overload or severe impact.



Examples of true brinelling causes

- Using a hammer to install a bearing
- Dropping a bearing
- Pressing a bearing onto a shaft by applying force to the non-rotating ring

These indentations are evident in the raceways and can increase bearing noise and vibration, leading to premature bearing failure.

These faults have been found in bearings and have been the cause of concern of failures in industries. Each one of the fault do exist independently or can herald into multiple faults.

The picture below depicts the vital components of some of different kinds of bearing that exist in the industries:

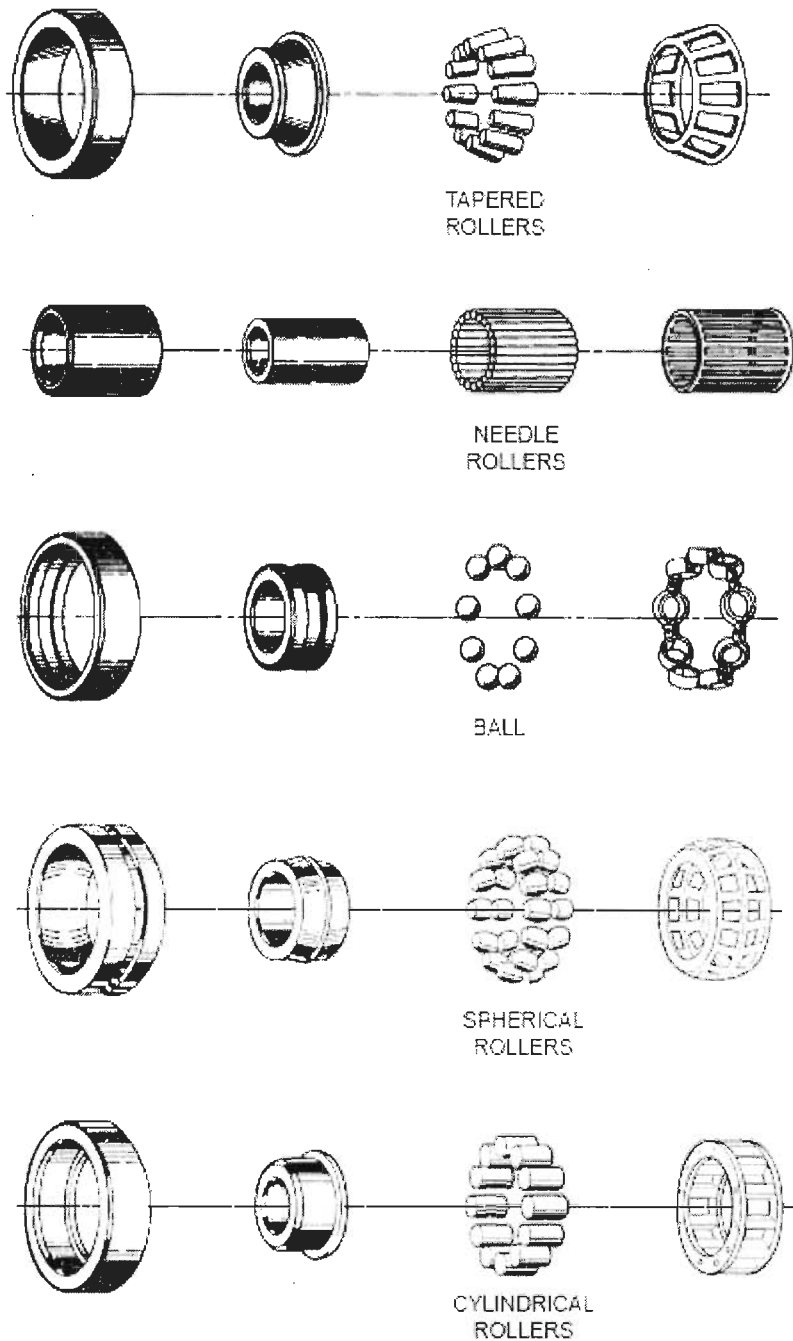


Figure 2.3: Five basic types of bearings: tapered, needle, ball, spherical and cylindrical. Each is named for the type of rolling element it employs.

To sense and attain the signature of these faults the vibration parameter was exploited. Vibration and shock are an ever present reality in the world of rotating electrical machines.

These vibrations generated or transmitted might be desirable, disturbing or even destructive. Hence, the need to understand the causes, effect, and the need to classify so that it becomes a helpful tool to pinpoint a fault before failure really damages a component, multiple components or brings the machine to a stand still. This research work proceeds to introduce Data Acquisition which has been implemented to acquire the vibration signal in this research.

2.2 DAQ Components

Data Acquisition (DAQ) is the sampling of the real world signals such as vibration, current, voltage, speed and temperature to generate data that can be further analyzed, diagnosed and finally, conclude it, to a meaningful and informative signature. DAQ typically involves acquisition of signals in an accurate manner, obtaining the waveforms and processing the signals to obtain desired information. The components of data acquisition systems include appropriate sensors that convert any measurement parameter to an electrical signal, which is acquired by data acquisition hardware. Companies, Industries, Researchers and Experts of FDEM have built different monitoring equipment according to their parameters of interest but no hard and fast rule has been assigned to the methodology. The DAQ of this research work comprises of Transducers, Signal Conditioning Unit, and finally, the software of LabVIEW that offers a graphical programming environment optimized for data acquisition. The data is then stored in the EXCEL sheet from which analysis is carried out.

Contd...

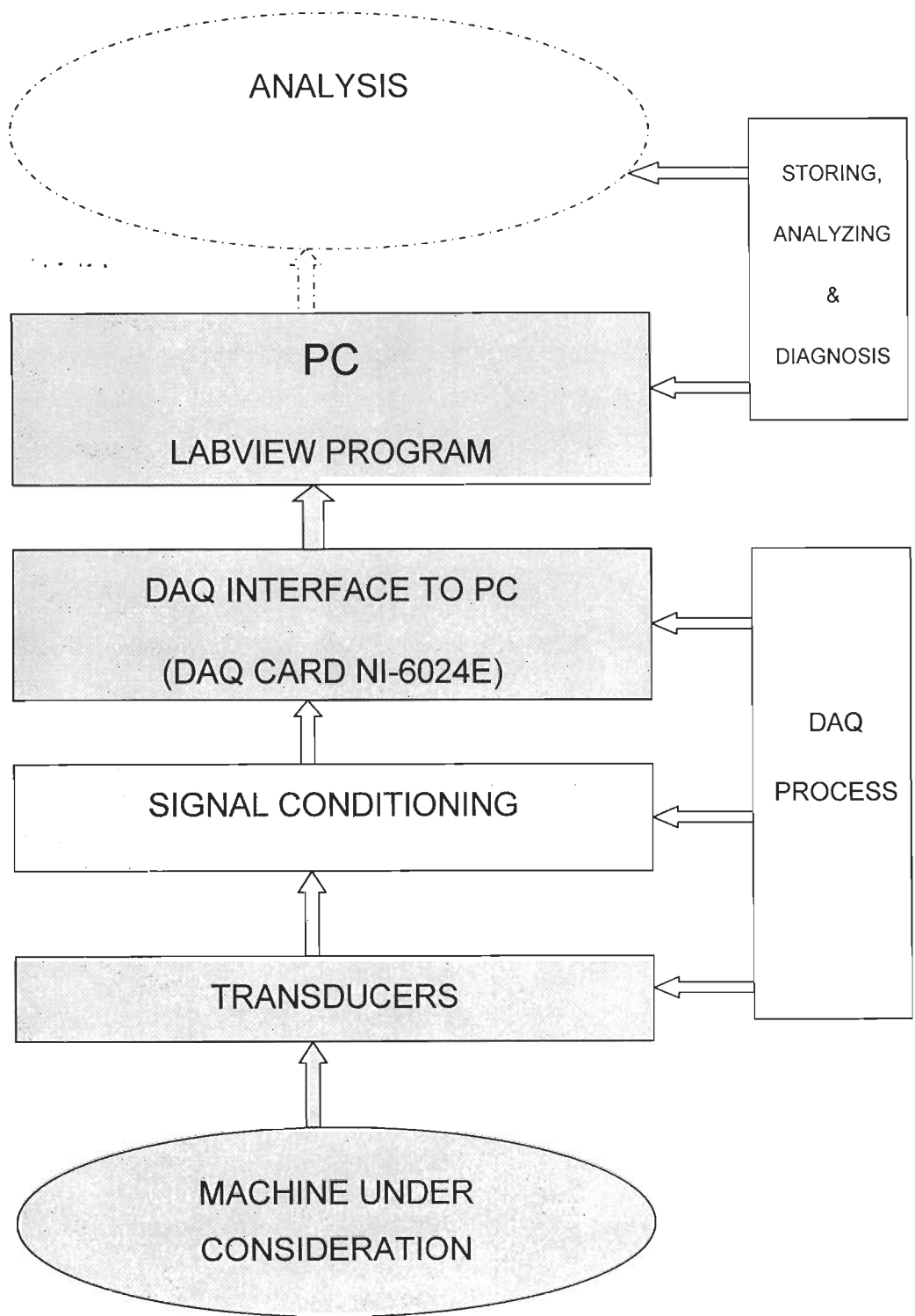


Figure 2.4: Flow Diagram of the DAQ for FDEM

2.3 Transducers in DAQ

Transducers are sensitive sensors that pick up the signals by responding to the behaviour of the induction machine. This research work incorporates the following transducer:

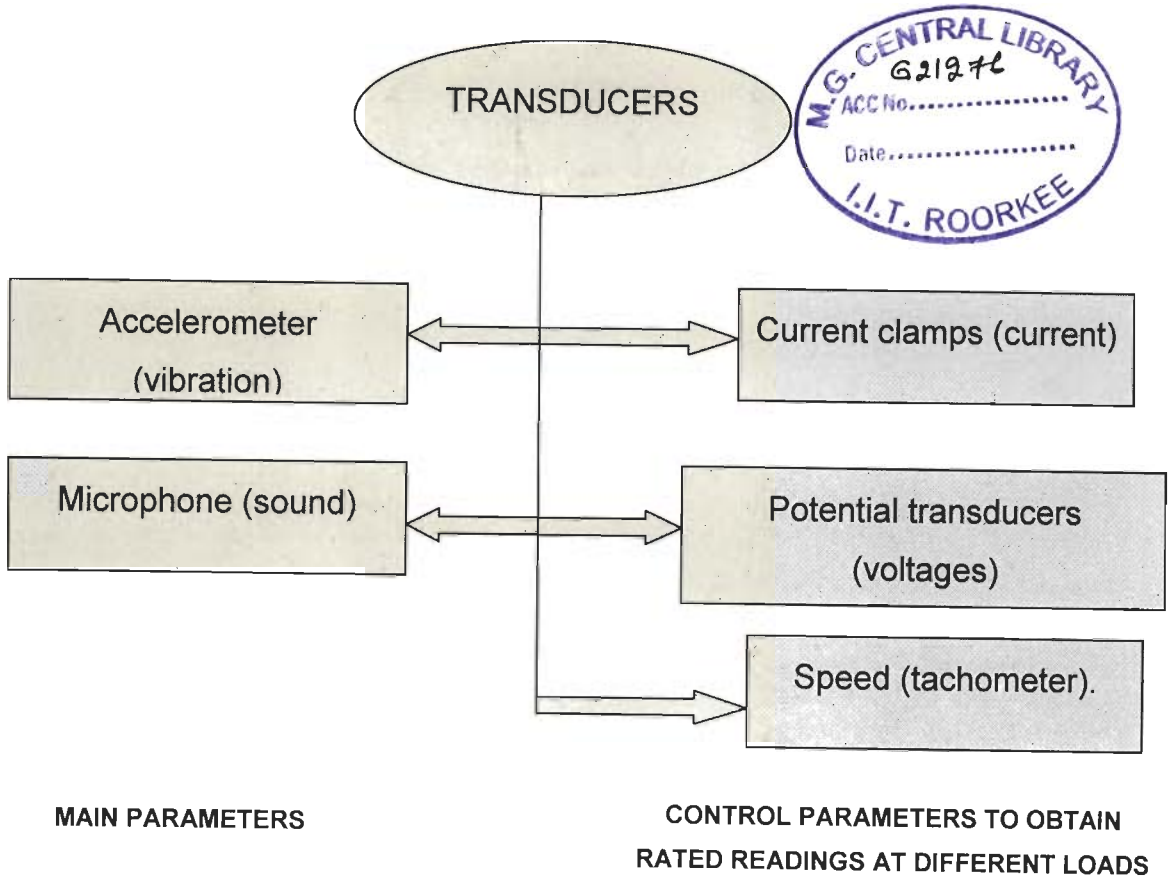


Figure 2.5: Transducer and experimental setup used in this work

This present work uses the current, voltage and speed to drive the induction motor at rated values at four load conditions whereas the vibration signal is the main focus of our study due to its random nature. The vibration and sound signals were acquired on which analysis is prosecuted after adjusting the motor at rated speed. This provides a systematic and controlled method of condition monitoring.

2.3.1 Accelerometer – (Vibration Sensor): Vibration can be measured in terms of acceleration, velocity and displacement. The choice of the parameter depends on the size of the machine as well as the frequency range. No hard and fast rule has been applied by the

condition monitoring experts on the choice of parameter. The table below gives the guidelines for selecting an accelerometer. They are as follows:

| |
|--|
| <p>Variables</p> |
| <p>Frequency range(Hz): Piezoelectric accelerometers have an upper and lower useable frequency. The upper frequency is determined by the accelerometer's natural frequency and the lower limit by the time constant of the sensor's internal circuitry or external charge amplifier. The accelerometer should be used within the flat portion of the response curve. In this range, the specified sensitivity lies within a defined amplitude tolerance band (usually $\pm 5\%$).</p> |
| <p>Measuring Range(+/-g): For low impedance sensors, selection should be such that the expected peak values of acceleration are within the measuring range. If the magnitude of the measuring range is not precisely known, a ± 500 g accelerometer may be used to establish the measurement scale. Then an accelerometer with the applicable range can be selected. Alternatively, it is possible to use a high impedance (charge mode) accelerometer with a charge amplifier to resolve vibration amplitudes over several decades of g levels.</p> |
| <p>Acceleration Sensitivity(mV/g): The sensitivities listed in catalogs are nominal values. A calibration certificate containing the exact value is provided with each sensor. Since the available full scale voltage is ± 5 volts, the sensitivity can be determined by dividing the expected acceleration range into the full scale voltage. For example, a ± 50 g range indicates a sensitivity of 100mV/ g.</p> |
| <p>Operating Temperature(OC): High impedance sensors can be used up to 250°C without problems. Due to the limitations of internal electronics, low impedance accelerometers are operable up to 165°C as a maximum.</p> |
| <p>Ground Isolation: If current loop problems are likely to occur, ground isolated accelerometers are recommended. For example, the ignition of a car engine often causes such problems. This condition can be prevented by selecting a ground isolated unit or installing an adhesive mounting pad under the accelerometer.</p> |
| <p>Addition of Mass: Adding mass (such as an accelerometer) to a vibrating structure can alter the frequency of the vibration. This is sometimes referred to as "mass loading". As a general rule, the mass of the sensor (and mounting accessories) should not exceed 10% of the mass of the vibrating structure.</p> |

Moreover, MK-500 manual describes the three kinds of vibration- detecting sensors and it can be depicted by the diagram shown below:

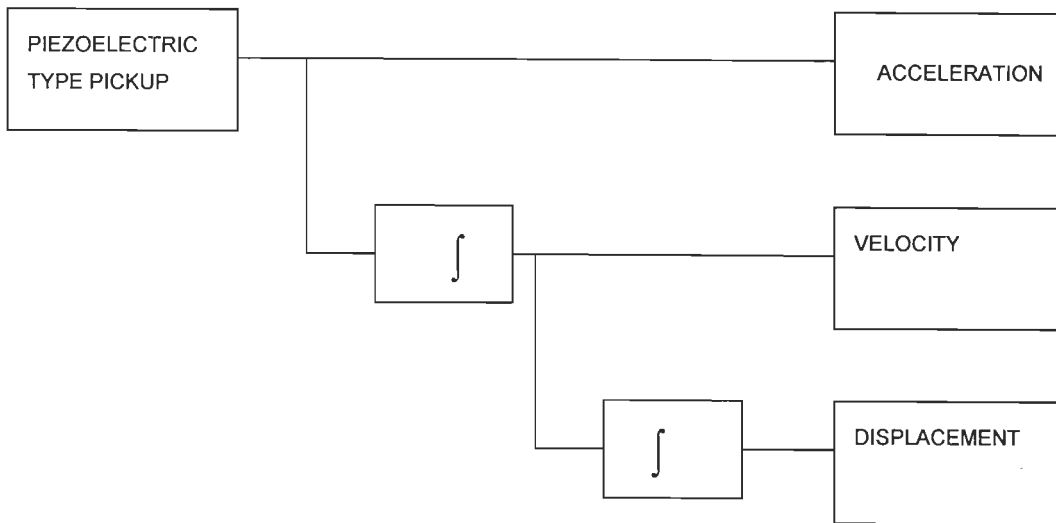


Figure 2.6: Main measurement considered for vibration monitoring

Acceleration, velocity and displacement have been the ways of monitoring the vibration signals. Papers suggest for machines producing less vibration velocity is in rampant use but as the machine gets larger and the severity level of vibration increases than acceleration is the ultimate choice. Another added advantage mentioned in the literature is that mathematicians vouch for integration rather than differentiating the signal and hence the velocity and displacement can easily be attained by the acceleration signal by a simple integration. Also, shock impacts can only be attained by an accelerometer because of the higher and broad useable frequency ranges.

This research work succumbs to the piezoelectric accelerometer which is connected to MK-500 Analyzer. The details of this PU-601R are fully described in Appendix (A-1) and the advantage of this instrument was that it takes care of all the above variables.

Principle of operation of Accelerometer

The piezoelectric accelerometer is based on a property exhibited by certain crystals where a voltage is generated across the crystal when stressed. This property is also the basis for such familiar sensors as crystal phonograph cartridges and crystal microphones. For accelerometers, the principle is

shown in Figure 2.7. Here, a piezoelectric crystal is spring-loaded with a test mass in contact with the crystal. When exposed to an acceleration, the test mass stresses the crystal by a force ($F = ma$), resulting in a voltage generated across the crystal. A measure of this voltage is then a measure of the acceleration. The crystal per se is a very high-impedance source, and thus requires a high-input impedance, low-noise detector. Output levels are typically in the millivolt range. The natural frequency of these devices may exceed 5 kHz, so that they can be used for vibration and shock measurements.

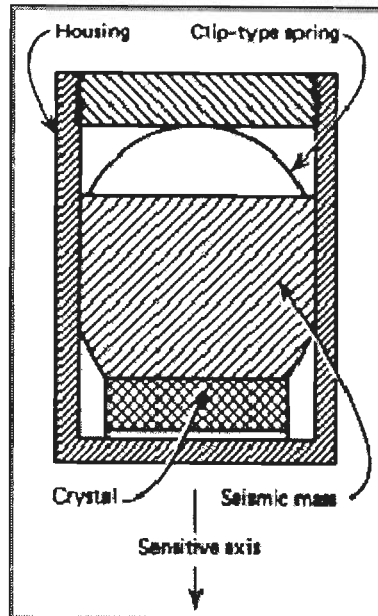


Figure 2.7: A piezoelectric accelerometer

2.3.2 Current Clamps-(Current)

I400s AC current clamp is a current transformer for checking the loading of the machine. The core of the transformer can be split with the help of a trigger switch and therefore core can be clamped around a live conductor to measure the current without breaking the circuit. The current passing through a conductor produces a magnetic field around it, according to Faraday's law this varying magnetic flux is cut by the secondary winding which is on the core. Due to this action there is the voltage across the secondary winding which is in the order of 1 or 10mV/A. By using this sensor we can measure the range of current between 40-400A. Details of this sensor are clearly mentioned in Appendix (A-2). The output of the sensor is connected directly to the BNC 2120 as an analog input.

2.3.3 Potential Transducers- (Voltages)

A simple potential transformer is used as a voltage transducer .It consists of iron core with two sets of isolated windings. The first winding is the primary winding which is connected between two phases of the machine while the second is connected to the monitoring system .The PT provides 4 Volts at the output for 440 Volt sinusoidal inputs. This was developed by S.A.Kazzaz [129]. The outputs are fed to BNC2120.

2.3.4 Speed -(Tachometer)

The speed was monitored by a tachometer. The speed was maintained at the rated value of the machine. Researchers have had a controversy that whether speed has an effect on faults diagnosis of rotating electrical machines.

Note: The focus of this work is the vibration parameter. The rest of the parameters were vital to maintain the machine on its rated speed and loading conditions were also considered. Four load conditions were taken into consideration, the no load, slight load, half load and three quarter load. This led to a complete test of the machine and the behavioural patterns as well as the signatures were established.

2.4 Signal Conditioning Unit

The term signal conditioning unit is unanimous in Digital Signal Processing. Different transducers acquire different nature of data which might have

- a) low signal intensity
- b) very high signal intensity
- c) noise riding on the signal
- d) controlling the resolution is the greatest issue when acquiring the data for faults in electrical machines
- e) multiplexing becomes important when two or more signals are required and
- f) the most important fact is direct signals from transducers cannot be fed to the PC.

Researchers have been using either micro processors or the PC for DAQ and the analog inputs require signals with a maximum of 5V or else destroy the gadget. These analog signals need to be broken down to a digital signal for the PC to recognize it and is reconstructed back to attain its originality. The process is shown below:

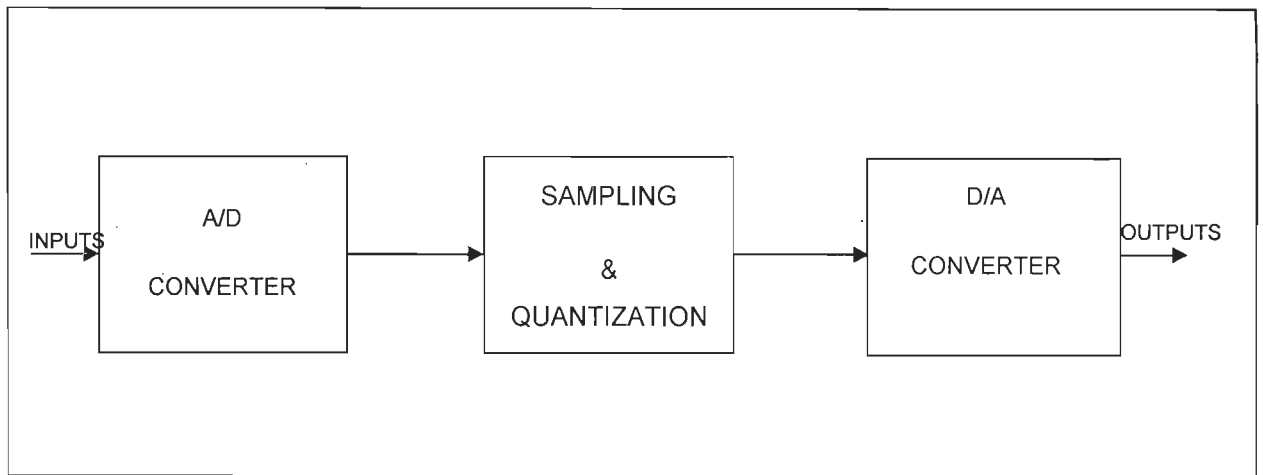


Figure 2.8: Signal Processing

The individual analog signals are first amplified to the required level and are fed to analog to digital converter. This meticulously breaks the signal using the sampling theorem and quantizes the signal to make it digital. They are then processed by the PC and ideally should be reconstructed back to attain its originality by the digital to analog converter. In this research work the Labview program that stores the data in an EXCEL file is in the discrete form which makes the analysis part easier and accurate. This means the de-quantized signal has been retrieved by attaining discrete values and the final original signals is carried out by the MATLAB, EXCEL or Labview software.

The three elements used for signal conditioning unit are as follows:

- a) MK-500
- b) BNC-2120
- c) NI-6024E

Contd.....

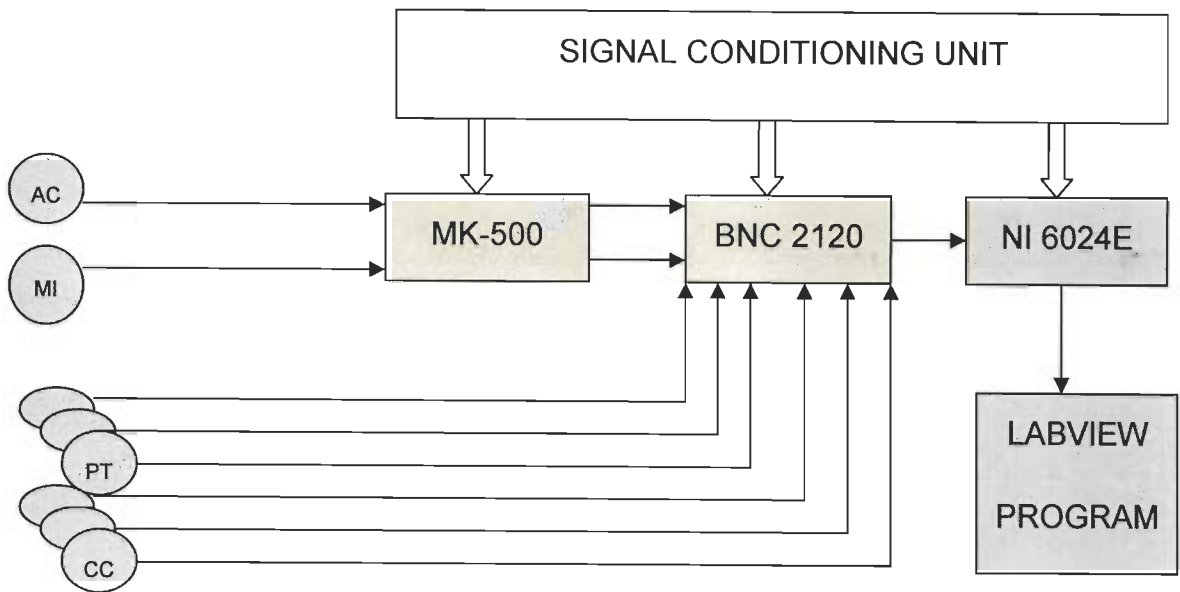


Figure 2.9: Signal conditioning unit

The above defines the elements used in the experimental SCU setup. The transducers input of acceleration and microphone are fed to the MK-500 to amplify and filter it to the required level after which it is fed to the BNC2120. Meanwhile, the three current clamps and potential transformer output are inserted into the BNC 2120. These signals are multiplexed and thus proceed to the NI 6024E card that converts this multiplexed signal from analog to digital form for the PC to understand. To access these signals the Labview program is used and data is retrieved in a discrete form.

2.4.1 MK-500

The MK-500 has a 12 bit /word ADC card which is a signal conditioning unit for vibration signal acquired from the Accelerometer. This has the facility of setting the signal, mode, range, frequency, filters (i.e. both HPF and LPF), rotor speed, data length, and average. The noise is filtered from the vibration signal.

A combination of frequency and data length yields the resolution of the signal strength of the machine (i.e. if the signal strength is low than a lower range is chosen or vice versa). The data is transferred to a BNC-2120 through a standard built in RS -232 interface. This Analyzer has the ability of

- a) Automatic Diagnosis
- b) Manual Diagnosis

This research work considers the latter since the resolution and combination of other settings were easily achieved. The settings of the MK-500 are given in Table 2.2 that finally yields a 0.625 Hz resolution.

Machine Analyzer MK-500 (Kwatetsu Advantech)

Normal Measurement Mode:

Table 2.2: Settings of the MK-500.

| | | | |
|------------|--------------|--------------|-------------|
| Signal: | Vibration | HPF: | 5 Hz |
| Mode: | Acceleration | LPF: | 40 KHz |
| Range: | 0.5g | Rotor Speed: | 1440 rpm |
| Frequency: | 500Hz | Data Length: | 2 Kilo word |
| Filter: | ON | Average: | 1 |

2.4.2 BNC-2120

The National Instrument Manual [Appendix A-3] defines the BNC-2120 is a desktop or DIN rail-mountable accessory you can connect directly to E Series devices (like NI 6024 E). The BNC-2120 has the following features:

- Eight BNC connectors for analog input (AI) connection with an optional thermocouple connector, an optional temperature reference and optional. resistor measurement screw terminals
- Two BNC connectors for analog output (AO) connection
- Screw terminals for digital input/output (DIO) connection with state indicators
- Two user-defined BNC connectors
- A function generator with a frequency-adjustable, TTL-compatible square wave, and a frequency- and amplitude-adjustable sine wave or triangle wave
- A quadrature encoder

2.4.3 NI-6024E

The 6023, 6024, and 6025 E Series boards are high-performance multifunction analog, digital, and timing I/O boards for PCI, PXI, PCMCIA, and Compact PCI bus computers. Supported functions include analog input, analog output, digital I/O, and timing I/O. The 6024E features 16 channels of analog input, two channels of analog output, a 68 –

pin connector and eight lines of digital I/O. It is a 12 bit analog to digital converter (ADC) resolution.

NI-DAQ refers to the NI-DAQ driver software for PC compatible computers unless otherwise noted. PXI, PXI stands for PCI extensions for Instrumentation. PXI is an open specification that builds off the Compact PCI specification by adding instrumentation-specific features.

2.5 PC LabVIEW Program

The PC Labview program is used to interface the signal conditioning unit and the end user. Data is acquired and stored in a user friendly manner, which is the discrete data, from where further analysis proceeds. LABORatory Virtual Instrumentation Engineering Workbench (LabVIEW) is a platform and development environment for a visual programming language from National Instruments. Each VI has three components: a block diagram, a front panel and a connector pane.

The server VI is divided into 3 Blocks:

- a) Data-Acquisition Block
- b) Output Generation Block
- c) Excelsheet Creation Block

The final Labview settings having a resolution 0.625 Hz had a Scan rate 0f 1280Hz and buffer size of 1280Hz with a Data length 50000 for two sets of bearings.

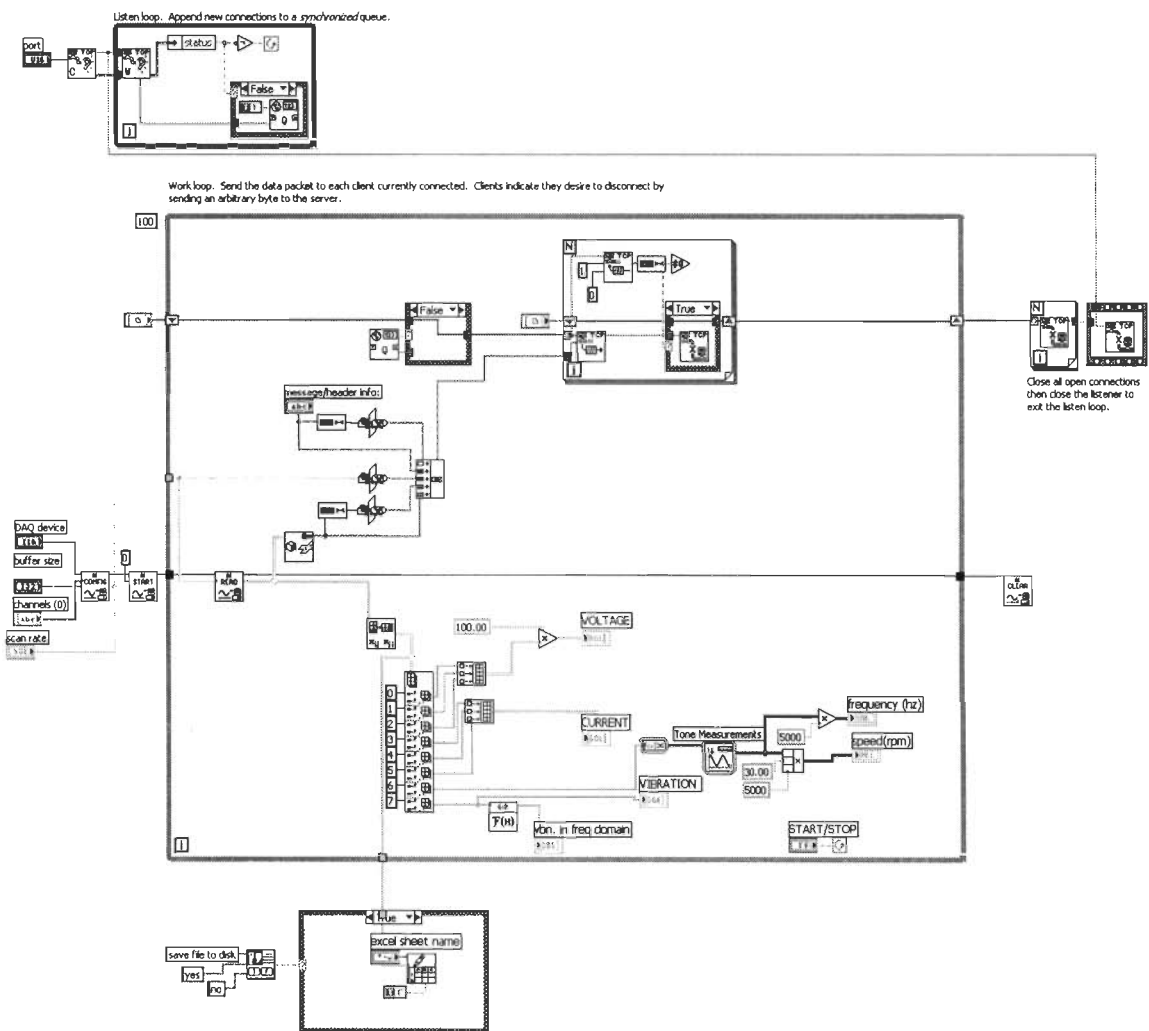
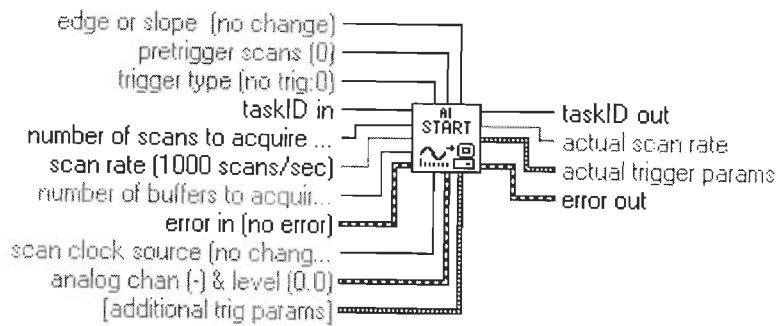


Figure 2.12: Labview PC program for DAQ

2.5.1 Data-Acquisition Block

The first block of this VI reads the DAQ device and configures it by taking the scan rate, buffer size and the number of channels used as input. This is done using the *AI (Analog Input) Config* and *AI Start* tools. We specify the port through which the DAQ card reads instantaneous samples.

AI START: starts a buffered analog input operation. This VI sets the scan rate, the number of scans to acquire, and the trigger conditions. The VI then starts an acquisition. Refer to *AI Start* for more information about this VI.

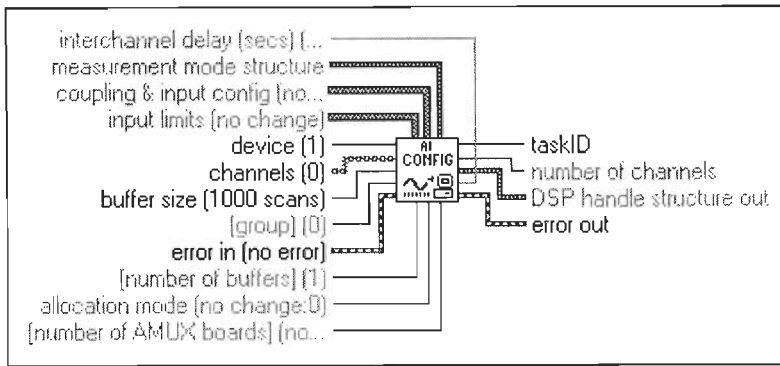


Number of Scans to Acquire: It is the total number of scans LabVIEW acquires before the acquisition completes. A scan is one point per channel. When the default input is -1, LabVIEW acquires exactly one buffer of data. The *buffer size* input to the AI Config VI determines the size of the buffer. The number of *total scans* includes any pre trigger scans requested. If you set *number of scans to acquire* to 0, LabVIEW acquires data indefinitely into the first (or only) buffer until you clear the acquisition with the AI Clear VI. In this case, the VI ignores the *pre trigger scans* input.

Scan rate: It is the number of scans/s to acquire. This is equivalent to the *sampling rate per channel*. The default for this VI is an input of 1000 scans/s. An input of -1 leaves the clock frequency unspecified. Use a rate of -1 when the clock frequency is not programmable on the device (i.e. for 43XX and 40XX series devices the rate is not independently programmable, but is determined by the notch frequency selection and the number of channels scanned). If you enter zero as the scan rate, LabVIEW disables the internal clock and allows you to use an external clock. Refer to the description of the AI Clock Config VI for more options with alternate clock sources.

taskID in identifies the group and the I/O operation.

AI Config : Configures an analog input operation for a specified set of channels. This VI configures the hardware and allocates a buffer for a buffered analog input operation. Refer to AI Config for more information about this VI.



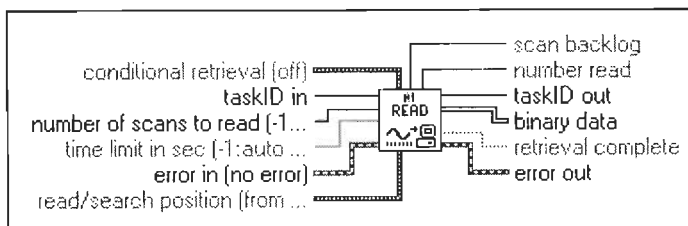
Channels : It specifies the set of analog input channels. The order of the channels in the scan list defines the order in which the channels are scanned during an acquisition. *channels* is an array of strings. You can use one channel entry per element or specify the entire scan list in a single element, or use any combination of these two methods. If x, y, and z refer to channels, you can specify a list of channels in a single element by separating the individual channels by commas, for example, x,y,z. If x refers to the first channel in a consecutive channel range and y refers to the last channel, you can specify the range by separating the first and last channels by a colon, for example, x:y.

Buffer size: It is the number of scans you want each buffer to hold. The default for this VI is an input of 1000 scans.

Device: It is the device number you assigned to the DAQ device during configuration.

AI Read:

It reads data from a buffered data acquisition. The AI Read VI calls the AI Buffer Read VI to read data from a buffered analog input acquisition. AI Read is a polymorphic VI that you can configure to output the following kinds of data:



Scaled Data:

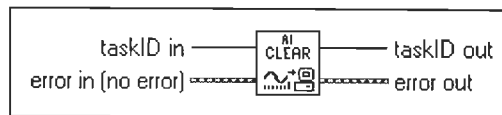
It is a 2D array that contains analog input data scaled to scaled data units. The data appears in columns, where each column contains the data for a single channel. The second (bottom) dimension selects which channel column. The first (top) dimension selects a single data point for that channel. The array must be transposed before graphing.

Number of Scans to Read

It is the number of scans the VI is to retrieve from the acquisition buffer. The default input is -1, which tells LabVIEW to set number of scans to read equal to the value of the number of scans to acquire control when the *AI Start* was called. If number of *scans to read* is -1 and *number of scans to acquire* is 0, LabVIEW sets *number of scans to read* to 100.

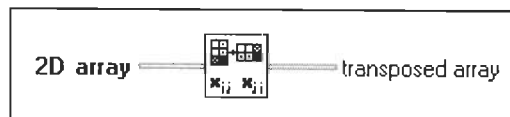
AI Clear

Clears the analog input task associated with **taskID in**.



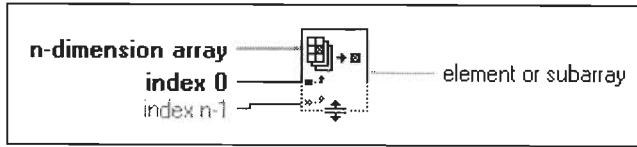
2.5.2 Output Generation Block

Transpose 2D Array: Rearranges the elements of 2D array such that 2D array $[i,j]$ becomes transposed array $[j,i]$. The connector pane displays the default data types for this polymorphic function.



2D array can be a 2D array of any type transposed array is the output array.

Index Array: Returns the element or subarray of n-dimension array at index. When you wire an array to this function, the function resizes automatically to display index inputs for each dimension in the array you wire to n-dimension array. You also can add additional element or subarray terminals by resizing the function. The connector pane displays the default data types for this polymorphic function.

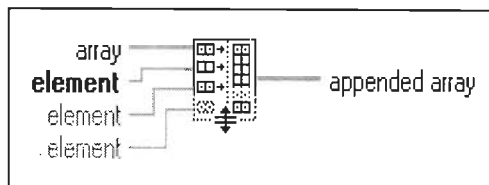


Element or subarray : It has the same type as the elements of n-dimension array. Rather than extracting an element of the array, you can extract a subarray of the array by leaving one or more of the index terminals unwired. For example, extract column 1 of a 2D array by specifying 1 in the column index and leaving the row index unwired.

If you index a 1D array and do not wire an input index terminal, this function extracts the first element of the array. If you grow the node and have more than one element or subarray output, this function extracts the first number of elements equal to the number of element or subarray outputs.

n-dimension array :It can be an n-dimensional array of any type. If n-dimension array is an empty array, the value of element or sub-array is the default of the data type of array (zero for numbers, FALSE for Boolean controls, and empty for string).

Build Array :



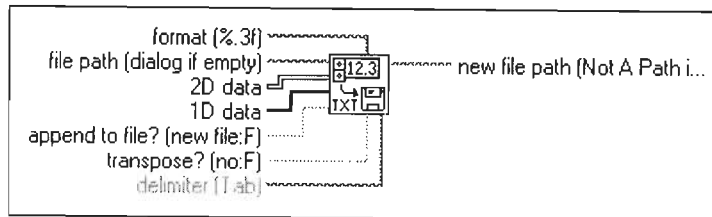
It concatenates multiple arrays or appends elements to an n-dimensional array. The connector pane displays the default data types for this polymorphic function Array or element can be any n-dimensional array or scalar element. All inputs must be either elements or 1D arrays or n-dimensional and (n-1)-dimensional arrays. All inputs must have the same base type. Build Array operates in one of two modes depending on whether you select the Concatenate Inputs option. If you select the Concatenate Inputs option, the function appends all inputs in order, forming an output array of the same dimensionality as the highest-dimension array input wired. If you do not select the **Concatenate Inputs** option, the function builds an output array of one dimension higher than the dimension of the inputs. The inputs must all be the same dimensionality.

2.5.3 Excel sheet Creation Block

This block allows the user to save instantaneous data samples in the form of an excel sheet for later use and analysis. The number of samples depends on the sampling rate which is input in the data acquisition block. The samples from all the eight channels are stored column wise in the sheet. When the VI is run, it asks the user whether he wants to save the data and the user can choose.

Write To Spreadsheet File:

Converts 2D or 1D array of single-precision numbers to a text string and writes the string to a new byte stream file or appends the string to an existing file. You also can transpose the data. The VI opens or creates the file before writing to it and closes it afterwards. You can use this VI to create a text file readable by most spreadsheet applications. This VI calls the Array to Spreadsheet String function to convert the data.



Format: specifies how to convert the characters to numbers. The default is `%.3f`.

File path: is the path name of the file. If file path is empty (default) or is Not A Path, the VI displays a dialog box from which you can select a file. Error 43 occurs if you cancel the dialog box.

Append to file? indicate whether to append the data to an existing file. If TRUE, the VI appends data to an existing file. If FALSE, the VI replaces data in an existing file. If there is no existing file, the VI ignores the value of *append to file?* and creates a new file.

2D data contains the single-precision numbers the VI writes to the file if *1D data* is not wired or is empty

2.6 Final Diagram of the DAQ System Used

The schematic diagram of the Fault Detection is shown in Figure 2.13 and Figure 2.14

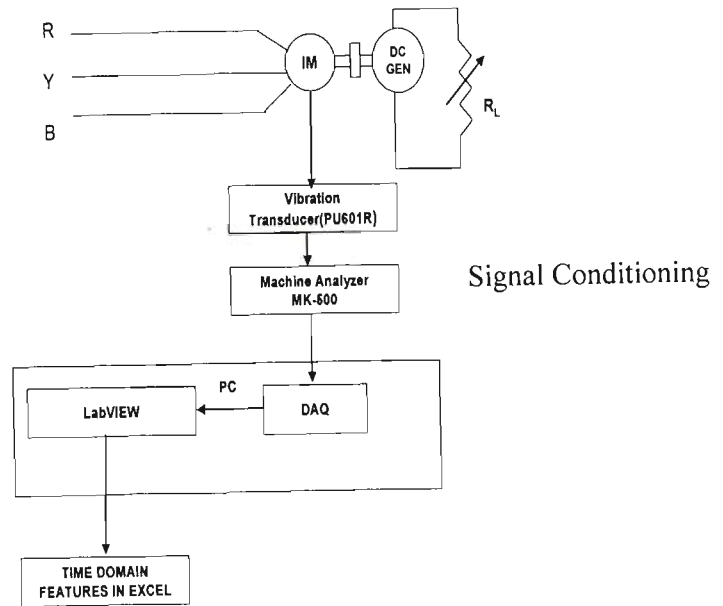


Figure 2.13 Final Diagram of the DAQ System Used

The present work is carried on three types of NBC 6308 bearings that are (a) healthy, (b) with an outer race fault, and (c) with an inner race fault. The faults were introduced and created by National Engineering Industries Limited (NEI), Jaipur, India, a manufacturer of bearings. Several runs were executed on a 7.5-kW induction machine with bearings of each type. The rating of the induction machine is specified in Table 2.1. This motor is coupled to a DC generator for four cases of loading that is no load, slight load, half load and three quarter load. The data from the above machine is obtained for localized or a single point defect. The experimental setup involves the acquiring of the vibration signal from vibration pickup PU-601R which is an analog signal fed into MK-500 machine analyzer of Kawatetsu Advantech make. A resolution of 0.625 Hz was obtained. This data is processed with sampling frequency $f_s = 1280\text{Hz}$ which is then interfaced to the PC using the NI-6024E DAQ card. The 12-bit DAQ card converts the data into a digital form and this is recognized by the PC using the Labview software stored as a discrete data in an Excel file. The Labview program has settings as in Table 3.2 to maintain a 0.625-Hz resolution and this data is reconstructed to obtain the original discrete analog signal on which analysis is executed. The data flow transmits via the National Instrument DAQ card (6024E) to the PC. This is finally accessed using the Labview

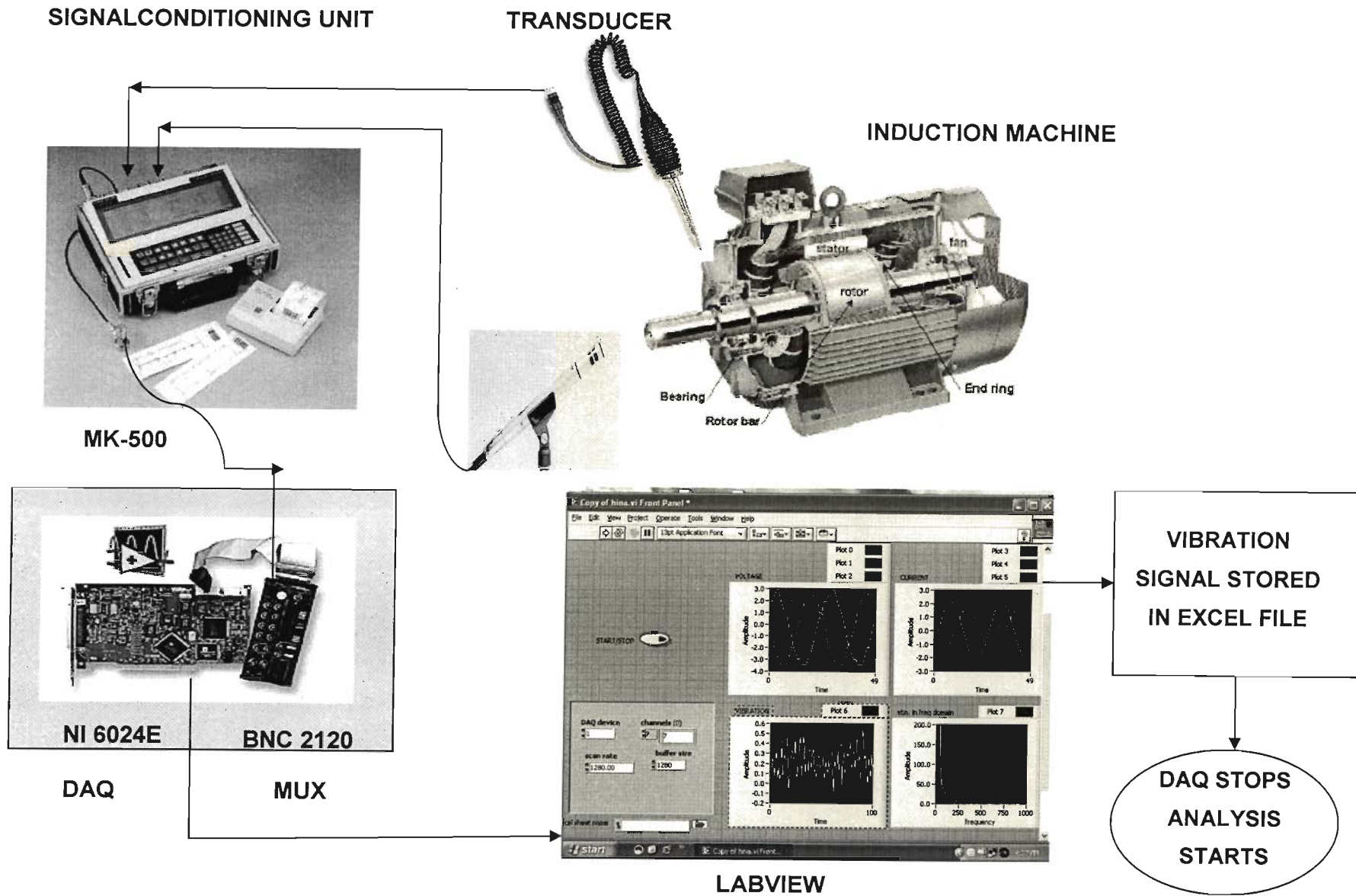


Figure 2.14 Condition Monitoring methodology at a glance

and the settings provided after which the data was transferred in the EXCEL file for further analysis.

2.7 Conclusions

The process of data acquisition from rotating machine to the PC is described in this chapter with details of transducer, signal conditioning and processing.

Analysis Techniques

This chapter discusses different methods for FDEM, reference to analysis techniques, and the analysis technique used in present work.

3.1 Introduction

This introduces the analysis techniques existing for FDEM and why vibration is a powerful tool. The advantage of using acceleration over velocity and displacement is highlighted. The different methods that can be applied is mentioned. The major measurement technology according to [16] can be stated as:

1. Vibration
2. Lubricant Analysis
3. Thermography
4. Ultrasonics
5. Acoustic Emission
6. High Frequency vibration

The most versatile way to fault diagnostic of electrical machines is the vibration approach which has been used in this work. Firstly, the raw time signal has been shown and is further supported by the statistical technique which involves both descriptive and inferential statistics. A further study of the frequency domain signal is taken under consideration whereby the FFT is evaluated for a rectangular window. One of the reasons that vibration data is collected on the bearing housing is that all the forcing frequencies are transmitted through the bearings from the rotating element. These same forces are also at work degrading the life of the bearing. This degradation will manifest itself in four ways as BCF. The results obtained by this approach can be referred to as in chapters 4, 5, 6 and 7.

3.2 Drawback from Literature Review Techniques

An intensive literature review reveals that numerous analysis techniques have been used to extract features but mentions their own merits and demerits of each technique. This throws

light to why this research work has considered statistics as a merge and a supportive tool in FDEM? This section will be divided into the signal processing techniques as time, frequency, time frequency and finally the other techniques. A lot of paradoxes exist in the literature review of signal processing techniques.

3.2.1 Time Domain Technique

B. Samanta and K. R. Al-Balushi [13] uses the features of time signals as inputs to the ANN and concludes that the ANN-based approach has its inherent shortcomings, that the ANN needs to be trained for each machine condition: normal and defective with different fault types and severity levels. Another limitation of the ANN-based approach is that the numerical values and the ANN structure would not probably be optimal for another machine. Bo Li et al [12] suggest in the future, incorporating the time domain signal, specifically the presence of peak amplitudes, the severity of the defect should be ascertainable. C. Wang and J. C. S. Lai [24] the overall vibration behaviour are analyzed, but concludes, that despite these simplifications, results obtained under these conditions are within 10% of the values determined from the experimental modal testing.

3.2.2 Statistical Techniques

D. Dyer, and R.M. Stewart [28] implements statistical kurtosis, and observes, that it remains constant for an undamaged bearing irrespective of load and speed, yet changes with damage and further summarizes that the technique is applicable to all types of rolling element bearings but faced problems in interpreting the results from split bearings and from those in close proximity to cavitation. D. Stegemann [26] categorizes modern techniques into *a)* statistical time values *b)* spectral functions and *c)* cepstral values and finally concludes, that the prove and applicability and reliability of the vibration monitoring system for failure root cause analysis and process optimization is dependent on certain operation condition. J. Ilonen et al [59] studies the discriminative energy functions which reveal discriminative frequency-domain regions, where failures can be identified and concludes, that the method also lacks generality due to its Gaussianity assumption, but it still succeeds in many practical situations. The Gaussianity limitation can be overcome by the proposed extensions using Gaussian mixture models, and the Kullback–Leibler divergence and suggests that these improvements will be studied in the future versions of the tool. J. Antoni and R.B. Randall [58] shows how the Spectral Kurtosis SK can be efficiently used and concludes that SK offers the rather unique opportunity to find out which frequency band should be processed and further refutes

the common belief that envelope analysis must rely on expertise. P. Loughlin and F. Cakrak [105] uses the conditional moments, for a simple physical interpretation, namely, they are the mean, median and mode frequencies at a given time, and the spread about the mean frequency at a given time (the 'instantaneous spectral bandwidth'). They characterize the faults well, and can differentiate between different fault classes. Finally, it concludes that these statistics can be computed in real time, distinguishes between different fault conditions, and provide a clear physical description of the process. Consequently, they are simple and effective features for on-line monitoring and diagnosis of developing faults, and they contribute to our understanding of transient development and propagation. P.K. Dunn [104] implements three tools that cover the areas of the central limit theorem, the normal approximation to the binomial, and the bivariate normal distribution. P.Forster and C.L.Nikias [103] a new array processing method is presented for bearing estimation, based on the cross bispectrum of the array output data, and concludes, that when additive noise, is spatially correlated Gaussian, the bispectrum based method can yield better bearing estimates than the stochastic maximum likelihood, with known cross spectral matrix, provided, the source skewness is large enough. P. Vlok et al [107] illustrated how statistical Residual Life Estimates (RLE) of bearings can be used to justify maintenance practices, and concludes, that while using RLE as a benchmarking tool one should introduce procedures of monitoring process changes that could impact additionally measured covariates. R.B.W. Heng and M.J.M. Nor [114] present a study on the application of sound pressure and vibration signals to detect the presence of defects in a rolling element bearing, using a statistical analysis method. The well established statistical parameter such as the crest factor and the distribution of moments, including kurtosis and skew, are utilized in the study, and concludes, that the first study reveals, that the statistical parameters calculated from the results are affected by the shaft speed. This is contrary to the findings of other researchers. Secondly, it highlights, that this study also reveals, that there are no significant advantages in using the beta function statistical parameters, compared to using kurtosis and crest factor, for detecting and identifying defects in rolling element bearings. S.Seker and E. Ayaz [137] studies statistical behavior of vibration test data—acquired from seven accelerated aging processes undertaken for a three-phase, 5 HP, squirrel-cage induction motor—is examined, and concludes, that it is found, that statistical examination of vibration measurements related to each aging cycle has a Gaussian distribution. The second moment, also termed “standard deviation,” appears to be the most dominant parameter employed throughout the analysis. S. Thanagasundram and F.S. Schlindwein [138] concludes that, results obtained with the AR

method for fault classification purposes were conclusive, showing that the system is able to identify and classify defective bearings for a set of used experimental data. T. Williams et al [143] uses vibration metrics such as: root mean square, peak value, kurtosis and crest factor and are recorded through the test duration, from accelerometers and acoustic emission sensors, and concludes, that the new system is capable of providing 'real' crack information. T.W.S Chow and G. Fei [145] uses Bispectrum analysis and concludes, that results indicated bispectrum magnitude of the dominant component, caused by the machine rotation, increased with the increase in the level of asymmetrical fault. But the bispectrum magnitudes of harmonic components were diminished due to the decrease in m.m.f when the level of the asymmetrical fault increased. W.J.Wang et al [151] reports on the application of nonlinear dynamics and higher-order spectra, with particular regard to the correlation dimension and bispectra and concludes, that although the methods of correlation dimension are valuable in the understanding of nonlinear systems, they do not present detailed information about nonlinear mode coupling on a frequency by frequency basis. Such frequency domain information is necessary in order to classify different faults. Moreover, the Gaussian noise contained in the signals can be suppressed in the bispectra. Therefore, a combination of correlation dimension and higher-order spectra offers a good description of a nonlinear system. W.J.Wang et al [152] gear tooth damage detection is conducted using the beta kurtosis and the continuous wavelet transform, based on the overall residual signal. The beta kurtosis of original signal average is also shown here to be useful in detecting excessive gear run-out. Test results from printing presses demonstrated the viability of the proposed methods, and conclude that more tests are currently being conducted to apply the proposed techniques to other machines where the rotation synchronization on different stages is required. W.Reimche et al [154] basics of comprehensive vibration using statistical time values for general signal description and threshold comparison, envelope analysis and spectrum, phase and correlation analysis of multi sensor arrangements are approached. Hints are also given to data reduction using cepstral and coherence analysis in combination with the extraction of machine or fault specific characteristic patterns as input values of vector or neural classification. Y.Choi and Y.Kim [157] proposed method is 'minimum variance cepstrum' because it minimizes the variance of the signal power in its cepstrum representation, and discusses in the results, that the proposed signal processing method is able to detect a periodic pulse signal as early as possible. It is independent of the level of noise as the theory proved and also as the experiment demonstrated.

3.2.3 FFT Technique

A. Stavrou et al [6] says that some of the specified frequency components were redundant, but whether or not this would be the case for other machines and for the same harmonics requires further investigation. A. Siddique et al [9] clearly distinguish the relevant frequency components from other components due to time harmonics, machine saturation, etc. C. K. Mechefske [18] based largely on the FFT frequency spectra; do not effectively accomplish these tasks when applied to low speed rotating machinery and concludes that the AR model based procedure has been shown to accomplish this task and the future work will evaluate the procedure when using signals that represent gradual deterioration in bearings. H. Ocak and K.A. Loparo [48] presents two separate algorithms, for estimating the running speed and the bearing key frequencies of an induction motor using vibration data, and concludes, that the magnitude of the peak increases as the fault diameter increases. This only applies in the early stages of a fault. In more advanced stages of bearing failure, the magnitudes of the spectrum at the defect frequencies often reduce to normal like levels. J P Dron et al [57] presents parametric spectrum analysis using high resolution technique. However, the complexity of these techniques necessitates many precautions when they are implemented; consequently, they should not replace conventional methods, but supplement them. J. Pineyro et al [61] deals with second order power spectral density and states one of the main drawbacks is the amount of memory needed during data processing. J. R. Stack et al [62] AM detector is computed, which only requires knowledge of the bearings characteristic fault frequencies. This method does not require training from various faulted bearings, nor does it require baseline data from the machine being monitored. J. R. Stack et al [63] examines machine-vibration spectra for peaks with phase-coupled sidebands, occurring at a spacing predicted by the model and discusses in the experimental results that a major difficulty is to quantify how challenging it should be to detect a given artificially seeded defect. J. R. Stack et al [66] as bearing health degrades, the modeled spectrum deviates from its baseline value; the mean spectral deviation is then used as the fault index and in the results discusses that as the load level of the machine increases, the magnitude of the fundamental and its harmonics increase drastically. However, the magnitudes of the various bearing fault signatures do not change significantly with load. This phenomenon adds difficulty to the process of current-based bearing condition monitoring. M. Bodruzzaman et al [83] mentions that when the frequencies of interest are closely spaced, the Fourier Transform spectrum analysis fails to resolve these frequencies and hence High resolution frequency estimation approach such as Forward –

Backward Linear Prediction (FBLP) method is adopted to identify all the prominent frequencies in a certain bandwidth. M.E.H.Benbouzid et al [84] used the FFT, and concludes, that the stator current high resolution spectral analysis, proposed as a medium for induction motor fault detection, has definite advantages over the traditionally, used FFT spectral analysis. M.E.H.Benbouzid et al [86] applies MCSA and concludes that Extensive experimental studies are necessary to fully assess usefulness of the proposed technique. P. D. McFadden and J. D. Smith [102] concludes, that the frequencies of components from defects are independent of position, but that the phase angles of these components are related to the position of the defect, and the frequency of the component. R.R.Schoen [120] correlates the relationship between vibration and current frequencies, caused by incipient bearing failures, but concludes, that the test results clearly illustrate that the stator current signature can be used to identify the presence of bearing fault. S.A. McNerny, and Y.Dai [127] develop a laboratory module but concludes, that after reviewing the basic operation of rolling element bearings and the characteristics of idealized bearing fault vibration signatures, the shortcomings of conventional spectral analysis were illustrated with a synthetic signal generated in MATLAB. The basis and effectiveness of envelope analysis for bearing fault analysis were then examined. S. M.A.Cruz [130] describes the use of multiple reference frames for the diagnosis of stator, rotor, and eccentricity faults, in line-fed and Direct Torque Controlled (DTC), inverter-fed induction motors, but concludes, that the proposed method avoids the burden of computation of FFT's, which require intensive computation resources and long sampling periods, necessary to obtain a good spectral resolution. S. A. Ansari et al [126] a PC-based vibration analyzer was developed, and this computes frequency spectra, root mean square amplitude, and other peak parameters of interest, and further discusses, that the probable cause of excessive vibration is the bearing defect, since the bearing noise gives rise to a wide range of vibration frequencies-each bearing component velocity producing individual characteristic frequency. S. Nandi et al [131] suggests that all the low and high frequency harmonics expected to be present in a mixed eccentric machine, but concludes, that the effects of saturation and slot effects on eccentricity related current harmonic components, are yet to be studied.

3.2.4 STFT Technique

R.B. Randall [124] STFT with WA for the time/frequency decomposition, and for determining the optimum combination of centre frequency and bandwidth for maximizing the Spectral Kurtosis (SK) and concludes, that the original definition of the SK uses the STFT for

the time/frequency decomposition, but also mentions the use of wavelets as an alternative, also for the equivalent of the kurtogram. W.J.Wang and P.D.McFadden [150] applies the spectrogram to the calculation of the time frequency distribution, of a gear vibration signal is examined, and concludes, that the spectrogram has advantages over the Wigner –Ville distribution (WVD), for the analysis of the vibration signals, and further states, that the spectrogram gives a clear one- to- one time frequency distribution of the energy in the signal due to the damage, and also provides a high sensitivity to changes of short duration in the signal.

3.2.5 Wavelet Transform Technique

A. Sedighi et al [5] combines wavelet transform and statistical technique as a fault detector discusses that a larger set of data for High Impedance Fault (HIF) tests could not be obtained from the real network. B. Liu et al [10] employs matching pursuit with time –frequency atoms to and concludes that since the signature obtained this way contained less unrelated components to the defects than traditional band pass filtering, thus it had a higher signal to noise ratio and gave more explicit information for the failure detection. Brian T [14] suggests in its future work that focus on developing advanced and efficient signal processing techniques using wavelet transformation and neural-fuzzy networks to relate signal features to specific bearing faults. C. K. Mechefske and J. Mathew [18] further investigate the sensitivity and robustness of the presented wavelet customization technique for the condition monitoring of other types of machine structures and systems.

C. Li et al [19] describes WPT-RST and suggests that it offers an alternative approach for the fault detection of bearing. Further more, it attains nearly the same accuracy, compared with Artificial Neural Network. F. Wan [34] investigates using Harmonic Wavelet Transform (HWT). Three non-linear factors, non-linear oil film forces, rotor–stator rubbing and the presence of crack, are taken into account, and concludes firstly, that HWT may be a feasible and efficient technique to analyze a multi-non-linear factors rotor. Secondly, the effect of the bearings oil film force on system is significant and should be considered adequately. Thirdly, the effect of multi-non-linear factors is coupling and must be considered simultaneously. It is necessary to consider each vital factor and set up a reasonable non-linear dynamic model. Then, detection and diagnosis of rotor bearing system can be performed accurately. G.K. Singh and S. A. S. Ahmed [42] concludes, that WT can be used effectively to specify one-machine fault at a time, while it cannot treat multiple faults simultaneously. However, the use

of wavelet and FT together, can provide an effective tool for extracting important information about the machine's condition. G.G. Yen, and K.Lin [37] investigates the feasibility of applying the WPT to the classification of vibration signals and concludes, that although the wavelet packet node energy provided us with a multiresolution view of a signal, it simultaneously introduced a higher dimension space, compared to the original time-domain signal. To reduce the dimensionality, it was shown that LDA had some practical problems when the feature dimension was relatively high, compared to the number of collected samples, since it involved calculation of the inverse of the covariance matrix. H. Zhengjia et al [53] uses Signal decomposition via wavelet transform and wavelet packet, provide an effective approach of multiresolution analysis and suggests that Multiresolution signal decomposition, in tandem, with autoregressive spectrum, energy monitoring, fractal dimension analysis, etc., can provide desirable results from the independent frequency bands. H. Yang [52] presents an application of this new basis pursuit method and the results obtained using this new technique were compared with Discrete Wavelet Packet Analysis (DWPA) and the Matching Pursuit Technique, and concludes, that the limitation of basis pursuit is that, its computation, tends to take longer in comparison with DWPA and matching pursuit, using the same length of data. However, this disadvantage is offset by the fact that basis pursuit can use shorter data lengths than the other techniques. I. S. Cade et al [56] uses wavelet analysis, and concludes, wavelet coefficients will only be nonzero during the transient response. In the case of rotor/bearing contact, it has been shown that nonzero coefficients will also be present only during the transient response. J.Zarei, and J.Poshtan [70] uses Meyer wavelet, in the wavelet packet structure, with energy comparison as the fault index. The advantage of this method is in the detection of incipient faults, and concludes, that the frequency bands in defect detection are more tolerant due to the fact, that the actual bearing-defect induced vibration frequency, may vary slightly from the predicted values due to slippage that occurs within bearing. J.Lin and L. Qu [69] a denoising method based on wavelet analysis is applied to feature extraction for mechanical vibration signals, and concludes, that Donoho's "soft-thresholding denoising" method does not behave well in these two applications. Therefore, this denoising method based on Morlet wavelet has more advantages than Donoho's & soft-thresholding denoising" method in feature extraction, from these impulse signals. K Mori [74] applies DWT to vibration signals to predict the occurrence of 'spalling' in ball bearings. The values of the wavelet coefficients during these impulsive responses, increase, as the occurrence of 'spalling' comes near. Prediction of 'spalling' is possible by monitoring the trend of the wavelet coefficient maximum values. K.

Kim, and A. G. Parlos [73] the motor current predictor is developed for a wide range of healthy operating conditions. The resulting motor current residuals are nonstationary, and a wavelet packet decomposition algorithm is used to separate the different harmonics, and to compute the fault indicators. L.Eren and M.J. Devaney [78] analyze wavelet packet decomposition to detect bearing defects and concludes that the use of such bands in defect detection is more tolerant of the fact that the actual bearing-defect induced vibration frequencies may vary slightly from the predicted values due to slippage that occurs within the bearing. L.Eren and M.J. Devaney [91] describes DWT to detect bearing faults. The frequency sub bands for bearing pre-fault and post-fault conditions are compared to identify the effects of bearing/machine resonant frequencies as the motor starts, but concludes, that this monitoring, on each start, is achieved in a non invasive manner. P.W, Tse [108] finds the WA and the FFT with ED methods. However, to diagnose the faults of inner-race and roller, the tool of WA is found to be easier and concludes that WA does provide good resolution in frequency at the low frequency range, and fine resolution in time at the high frequency range. P.W. Tse et al [109] an innovative wavelet called exact wavelet analysis has been designed, but concludes, that this technique is particularly suitable for detecting randomly occurring faults. S. Prabhakar [136] uses Discrete Wavelet Transform (DWT). Vibration signals from ball bearings having single and multiple point defects on inner race, outer race and the combination faults have been considered for analysis. The impulses in vibration signals due to bearing faults are prominent in wavelet decompositions, but in the results and discussion, it pinpoints that kurtosis values increase as the bearing defects increase, i.e., $(\text{kurtosis})_{\text{good}} < (\text{kurtosis})_{\text{single defect}} < (\text{kurtosis})_{\text{two defects}}$. However, with these values, one cannot pinpoint the location of the defect in the bearing. T W. S. Chow and S.Hai [147] a wavelets-transform based technique is used to design specified narrow filter banks. Gaussian-enveloped, oscillation-type wavelet, is employed, and concludes, that as a family of wavelet functions is created with the same shape as the mother wavelet, a Gaussian-enveloped oscillation wavelet is employed in this paper because of its versatility in allowing the parameters of the filter banks to be selected. T. Zhang [144] In order to increase the Signal Noise Ratio, an approach to extract fault features from their vibrations, with envelope analysis and orthogonal decomposition of wavelet is presented, where envelope analysis is used as the preprocessing of the decomposition, and concludes, that the proposed method can be used to pick up other kinds of fault characteristics besides rolling bearing.

3.2.6 Artificial Neural Network Technique

A. Murray and J. Penman [4] that HOS when implemented in conjunction with an ANN diagnostic system, it has been shown that HOS can improve recognition performance. R. J. Povinelli [115] uses full covariance Gaussian Mixture Models of time domain signatures and the results show that the proposed method is robust, significantly outperforming the time delay neural network used as a baseline. T.Han et al [142] describes the DWT, GA and ANN techniques, and concludes, that the disadvantage of DWT, which results in feature dimension increasing, can be overcome by feature selection using GA. Also the difficulty of neural network parameter setting has been solved through GA optimization. T W. S. Chow and H.Tan [146] two different state-of-the-art HOS-based methods, namely, a nonparametric phase-analysis approach, and a parametric linear or nonlinear modeling approach, are used for machine fault diagnostic analysis, and concludes, that although the order-recursive linear identification approach, does not require the model order to be known *a priori*, it provides less accurate approximation to the measured vibration signals compared with the approach of quadratic nonlinear modeling.

A.J. Hoffman and N.T. Van der Merwe [7] states that Neural Networks are the best known technique to approach such a problem and conclude that it was demonstrated that incomplete training sets will lead to faulty diagnostic decisions. Bo Li et al [11] results show that neural networks can be effectively used in the diagnosis of various motor bearing faults through appropriate measurement and interpretation of motor bearing vibration signals. F. Filippetti et al [32] also states that a neural network can substitute in a more effective way the faulted machine models used to formalize the knowledge base of the diagnostic system when inputs and outputs are suitably chosen and mentions that this procedure substitutes the statement of a trigger threshold, required by the diagnostic procedure based on the machine models. I.E. Alguindigue et al [54] proposes a vibration monitoring methodology for rolling element bearings (REB) based on neural network technology and concludes that neural networks can provide a methodology for improving the analysis of spectra for vibration analysis, and may provide a viable complement to PSD analysis for monitoring and diagnostics of vibrating components. L.Eren, A. Karahoca and M.J. Devaney [79] studies Radial Basis Function Neural Networks and suggests that these are used to improve the bearing fault detection procedure, and concludes, that the line current data, they can provide, yields a useful predictive maintenance diagnostic when analyzed by the discrete wavelet packet transforms. M. Kalkat et al [88] illustrates, the effectiveness of the artificial NN predictor for vibration

analysis of a rotor-bearing system and discusses the experimental results, that the hidden neuron size plays an important role during the training of the network. When size of the neuron was increased, the training time of the network increased. M. F. White [89] develops a neural network-based incipient fault detector for small and medium size induction motors. The neural network-based incipient fault detector avoids the problems associated with traditional incipient fault detection schemes, by employing more readily available information such as rotor speed and stator current. M. Xu and T. Alford [92] applies different techniques, and summarizes, that monitoring the induced current frequencies to detect the characteristic bearing failure, involves suppressing the more dominant power system harmonics and then analyzing the remaining current spectrum. WPD provides a means to assess this spectrum, which is less sensitive than the FT to variations in the motor speed, which may result from changes in mechanical load or line voltage. A radial basis neural network then provides an effective means of detecting two common sources of bearing failure. N.S. Vyas and D. Satishkumar [98] discusses a neural network simulator built for prediction of faults in rotating machinery. A back propagation learning algorithm and a multi-layer network have been employed, and concludes, that It has been found that the testing success in addition to the input and hidden layer architecture, is crucially dependent on the two training parameters, namely the learning rate coefficient and the momentum. These parameters do not show a linear pattern of behavior and their role needs to be investigated further. R.R.Schoen et al [119] presents a method for online detection of incipient induction motor failures, which requires no user interpretation of the motor current signature, even in the presence of unknown load and line conditions, and concludes, that the combination of rule based frequency filter and a neural network, maximizes the systems ability to detect the small spectral changes produced by incipient fault conditions. R.M. Tallam et al [116] proposes an on-line training algorithm for Neural Network (NN) based fault detection schemes, but conclude that the COT algorithm is a viable solution for real-time implementation of any NN-based fault detection scheme. However, continual training, results in an inability to detect a fault that develops very slowly compared to the time between weight updates. Further work is in progress to overcome this drawback. R.M. Tallam et al [117] also proposes a neural network scheme for turn fault detection in line-connected induction machines is extended to inverter-fed machines, with special emphasis on closed-loop drives, and concludes, that experimental results showed that the scheme is insensitive to arbitrary supply voltage variations and non-idealities in the machine or instrumentation. R.M. Tallam et al [118] uses a feed-forward neural network, which learns the model of a healthy machine, and

has been used in conjunction with a Self-organizing Feature Map (SOFM), to visually display the condition of the monitored machine, and concludes, that experimental results have been provided to show that this method is not sensitive to unbalanced supply voltages or asymmetries in the machine and instrumentation. Z. Chen [158] applies the evolutionary strategy for classification problems is presented which includes GKMT and HENN, and concludes, that the comparison of the performance of the HENN and the BP algorithm shows, that HENN is superior to the BP algorithm

3.2.7 Fuzzy Technique

G. Goddu et al [38] used the frequency spectrum of the bearing vibration signal using a fuzzy logic fault diagnosis methodology, and suggests, future research should extend it by incorporation of intelligent membership function optimization, as well as, employing the method on a real data set. P. V. Goode and M.Chow [106] applies the neural fuzzy system that can provide quantitative descriptions of the motor faults under different operating conditions, as well as, qualitative heuristic explanations of these operating conditions, and the fault detection procedures through fuzzy rules and membership functions. W. Wang [153] develops a new neuro-fuzzy diagnostic system, whereby the strengths of three robust signal processing techniques are integrated. The adopted techniques are: the continuous wavelet transforms (amplitude) and beta kurtosis based on the overall residual signal, and the phase modulation by employing the signal average, and concludes, that research is underway to develop a neuro-fuzzy prognostic system to verify the diagnostic results, and to adaptively update its knowledge (rule) base, to further improve the reliability of this diagnostic system. X.Lou, and K.A.Loparo [156] deals with a new scheme based on the wavelet transform and neuro-fuzzy classification, and concludes, that using the wavelet transform together with fuzzy logic to quantify the degree of severity of an incipient fault, is a promising technique for prognostics. Further investigations should be conducted on optimal wavelet decomposition in the sense of best performance in incipient fault detection, isolation and severity monitoring. A more challenging task is to explore identifying simultaneous multiple faults through the smart use of time-scale analysis and other techniques, in systems science and engineering.

3.2.8 Acoustic Emission Technique

A. M. Al-Ghamd and David Mba [3] utilizes AE and established, the smooth defect could not be distinguished from the no-defect condition for ORF. Furthermore, their work presents two

important features; firstly, AE was more sensitive than vibration to variation in defect size, and secondly, that no further analysis of the AE response was required in relating the defect source to the AE response, which was not the case for vibration signatures. C. James Li and S. Y. Li [20] use AE on bearings, the linear discriminant functions have been established to detect defects on the outer race of the roller bearings and further suggest that AE is found to be a better signal than vibration when the transducers have to be remotely placed from the bearing. Q. Sun et al [112] state of art paper summarizes the emerging future directions in acoustic noise mitigation studies. L. M. Rogers [81] describes a methodology for the reliable detection of incipient damage due to fatigue, fretting and false brinelling in large, heavily loaded, rolling element bearings and It has been found that combining acoustic emission source location, and spectrum analysis of the associated time-domain signatures, has produced a powerful diagnostic tool, for the detection of micro-damage to the various working faces of the bearing, under variable speed and loading conditions, before any metal loss is evident in the bearing lubricant, and concludes, that whereas in the past, bearing condition diagnostic systems using accelerometer have fully met the needs of industry, the trend towards increasing power, complexity and tolerance of modern machinery, requires improved detectability of incipient damage mechanisms, so to avoid the serious consequences of an in-service failure. It has been shown in this paper, that by combining acoustic emission source location with signal envelope spectrum analysis, it is possible to identify different wear processes occurring at different times in different parts of complex machinery. The method has provided reliable information on the condition of the main bearings of marine propulsion engines, before microscopic loss of metal from the rolling contact faces of the bearing is detectable in the lubricant.

3.2.9 Independent Component Analysis (ICA)

S. Pöyhönen et al [141] applies ICA to multi-channel vibration measurements of an induction motor to fuse the measurement information of several channels, and provide robust and reliable broken rotor bar detection, and concludes, that however, further studies are required with measurements from other faults to conclude overall usefulness of data fusion of vibration measurements, because the broken rotor bar was quite easily detected based on the main vibration measurement. Also, building a multi-class classifier for detection of several faults may degrade the classification results. S. Han et al [135] proposed method utilizes ICA estimation of unifying structure, which includes mutual information and time structure. If the signals have no time correlation, their complexity may be achieved by their entropies, and

concludes, that the results provide more accurate defect analysis with noisy corrupted data, over conventional ICA, is a feasible approach for extraction of a machine signal from noisy measurements.

3.2.10 Other Techniques

B. Raison [17] employed cepstrum and parcels summation was used for bearing monitoring but concludes that the last method seems to be very promising and the signal transformations before parcels summation and the algorithm in itself must be carefully detailed and explored. D. Ho and R. B. Randall [25] application of Self-Adaptive Noise Cancellation (SANC) in conjunction with envelope analysis in order to remove discrete frequency masking signals was used. The subsequent envelope analysis can then be performed by using the Hilbert transform technique or band-pass rectification, but concludes, that techniques such as SANC can be used to remove discrete frequency noise from the signal before performing envelope analysis. Since this requires real-valued signals as inputs, band-pass rectification is a faster way of performing envelope analysis than the Hilbert transform technique. However, band-pass rectification will also need the extra zero padding used for analyzing the squared envelope in order to move the pseudo-sum frequencies outside the frequency range of interest and thus time records will have double the number of samples. F.F. Costa et al [35] considers Broken cage bars, and further conclude that the operation of acquiring and suppressing fundamental component of the signal must be performed in real time via the recursive algorithm. F. Briz et al [29] using an injected high-frequency carrier signal is presented and analyzed and concludes that while broken rotor bar detection has been shown to be viable with a machine having semi-open rotor slots, the rotor-fault-related component in the negative-sequence, carrier-signal current spectrum was found to be too small for the case of closed-rotor-slot machines to allow reliable rotor fault detection. F.Filippetti et al [31] a new and simple procedure based on a model which includes the speed ripple effect is developed. This procedure leads to a new diagnostic index, independent of the machine operating condition and inertia value, that allows the implementation of the diagnostic system with a minimum configuration intelligence, and concludes, that an experimental proof of the improvement in the fault diagnosis and of the independence of the sum of the current components on inertia are given. F. C. Trutt [30] presents a theoretical and experimental analysis of a voltage mismatch technique that may be used in operating situations to monitor the health of induction motor windings, and concludes, that both voltage mismatch parameters are seen to predict deterioration independent of whether this deterioration acts to

create more balance or to create more unbalance in the motor. Future research should include more extensive experimental testing on a variety of induction motor systems, in order to provide additional verification of the proposed monitoring scheme. H. Nejjari and M. E.H. Benbouzid [51] proposes methodology based on the so-called Park's vector approach. In fact, stator current Park's vector patterns are first learned, using ANN's, and then used to discern between "healthy" and "faulty" induction motors, and concludes, that it was tested on both classical and decentralized approaches. H. Guldemir et al [50] the machine with offset (eccentric) rotor has been studied. This study has proved that some of the components in the line current spectrum of an induction motor are a function of eccentricity. The magnitudes of these components increase when the level of eccentricity increases. These harmonics are used to monitor the eccentricity of the motor. H. Ocak and K.A. Loparo [46] introduces a new bearing fault detection and diagnosis scheme based on Hidden Markov Modeling (HMM) of vibration signals. The technique allows for online detection of faults by monitoring the probabilities of the pre-trained HMM for the normal case. It also allows for the diagnosis of the fault by the HMM that gives the highest probability. H. Ocak and K.A. Loparo [47] introduced a new bearing fault detection and diagnosis scheme based on hidden Markov modeling (HMM) of vibration signals. In this new scheme, HMM models were trained to represent various bearing conditions. These models were then used to detect both single and multiple bearing faults based on the model probabilities, and concludes, that the method has been extended to address the problem of bearing prognostics. H. Henao et al [45] proved that a simple external stray flux sensor is more efficient than the classical stator current signature analysis, to detect inter-turn short circuit in three-phase induction machines, and concludes, that this detection technique is more reliable than the MCSA, especially when the number of shorted turns is small, compared to the total number of turns in a phase winding. J. R. Stack [64] research introduces the notion of categorizing bearing faults as either single-point defects or generalized roughness, and in the conclusion suggests, generalized roughness faults produce unpredictable (and often broadband) changes in the machine vibration and stator current. J. L. Kohler [60] addresses the level of turn-to-turn insulation deterioration that can be resolved using an online monitoring technique, based upon an effective negative-sequence impedance detector and concludes, that a fault in the presence of the supply unbalance can cause the detector to change unpredictably at very low levels of deterioration, because the effect of the fault, combined with the supply unbalance may initially cause the motor currents to become more balanced. J. Shiroishi et al [68] investigates defect detection methodologies for rolling element bearings through vibration

analysis. Specifically, the utility of a new signal processing scheme combining the High Frequency Resonance Technique (HFRT) and Adaptive Line Enhancer (ALE) is investigated, and concludes, that results from this study show that increasing RPM tends to decrease sensitivity to defects. K Mori et al [74] describes a coherent strategy for intelligent fault detection. These encompass: (i) a taxonomy for the relevant concepts, i.e. a precise definition of what constitutes a fault etc., (ii) a specification for operational evaluation which makes use of a hierarchical damage identification scheme, (iii) an approach to sensor prescription and optimization, and (iv) a data processing methodology based on a data fusion model. K.Siwiek et al [76] uses external measurements of the voltage and current in this circuit, and concludes that once the network was trained, the recognition of fault is done immediately, irrespective of the size of the circuit. Thus, the solution is suited for the real time applications of fault location. S. Kumaraswamy et al [139] an attempt has been made to study the vibration level of various machine tools to explore the possibility of establishing the standard vibration level. Till today no vibration standards are available for determining the acceptable vibration level for specific machine tools. M.Haji, and H.A. Toliyat [90] a pattern recognition technique based on Bayes minimum error classifier, is developed, to detect broken rotor bar faults in induction motors at the steady state and concludes that without loss of generality, the algorithm can be revised to include other faults such as eccentricity and phase unbalance. Also, if appropriate features are derived, this method can be applied for fault classification in other electric machines like DC machines. M. Xu and T. Alford [92] the induction motor operating principles and motor current measurement, are described. The characteristics of two types of induction motor problems, namely broken rotor bars and air-gap eccentricity, in the measured spectral data are discussed, and one of the conclusions is that the broken rotor bar problem was not evident in the vibration measurement but consistently showed up in the current spectrum. This is not uncommon in detecting rotor problems, because, the damping and other effects exist in the signal transmission path for motor vibration measurement. M. Bai et al [93] develops a system composed of a signal processing module and a state inference module. In the signal processing module, the Recursive Least Square (RLS) algorithm and the Kalman filter are exploited to extract the order amplitudes of vibration signals, followed by fault classification using the fuzzy state inference module signals. In addition, more sophisticated methods in the areas of speech and pattern recognition are being sought, in an attempt to enhance the feature extraction and intelligent inference. P.Chen et al [100] proposes a fault diagnosis method for plant machinery in an unsteady operating condition using Instantaneous Power Spectrum (IPS) and Genetic Programming (GP). IPS is

used to extract feature frequencies of each machine state from measured vibration signals, for distinguishing faults by relative crossing information. GP can sensitively reflect the characteristics of signals for precise diagnosis. Q. Sun et al [112] proposed technique contains effective feature extraction, good learning ability, reliable feature fusion, and a simple classification algorithm, and finally, concludes, that future development of the technique will be directed towards the ability to estimate the remaining life of mechanical components. R. Yan, and R. X. Gao [122] presents a machine health evaluation technique using the Lempel-Ziv complexity as a numerical measure, but concludes, that research is being continued to analyze vibration signals from different defect locations, and on different types of bearings, to systematically validate the utility of this technique. S. Nandi and H.A. Toliyat [32] the method proposed in this paper monitors certain rotor-slot-related harmonics at the terminal voltage of the machine, once it is switched off, but concludes, that Unlike negative-sequence current or impedance measurements, this technique is insensitive to supply voltage unbalance. The faulty phase can be detected, too. The very nature of the test also suggests that the supply harmonics have little influence on detectability. W.T.Thomson and R.J.Gilmore [155] presents the fundamentals on MCSA plus data interpretation, and the presentation of industrial histories, and concludes, with the advantages of using MCSA as a tool for assessing the operational condition of three phase induction motor. The study presented in this paper is of an exploratory character. Further investigations are required to fully establish the method.

3.3 Parameters for FDEM

Parameters that can be measured during FDEM are vibration, sound, current, voltage, temperature, speed. The vibration has been the focus because of the following reasons

- Vibration possesses both classification of signals that is deterministic and random which is the property that has been fully utilised in this thesis
- All the forcing frequencies are transmitted through the bearing element to the bearing housing
- Only parameter that responds to subtle changes in current and voltages imbalances
- Senses and reflects misalignment discrepancies in the spectrum
- All electrical and other faults can easily be captured through this parameter

- Versatility of this parameter can also sense a sudden impact which is a prime concern for shocks.
- The behavioural pattern of this parameter is not limited to this machine but can be extended to larger machines since vibration sets threshold values above which a fault is declared

It should be noted that since current, voltage, speed and temperature are deterministic signals hence much fault finding information might not be easily revealed in these parameters. However these parameters are used to control the machine to rated values upon which FDEM was performed.

3.4 Importance of Vibration Parameter

Vibrations may be classified as deterministic or random signals. This parameter has been a point of focus since the evolution of FDEM. The major reason being that all fault component are captured in this parameter that is both deterministic and non deterministic. Moreover, vibration is known to be mechanical in nature but an electrical fault is easily reflected and can be captured by this parameter if the DAQ and analysis is accurate.

3.4.1 Deterministic Vibration: Deterministic follows an established pattern so that the value of the vibration at any designated future time is completely predictable from the past history. It is characterized by regular and repeating pattern. A further important category of deterministic vibration is shock vibration characterized by the fact that its excitation is non periodic.

3.4.2 Random or Stochastic vibrations: the excitation is non deterministic examples include are wind, velocity, road roughness and ground motion during earthquakes. This can further be classified into stationary random vibrations whose statistical characteristics do not change with time. On the contrary, for non stationary random vibrations these statistical properties vary within time intervals considered essential for their proper description.

3.4.3 Choice of using acceleration: Vibration from machines contains wide range of sinusoidal and random components. The signal processing handbook [160] mentions that amplitude measurement is particularly important with plain bearings, since it indicates the risk of abrasion. Velocity is related, through number of stress reversals, to potential fatigue failure. Acceleration is related to force and thus a possible development to wear.

3.5 Analysis Techniques Used in Present Work

The DAQ described in Chapter 2 of the parameter reconstructed results in the original signal waveform using EXCEL. The extracting of information can be accurate if and only if a proper and an exact signal are achieved. This can be attained if sampling, quantization and reconstruction have been properly executed. If a mismatch occurs the data is corrupted and the information hides. Once a proper signal is attained the features can be extracted by using any signal processing technique to analyze the behaviour of the signal. In a broad sense the signal processing (SP) techniques can be divided as follows:

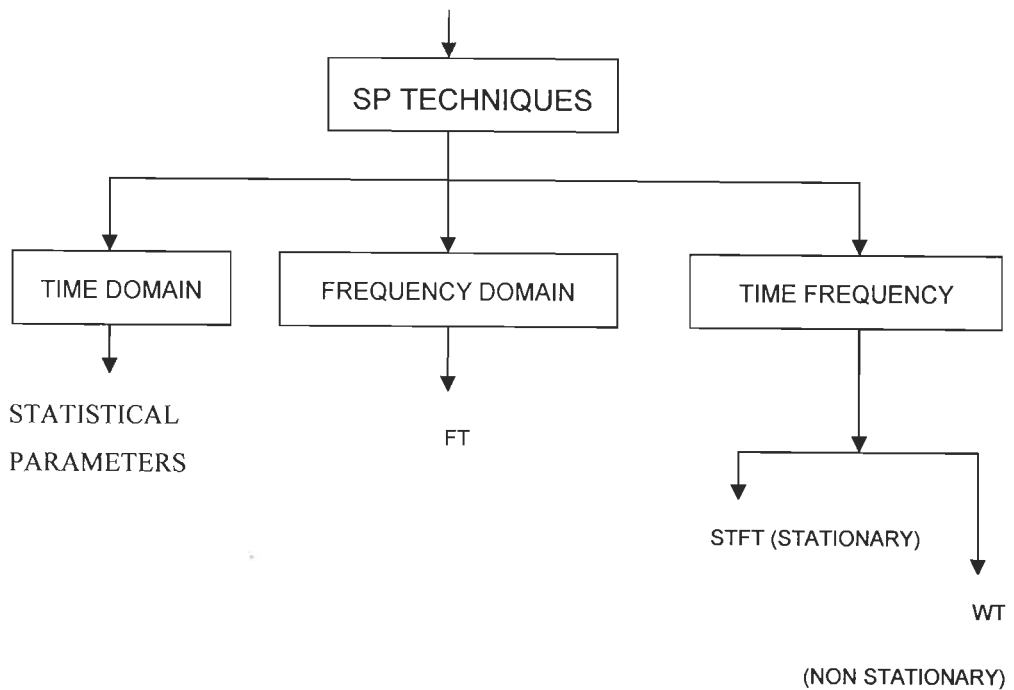


Figure: 3.1 Basic Analysis Tools Used in FDEM

The above diagram shows the basic SP techniques used in FDEM. The system can be made intelligent by using AI techniques. Notwithstanding, newer techniques used in FDEM are a merge of SP techniques and other fields such as AI, statistics and many more. This work uses one of these kinds of approach and it focuses on time domain embedded with statistical analysis. This evolves numerous dimensions to the time domain signal and gives it a new meaning entirely. A common belief of DSP experts is that information cannot be deciphered in the time domain and hence the signal is translated to frequency, STFT or WT and than

features can be extracted. But this merge of time plus statistics evolves better dimension for fault diagnosis of electrical machines. The bearing characteristic frequency BCF was also calculated to show that the results are an affirmative.

3.5.1 Time Domain

The acceleration mode of the vibration signal is taken into consideration and a plot of acceleration [g] versus time is plotted for four cases –that is no load, slight load, half load and finally three quarter load for three categories namely

- a) fault free bearing
- b) outer race fault and
- c) inner race fault

According to the type, severity and load it can be seen that the dispersion increases in the time plot. To support this observation the statistical parameters are applied to confirm these deviations. In this research work a complete new approach is given to FDEM whereby a subtle application of the statistical parameters and inferences unravel the hidden information of the time signal. Hence, this work strongly recommends that if a supportive tool such as statistical techniques are incorporated in a time signal not only it describes the features but speaks volumes of the information hidden in the time domain signal which defies the myth that time signal has no information of interest. This will lead to a more futuristic way of defining FDEM.

Implementation of Statistics in FDEM: Statistics have been applied to many fields of study which includes Business, Biotechnology, Biomedical, Population index, Sensex indices and many other upcoming fields amongst which in this research work it is applied for fault diagnosis in FDEM. *Statistics* refers to the body of techniques used for collecting, organizing, analyzing, and interpreting data. The data may be quantitative, with values expressed numerically, or they may be qualitative, with only one characteristic preferred and tabulated. Statistics are used in vibration to help make better decisions by understanding the sources of variation and by uncovering patterns and relationships in vibration data.

Descriptive statistics include the techniques that are used to summarize and describe numerical data for the purpose of easier interpretation. These methods can either be graphical or involve computational analysis. This work treats all the existing parameters as a whole unit for FDEM. The terms below appear in the order they are produced by Excel's Descriptive Statistics. Each term is followed in capital letters by the Excel function that produces the

same value, a definition or explanation of the statistic, and then the relevant equation. Note that the mean, standard error, median, mode, standard deviation, range, minimum, maximum, sum and confidence level all have the same units as the sample values x_i .

Measure of Central Tendency (MCT): This is defined by the mean, standard error, median, and mode of the vibration signal. The mean, median, mode is a good measure of the central tendency for roughly symmetric distributions but can be misleading in skewed distributions. Therefore, other statistics such as the median may be more informative. The acceleration levels (g) can be measured by the central tendency which usually swings around the zero value both in positive and negative directions. This study reveals that as the severity increases this should reflect in the parameters governed by this class.

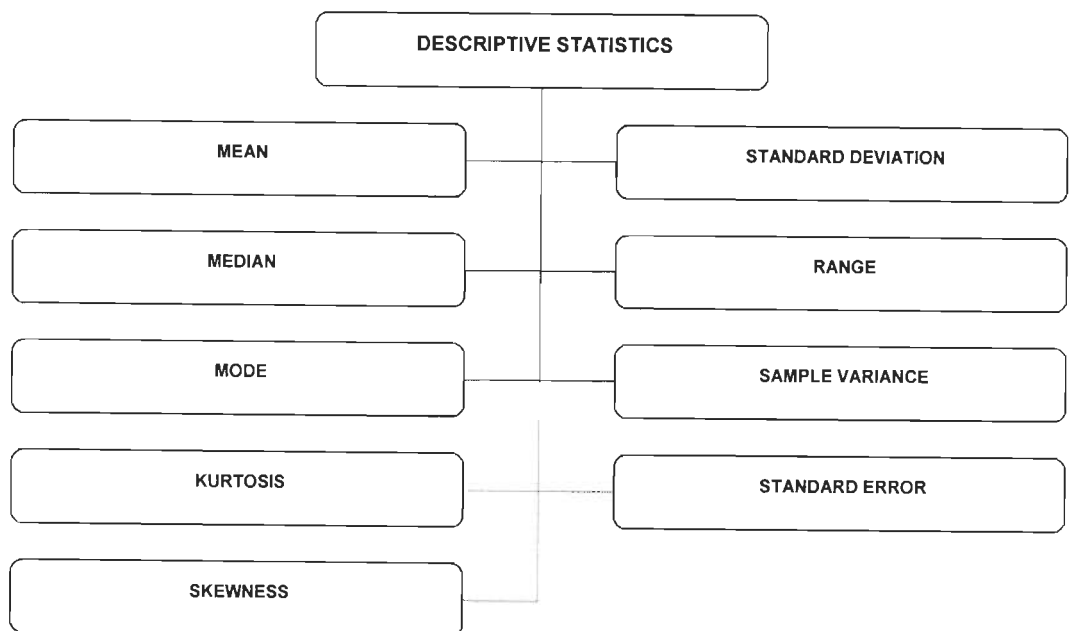


Figure 3.2 Classification of statistical parameters

Measure of Variability (MV): This is the amount of variance that occurs and is measured by the standard deviation, sample variance, range, minimum and maximum.

Range: shows the dispersion in the samples which can also be seen in the cumulative distribution function. If the range is less sample variance and dispersion is also less as seen in the case of the healthy machine. This eventually relates to the standard deviation.

Sample variance: portrays the amount of variance in the samples. A large variation shows a larger amount of dispersion.

Standard deviation: as the standard deviation increases the dispersion increases which in turn gives a significant change in the time signal. This can be verified from the range parameter showing the spread of the Gaussian curve along the independent axis.

In the results of this research work it can be seen that an increase in variability is reflected from a healthy to an outer race and inner race defect which is in accordance to the laws of statistics. The parameters of this class are the focus of this work since a dramatic change occurs at incipient stage. The most sensitive parameter for an incipient stage for fault detection is the measure of variability (MV) that could change the perception of FDEM.

Measure of Dispersion (MD): This indicates the dispersion in the vibration signal and is defined by the kurtosis and skewness,

Kurtosis: the fourth sample moment around the mean indicates the degree of peakedness of the distribution. For a good quality surface, it can be shown theoretically that the kurtosis coefficient takes on the approximate numerical value of 3 to 3.5

Skewness: is the average cubed deviation from the mean. Due to symmetrical distribution of a healthy machine the value is close to zero in the case of healthy machine but when a fault occurs this value has a tendency to change.

Until now researchers have segregated one parameter from the rest, the focus being dispersion, but this work suggests that this becomes a guiding line to fault detection. It has been suggested that kurtosis coefficient takes on numerical value of 3.0 to 3.5 and the skewness value lies around 0 for an induction machine.

Description of the parameter with formula:

Mean (AVERAGE): The sum of all samples divided by the number of values:

$$\bar{x} = \frac{\sum_{i=1}^n x_i}{n} \quad \text{where } n = \text{total number of samples} \quad 3.1$$

Standard Error: The population standard deviation of many measurements of a mean of n samples. It is estimated by the standard deviation of one measurement of the mean divided

by the square root of n:

$$\frac{s}{\sqrt{n}} = \sqrt{\frac{\sum_1^n (x_i - \bar{x})^2}{n}} \quad 3.2$$

Median (MEDIAN): If n is odd, the value of x_i for which half of the remaining values are larger and half are smaller. If n is even, the average of the two values in the middle.

Mode (MODE): The most frequently occurring value, if any.

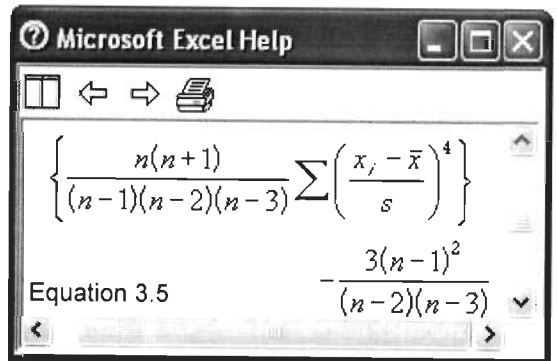
Standard Deviation (STDEV): From Excel’s Help on this function, “The standard deviation is a measure of how widely values are dispersed from the average value (the mean).”

$$s = \sqrt{\frac{\sum (x_i - \bar{x})^2}{n}} \quad 3.3$$

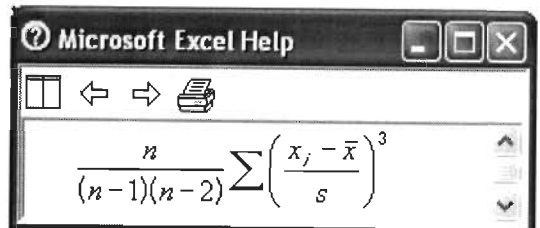
Sample variance (VAR): Square of the standard deviation:

$$s^2 = \frac{\sum_1^n (x_i - \bar{x})^2}{n} \quad 3.4$$

Kurtosis (KURT): From Excel’s Help on this function, “Kurtosis characterizes the relative peakedness or flatness of a distribution compared with the normal distribution. Positive kurtosis indicates a relatively peaked distribution and is known as leptokurtic. Negative kurtosis indicates a relatively flat distribution and is known as platykurtic.”



Skewness (SKEW): “Skewness characterizes the degree of asymmetry of a distribution around its mean. Positive skewness indicates a distribution with an asymmetric tail extending toward more positive values. Negative skewness indicates a distribution with an asymmetric tail extending toward more negative values.”



3.6

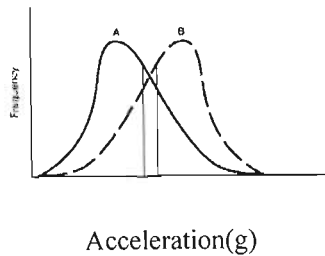


Figure 3.3: Two skewed distribution curves.

The above graph shows the two skewed distribution curves. Curve A defines the positive skewness and curve B represents the negative skewness.

Range: Maximum value minus minimum value. (Usually increases as n increases, making it a poor measure of the dispersion or spread of the population values.)

Minimum (MIN): Minimum value.

Maximum (MAX): Maximum value.

Sum (SUM): Sum of all values, $\sum_{i=1}^n x_i$ 3.7

Count (COUNT): Number of values, n

Confidence Level (chosen %):

If the population is normally distributed and you choose the default of 95% ($\alpha = 0.05$), then the probability is 95% that $\mu = \bar{x} \pm \text{ConfidenceLevel}$.

3.5.3 Inferential statistics: include those techniques by which decisions about a statistical population or process are made based only on a sample having been observed. Because such decisions are made under conditions of uncertainty, the use of probability concepts is required. The inferential statistics can be classified into probability density function and cumulative distribution function as shown in Figure 3.6.

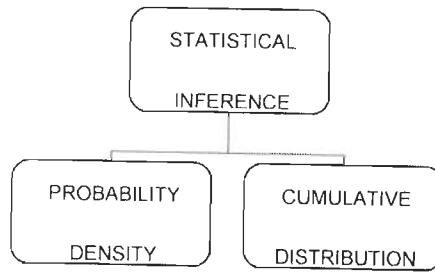


Figure 3.5: Classification of statistical Inference

The Normal Probability Distribution

The *normal probability distribution* is a continuous probability distribution that is *both symmetrical* and *mesokurtic*. The probability curve representing the normal probability distribution is often described as being bell-shaped. The normal probability distribution is important in statistical inference for three distinct reasons:

1. The measurements obtained in many random processes are known to follow this distribution.
2. Normal probabilities can often be used to approximate other probability distributions, such as the binomial and Poisson distributions.
3. Distributions of such statistics as the sample mean and sample proportion are normally distributed when the sample size is large, regardless of the distribution of the parent population. As is true for any continuous probability distribution, a probability value for a continuous random variable can be determined only for an *interval* of values. The height of the density function, or probability curve, for a normally distributed variable is given by

$$f(X) = \frac{1}{\sqrt{2\pi\sigma^2}} e^{-[(X-\mu)^2/2\sigma^2]} \quad 3.8$$

where e is the constant 2.7183,

μ is the mean of the distribution,

and σ is the standard deviation of the distribution.

Since every different combination of μ and σ would generate a different normal probability distribution (all symmetrical and mesokurtic), tables of normal probabilities are based on one

particular distribution: *the standard normal distribution*. This is the normal probability distribution with $\mu = 0$ and $\sigma = 1$. Any value X from a normally distributed population can be converted into equivalent standard normal value z by the formula:

$$z = (X - \mu) / \sigma \quad 3.9$$

Any z value restates the original value X in terms of the number of units of the standard deviation by which the original value differs from the mean of the distribution. A negative value of z would indicate that the original value X was below the value of the mean.

Cumulative Frequency Distributions

A *cumulative frequency distribution* identifies the cumulative number of observations included below the upper exact limit of each class in the distribution. The cumulative frequency for a class can be determined by adding the observed frequency for that class to the cumulative frequency for the preceding class. The graph of a cumulative frequency distribution is called an *ogive*. For the less-than type of cumulative distribution, this graph indicates the cumulative frequency below each exact class limit of the frequency distribution. When such a line graph is smoothed, it is called an *ogive curve*.

$$F(X) = \int f(x) dx \quad 3.10$$

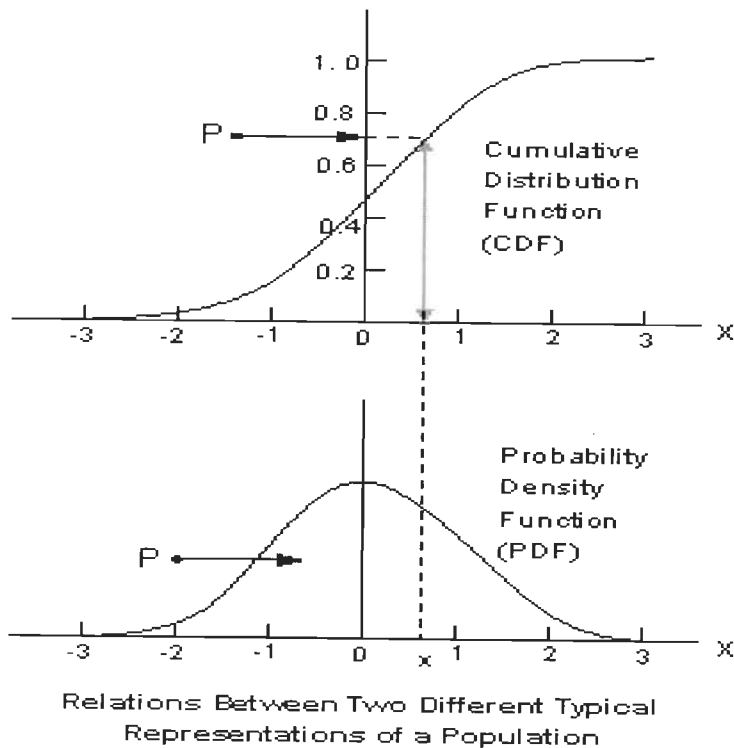


Figure 3.5 Relation showing the PDF and CDF

3.6 Frequency Domain: A very common approach used in DSP is the FFT to perform the DFT with only $N \log_2 N$ operations. The frequency resolution is given by

$$\text{Frequency Resolution} = \text{Number of samples} / \text{Sampling frequency}$$

According to the thesis S.A.S.Kazzaz [129] the FFT is a powerful tool for signal analysis but states the major drawback which is of utmost importance and hence is given below:

- 1- the resolution of the frequency is same for low and high frequency regions. This may lead to inaccurate information pertaining to the low frequency region.
- 2- If there is non stationary part of the signal, the spectrum will demonstrate uncertain information about its frequency content and its location in time domain.
- 3- If the frequency component is not equal to an integer multiple of the step frequency (resolution), the amplitude of the component in the spectrum can not be related to its amplitude in time domain.

- 4- In order to obtain high frequency resolution, sampling frequency and the number of samples must be adjusted. However, memory size and the speed of the DAQ play a role in selecting values of the frequency resolution.

Based on the above drawbacks this research focuses its attention on the acquiring of signals with sampling frequency that gives a 0.625 Hz resolution. And further exploits the STFT to determine the BCF.

3.7 Short Time Fourier Transform STFT

The difference between the STFT and FFT is that in STFT the signal is divided a small segment using a window function (w) instead of taking the whole signal. The FFT is performed on this truncated series. The machine vibration data is repetitive due to its rotational behaviour hence this concept is fully utilized to achieve the desired results. The rectangular window was implemented in this research work.

The expression is given as below

$$X(f, k) = \sum_{n=0}^{N-1} W(n-k)x(n)e^{-j2\pi f n} \quad 3.11$$

Where $W(n-k)$ the window function and k is is the width of the window.

The width and the type of the window depend on the topology of the signal and the information to be extracted. The width of the window is adjusted to make each segment of the signal stationary .Then the spectrum will give the frequency components of that non stationary part of the signal that corresponds to that particular segment.

. Figure 3.6 above is a flow diagram of the Analysis Techniques implemented in this research work. After acquiring the vibration signal the time domain and frequency domain signal is analyzed.

Time Domain Analysis: The analysis is further incorporates statistical techniques in tandem with time domain signal and it as follows:

- 1) the signal is considered in original time plot
- 2) the statistical analysis is computed in two components

- a) Statistical Parameters: the mean, standard error, median, mode, standard deviation, sample variance, kurtosis, skewness, range, minimum, maximum and confidence interval at 95%.
- b) Statistical Inference: where the PDF and CDF are calculated and plotted.

Frequency Domain Analysis: The FFT was determined and plotted to find the Bearing Fault Frequency BCF.

Table 3.1: Formula as well as calculated frequencies of the bearing defects.

| Faults | Formula | Calculated Frequency (Hz) |
|------------------|--|---------------------------|
| Outer race fault | $f_o(Hz) = (N/2)fr[1 - b \cos(\beta) / d]$ | 64.6 |
| Inner race fault | $f_i(Hz) = (N/2)fr[1 + b \cos(\beta) / d]$ | 103.3 |
| Ball spin | $f_{bd}(Hz) = dfr / 2b[1 - [b \cos(\beta) / d]^2]$ | 49.2 |
| Train defect | $f_{td}(Hz) = fr / 2[1 - b \cos(\beta) / d]$ | 9.2 |

where, the rotational frequency fr is at 24Hz, b =ball diameter=15mm, d =pitch diameter=65mm, β =defines the contact angle=0 degrees, N =number of balls =7

3.6 Conclusions

Many techniques have been proposed, as described in this chapter, for fault diagnosis. Each of the analysis techniques has its own advantages/drawbacks. In present work time domain analysis has been employed. The findings have been found to agree with the frequency domain approach based on Bearing Characteristic Frequency (BCF). The Signal Processing Techniques is the root of analysis for all techniques.

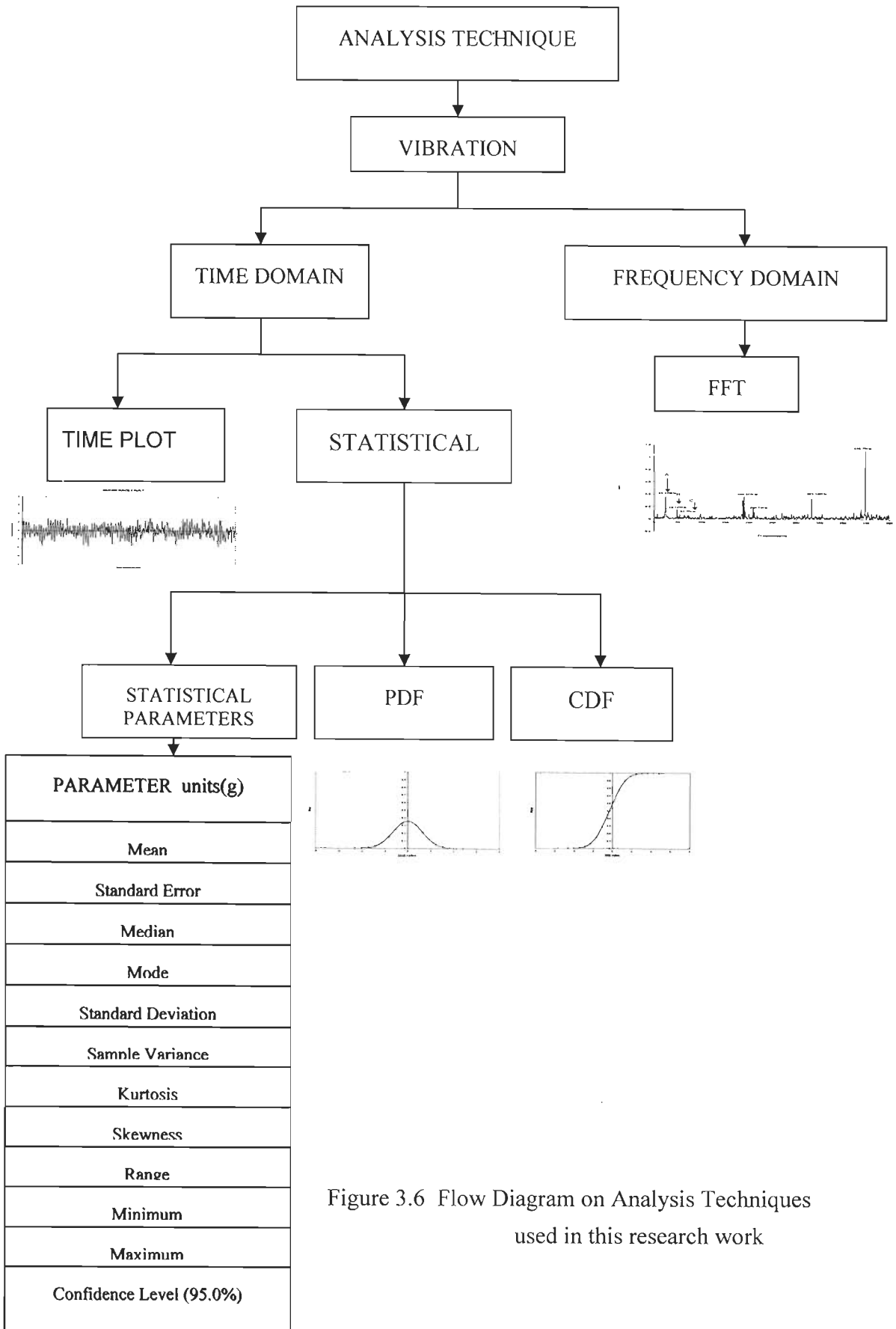


Figure 3.6 Flow Diagram on Analysis Techniques used in this research work

Behaviour of the Vibration Data

This chapter, introduces chitest as a validation test of vibration signal, states the advantages and its application. Further the conditions of validity of chitest, defines goodness to fit, final steps of chitest and the guidelines to calculate chitest are explained.

4.1 Introduction

In statistics a need arises to understand the data as well as to verify that the distribution which it is representing is of a proper fit. Vibrations are random in nature and hence a need for the clarification is necessary. This in turns serves as a guideline to the choice of analysis technique to be applied. For instance, at an incipient stage the bearing fault in this research work elaborates that data is a Gaussian distribution and these results need to be validated by a statistical technique. A controversy whether the data is Gaussian or Non Gaussian has been a concern. G. Keller[40] suggests that chitest is a non parametric test that ascertains the behaviour of the data. L.R. Kadiyali [82] highlights the process of chi square test for random process. A thorough literature review reveals that Independent Component Analysis (ICA) has been used by some researchers for FDEM whereas a guideline to ICA suggests ICA technique can only be applied if the data is non Gaussian. Hence, this becomes a prime concern of the behaviour of vibration in electrical machines. This research work classifies and categorically proves that vibration data is Gaussian at an incipient stage and has been validated by a non parametric test the chi square test χ^2 .

4.2 Chitest for Behaviour Analysis of Data

Statistics defines these tests broadly in two categories that are the parametric and non parametric tests.

Parametric Tests: when statistics is under the assumption that data follow some common distribution than it can be classified as a parametric test. These include t-test, ANOVA and linear regression.

Non Parametric Tests: These are also known as the distribution free tests since they do not

make the assumption that the data follow some distribution. These include Mann Whitney test, Wilcoxon Signed test, Kruskal Wallis test and others. Another test is the chitest and it is one of the most versatile validation test for vibration signal and holds no bias against accepting a distribution or rejecting the hypothesis. This test also caters for large sets of data N. In this research work 50000 discrete data points are considered for only one vibration signal. This cannot be satisfied by any other parametric or non parametric tests.

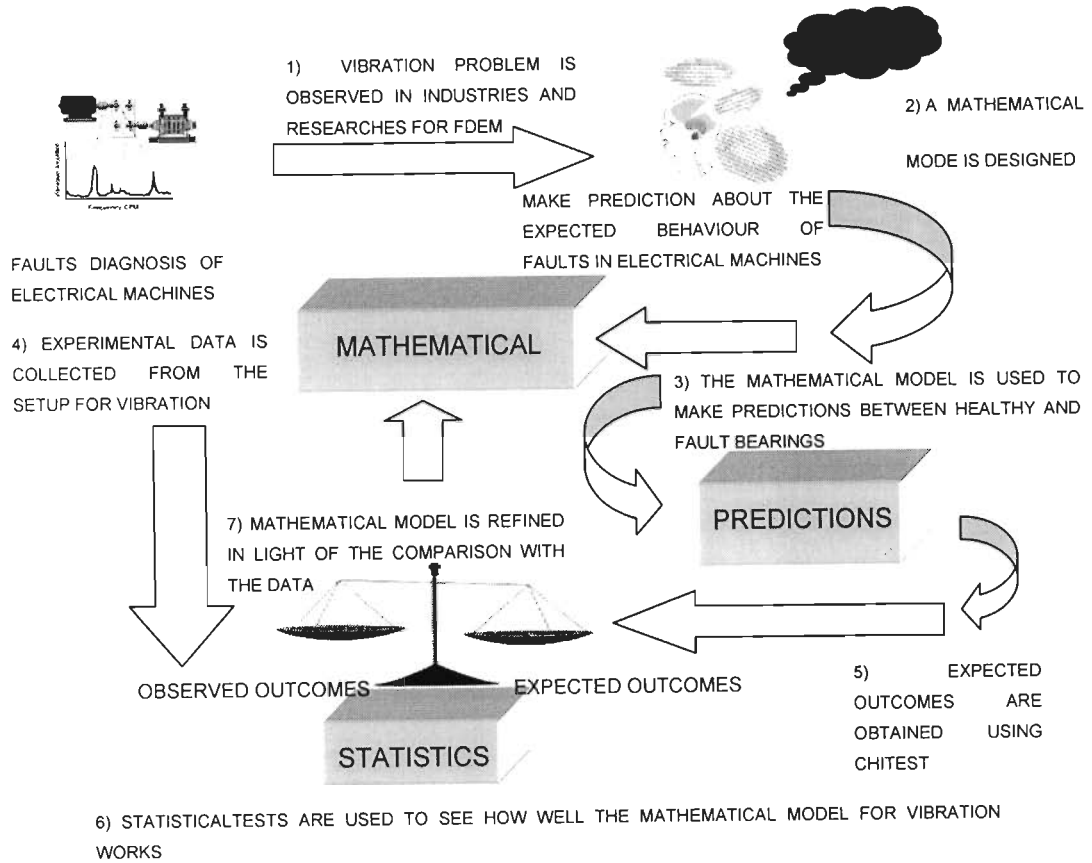


Figure 4.1: Need for a validation test for a Vibration Signal

The above diagram shown in Figure 4.1 shows that statistical test is used to see how well the mathematical model for vibration works. It has a balance where the observed outcomes and the expected outcomes are weighed. The observed and expected value is less than the chi squared critical value than the hypothesis is accepted. The observed and expected value is weighed so that they do not exceed the critical value point. Else the hypothesis is rejected.

4.3 Advantages of Chitest

- It defines a difference in proportions between groups in terms of the overall ratio of the dependent variable.
- It handles large data size such as the vibration signal having 50000 data points. The other techniques are limited to the size of the data.
- It is further defined by two types of test the testing of proportions with contingency table and Goodness to fit test. This work utilizes the latter.
- The degree of freedom depends upon the particular distribution being tested.

4.4 Applications of Chi Square Distribution

The Figure 4.2 shows the three important regions found in chitest.

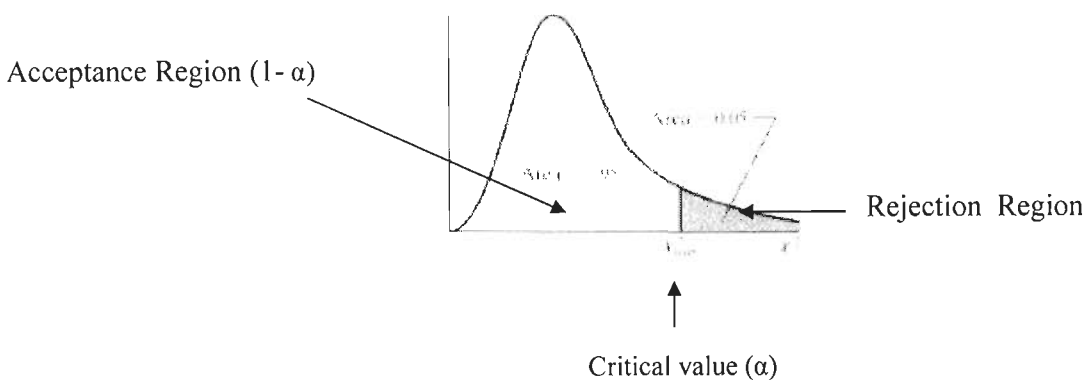


Figure 4.2 Critical values for 95% confident interval (Kadiyali[82])

The plot shows the acceptance region, rejection region and the critical value. The chitest that is carried out is on the principle that if the observed values and the expected values are above the critical value than the hypothesis becomes null and it is rejected and if the values are less than the critical value than the hypothesis is accepted and that in turn implies that it is a “goodness to fit” distribution. To find the Critical values (α) of the chi-square distribution refer to Appendix A 6. The critical value of chi-square significance level $\alpha = 0.05$ and a Degree of freedom $d.f=8$ is 15.51. Therefore, any value above 15.51 rejects the hypothesis saying the distribution is not a fit.

- a) To test if the hypothetical value of the population variance is $\sigma = \sigma_0^2$
- b) To test the goodness to fit.
- c) To test the independence of attributes.
- d) To test the homogeneity of independent estimates of the population variance.
- e) To combine various probabilities obtained from independent experiment to give a single test of significance.
- f) To test the homogeneity of independent estimates of the population correlation coefficient

4.5 Conditions of the Validity of Chitest

Chitest is an approximate test for large number of values of n. For the validity of chi square test of goodness to fit between theory and experiment, the following conditions must be satisfied:

- a. The sample observation should be independent.
- b. Constraints on the cell frequencies ,if any , should be linear
 - i. (ie $\Sigma O = \Sigma E$)
- c. N, the total frequency should be reasonably large, say, greater than 50.
- d. No theoretical cell frequency should be less than 5.(The chi square distribution is essentially a continuous distribution and cannot maintain its character of continuity if cell frequency is less than 5)

Chitest depends only on the set of observed and expected frequencies and on d.f .It does not make any assumptions regarding the parent Population from which the observation are taken. Since it does not involve any population parameters, it is termed as a statistic and the test is known As Non Parametric Test or Distribution Free Test.

Goodness to Fit Test

This test enables us to find if the deviation of the experiment from theory is just by chance or is it really due to the inadequacy of the theory to fit the observed data. If f_i ($i=1,2,\dots,n$) is a set of observed frequencies and e_i ($i=1,2,\dots,n$) Is the corresponding set of expected frequencies then chitest is given by

$$\chi^2 = \sum_{i=1}^n \left[\frac{(f_i - e_i)^2}{e_i} \right] \quad 4.1$$

if

$$\sum_{i=1}^n f_i = \sum_{i=1}^n e_i \quad 4.2$$

Follows chi square distribution with (n-1) d.f.

Decision Rule

$$\text{Accept } H_0 \text{ if } \chi^2 \leq \chi_{\alpha}^2 (n - 1) \quad 4.3$$

$$\text{Reject } H_0 \text{ if } \chi^2 > \chi_{\alpha}^2 (n - 1) \quad 4.4$$

Where

χ^2 Is the calculated value and

$\chi_{\alpha}^2 (n - 1)$ Is the tabulated value of chi square for (n-1) d.f

And level of significance α .

4.6 Final Steps for Chitest

- a) Formulate a null hypothesis indicating a hypothesized distribution for the population
- b) Establish categories for the population.
- c) Use a simple random sample of n items and record the observed frequencies for each class or category.
- d) Use the assumption of null hypothesis is true and determine the expected frequencies for each category.
- e) Multiply the category proportions in step4 by the sample size to determine the expected frequencies for each category.
- f) Use the observed and expected frequencies and compute chitest from the above equation.
- g) Apply the decision rule to accept or reject the hypothesis.

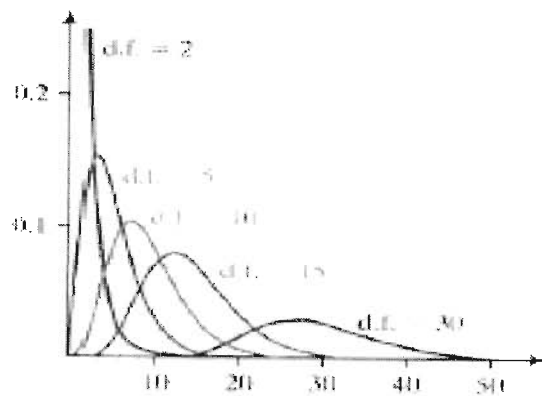


Figure 4.3: Chi square distribution for different d.f. (Kadiyali[82])

Figure 4.3 show plots of chi square distribution of different levels of Degree of freedom (d.f). It is a plot of probabilities of chi square values versus the chi values and shows the behaviour at different levels of d.f.

4.7 Guideline for a Chitest

- a) select the class limit
- b) subtract the mean
- c) divide by the standard deviation
- d) find the probability
- e) find the frequency
- f) $\text{chitest} = \frac{(o-e)^2}{e}$ where o=observed frequency ,e=expected frequency
- g) compare it with the observed frequency

The **observed frequencies** are the actual number of observations that fall into each class in a frequency distribution or histogram.

The **expected frequencies** are the number of observations that should fall into each class in a frequency distribution under the hypothesized probability distribution.

4.8 Results and Discussion

The three cases considered were the healthy, outer race fault and inner race faults and the results are shown as below: These indicate the chitest value of the vibration signal for a degree of freedom being 8 and a chi square estimated at 8 d.f and 5 percent significance level is 15.51.

Any value above the significance level will force the chitest to be rejected and values below this will accept that the test is Gaussian. From the table below it can be observed that all the values fall below and hence this strongly recommend that at an incipient stage the distribution of a Gaussian kind.

Table 4.1: The chi square values

| Bearing Condition | No Load | Slight Load | Half Load | Three Quarter Load |
|----------------------|---------|-------------|-----------|--------------------|
| Healthy (Fault Free) | 14.83 | 3.23 | 5.14 | 10.98 |
| Outer Race Fault | 9.38 | 2.7 | 5.76 | 10.73 |
| Inner Race Fault | 3.22 | 3.64 | 3.6 | 5.7 |

Figure 4.4 represents the no load condition of a healthy machine. The first curve shows the plot of expected value and the second curve shows the observed value. The third curve gives the chi square value and is such that if the amplitudes are added it gives the final chi square value which is shown in Table 4.1 to be 14.83 which is less than the estimated chi square value of 15.51 and hence the test is accepted. The acceptance is an affirmation that it is a Gaussian distribution.

Chi Square Test on Healthy Machine

Healthy No Load Condition

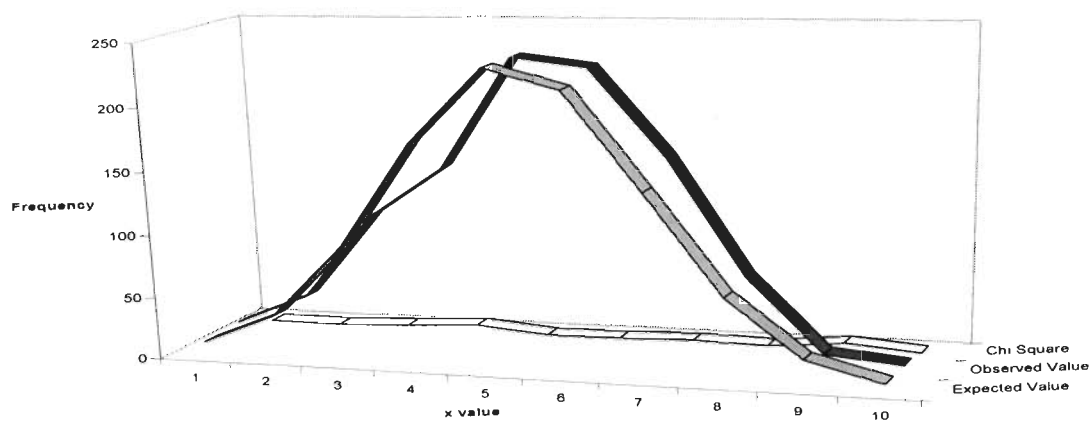


Figure 4.4: Observed and expected frequency for no load vibration for healthy bearing

Healthy Slight Load Condition

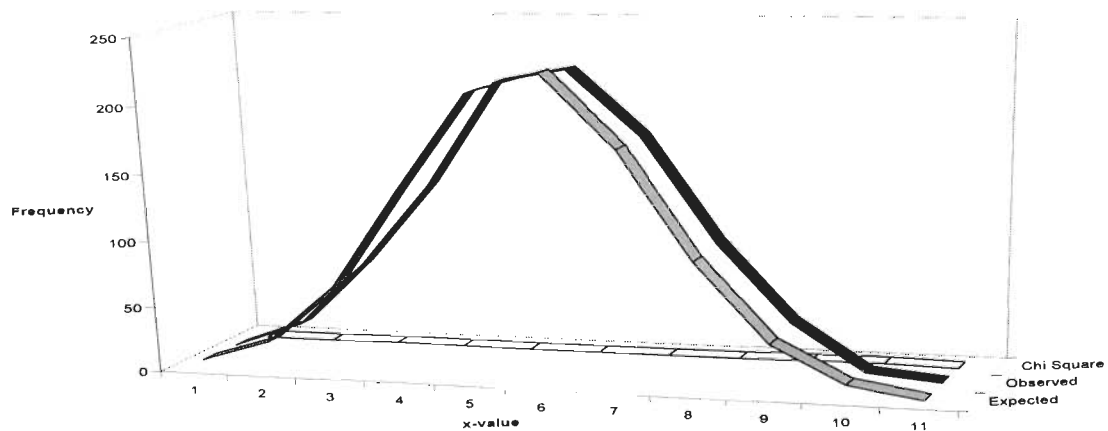


Figure 4.5: Observed and expected frequency for slight load vibration for healthy bearing

The above Figure 4.5 shows a healthy machine with slight load and has a chi square value to be 3.23 given in Table 4.1 which is less than 15.51 and hence the chi theory is accepted. The signal is Gaussian.

Healthy Half Load Condition

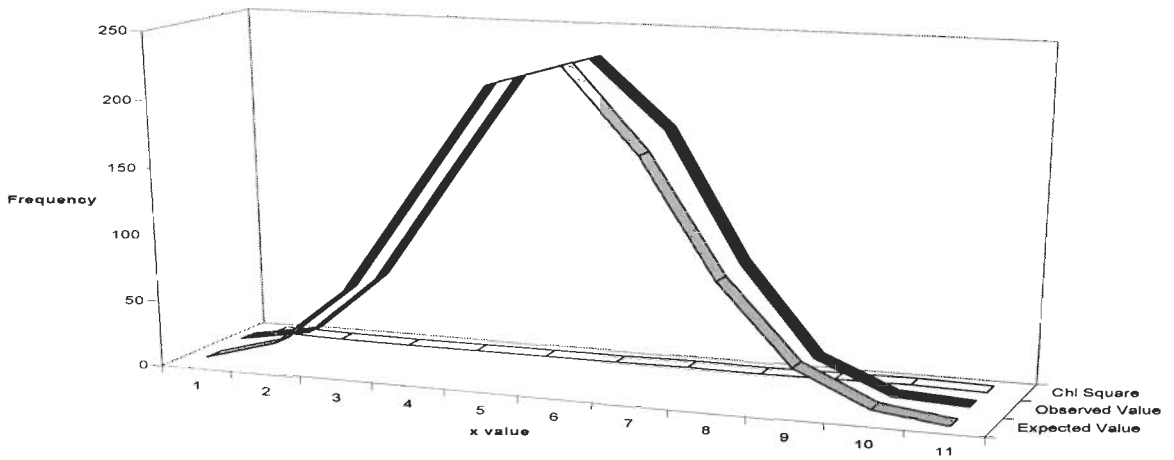


Figure 4.6: Observed and expected frequency for half load vibration for healthy bearing
 The above Figure 4.6 shows a healthy machine with Half load and has a chi square value to be 5.14 given in Table 4.1 which is less than 15.51 and hence the chi theory is accepted. The signal is Gaussian.

Healthy Three Quarter Load Condition

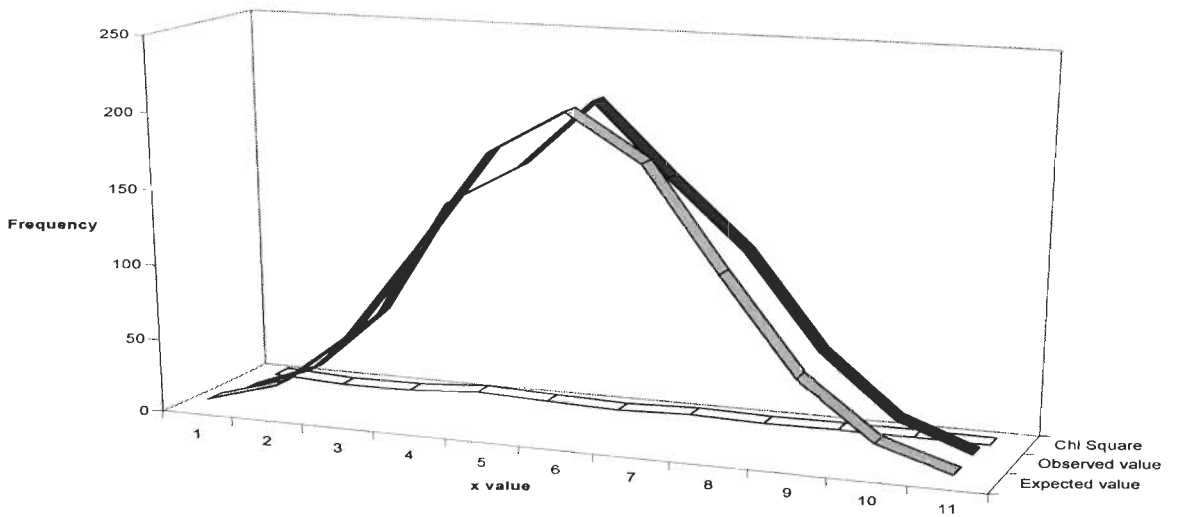


Figure 4.7: Observed and expected frequency for three quarter load vibration for healthy bearing.

The above Figure 4.7 shows a healthy machine with Three Quarter load and has a chi square value to be 10.98 given in Table 4.1 which is less than 15.51 and hence the chi theory is accepted. The signal is Gaussian.

Chi Square Test on Outer Race Fault

Similar chi square test were performed for the outer race fault at an incipient stage as was performed for the healthy condition. Four load conditions are shown below.

Outer Race Fault No Load

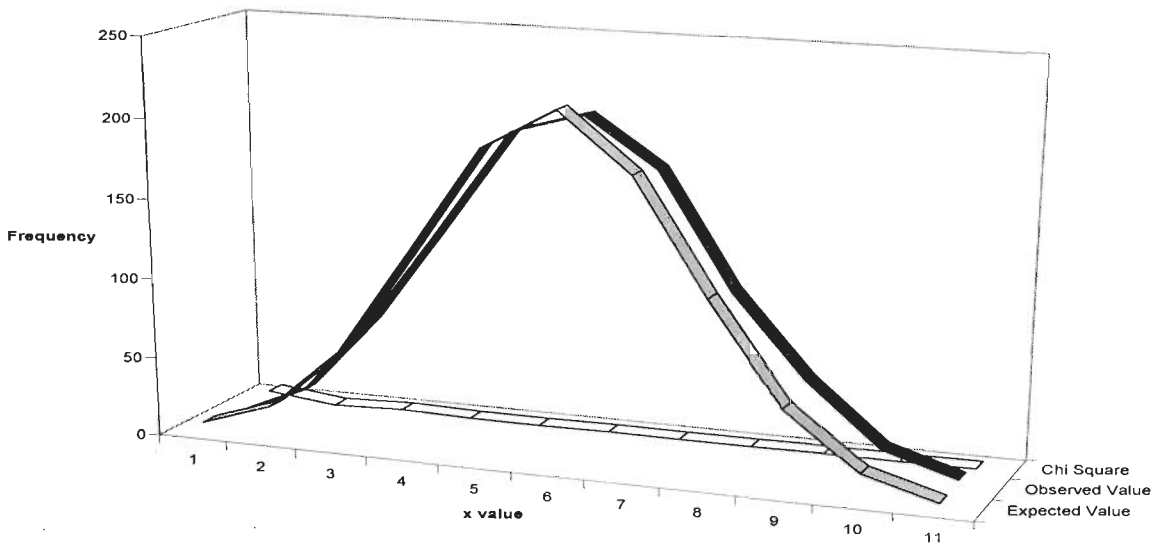


Figure 4.8: Observed and expected frequency for no load vibration for ORF

The above Figure 4.8 shows a outer race fault with No load and has a chi square value to be 9.38 given in Table 4.1 which is less than 15.51 and hence the chi theory is accepted. The signal is Gaussian.

Outer Race Fault Slight Load

The Figure 4.9 below shows an outer race fault with Slight load and has a chi square value to be 2.7 given in Table 4.1 which is less than 15.51 and hence the chi theory is accepted. The signal is Gaussian.

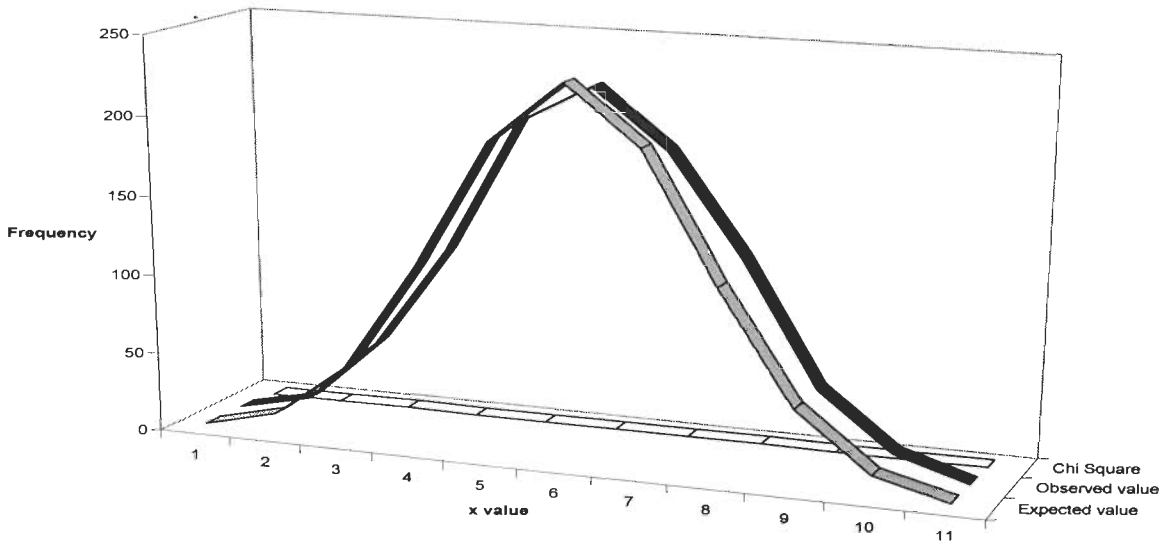


Figure 4.9: Observed and expected frequency for slight load vibration for ORF

The Figure 4.10 below shows an outer race fault with Slight load and has a chi square value to be 5.76 given in Table 4.1 which is less than 15.51 and hence the chi theory is accepted. The signal is Gaussian.

Outer Race Fault Half Load

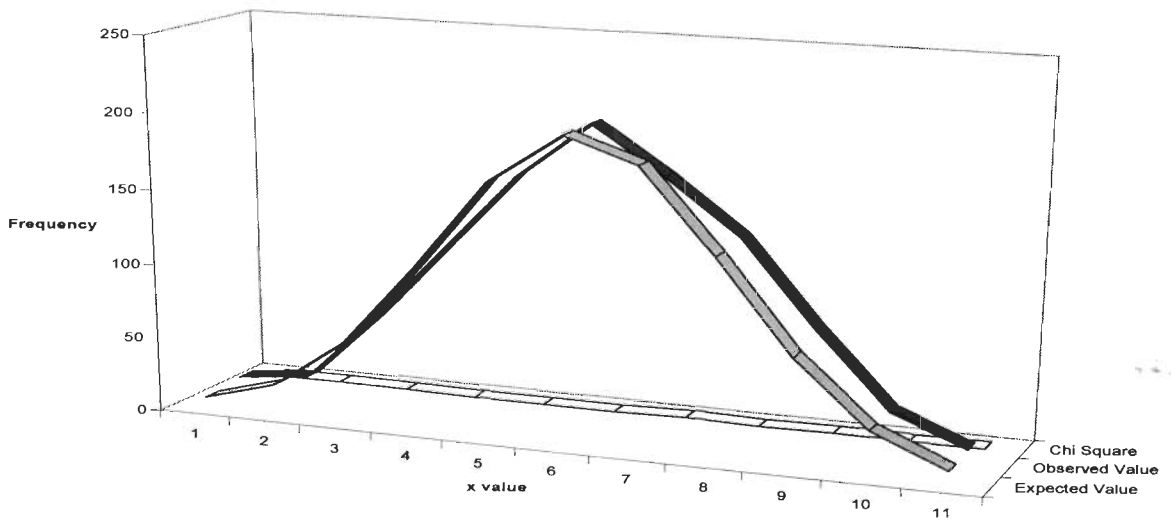


Figure 4.10: Observed and expected frequency for half load vibration for ORF

Outer Race Fault Three Quarter Load

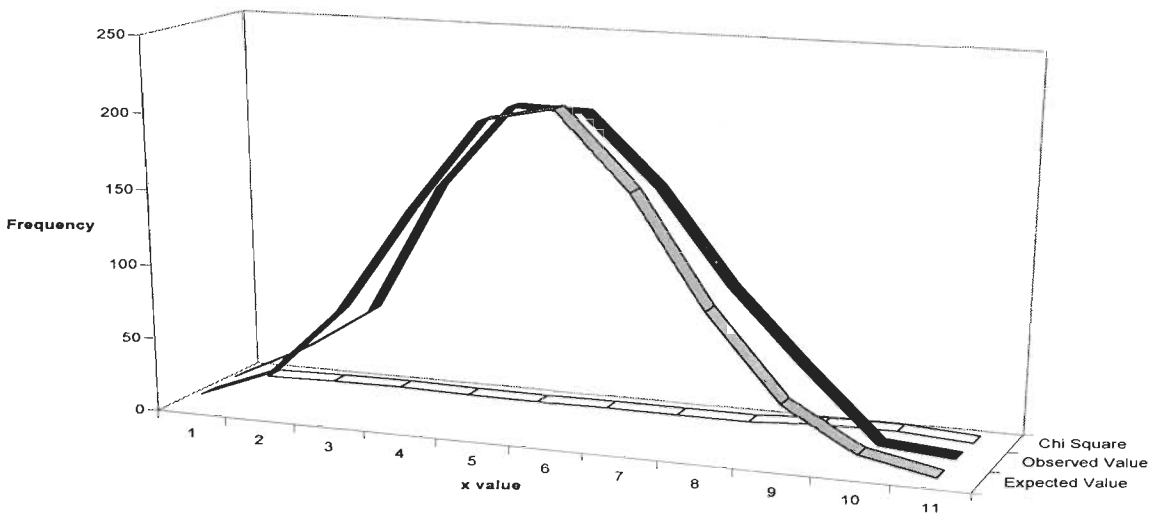


Figure 4.11: Observed and expected frequency for three quarter load vibration for ORF

The above Figure 4.11 shows an outer race fault with Three Quarter load and has a chi square value to be 10.73 given in Table 4.1 which is less than 15.51 and hence the chi theory is accepted. The signal is Gaussian.

Chi Square Test on Inner Race Fault

Similar chi square test were performed for the inner race fault at an incipient stage as was performed for the healthy and outer race fault condition. Four load conditions are shown below.

Inner Race Fault No Load

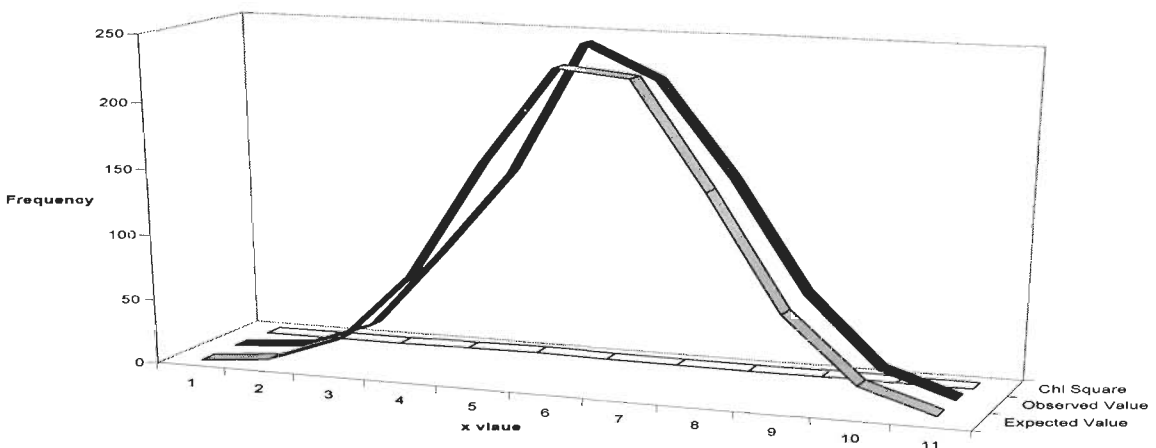


Figure 4.12: Observed and expected frequency for no load vibration for IRF

The above Figure 4.12 shows an inner race fault with No load and has a chi square value to be 3.22 given in Table 4.1 which is less than 15.51 and hence the chi theory is accepted. The signal is Gaussian.

Inner Race Fault Slight Load

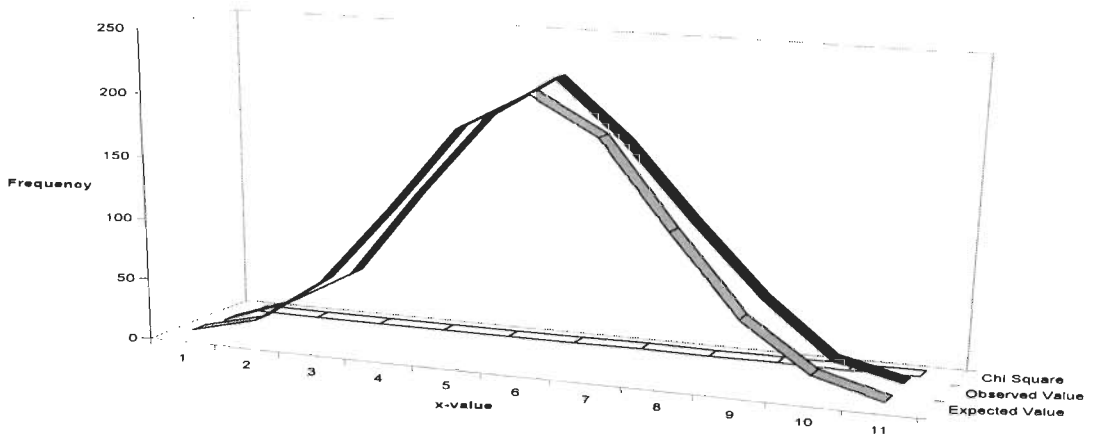


Figure 4.13: Observed and expected frequency for slight load vibration for IRF

The above Figure 4.13 shows an inner race fault with Slight load and has a chi square value to be 3.64 given in Table 4.1 which is less than 15.51 and hence the chi theory is accepted. The signal is Gaussian.

Inner Race Fault Half Load

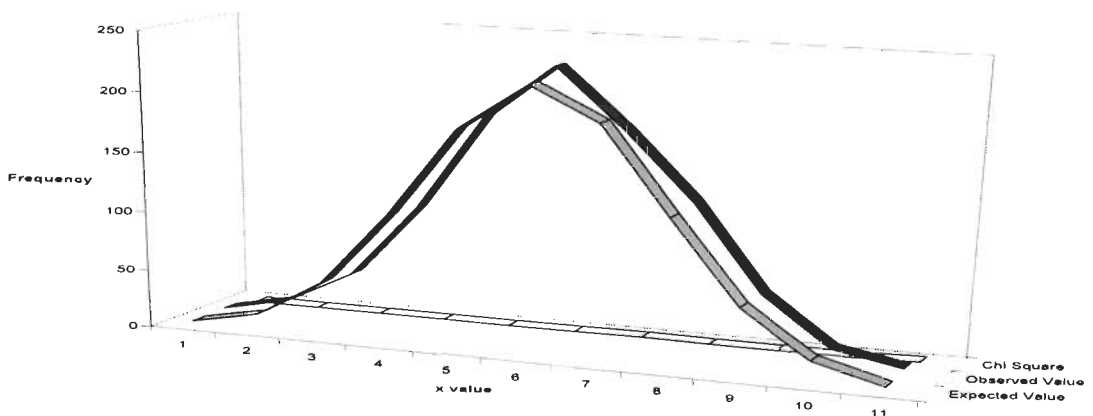


Figure 4.14: Observed and expected frequency for half load vibration for IRF

The above Figure 4.14 shows an inner race fault with half load and has a chi square value to be 3.6 given in Table 4.1 which is less than 15.51 and hence the chi theory is accepted. The signal is Gaussian.

Inner Race Fault Three Quarter Load

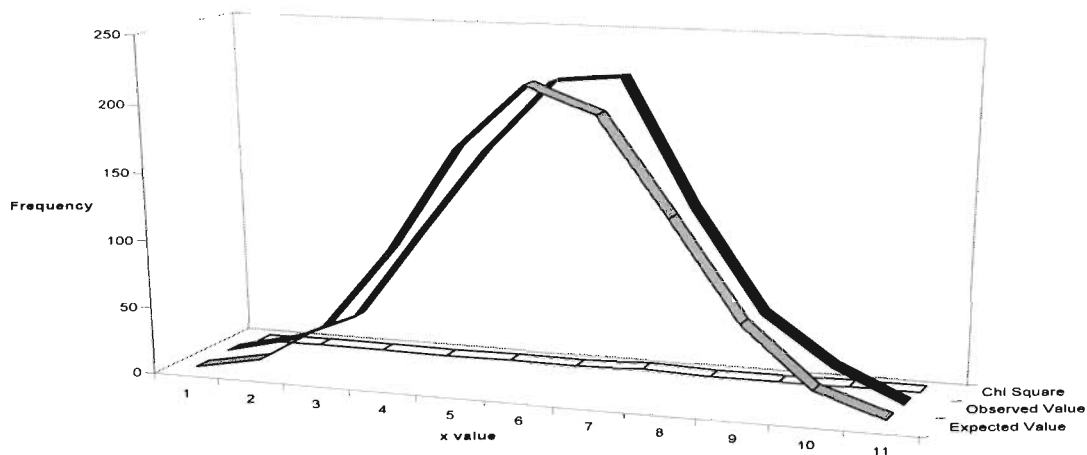


Figure 4.15: Observed and expected frequency for three quarter load vibration for IRF

The above Figure 4.15 shows an inner race fault with Three Quarter load and has a chi square value to be 5.7 is given in Table 4.1 which is less than 15.51 and hence the chi theory is accepted. The signal is Gaussian.

4.9 Conclusions

The chitest was executed for three conditions namely healthy, outer and inner race faults with further four conditions of no load, slight load, half load and three quarter load and the results show that the degree of freedom is 8 and the significance level at d.f=8 is 15.51. The goodness of fit test was executed and the results show that for an incipient stage fault, when the motor was driven at its rated value is Gaussian. Thus, describes the further analysis techniques that can be implemented on the vibration signal.

The most important observation was that from no load to three quarter load for both healthy and faulty condition at an incipient stage the results are found to be normally distributed.

A Statistical Approach for Fault Diagnosis of Ball Bearings in Electrical Machines

In this chapter, diagnosis of, outer race fault and inner race fault are considered. The analysis technique used are; statistical parameters and statistical inference. Frequency domain analysis is also carried out to validate the results.

The aim of this chapter is to compare the variations of a time domain signal of machine vibrations when the bearing is (a) healthy (fault free), (b) having a fault in the outer race and (c) having a fault in the inner race. The statistical approach is used to investigate and classify the faults. The well known frequency domain analysis is carried out to verify the results of the statistical analysis. The proposed analysis technique implies a clear indication of the changes that occur even when a fault is at an incipient stage.

5.1 Introduction

The constant running of a rotating machine causes a continuous wear and tear. M.L. Sin et al [97] suggest that 40% of induction machine faults are caused due to the bearings. T. Williams et al [143] further categorize the bearing related faults as 18% for outer race faults, 64% for inner race faults and 18% for other bearing-related defects in ball bearings. J.R.Stack, et al and N.Tandon, et al [64,99] describes the faults to be grouped as localized or distributed and the intention is to clearly separate bearing faults according to the effect the fault has on the measurable machine parameter (e.g. Vibration).

This chapter treats a localized fault which depicts a fault at its incipient stage. The parameter under consideration is vibration whereby K.Gilman, [71] states that although acceleration amplitude at a given frequency does constantly change, its average value tends to remain relatively constant. S.Nandi, and H.A. Toliyat, [133] affirms that even under normal operating conditions with balanced load and good alignment, fatigue failures may take place. These faults may lead to increased vibration and noise levels as reported by N.Tandon, et al and S.Nandi, et al [99, 133]. K.Mori, et al [74] applied discrete wavelet transform (DWT) to vibration signals to predict the occurrence of spalling in ball bearings but eventually the paper states that as the threshold value cannot be chosen in a systematic way at present, further

investigation will be necessary.

This study pinpoints a specific fault and highlights the region of interest when a fault has just erupted. Statistical technique can be divided into descriptive statistics which is defined by statistical parameters and statistical inference. These terms will be explained later. Descriptive statistics deals with collecting, processing and analysis of data in a way that makes it comprehensive. G.Keller & B. Warrack, [40] and S.Seker, et al [137] shows that statistical parameters such as mean value, standard deviation, skewness and kurtosis are analyzed, and define a critical situation related to the degradation of the motor bearing as determined by one of these statistical parameters. They establish that standard deviation is most important and is used for the determination of the bearing damage level.

They further report that for a perfect normal (Gaussian) distribution, the skewness factor is zero which is also stated by [49,114,141] and kurtosis factor is three stated in [49, 99, 114, 129,141,143]. N. Tandon, et al, S. A. S.Kazzaz, S. Wadhvani, and T.Williams. et al [99, 129,140,143] also have evaluated the peak and crest factor. The vibration signal is random in nature and researchers have only classified data of healthy bearing as Gaussian and when a fault occurs the signal has been said to be non Gaussian. H.R. Martin et al and R.B.W. Heng, et al [49, 114] quote that for the bearing in a correctly lubricated condition, the kurtosis for normal distribution is given in the range of 3.0 to 3.5. Some of the researchers suggest that as a fault occur the kurtosis value increases and others say that the kurtosis value decreases. This chapter eradicates this controversy and shows that for a single point defect the kurtosis remains fairly constant as seen in Table 4.

The statistical inference deals with interpreting data and concluding from the results obtained for the same data as stated in G.Keller, and B.Warrack, [40]. K.Gilman, [72] defines a key concept that many random processes have so called Gaussian amplitude probability distribution.

The probability density function have been approached by K.Gilman, and S.Seker, et al [71, 49,72,129] and it has been noted that vibration signature of a healthy machine exhibits a Gaussian probability density. N. Tandon, et al [99, 129] mention that as the machine develops a fault, its vibration begins to generate a distribution that deviates from Gaussian. K.Gilman, [72] also defines that the signal spends a greater percentage of its time at higher amplitude levels, and the waveform becomes less smooth and spiky. In this chapter, the cumulative distribution is also considered that shows not only the range by which the distribution has spread but also the acceleration levels for different faults at different probabilities.

This chapter categorizes the statistical parameters into three measures:

- i) Measure of central tendency-MCT
- ii) Measure of variability -MV
- iii) Measure of dispersion-MD

This chapter also focuses on the frequency domain method in which J.R. Stack, et al [64] states that a single point defect produces one of the four characteristic fault frequencies depending on which surface of the bearing contains the fault. A.Choudary, et al , J.R. Stack, et al and T. Williams, et al [2,64,143] suggest that as the fault increases in severity the magnitude of the broadband changes in machine vibration increases accordingly. M.L. Sin, et al and S.Nandi, et al [97, 133] also mention the effectiveness of evaluating the FFT and verifying it by the Bearing Characteristic Frequency (BFC).

5.2 Analysis of the Data Acquired

The vibration data was sensed by the accelerometer and was processed. This has been fully described in chapters 2 and 3. The acquired vibration signal is stored in an Excel file. This allows the analysis and inferences to be easily executed. This chapter shows three conditions: (a) when the bearing is healthy, (b) with outer race faults, and (c) with inner race faults and results are classified as case1, case2 and case3 respectively. Firstly, the time representation is given for the three cases. Secondly, the statistical analysis is divided into two components a) statistical parameters are evaluated for the three cases. b) the statistical inferences which incorporates PDF and CDF are considered for the above mentioned cases. Lastly, the FFT is calculated to establish the Bearing Characteristic Frequency BCF.

5.2.1 Time Domain Signal: Figure 5.1, 5.2 and 5.3 show time domain representations for the first 500 samples (i.e. depicted on a 0 to 0.8 ms scale) that have been selected from total 50000 samples acquired. The time domain signal shows that for a healthy bearing the magnitude swing is minimum whereas for an outer race fault and inner race fault the amplitude swing has considerably increased. An increase in the amplitude of the vibration signal indicates an increase in the range. This infers that as fault is introduced the variation in the time domain signal increases which further reflects in a rise in deviations, sample variance and standard deviations. The statistical parameters are compiled in Table 5.1 for a healthy, outer race fault and an inner race fault and the vibration signal for the three cases is shown in Figures 5.1, 5.2 and 5.3 respectively.

Case1: Healthy Bearing

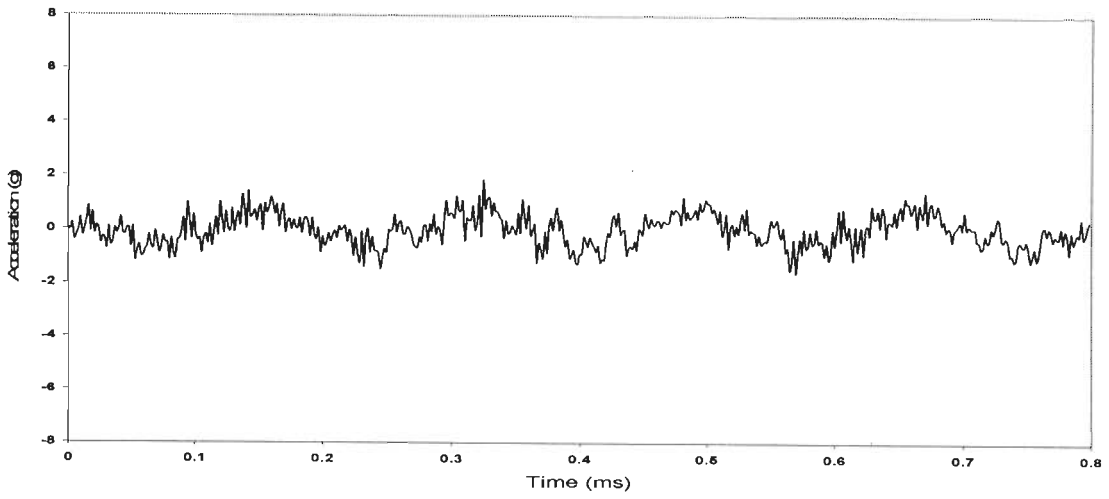


Figure 5.1: Vibration signal for a healthy bearing.

Case2: Outer Race Fault

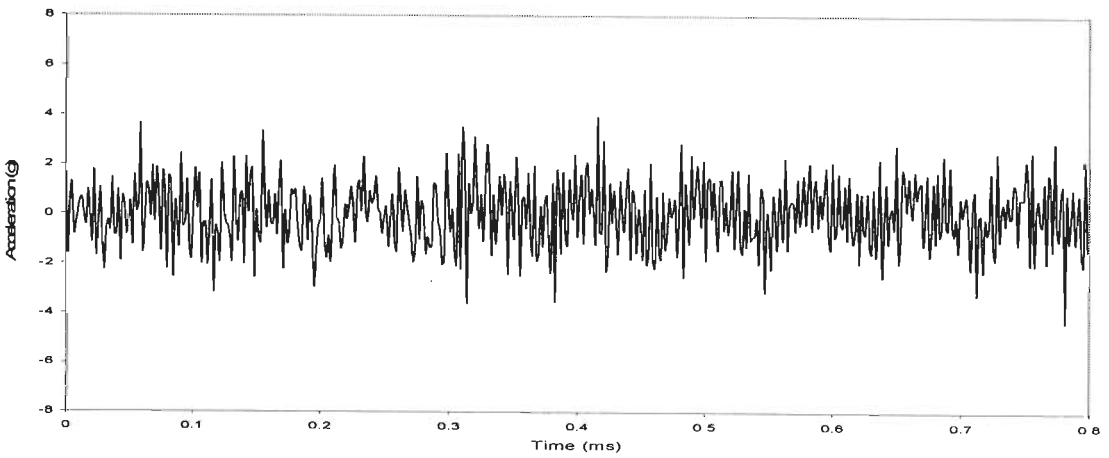


Figure 5.2: Vibration signal for an outer race bearing fault.

Case3: Inner Race Fault

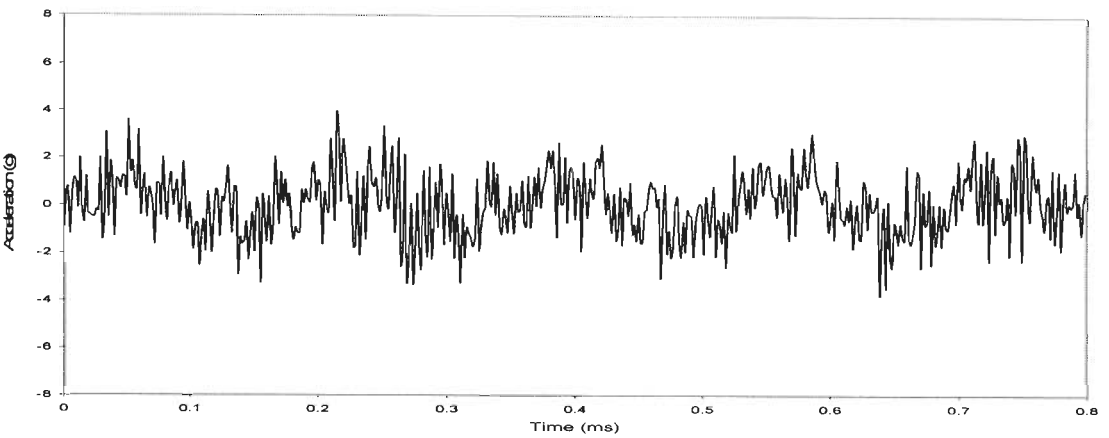


Figure 5.3: Vibration signal for an inner race bearing fault.

5.3 Statistical Parameter

The descriptive statistics involves the calculation of the mean, standard error, median, mode, standard deviation, sample variance, kurtosis, skewness, range, minimum, maximum, count and confidence interval as given by G.Keller[40]. S.Serker and E.Ayaz [136] quote that the data analysis is by means of the statistical parameter such as mean value, standard deviation, skewness and kurtosis but this chapter shows that all parameters play an important role in understanding the vibration signal.

Table 5.1: A comparative study of the statistical values obtained for a bearing under the condition (a) healthy, (b) outer race faults, and (c) inner race faults.

| BEARING FAULT CONDITION | | | |
|--------------------------------------|---------|------------|------------|
| PARAMETERS | HEALTHY | OUTER RACE | INNER RACE |
| Mean (g) MCT | -0.004 | -0.009 | -0.003 |
| Standard Error (g) MV | 0.003 | 0.006 | 0.006 |
| Median (g) MCT | -0.015 | 0.000 | -0.024 |
| Mode (g) MCT | -0.269 | 0.073 | -0.176 |
| Standard Deviation (g) MV | 0.603 | 1.261 | 1.378 |
| Sample Variance (g ²) MV | 0.364 | 1.589 | 1.899 |
| Kurtosis MD | 3.344 | 2.766 | 3.040 |
| Skewness MD | 0.057 | -0.034 | 0.047 |
| Range (g) MV | 4.346 | 9.512 | 11.538 |
| Minimum (g) | -2.114 | -4.902 | -6.089 |
| Maximum (g) | 2.231 | 4.609 | 5.449 |

| | | | |
|--------------------------------|--------------|--------------|--------------|
| Confidence Level(95.0%) (g) | 0.005 | 0.011 | 0.012 |
|--------------------------------|--------------|--------------|--------------|

As described in chapter 3, the statistical parameter can be subdivided into 1) measure of central tendency 2) measure of variability 3) measure of dispersion. Table 5.1 shows a comparative study obtained for the three cases under consideration in this chapter.

- 1) Measure of Central Tendency (MCT): A good measure of the central tendency is defined by the mean, median and mode as given by G.Keller, et al [40]. The mean, median, and mode have almost zero value as indicated in Table 5.1. This central tendency swings about zero value for healthy and faulty conditions and is very small. This study shows that MCT is not much affected at an incipient stage.
- 2) Measure of Variability (MV): This measure of variability is the range, variance, standard deviation and standard error as given by G.Keller, et al [40]. The standard error indicates how much variability exists in a distribution of sample means. Table 5.1 shows that each of the three parameters of the variability has a minimum value for healthy bearing and an increase in variability for an outer race and inner race fault. For example, the value of range is 4.436g, 9.512g and 11.53g for healthy, outer race and inner race faults respectively. This study shows that these parameters have a significant role at the incipient stage.
- 3) Measure of Dispersion (MD): The kurtosis and skewness portrays the measure of dispersion. M.L.Sin, et al [97] state that for a good quality surface, it can be shown theoretically that the kurtosis coefficient takes on the numerical values of 3.0 to 3.5. Table 5.1 indicates that the kurtosis value is very close to 3.0 for all the three cases that shows that if the value of kurtosis is 3.0 then it should follow a Gaussian distribution. Similarly, the skewness for the three cases remains at zero. This study shows that MD is not much affected at an incipient stage.

The minimum and maximum values also increase gradually showing a distinct spread in the range. As seen in Table 5.1, the confidence level is 0.005g for healthy, 0.011 g for outer race fault, and 0.012 g for the inner race fault at 95% confidence interval. This further implies that the significance level is highest for a healthy bearing.

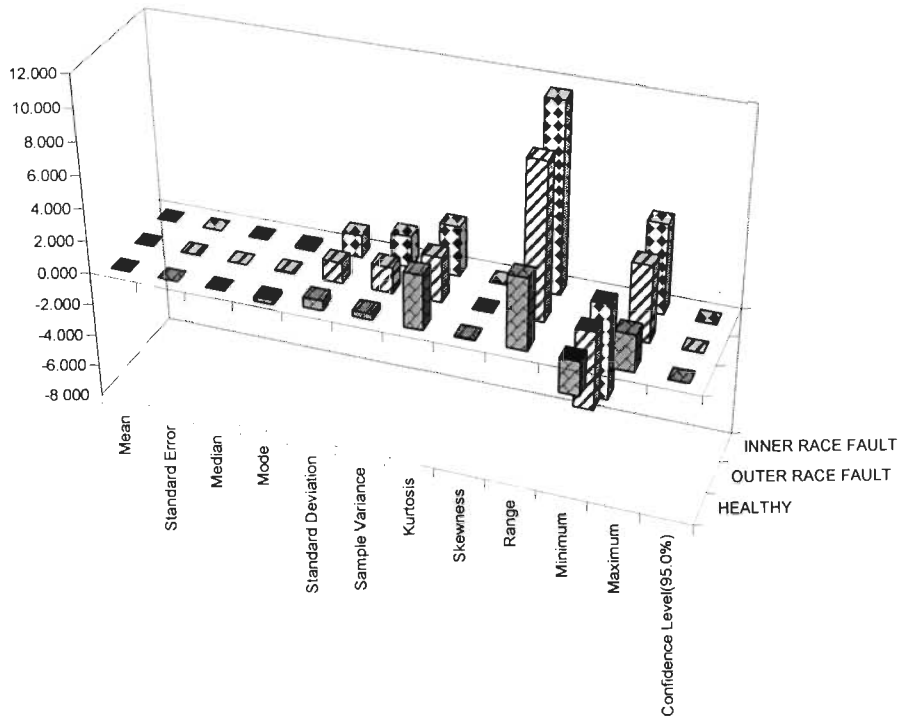


Figure 5.4: A 3-D plot showing the behaviour of the statistical parameters in the three cases.

The values obtained in Table 5.1 are pictorially depicted as the 3-D plot which shows the distinctive behaviour of the statistical parameters for the three cases as in Figure 5.4. This graph shows that for a single point defect at an incipient stage, the parameters of importance are the measure of variability. The graph shows that the bars have a significant change for standard deviation, sample variance, range, minimum and maximum values.

5.4 Statistical Inferences

A key concept is the fact that many random processes have so called Gaussian amplitude probability distributions. This means that the positive peaks in the random signal, when accumulated will distribute in a Gaussian manner as stated by K.Gilman, [71]. From Table 5.1 it has been calculated that kurtosis is near about 3, this confirms that it is a Normal distribution. Hence, in this chapter the probability density and cumulative distribution are considered which are classified under the statistical inferences.

5.4.1 Probability Density Function

To analyze the vibration signal for a bearing in good condition, along with a sample probability density function (PDF) portrays that a bearing in good condition has a vibration probability density that depicts a roughly Gaussian (bell shaped) curve. N.Tandon and

A.Choudhury [99] quote that the probability density of the acceleration of a bearing in good condition has a Gaussian distribution, whereas a damaged bearing results in non-Gaussian distribution with dominant tails because of a relative increase in the number of high levels of acceleration, whereas, K.Gilman, [71] states that the measurement of random processes is statistical in nature; all the concepts and definitions of statistics apply as suggested by K.Gilman, [72] state that the power spectral density seems to imply that it has something to do with distribution of power over a spectrum or frequency range.

In Table 5.1 it can be seen that the kurtosis lies in the range of 2.7 to 3.3 irrespective of damaged or non damaged bearing for a single point defect indicates a behaviour that might be close to the normal distribution. This data was further validated by the χ^2 -test which clearly shows that it satisfies the distribution. Chi square estimated at 8 Degree of freedom and 5% of significance level is 15.51 and the χ^2 -values obtained are 5.14, 5.76 and 3.61 for a healthy bearing, an outer race, and an inner race fault, respectively. Thus the results of this chapter show that the vibration signals are Gaussian in nature irrespective of healthy and non healthy conditions.

The statistical inference can be derived from the probability density function which is represented as the Gaussian distribution function and is given by the equation that has been explained in chapter 3.

$$f(x) = (1/\sigma\sqrt{2\pi})\exp(-1/2)(x - m/\sigma)^2$$

Case1: Healthy Bearing

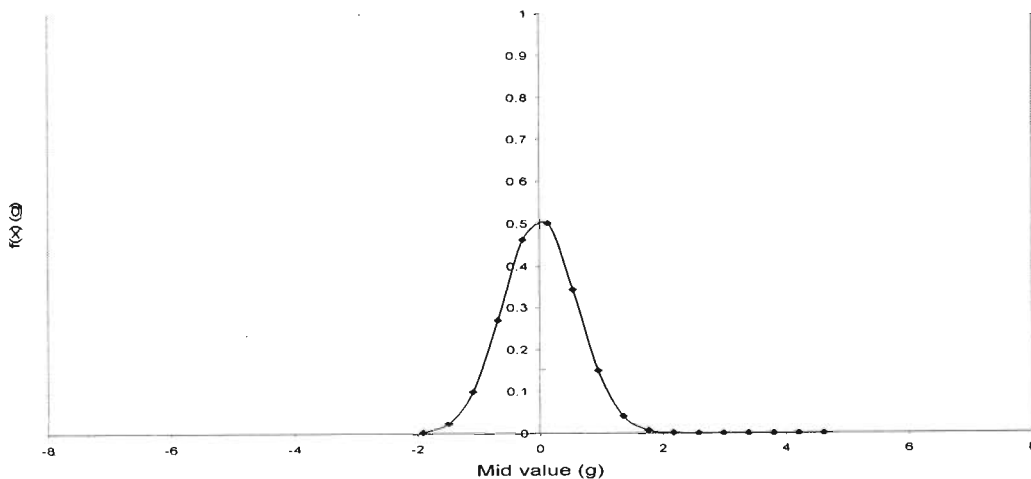


Figure 5.5: Probability density function of healthy bearing data.

Case2: Outer Race Fault

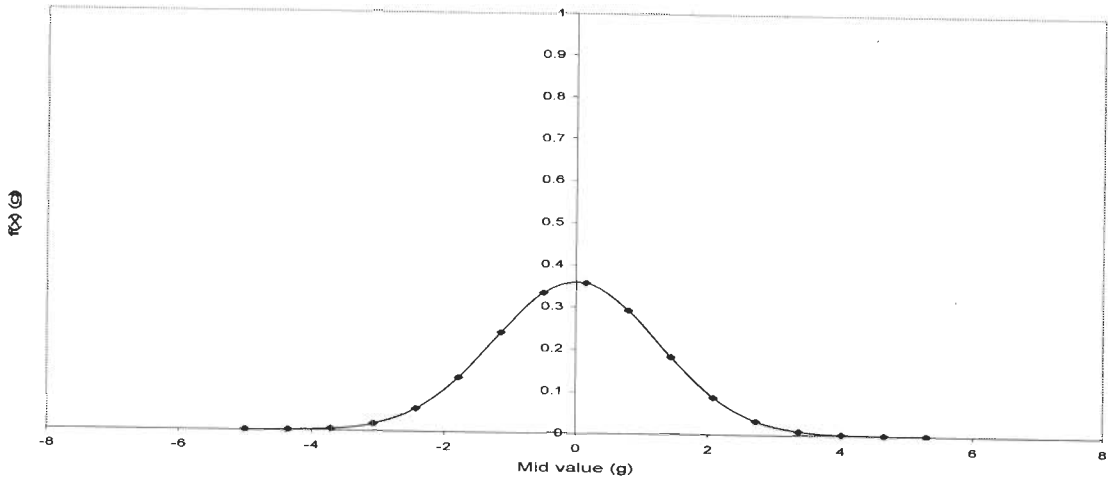


Figure 5.6: Probability density function of an outer race bearing fault.

Case3: Inner Race Fault

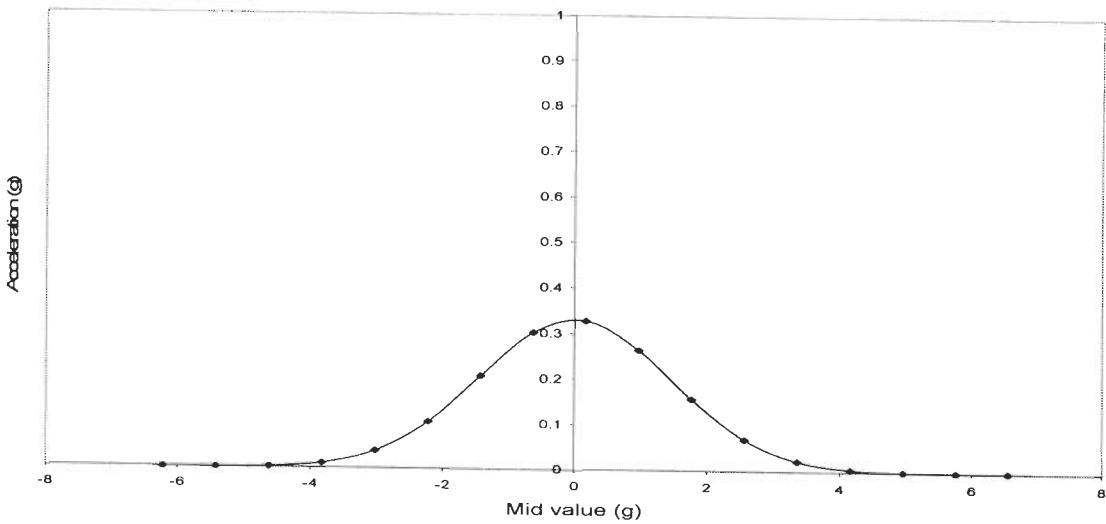


Figure 5.7: Probability density function of an inner race bearing fault.

The probability density function indicates that as the measure of variability increases the spread increases which can be seen in Figure 5.5 - 5.7. The healthy machine has higher maximum value than the non healthy machine. For case1, case2 and case 3, $f(x)$ is 0.50g, 0.35g and 0.33g, respectively whereas the range of case1, case2 and case 3, is 4.34g, 9.51g and 11.54g, respectively. This shows that as the magnitudes of $f(x)$ decreases, the range increases gradually for a healthy bearing, an outer race fault, and an inner race fault. The lesser the range variation of the signal the lesser is the fault indicating a healthy machine. But in the third case, for an inner race fault the $f(x)$ value is minimum which means the amplitude has dipped

significantly, but the range is high; this study implies that higher the spread, lower the $f(x)$, and the larger is the variation in the time domain signal clearly indicating a fault.

5.4.2 Cumulative Distribution Function

The cumulative distribution function (CDF) is given by the following equation given in chapter 3

$$F(X) = \int f(x)dx$$

Where $F(x)$ =cumulative distribution function

The probability density function was calculated for 50000 samples and the cumulative distribution is evaluated for these values of the probability density function.

Case1: Healthy Bearing

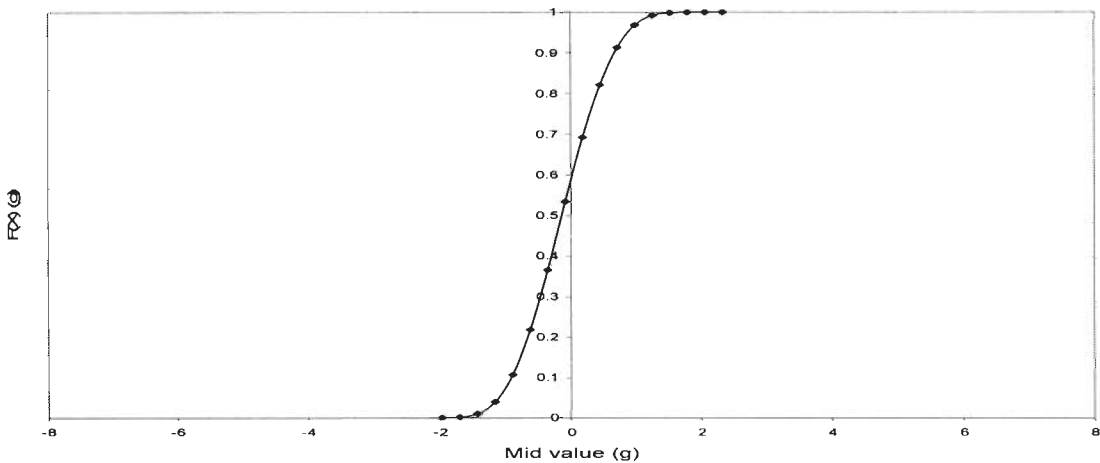


Figure 5.8: Cumulative distribution function of a healthy bearing

Case2: Outer Race Fault

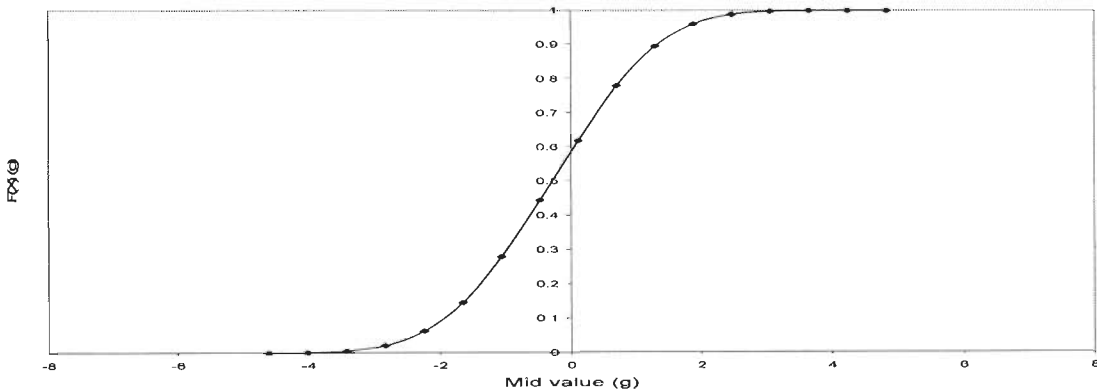


Figure 5.9: Cumulative distribution function of an outer race fault

Case3: Inner Race Fault

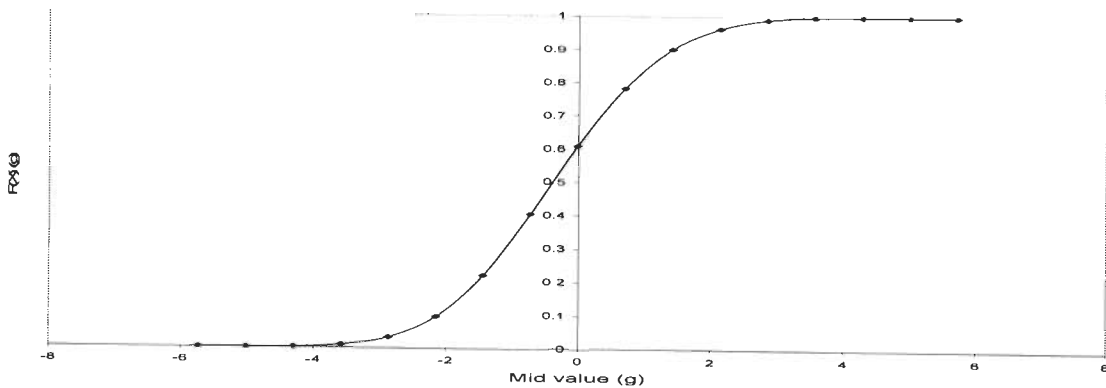


Figure 5.10: Cumulative distribution function of an inner race fault

In Figures 5.8, 5.9 and 5.10 it can be seen that at 10% and 90% the acceleration levels are shown by the g-values and are (-0.9g to 0.7g), (-1.65g to 0.89g), (-2.15g to 1.42g) for the healthy bearing, outer race fault, and inner race fault, respectively. The variations obtained for probability density functions are reflected on the cumulative distribution function where the maximum dispersion can be seen in Figure 5.10 of an inner race fault. This variation in range shown in PDF is reflected in CDF. Case1 gives a sharp curve with least range; case 2 shows a much wider range and a more sloping curve and finally case 3 gives the a steep slope with highest range indicating a spread in the curve of both PDF and CDF.

5.5 Frequency Domain Signals

Frequency Analysis using Fourier Transform is the most common signal processing method as stated by M.L. Sin, [97]. A single point defect produces one of the four characteristic fault frequencies depending on which surface of the bearing contains the fault. These predictable frequency components typically appear on the machine vibration. The presence of a defect causes a significant increase in the vibration level quoted by J.R. Stack, et al, N. Tandon, et al and S.Nandi, et al, [64, 99,133].

Bearing fault-related defects can be categorized as outer bearing race defect, inner bearing race defect, ball defect and train defect. A NBC 6308 bearing having 7 balls was employed. The vibration frequency was characterized according to the defects given by M.L.Sin, T.Williams, et al, J.R.Stack, et al, S.Nandi, et al, and A.Choudhary, et al [97,143,,64,2] :

From chapter 3 the BCF for f_o, f_i, f_{bd}, f_{td} are the characteristic vibration frequencies which are 64.62Hz for outer race, for inner race 103.38Hz, for ball defect 49.23Hz and for train defect 9.23Hz for bearing number 6308. These frequencies are of interest for fault detection.

Table 5.2 shows the BCF in terms of the calculated value. The practical results are as shown below. To obtain these results the number of samples considered to evaluate are $2^{11}= 2048$ and $2^{12}= 4096$ data points on which FFT was evaluated and only one average value was considered. This consideration was also taken care of in the Machine Analyzer.

| Type of Bearing | Calculated Value | Practical Value | Practical Magnitude |
|-----------------|------------------|-----------------|---------------------|
| Outer Race | 64.62Hz | 63.75Hz | 0.0747g |
| Inner Race | 103.38Hz | 99.375Hz | 0.4906 g |

Table 5.2: A comparative study of the calculated and the practical value magnitudes of the FFT spectra for the three cases.

Case1: Healthy Bearing

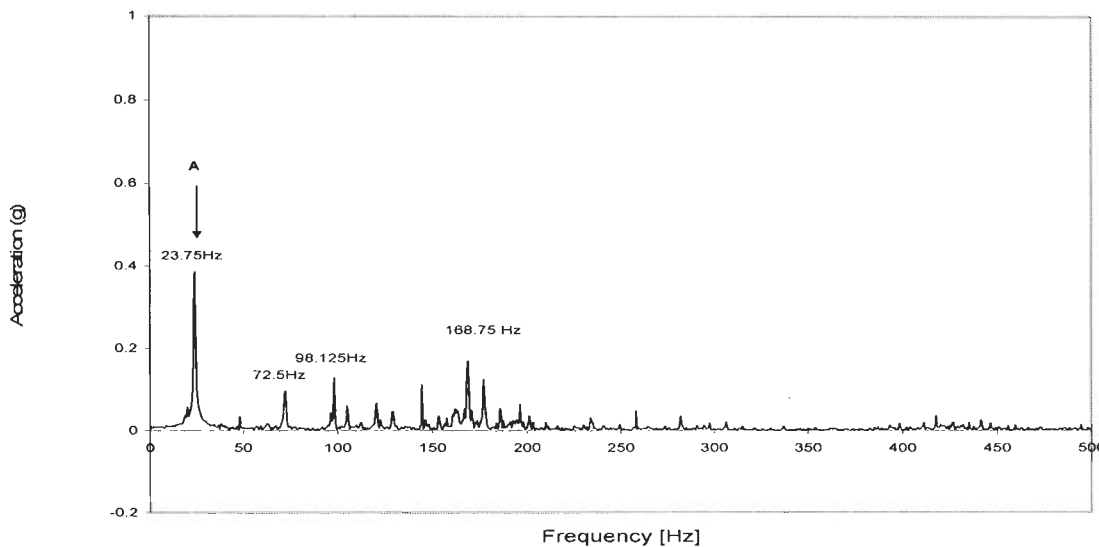


Figure 5.11: Frequency spectrum of a healthy machine.

Case2: Outer Race Fault

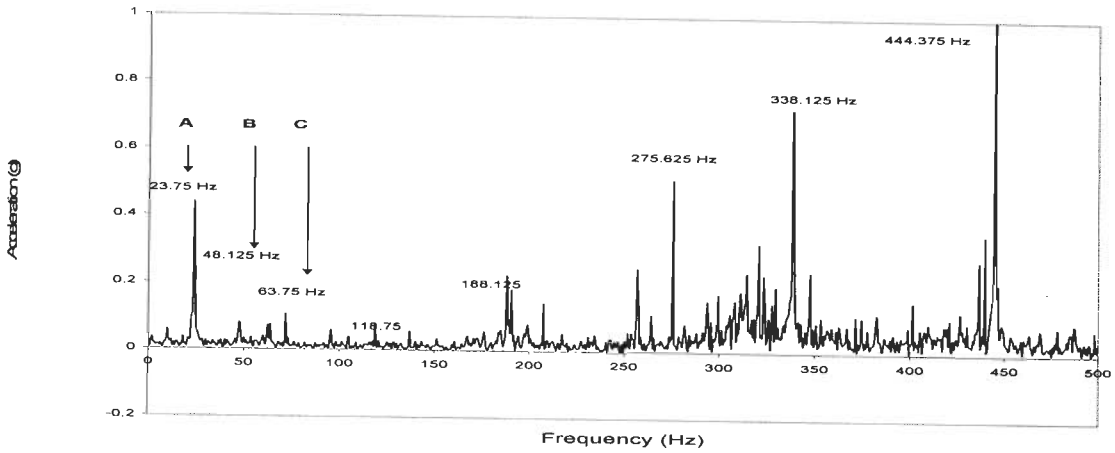


Figure 5.12: Frequency spectrum of an outer race fault.

Case3: Inner Race Fault

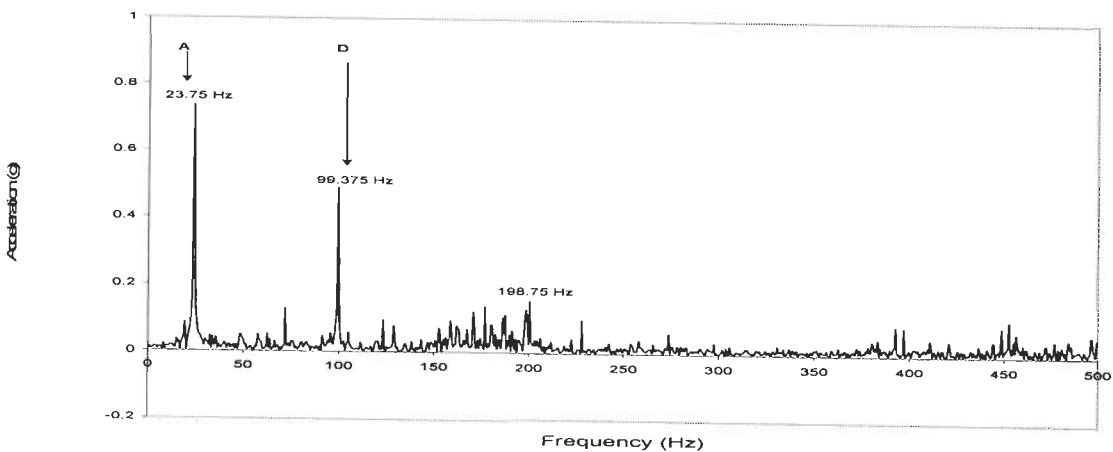


Figure 5.13: Frequency spectrum of an inner race fault.

As shown in Figures 5.11, 5.12 and 5.13 the significant frequencies of interest are given as A, B, C and D. Where the bearing characteristic frequency (BCF) obtained from the vibration data is given as

1. A-Rotational frequency
2. B-Ball Spin Frequency
3. C-Outer Race Frequency
4. D-Inner Race Fault

The healthy spectrum shows the peak at 23.75Hz which is the rotational frequency; rest of the components is not significant. Meanwhile, in Table 5.2 it can be seen that a peak has erupted at 63.75 Hz which signifies an outer race fault and similarly for an inner race fault the peak is at 99.375Hz.

The respective magnitudes are shown in Table 5.2. These peaks have erupted and it is speculated that as the severity of fault increases the magnitude levels should rise.

Discussion: This compares the three signals the healthy (fault free), outer race fault and inner race fault. The different comparisons are as given below:

Time Signal

The time domain signal is depicted in Figures 5.1, 5.2 & 5.3 for healthy bearing, an outer race fault and an inner race fault, respectively. Figure 5.1 show a minimum variation of the vibration signal followed by an increase in variations in Figure 5.2 and the maximum variation is obtained in Figure 5.3. This increase in variation is an indication of an increase in the measure of variability.

Statistical Parameter

As shown in Table 5.1, the central tendency parameters are swinging near zero for both healthy and faulty conditions. This is because the fault is a point fault. In the case of an increase in severity, changes might occur in the statistical parameters with an increase in standard deviation, range, sample variance and kurtosis.

The measure of variability parameter increases gradually from healthy bearing, outer race fault and inner race fault. The measure of the dispersion parameter shows that kurtosis value are very close to 3 which is due to the point defect but as the severity of fault increases the kurtosis value falls below 3 whereas the skewness value is at zero.

The minimum and maximum values of the vibration data for a healthy, outer race fault and inner race fault in Table 5.1 show the symmetry of the random data which is a necessary criteria to obtain a Gaussian curve and these increases both on negative (minimum) and positive (maximum) value gradually showing a distinct spread in the range according to the type of fault.

The confidence interval at 95% shows the values increase from 0.005 to 0.011 and 0.012 a gradual change from healthy, outer race fault and inner race fault respectively.

This research work indicates that each parameter plays an important role in fault diagnosis in electrical machines. No parameter can be isolated or segregated in determining the behaviour. An overall behaviour of each value shows changes that classifies and identifies the fault. This is how the descriptive statistics play an important role.

The central tendency gives the orientation of the data it signifies whether the data is near about zero which is a critical criterion for a vibration signal. The measure of variability (i.e. range, variance, standard deviation and standard error) gives a sense of how much variations are found in the time signal which is verified by the parameters that inner race fault has maximum variations. The measure of dispersion does not have significant change in the three cases due to a single point defect. It is speculated that if a severity of fault is obtained the values of kurtosis and skewness will also change.

Hence, this study finds a link that if the kurtosis is 3.0 and skewness is zero it is a Gaussian distribution function. Thus, this has inferred that PDF and CDF calculation provides the deterioration of the PDF and provides the acceleration levels at different probabilities.

Statistical Inference

This leads to the statistical inference of plotting the density function and is depicted in Figures (5.5, 5.6, and 5.7) and the cumulative distribution function is depicted in Figures (5.8, 5.9, and 5.10) for healthy bearing, an outer race fault, and inner race fault, respectively. In PDF and CDF, the central tendency defines the criteria that normalized PDF has a zero mean with a PDF that can have a maximum of 1. Here the PDF and CDF are calculated, evaluated and plotted in all the three cases and it can be seen that the measure of variability is minimum in healthy bearing, followed by outer race faults, and maximum in inner race fault. This indicates more clearly in the plot of CDF of how the slope becomes steep as the variations increases as a fault occurs and is shown for the three cases with maximum probability to be 1. As the measure of variability or spread increases, the value of $f(x)$ decreases. This study also indicates that as for a single point defect fault introduces changes in central tendency (i.e. mean, median and mode) and dispersion (i.e. skewness and kurtosis) might not have significant changes. But according to the type of fault changes in variability increases and hence this depicts our incipient fault detection. The measure of dispersion has not much changed for a single point fault. Moreover, the values of dispersion in Table 5.1 have a clear-cut indication that the

vibration signal is Gaussian in nature.

This study proves the authenticity of vibration being Gaussian irrespective of a damaged bearing by both the descriptive and inferential statistics. The final verification is executed by calculating and experimentally observing the bearing characteristic frequency which is indicated in Table 5.2

The result shows that for a healthy machine as in Fig (5.11), there is a sharp peak at 23.75Hz which is the rotational frequency; the rest of the spectrum components are considerably down. The outer race fault is seen in Fig (5.12); a small rise of a peak can be seen at 63.75Hz. The inner race fault shown in Fig (5.13) has a sudden erupted peak at 99.375Hz which is very close to 103.38 Hz. As mentioned earlier by Tandon and Choudhary [99], due to slipping or skidding the frequencies have drifted. This drift is permissible in the ± 5 Hz range.

5.6 An Overview of Healthy, Outer and Inner race fault

The diagram shows the PDF of the three waveforms at the half load condition for a Healthy (Fault Free), Outer race fault and Inner race fault. As a fault occurs the magnitudes dip of the PDF. For an Healthy, outer race fault and inner race fault the maximum value of the magnitude is 0.501g, 0.355g and 0.328g respectively.

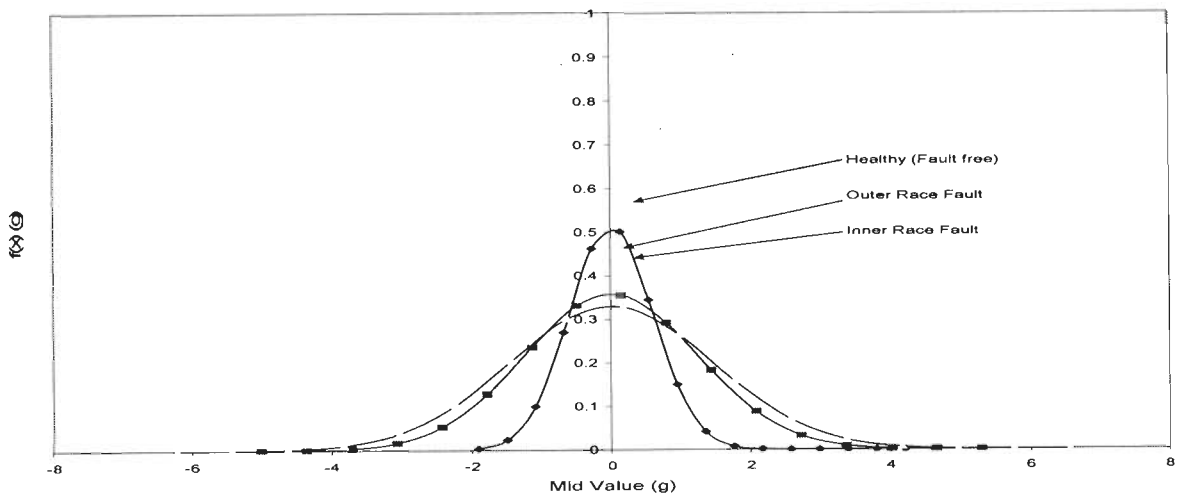


Figure 5.14: A comparative PDF diagram showing the Healthy (Fault Free), ORF and IRF.

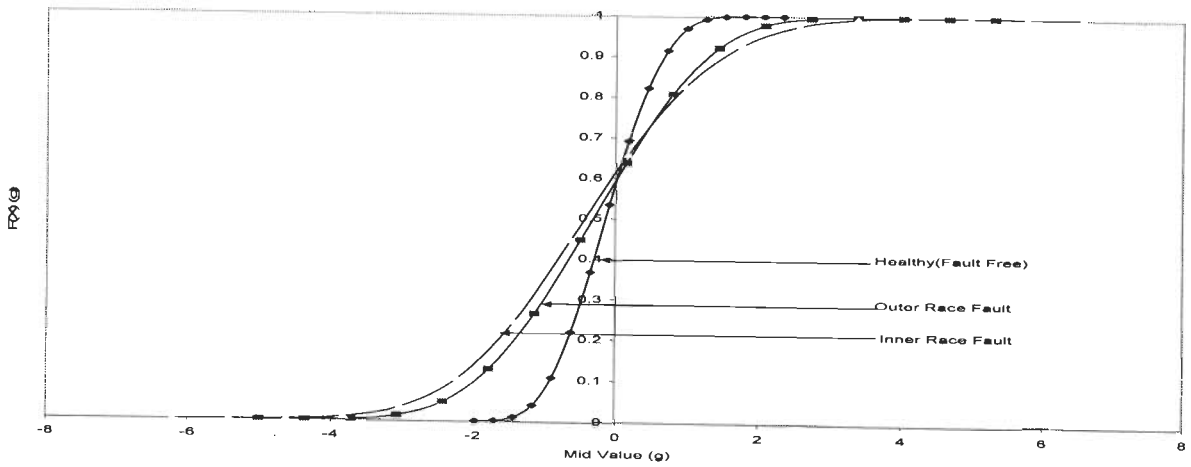


Figure 5.15: A comparative CDF diagram showing the Healthy (Fault Free), ORF and IRF.

The three CDF curves shows for a half load the Healthy (Fault free), the outer and the inner race fault. The Healthy curve has a minimum range and steepness and the maximum range and steepness is found for inner race fault.

5.7 Repeated Runs showing the Statistical Parameters:

The Table 5.3 below depicts the consistency of the results for an outer race fault at half load. As mentioned in the previous chapters a total of 104 runs were analyzed for one fault and 26 runs were carried for one kind of loading condition. Two bearings were used hence each bearing had 13 runs out of which seven runs can be seen below.

Table 5.3 shows seven repeated runs of the machine for half load outer race fault

| | Run-1 | Run-2 | Run-3 | Run-4 | Run-5 | Run-6 | Run-7 |
|-------------------------|-----------|-----------|-----------|-----------|-----------|-----------|-----------|
| Mean | -0.007645 | -0.007655 | -0.007660 | -0.007665 | -0.007670 | -0.007675 | -0.007680 |
| Standard Error | 0.007106 | 0.007106 | 0.007106 | 0.007106 | 0.007106 | 0.007106 | 0.007106 |
| Median | -0.004883 | -0.004893 | -0.004898 | -0.004903 | -0.004908 | -0.004913 | -0.004918 |
| Mode | 0.214844 | 0.214834 | 0.214829 | 0.214824 | 0.214819 | 0.214814 | 0.214809 |
| Standard Deviation | 1.588894 | 1.588894 | 1.588894 | 1.588894 | 1.588894 | 1.588894 | 1.588894 |
| Variance | 2.524584 | 2.524584 | 2.524584 | 2.524584 | 2.524584 | 2.524584 | 2.524584 |
| Kurtosis | 2.838881 | 2.838881 | 2.838881 | 2.838881 | 2.838881 | 2.838881 | 2.838881 |
| Skewness | -0.004902 | -0.004902 | -0.004902 | -0.004902 | -0.004902 | -0.004902 | -0.004902 |
| Range | 12.397461 | 12.397461 | 12.397461 | 12.397461 | 12.397461 | 12.397461 | 12.397461 |
| Minimum | -6.127930 | -6.127940 | -6.127945 | -6.127950 | -6.127955 | -6.127960 | -6.127965 |
| Maximum | 6.269531 | 6.269521 | 6.269516 | 6.269511 | 6.269506 | 6.269501 | 6.269496 |
| Confidence Level(95.0%) | 0.013927 | 0.013927 | 0.013927 | 0.013927 | 0.013927 | 0.013927 | 0.013927 |

5.8 Conclusion

This chapter describes the analysis of time domain vibration signal of a rotating electrical machine for fault diagnosis. The approach is to first observe the variations in raw time data signal consequent to a fault by statistical methods. This method is subdivided into Descriptive statistics which involves the evaluation of all the parameters of concern, and inferential statistics that is given by the PDF and CDF representation. This research work establishes a relation between the time domain signal, descriptive statistics and inferential statistics and is verified by the FFT analysis.

Finally the Bearing Characteristic Frequency (BCF) is calculated and experimentally obtained to ultimately verify the results of statistical methods for the time domain analysis. The experimental results justify the study of bearing fault using statistical approach.

Important observations made in this study

The present research work is on NBC 6308 ball bearing installed in a 7.5 -kW Induction Machine. Here, two identical bearing carrying known faults are taken, for which several runs are taken. The results were consistent and hence each representation depicts one run of the machine.

- 1) The resolution and the sampling rate are important to acquire vibration signal.
- 2) Each and every statistical parameter as presented here is equally important in the interpretation of a fault in rotating electrical machine. No parameter can be isolated or segregated to define faults.
- 3) An important observation is that as the magnitude of the PDF decreases with the nature of fault and the spread increases in the CDF there is an increase in the magnitude of corresponding frequencies in the FFT. The CDF defines the acceleration levels at different probabilities. This is a vital finding in this study and its significance can be related by capturing faults at incipient stage in fault diagnostics of electrical machines.
- 4) A comparison of the healthy, outer race and inner race is shown by superimposing the three cases for both PDF and CDF.
- 5) Lastly the repeated seven runs is seen to describe the consistency of the statistical parameter.

Experimental Investigations on Outer Race Fault

This chapter focuses on outer race fault under four load conditions that is no load, slight load, half load and $\frac{3}{4}$ loads. It specifically identifies the condition at an incipient stage and categorically gives an increase in the peaks of FFT as load increases and a decrease in peaks of the PDF was observed and CDF indicating a wider spread implying increased dispersions. A validity test was executed showing Gaussian distribution.

The aim of this research work is to identify Outer Race Fault (ORF) in the induction machine at different load conditions. The vibration data is acquired and analysis is done by computing the statistical parameters, probability density function and the cumulative distribution function. Finally the chi square test is used to validate the data findings.

6.1 Introduction

Prior to the advent of condition monitoring, traditional methods of determining a fault in a machine which involved feeling and sensing the vibration and observing a sudden rise in temperature by expert operators was utilized. But due to the human errors in prediction resulted in unwanted halts of the plants. This led to mounting sensors and analyzing signals acquired through these sensors. Eventually, the concept of fault detection in electrical machines at the time when fault has just started evolved.

The Outer Race Fault (ORF) contributes to 18% of the bearing faults according to research papers and study by T. Williams et al [143]. This research work identifies and classifies the outer race fault as Incipient Bearing Fault IBF. Time signal is observed, statistical parameters are extracted from the data, probability density function and cumulative distributions for different load conditions are also evaluated. Chi-square test is done to prove the distribution. Furthermore, the fault frequencies are determined and verified with the values available theoretically and practically.

S. Nandi and H. A. Toliyat [133, 134] describe the different types of faults and signatures they generate. It relates to the importance of IBF and the various faults that exist apart from bearing faults. N. Tandon, and A. Choudary [99] describe the methods for detection of defects in rolling element bearings using vibration and acoustic measurement.

H.R. Martin and F. Honarvar [49] used variations of the statistical moment analysis method to show potential for damage detection at a much earlier stage. This approach has several advantages over other methods as the measurements taken are essentially independent of load and speed. R.B.W. Heng and M.J.M. Nor [114] presented a study on the application of sound pressure and vibration signal to detect the presence of defects using statistical methods. W.Reimche et al [154] has shown the basics of comprehensive vibration analysis using statistical time values for general signal description and threshold comparisons, envelope analysis and spectrum, phase and correlation analysis of multi sensor arrangements. R.B.Randall [124] introduces a concept of Spectral Kurtosis (SK). It comprises of Short Time Fourier Transforms STFT and Wavelet analysis for determining the optimum combinations of centre frequency and band width for minimizing the Spectral Kurtosis SK. D.Dyer, and R.M. Stewart [28] proposed a method based on kurtosis coefficient, which remains constant for an undamaged bearing irrespective of load and speed, yet changes with damage. The extent of damage can be assessed from the distribution of this statistical parameter in the selected frequency. S.A. McInerny, and Y.Dai [127] described the envelope analysis and explained the connection between bearing fault signatures and amplitude modulation/demodulations. M.J. Devaney, and L. Eren [91] described the monitoring of induction motors current to detect bearing failures.

H.Ocak, and K.A.Loparo [48] introduce Hidden Markov Modeling (HMM) of vibration signals, which allows for diagnosis of the type of bearing faults by selecting the Hidden Markov Modeling with the highest probability. One of the techniques mentioned in papers is the wavelet analysis and Discrete Wavelet Transforms (DWT) [13, 14, and 15].

Flow Diagram of Identifying ORF

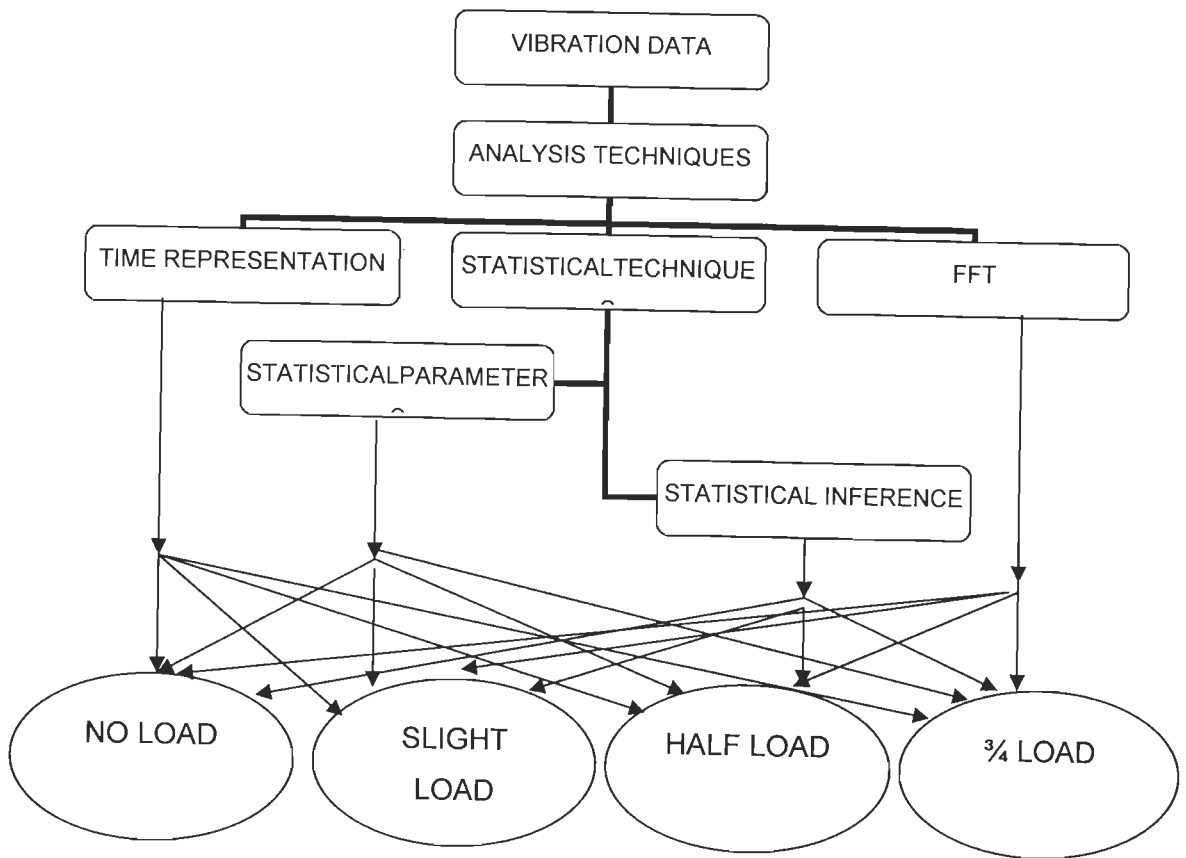


Figure 6.0: Flow diagram to detect ORF at different load conditions.

The flow diagram is a pictorial representation shown in Figure 6.0 of the methodology used to determine the outer race fault.

The aim of this chapter is to investigate the Incipient Bearing Failure (IBF) by acquiring vibration data and employing time domain, statistical techniques as well as the Fast Fourier Transforms (FFT) to identify a fault. Bearings are the point of focus with special attention to the outer race fault (ORF).

6.2 Analysis of the Data Acquired:

Investigation is carried out for four load conditions on the outer race fault. The motor was operated for no load, slight load, half load and three quarter load. For each case several runs were considered out of each one run is depicted in the runs.

6.2.1 Time Domain Signal

Figures 6.1, 6.2, 6.3 & 6.4 represents the time domain representations for the first 500 samples (i.e. depicted on a 0 to 0.8 ms scale) that have been selected from a total of 50000 acquired samples. Four load conditions are applied to obtain a behaviour pattern from minimum to maximum loading conditions. It can be seen from the figures that as the load increases from no load to three quarter load condition, the magnitude in the time signal increases.

No Load

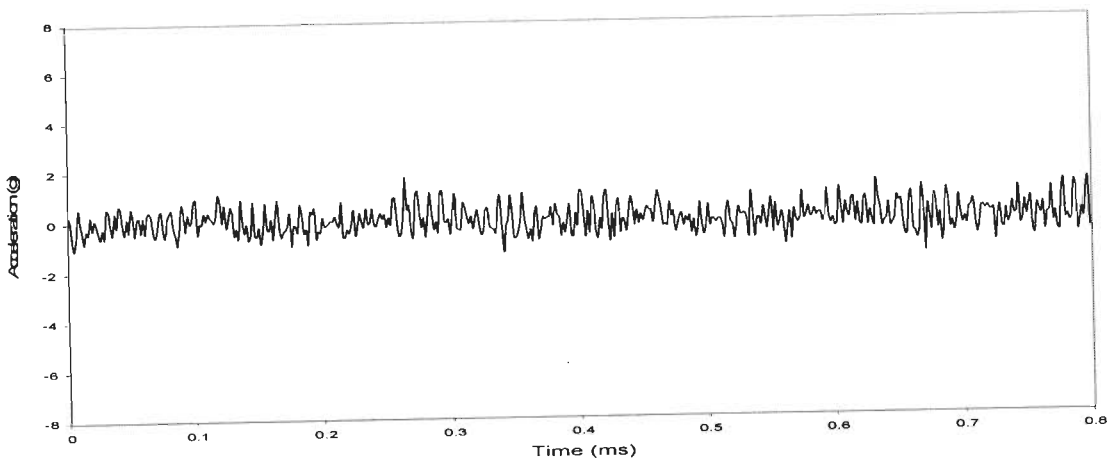


Figure 6.1: Vibration signal for outer race fault at no load.

Slight Load

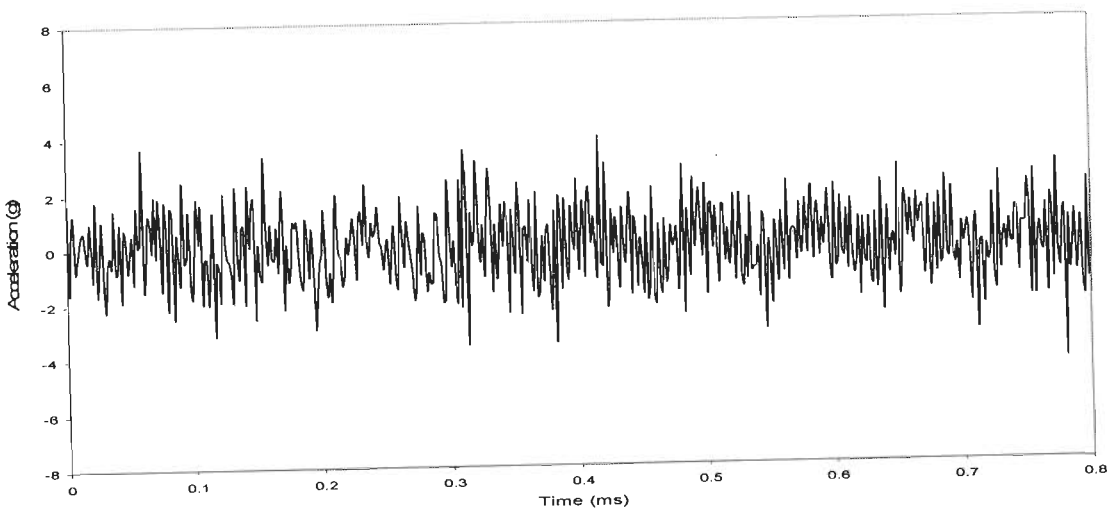


Figure 6.2: Vibration signal for outer race fault at slight load.

Half Load

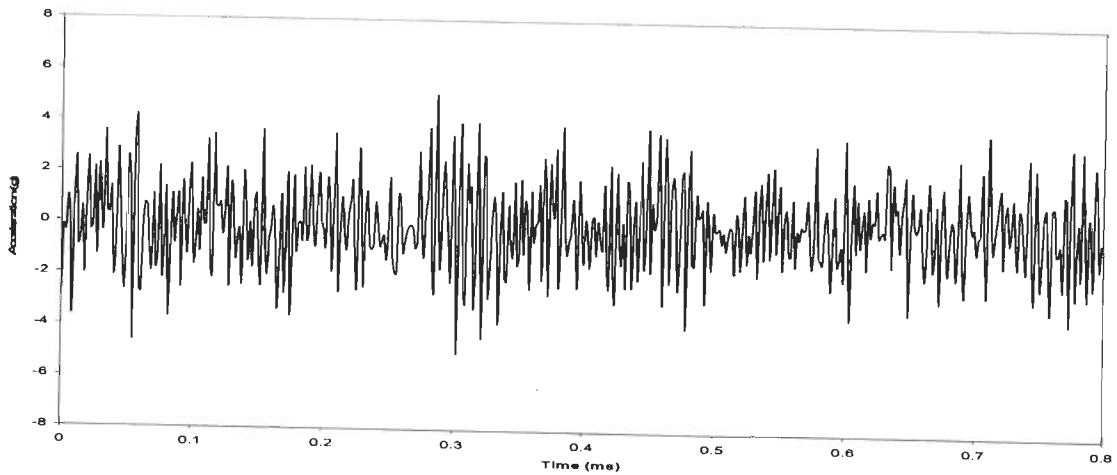


Figure 6.3: Vibration signal for outer race fault at half load.

Three Quarter Load

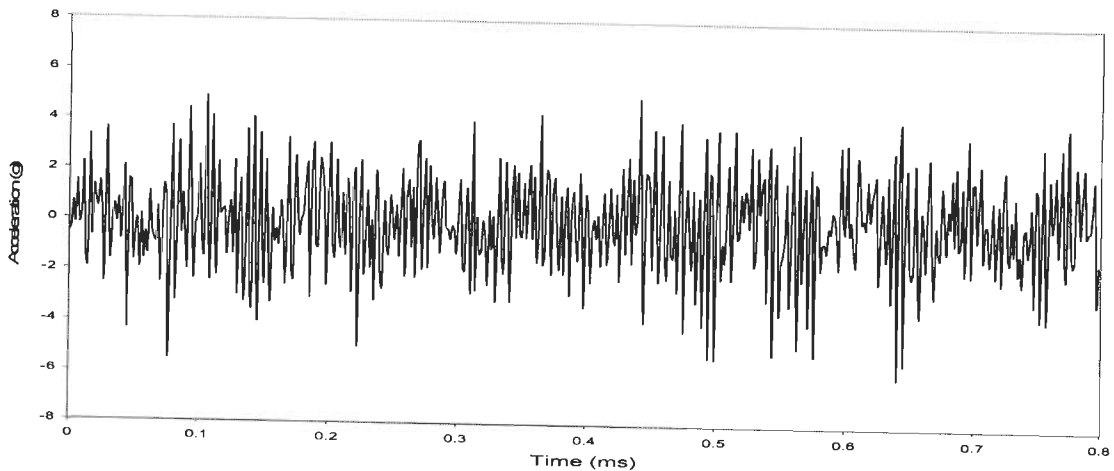


Figure 6.4: Vibration signal for outer race fault at three quarter load.

Statistical Analysis of the Acquired Data

In general, the statistical analysis can be divided into statistical parameter and statistical inferences.

6.2.2 Statistical Parameter

Literature suggests that statistical parameters have been used as a tool for fault diagnosis in a rolling element. J.Zarei, and J.Poshtan [70] suggest that kurtosis is not a popular method. R.B.W. Heng and M.J.M. Nor [114] give emphasis on the r.m.s, crest factor (CF) and kurtosis values. H.Ocak, and K.A.Loparo [47] state statistical analysis approach based on kurtosis and CF, and conclude that it lacks the ability to detect bearing defects.

R.B.W. Heng and M.J.M. Nor [114] state that for the bearing in a correctly lubricated condition, the kurtosis for normal distribution is given in the range of 3.0 to 3.5

The descriptive statistics involves the calculation of measure of central tendency, measure of variability and measure of dispersion as mentioned in chapter 3.

Table 6.1: Statistical Parameters for four load conditions for a Healthy Machine (Fault Free).

| PARAMETERS | HEALTHY (FAULT FREE) | | | |
|--------------------------------------|----------------------|-------------|-----------|--------------------|
| | No Load | Slight Load | Half Load | Three Quarter Load |
| Units | | | | |
| Mean (g) MCT | -0.003 | -0.005 | -0.004 | -0.005 |
| Standard Error (g) MV | 0.002 | 0.002 | 0.003 | 0.003 |
| Median (g) MCT | 0.000 | -0.044 | -0.015 | -0.029 |
| Mode (g) MCT | -0.034 | -0.210 | -0.269 | -0.229 |
| Standard Deviation (g) MV | 0.385 | 0.534 | 0.603 | 0.614 |
| Sample Variance (g ²) MV | 0.148 | 0.285 | 0.364 | 0.377 |
| Kurtosis MD | 2.957 | 3.494 | 3.344 | 3.474 |
| Skewness MD | -0.016 | 0.177 | 0.057 | 0.086 |
| Range (g) MV | 3.364 | 3.662 | 4.346 | 4.243 |
| Minimum (g) | -1.719 | -1.816 | -2.114 | -2.173 |
| Maximum (g) | 1.646 | 1.846 | 2.231 | 2.070 |
| Confidence Interval (95.0%) (g) | 0.003 | 0.005 | 0.005 | 0.005 |

Table 6.2: Statistical Parameters for four load conditions for an outer race fault.

| PARAMETERS | OUTER RACE FAULT | | | |
|--------------------------------------|------------------|-------------|-----------|--------------------|
| | No Load | Slight Load | Half Load | Three Quarter Load |
| Units | | | | |
| Mean (g) MCT | -0.008 | -0.009 | -0.008 | -0.008 |
| Standard Error (g) MV | 0.003 | 0.006 | 0.007 | 0.009 |
| Median (g) MCT | -0.020 | 0.000 | -0.005 | 0.000 |
| Mode (g) MCT | 0.132 | -0.044 | 0.215 | 0.376 |
| Standard Deviation (g) MV | 0.569 | 1.241 | 1.589 | 2.016 |
| Sample Variance (g ²) MV | 0.324 | 1.540 | 2.525 | 4.064 |
| Kurtosis MD | 2.914 | 2.772 | 2.839 | 2.904 |
| Skewness MD | 0.069 | -0.060 | -0.005 | -0.039 |
| Range (g) MV | 4.609 | 10.386 | 12.397 | 15.791 |
| Minimum (g) | -2.422 | -5.327 | -6.128 | -7.695 |
| Maximum (g) | 2.188 | 5.059 | 6.27 | 8.096 |
| Confidence Interval (95.0%) (g) | 0.005 | 0.011 | 0.014 | 0.018 |

In present work, a number of statistical parameters are found, for a given operating condition, to arrive at fault diagnosis. These parameters are given in Table 6.1 for a motor with healthy bearings and in Table 6.2 for load end bearing with outer race fault. Four loading conditions of the machine are considered: No Load, Slight Load, Half Load and Three Quarter Load.

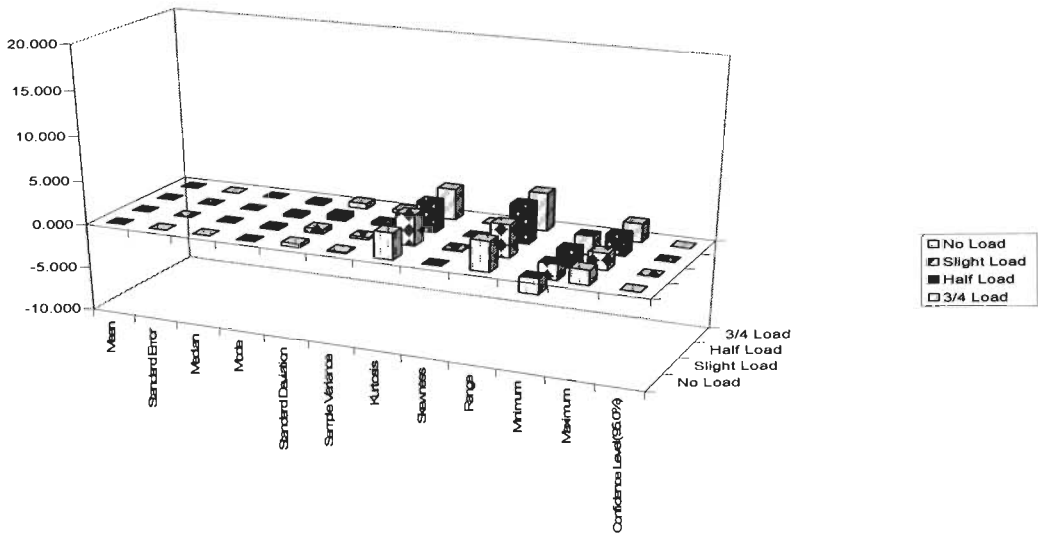


Figure 6.5: A 3-D plot showing the behaviour of statistical parameters at four load condition for Healthy Bearing.

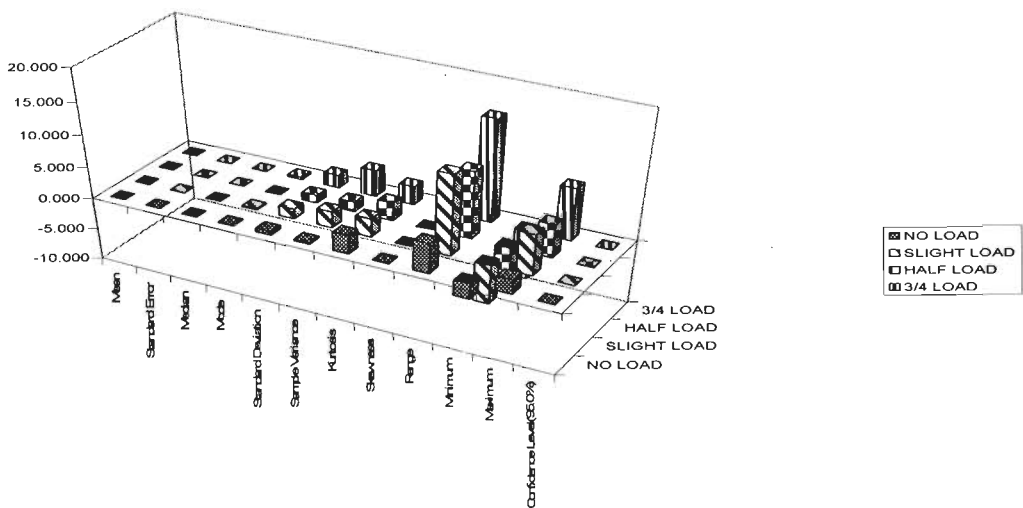


Figure 6.6: A 3-D plot showing the behaviour of statistical parameters at four load condition for ORF.

The statistical parameters in Tables 6.1 and 6.2 are plotted for the four load conditions as shown in Figure 6.5 and Figure 6.6 for a healthy machine and for ORF respectively; a 3-D plot indicates that the central tendency remains constant, the measure of variability shows variation and the measure of dispersion remains fairly constant for the four load conditions.

This indicates that only measure of variability is important in identifying incipient bearing fault for the loading condition of ORF. Further, Figure 6.5 and 6.6 compares the parameters of a healthy machine and an ORF pictorially.

6.3 Statistical Inferences

Statistical parameters are derived from vibration signal and the statistical inference is further extended by calculating the probability density function and cumulative distribution function. N. Tandon, and A. Choudary [99] suggests probability density of acceleration of a bearing in good condition has a Gaussian distribution, whereas a damaged bearing results in non Gaussian distribution with dominant tails because of a relative increase in the number of high levels of acceleration. D.Dyer, and R.M. Stewart [28] reveals that the measure of bearing condition is obtained by observing the changes in the probability at particular amplitude levels. Those above 3σ providing the most significant information. This research work clearly depicts that an outer race fault having a perfect Gaussian distribution for four different kinds of load conditions, namely, No Load, Slight Load, Half Load and Tree Quarter Load of an outer race fault. The probability density function and cumulative distribution function was calculated for 50000 samples.

This data was further validated by the χ^2 -test which clearly shows that it satisfies the distribution. Chi square is estimated at 8 Degree of freedom and 5% of significance level is 15.51 and the χ^2 values obtained are 9.38, 2.70, 5.76 and 10.73 for outer race fault at no load, slight load, half load & three quarter load respectively. Thus the results of this research work shows that the vibration signals are Gaussian in nature, irrespective of healthy and non healthy conditions of an ORF.

6.4.1 Probabilty Density Function

The statistical inference can be derived from the probability density function which is represented as the Gaussian distribution function and is given by the equation mentioned in chapter 3.

$$f(x) = (1/\sigma\sqrt{2\pi}) \exp(-1/2)(x - m/\sigma)^2$$

No Load:

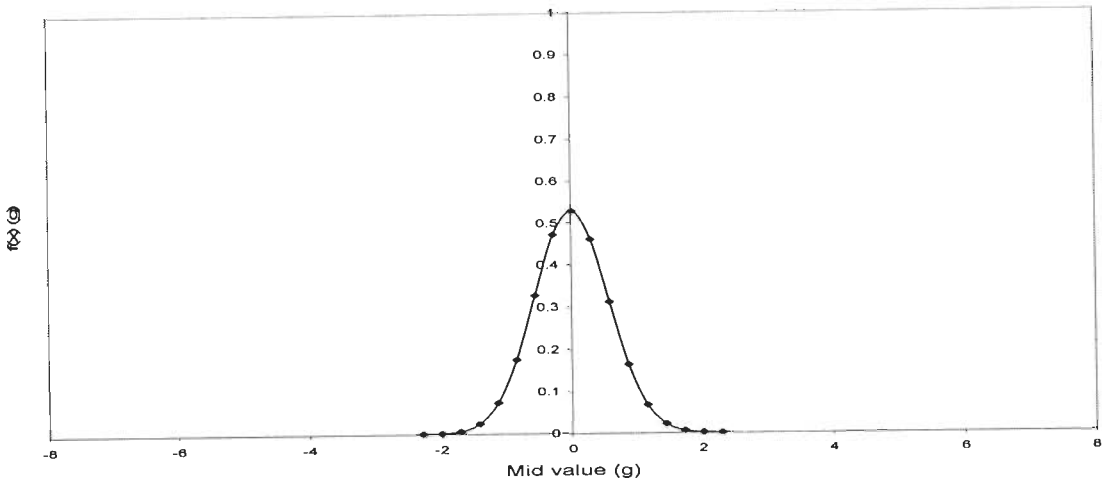


Figure 6.7: The probability density function for no load condition for outer race fault.

Slight Load:

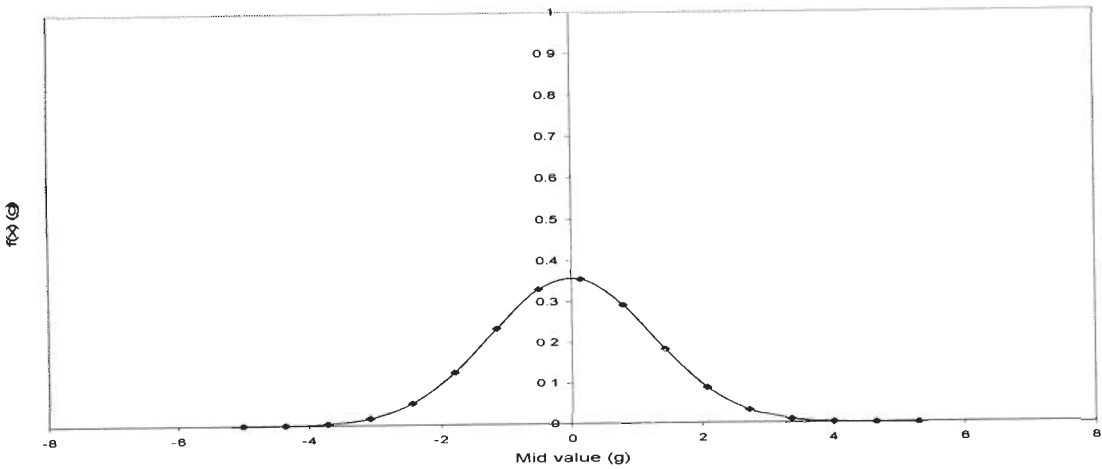


Figure 6.8: The probability density function for slight load condition for outer race fault.

Half Load:

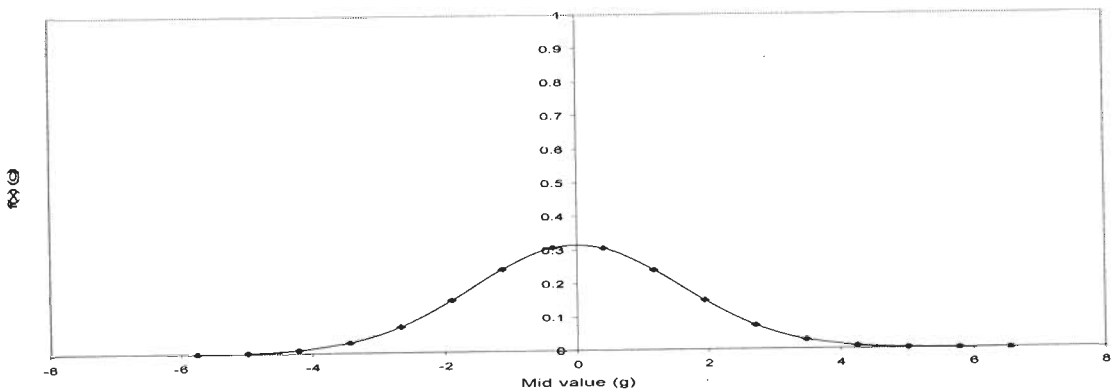


Figure 6.9: The probability density function for half load condition for outer race fault.

Three Quarter Load:

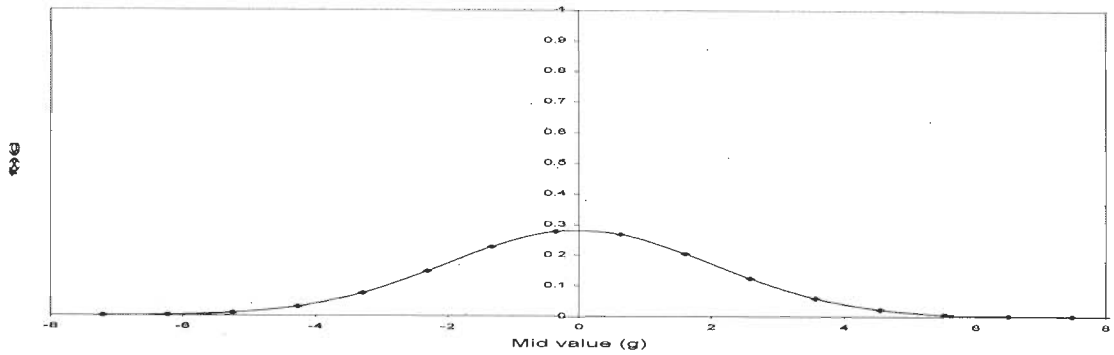


Figure 6.10: The probability density function for three quarter load condition for outer race fault.

Table 6.3: The practical value of magnitudes of the maximum value of PDF obtained for four different load conditions .

| Probability Density Function | | |
|------------------------------|-------------------------|----------|
| Load Conditions | Mid value at centre (g) | f(x) |
| No Load | 0 | 0.52865g |
| Slight Load | 0 | 0.35538g |
| Half Load | 0 | 0.30864g |
| Three Quarter Load | 0 | 0.27687g |

The probability density function plots are depicted in Figures 6.7, 6.8, 6.9, and 6.10. Table 6.3 shows the magnitudes fall as the loading increases. This relates to the fact that the range also increases. It is a clear indication of an increase in the measure of variability. Hence, this research work shows that as load increases the PDF decreases as seen in Table 6.3.

6.3.2 Cumulative Distribution Function

This research work gives a new concept of looking at the behaviour of variations by calculating the cumulative distribution function of the vibration signal. Again, the four

different kinds of load conditions namely, No Load, Slight Load, Half Load and Three Quarter Load of an outer race fault were evaluated.

The cumulative distribution function equation is $F(X) = \int f(x)dx$, where $F(x)$ = cumulative distribution function

No Load

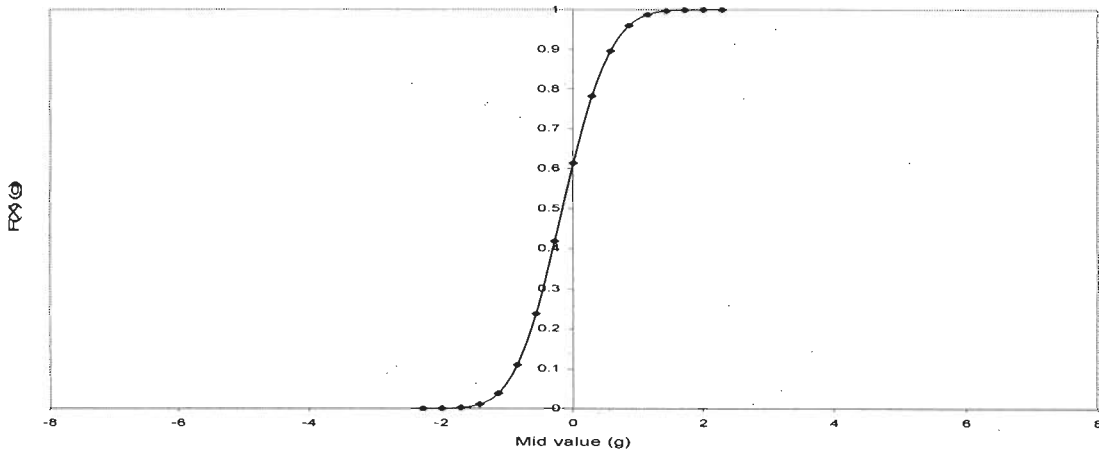


Figure 6.11: The cumulative distribution function for no load condition for outer race fault.

Slight Load

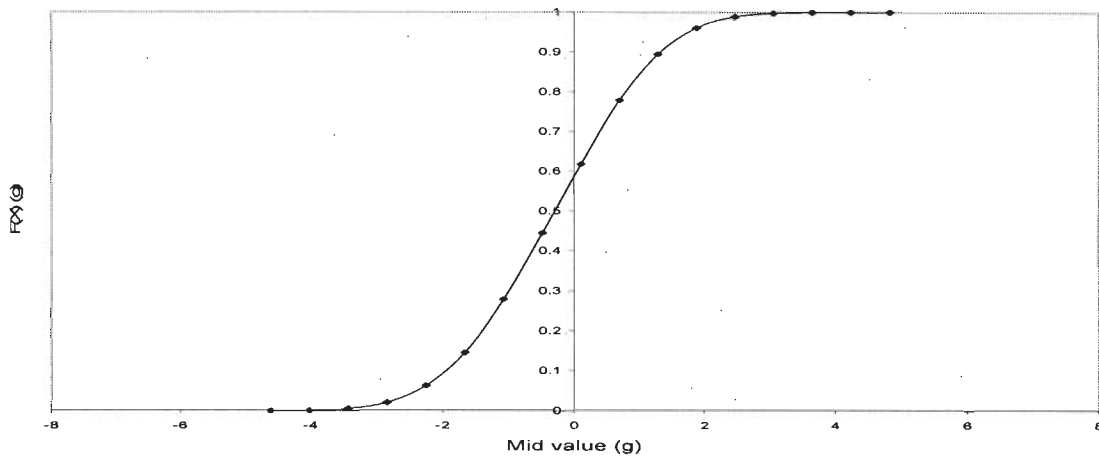


Figure 6.12: The cumulative distribution function for slight load condition for outer race fault.

Half Load

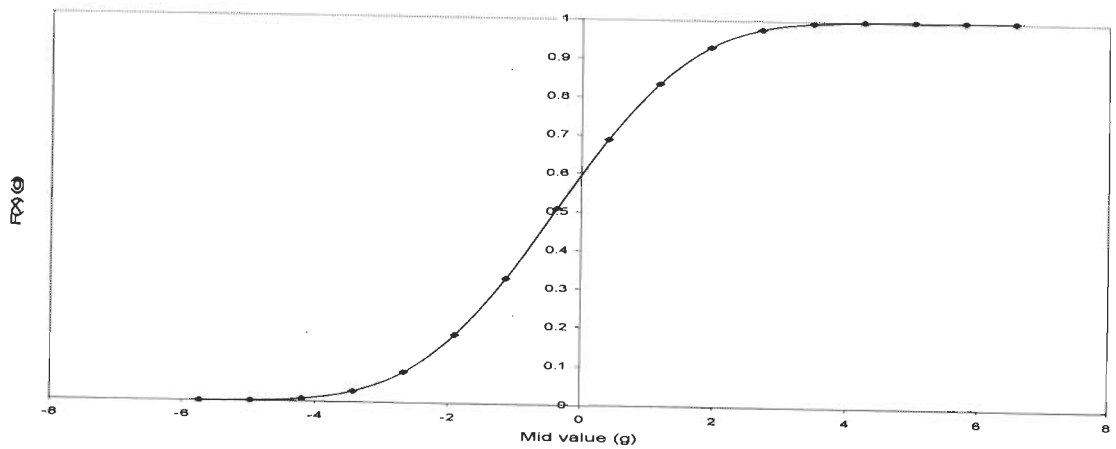


Figure 6.13: The cumulative distribution function for half load condition for outer race fault.

Three Quarter Load

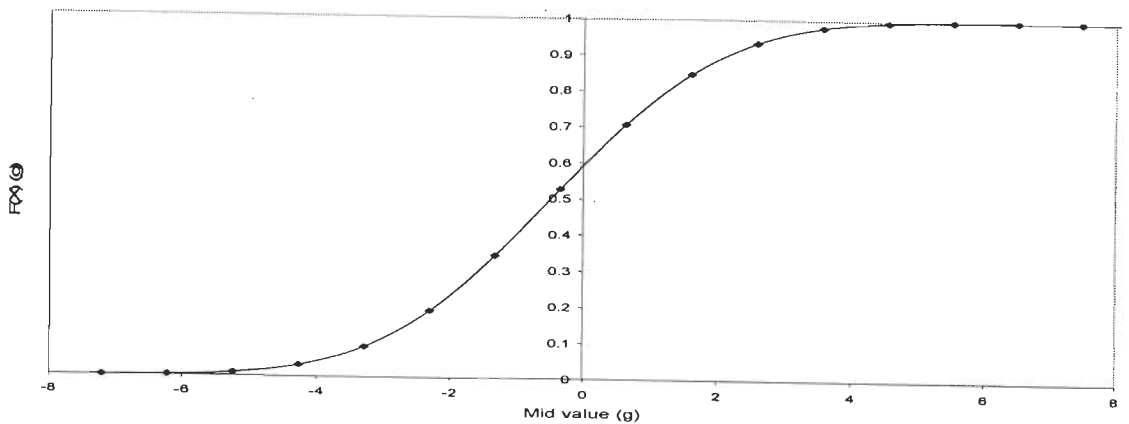


Figure 6.14: The cumulative distribution function for three quarter load condition for outer race fault.

From Figures 6.11, 6.12, 6.13, and 6.14 it can be seen that at 10% and 90% the acceleration levels are given by the g-values; at no load it ranges from (-0.85g to 0.57g), at slight load it ranges from (-1.78g to 1.43g), at half load it ranges from (-2.67g to 1.94g) and finally at three quarter load it ranges from (-2.1311g to 2.58g). At no load a sharp curve is found. As the load increases not only does the range increase, but the shape of the CDF expands indicative of large variation.

6.4 Frequency Domain Representation

The FFT is calculated to confirm that the position of peaks of the frequencies do tally with the theoretical frequencies expected. A peak at the characteristic fault frequency clearly indicates that a fault is captured at an incipient stage. Researchers do suggest that frequency spectra is difficult to find since Bearing Characteristic Frequency (BCF) has little energy and is overwhelmed by the noise and higher level macro structural vibrations. For normal speeds, these defect frequencies lie in the range of 500Hz. This research work considers a range of 500Hz and its BCF can be clearly seen in the FFT which has been calculated in EXCEL. The BCF for NBC 6308 with 7 balls is given by 64.6Hz as mentioned in chapter 3.

These Calculated Frequencies should be dominant according to the fault considered. The prevalent frequencies are calculated and the harmonics of each individual frequency do exist on the severity and intensity of the fault. The resolution that was considered to obtain the result below was 0.625Hz. As the resolution becomes high the peaks become more distinguished and can be easily classified. These frequency values sometimes drift between (+/-) 5Hz in practical data that sustains these discrepancies.

No Load

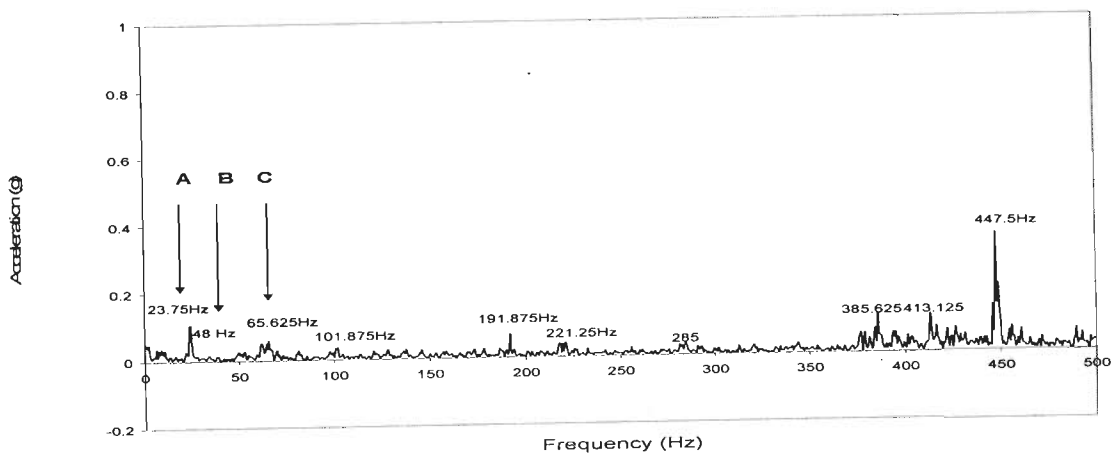


Figure 6.15: The FFT for no load condition for outer race fault.

Cont.....

Slight Load

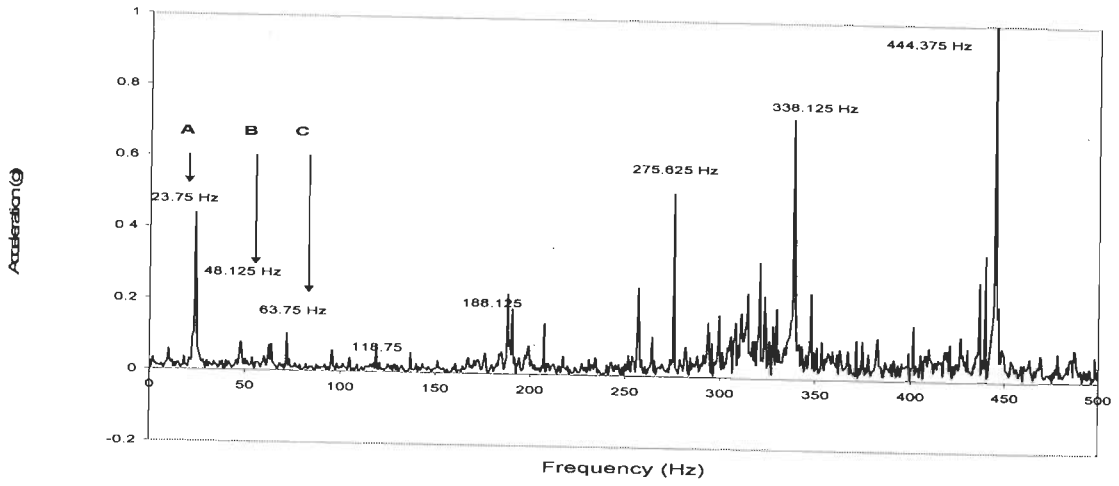


Figure 6.16: The FFT for slight load condition for outer race fault.

Half Load

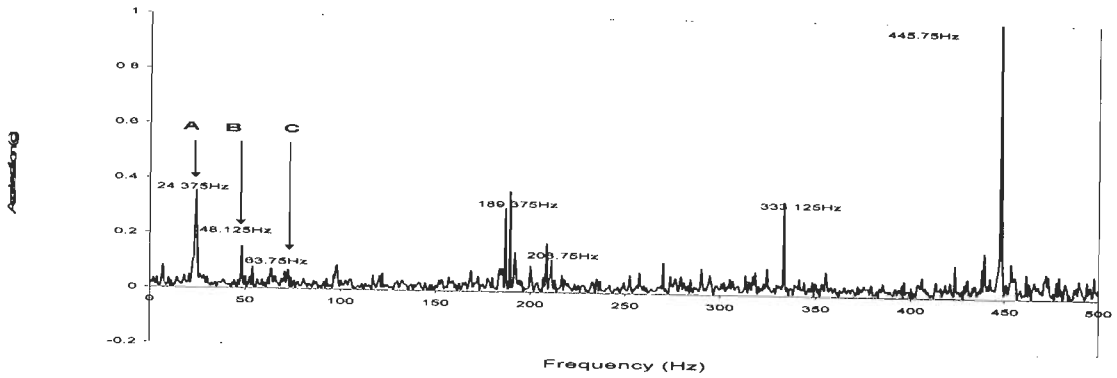


Figure 6.17: The FFT for half load condition for outer race fault.

Three Quarter Load

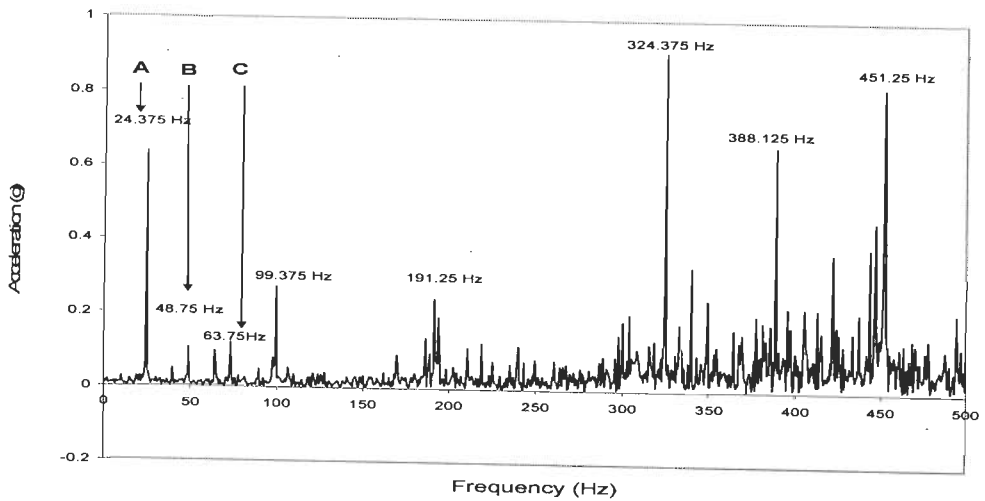


Figure 6.18: The FFT for three quarter load condition for outer race fault.

From Figures 6.15, 6.14, 6.15, and 6.16 the significant frequencies of interest are given as A, B, C. Where the bearing characteristic frequency (BCF) obtained from the vibration data is given as,

- A-Rotational frequency
- B-Ball Spin Frequency
- C-Outer Race Frequency

The rotational speed of the machine was 1440 rpm which was the rated value and the calculated frequency was 24Hz. The peak of the rotational frequency was at 23.75Hz of the spectrum.

Table 6.4: The practical value of magnitudes of the peaks obtained for four different load conditions.

| Load Condition | Fault Frequency | Magnitudes of these peaks |
|--------------------|-----------------|---------------------------|
| No Load | 63.75 Hz | 0.0507g |
| Slight Load | 63.75 Hz | 0.0741g |
| Half Load | 63.75 Hz | 0.0747g |
| Three Quarter Load | 63.75 Hz | 0.0947g |

Meanwhile from Figures 6.15, 6.16, 6.17, and 6.18 it can be seen that a peak has erupted at 63.75 Hz which signifies an outer race fault and as the load increases the peak increases. Table 6.4 shows the magnitudes obtained at the fault frequency. It is of practical interest that as the load increases the fault frequency magnitude at “c” rises.

6.5 Discussion

This research work describes a method for the detection of an outer race fault using statistics in tandem with time as a powerful fault diagnosis tool at an incipient stage. In chapter 2 of this research work the specification of an induction motor is specified and these vibration signal are taken from the front end bearing of the motor.

Time Signal: The vibration data signal is depicted in Figures 6.1, 6.2, 6.3, and 6.4. It can be seen that as the load increases the magnitude of the signal increases. The no load time signal has the least magnitude in the vibration signal for ORF.

Statistical Parameter:

These variations in magnitude of the time domain signal are further analyzed for values of the statistical parameter. In general, the statistical parameter can be divided into three categories as mentioned in chapter 3,

1) Measure of Central tendency (MCT) :

In Tables 6.1 and 6.2, it can be seen that the values are zero or very close to zero indicating an almost symmetric distribution. An excerpt from Tables 6.1 and 6.2 is depicted in the Table 6.5 below

Table 6.5: Measure of Central tendency (MCT)

| MCT | Comparing Outer Race Fault (ORF) and Healthy MCT | | | | |
|------------|--|--------------------|--------------------|--------------------|--------------------|
| | Units | No Load | Slight Load | Half Load | Three Quarter Load |
| Mean (g) | | -0.008 (-0.003) | -0.009 (-0.005) | -0.008 (-0.004) | -0.008 (-0.005) |
| Median (g) | | -0.020 (0.000) | 0.000 (-0.044) | -0.005 (-0.015) | 0.000 (-0.029) |
| Mode (g) | | 0.132 (-0.034) | -0.044 (-0.210) | 0.215 (-0.269) | 0.376 (-0.229) |

Data for a healthy machine is in parenthesis. For a three quarter load the median has a value of 0.000g for outer race fault and it tends to be -0.029g for healthy machine. Meanwhile, for the same load condition the value of mode is 0.376g for outer race fault and -0.229g for healthy machine. Indicating an almost zero value.

2) Measure of variability in terms of statistical parameter is represented by range, sample variance and standard deviation. An excerpt from Table 6.1 and 6.2 is depicted in the Table 6.6 below

Table 6.6: Measure of variability (MV)

| MV | Comparing Outer Race Fault (ORF) and Healthy MV | | | | |
|--------------------|---|---------|-------------|-----------|--------------------|
| | Units | No Load | Slight Load | Half Load | Three Quarter Load |
| Standard Error (g) | | 0.003 | 0.006 | 0.007 | 0.009 |

| | | | | |
|--|---------------|---------------|---------------|---------------|
| | (0.002) | (0.002) | (0.003) | (0.003) |
| Standard Deviation (g) | 0.569 | 1.241 | 1.589 | 2.016 |
| | (0.385) | (0.534) | (0.603) | (0.614) |
| Sample Variance (g²) | 0.324 | 1.540 | 2.525 | 4.064 |
| | (0.148) | (0.285) | (0.364) | (0.377) |
| Range (g) | 4.609 | 10.386 | 12.397 | 15.791 |
| | (3.364) | (3.662) | (4.346) | (4.243) |
| Minimum (g) | -2.422 | -5.327 | -6.128 | -7.695 |
| | (-1.719) | (-1.816) | (-2.114) | (-2.173) |
| Maximum (g) | 2.188 | 5.059 | 6.27 | 8.096 |
| | (1.646) | (1.846) | (2.231) | (2.070) |

The range has the value of 4.609g for a no load condition healthy machine and 3.364g for no load outer race fault. Similarly, the range for three quarter loading is 15.791g for outer race fault and 4.243g for a healthy machine. Similarly, the standard deviation increases from 0.614g to 2.016 g for three quarter loading.

It was mentioned that as the load increases the variation increases. This can be seen in Table 6.6. The maximum and minimum values are showing the degree of the spread of the data. It has also been observed in this study that as the load increases measure of variability has significant changes at Incipient Bearing Fault.

3) Measure of dispersion (MD) is given by the kurtosis and skewness. Since the fault is at an incipient stage the kurtosis and skewness remain close to 3 and zero respectively, which, does not in this case show a fault according to research papers.

Table 6.7: Measure of dispersion (MD)

| MD | Comparing Outer Race Fault (ORF) and Healthy MD | | | |
|--------------|--|--------------------|------------------|---------------------------|
| Units | No Load | Slight Load | Half Load | Three Quarter Load |
| | | | | |

| | | | | |
|-----------------|--------------------------|--------------------------|--------------------------|--------------------------|
| Kurtosis | 2.914 (2.957) | 2.772 (3.494) | 2.839 (3.344) | 2.904 (3.474) |
| Skewness | 0.069 (-0.016) | -0.060 (0.177) | -0.005 (0.057) | -0.039 (0.086) |

The measure of dispersion MD has no significant change for an outer race fault at an incipient stage which is observed in Table 6.7.

The above discussion shows that the most vital measure at an incipient stage is the measure of variability.

Probability Density Function (PDF): The PDF was calculated and Table 6.3 shows the results for four load conditions. As the load is increased, the magnitudes falls of the PDF, this can be seen in the results. On the other hand the range increases. This shows that a combination of a fall of magnitude and range gives a spread and an increase in dispersion of samples.

An important observation is that the PDF magnitudes fall as the load was increased and the signal remains Gaussian as indicated in chapter 4 even after loading the machine.

Cumulative Distribution Function (CDF): This research work has evaluated the CDF to see the behaviour of how these variations are indicated in the CDF. D.Dyer, and R.M. Stewart [28] quotes changes in the probability at particular amplitude levels, those above 3σ provide most significant information by observing these changes and hence Table 6.6 show the CDF and the variations from No load, slight load, half load and three quarter load respectively. The probability spread is maximum at three quarter load compared to the four load conditions. This shows that as the load increases at faulty condition the measure of variability increases and this can be seen by the spread of the CDF graph. At three quarter load the graph is steepest.

Frequency Domain Representation: The bearing characteristic frequency (BCF) was calculated and this value was found to be 64.62Hz whereas the practical value obtained in this result is 63.75Hz. These are depicted in Figures 6.15, 6.16, 6.17, and 6.18. Table 6.4 summarizes the peaks obtained and the respective magnitudes obtained. It can be seen that as the load increases the magnitudes of peaks of the FFT also increases. M.J. Devaney, and L. Eren [91] Suggests that motor current amplitude will increase with increased load, bearing baseline data should be collected with a healthy set of bearings under varying loads.

This research work deals with this condition by driving the load from no load to three quarter load which gives a near about full load condition, thus covering all the load conditions that covers the behaviour from minimum to its maximum values. H.Ocak, and K.A.Loparo [47] reveals that power spectrum amplitude peaks increase. W.Reimche [154] states that initiating and growing of defects in rolling element bearings of machines in most cases is detected by using statistical values.

This research work clearly indicates that as the load conditions increases in faulty machine, the magnitudes of the peaks do increase and this can be seen in Figure 6.15, 6.16, 6.17, and 6.18.

6.6 Trend of ORF with Load Variations

The diagram shows the PDF of the four waveforms at the No load, slight load, half load and three quarter load condition for a Healthy (Fault Free). Figure 6.19 shows the PDF of the four waveforms at the No load, slight load, half load and three quarter load condition for an Outer Race Fault. Figure 6.20 shows the CDF of the four waveforms at the No load, slight load, half load and three quarter load condition for a Healthy (Fault Free) and Figure 6.21 shows the CDF of the four waveforms at the No load, slight load, half load and three quarter load condition for an Outer Race Fault.

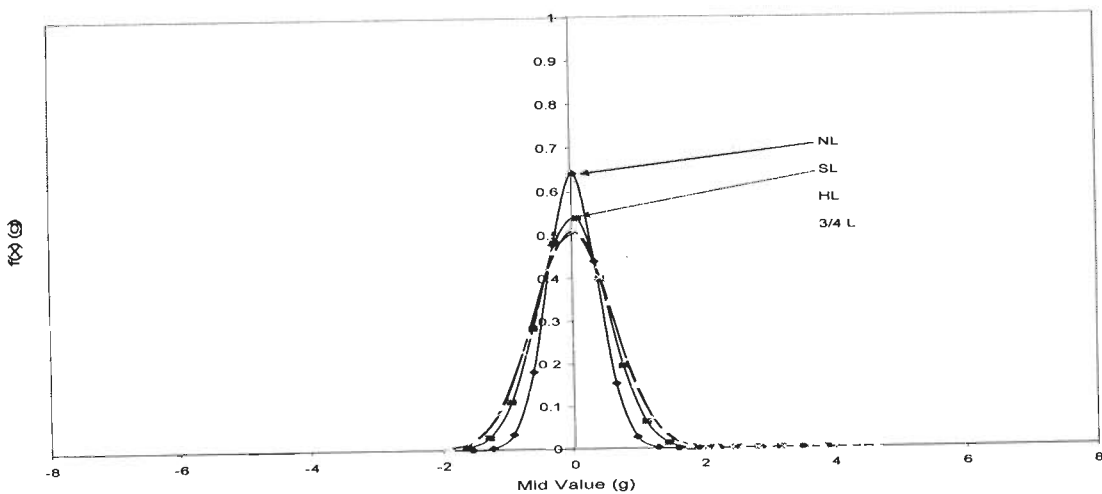


Figure 6.19: PDF of Healthy at four load condition

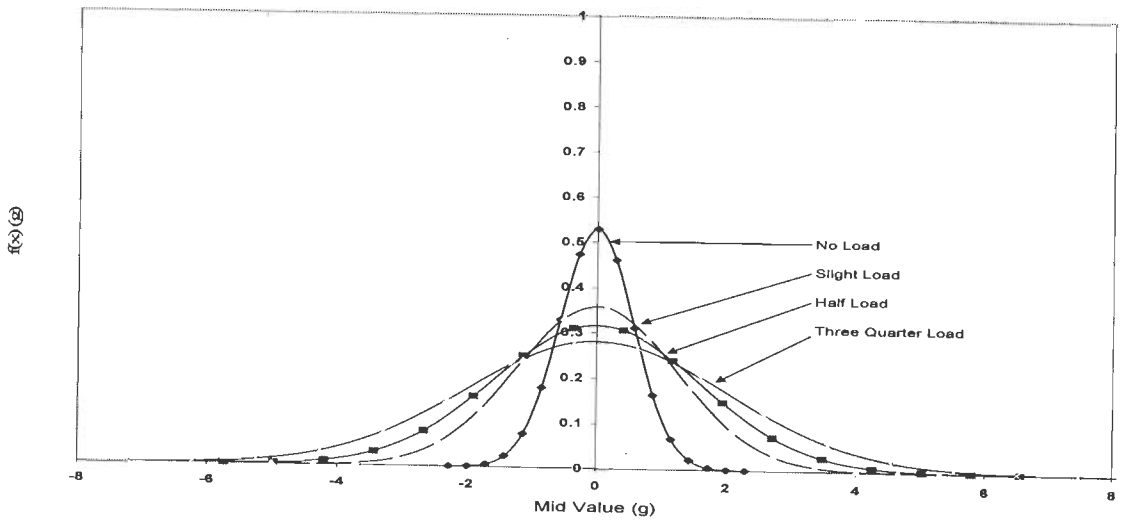


Figure 6.20: PDF of Outer race fault at four load condition

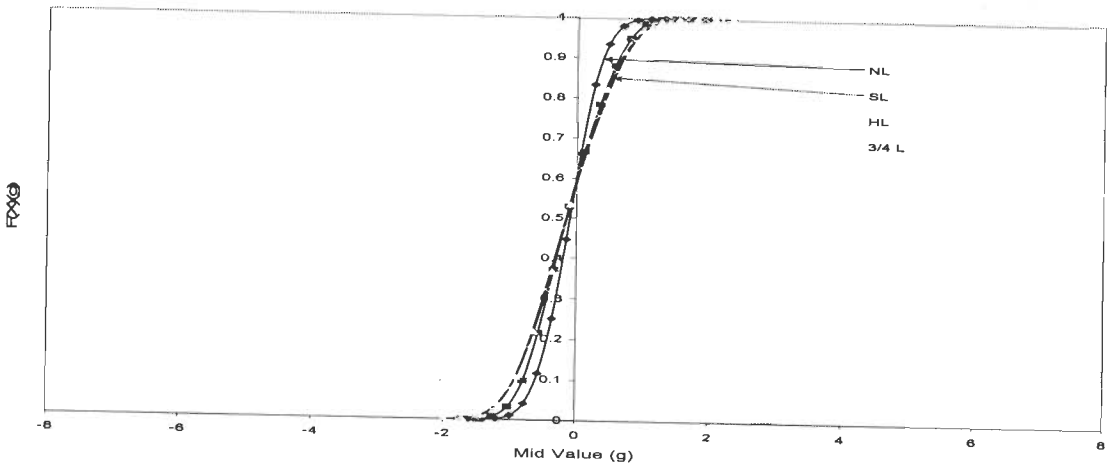


Figure 6.21: CDF of Healthy at four load condition

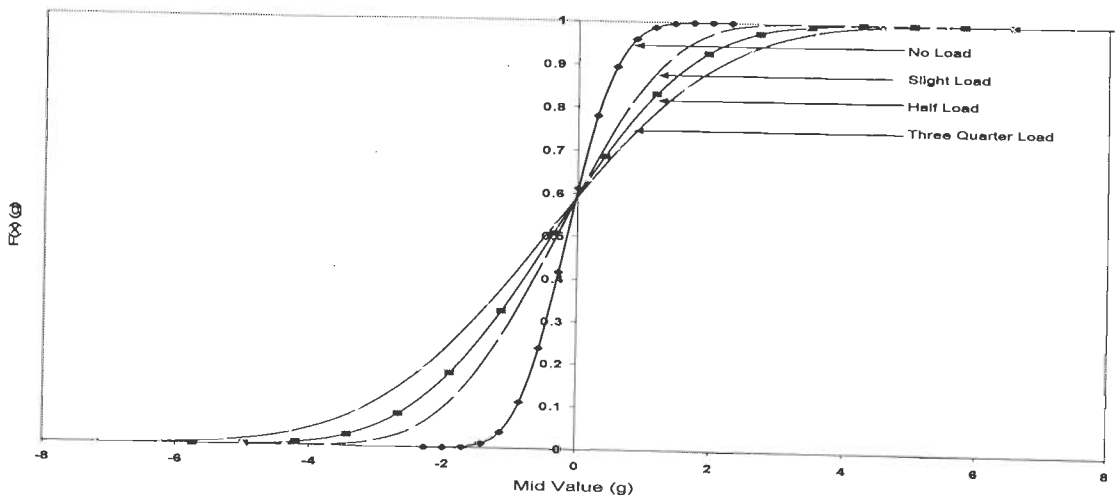


Figure 6.22: CDF of Outer race fault at four load condition

The above Figures 6.19 and 6.21 depicts the PDF and CDF responses of the healthy

machine responding to the four load conditions. The graph changes due to the loading and the PDF spreads significantly for a three quarter load but is still less compared to outer race fault. Similarly, Figures 6.20 and 6.22 depicts the PDF and CDF responses of the outer race fault responding to the four load conditions the PDF spreads as the fault traverses from no load to three quarter load and they are reflected in the CDF where the largest slope is found for three quarter loading.

6.7 Conclusion

It is a known fact that time domain signal contains and portrays no information but this research work shows that if the time characteristic is combined with statistical measures it becomes a powerful tool for vibration signal sensing for an outer race fault. The most important finding of this research work is as stated as follows:

- 1) As the load increases the measure of variability increases. This is clearly depicted in Figures 6.19 to 6.22
- 2) This research work suggests that one or two parameters is not a sufficient way to predict an incipient fault rather all statistical parameters become of vital importance for an ORF.
- 3) It has also been observed that changes in the measure of central tendency and dispersion are consistent at an incipient stage as indicated, but a crucial measure is the variability which changes.
- 4) This gives a clear picture that as the load increases the parameters have an increase in standard deviation, sample variance and range.
- 5) The cumulative distribution shows the probability variability of the signal. As the load increases the range increases and the plot of CDF can be seen.
- 6) It has been observed in the study of ORF that as the load conditions increases at Incipient Bearing Fault IBF the data still results in Gaussian distribution. This research work concludes that data remains normally distributed irrespective of healthy or faulty condition.
- 7) It also gives an important view that as load increases the probability distribution function decreases but the FFT fault peak magnitude increases.
- 8) Lastly, the overview shows the load condition derived for both Healthy and outer race fault which gives a comparative measure of the variability.

Experimental Investigations on Inner Race Fault of Ball Bearings of Electrical Machines using Statistical Analysis

This chapter deals with the inner race fault which is a 64% contributor of faults amongst all the bearing faults that exists. This fault was specifically pinpointed under four load conditions and different analysis techniques were applied to detect the existence of this fault. It is one of the most difficult faults to detect at an incipient stage since it is deep rooted and it hides behind the spectra. This chapter gives an insight how to classify the inner race fault using the statistical parameter and inference and eventually validating with the results with a non parametric test.

7.1 Introduction

Rotating parts are always a cause of worry because of the continuous rubbing and the tear and wear. The statistics of the industry show that bearings contribute 40% to the breakdown of electrical machines. Researchers define that 64% is contributed by inner race fault which is of great significance in this study. 18% is the outer race fault followed by the rest 18% as shown in Figure 7.1. The inner race faults are the deepest and the most difficult to detect. This research work contributes for a sure technique to classify the inner race fault. Vibration signal has been used to identify the fault in an electric drive. Four load conditions were introduced that drove the prime mover from no load to three quarter loading. This gives a clear picture of the fault when the induction machine is driven at its rated speed.

Researchers have mentioned different techniques for fault diagnosis of rolling elements in electrical machines. I.E Alguindigue et al [54] narrates that Neural Network NN was used for vibration monitoring and diagnosis and concludes that it can provide a methodology for improving the analysis of spectra for vibration analysis and may provide a viable complement to Power Spectral Density PSD analysis. P. W. Tse et al [109] introduces the Exact Wavelet Analysis (EWA) to extract fault related features that exhibit stationary and non stationary characteristics, making it particularly suitable for detecting randomly occurring faults.

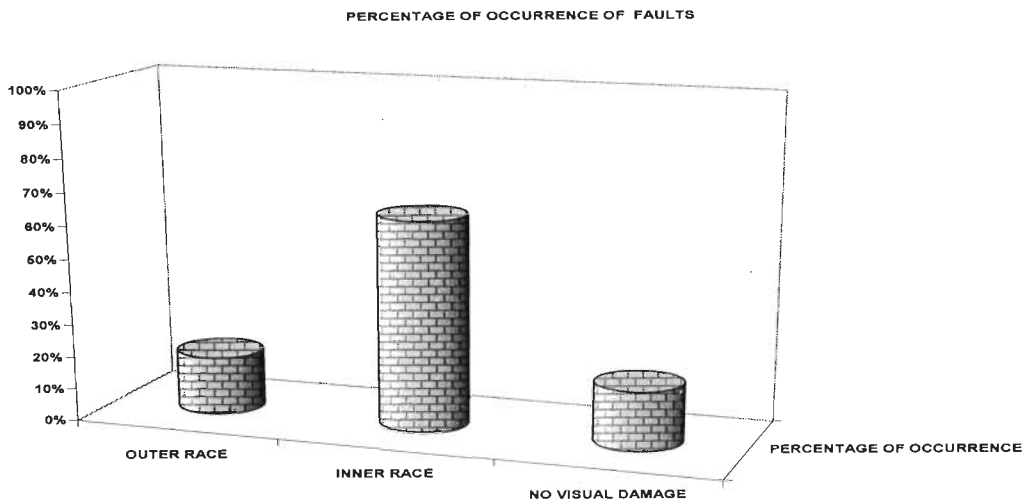


Figure 7.1: Percentage of occurrence of faults found in bearings.

It further states Continuous Wavelet Transforms CWTs have not yet been widely adopted by industry because this technique offers a major obstacle in the difficulty of interpreting the results that are generated by CWT. Inner Race Fault (IRF) was also considered and mentions that most of the frequencies that are embedded in the inspected signal are relatively low in frequency magnitude. Hence, IRF was discovered in the bearing later. Also, it mentions those obvious periodic impacts are hardly seen unless the damage of the defective component is very serious leading to a near fatal breakdown. An insight to the idea of machine fault diagnosis is defined as to detect the occurrence of faults as soon as possible or in other words, when the fault is at incipient level. Peter W.Tse [109] observes that the fault related impulses always possess concentrated vibration energy in a short burst, that is, have high frequency content or occur at low scale values.

X.Lou, and K.A.Loparo [156] deals with a new scheme for the diagnosis of localized defects in ball bearings based on wavelet transform and neuro-fuzzy classification. IRF was also considered but mentions that some faults will be undetectable until failure is imminent. H.Yang et al [52] presents an application of the new basis pursuit method in the extraction of features from signals collected from faulty rolling bearings with IRF and Outer Race Fault ORF. The results obtained were compared with Discrete Wavelet Packet Analysis (DWPA). It also mentions that the peak values at these frequency components, if detectable, are the features one seeks in interpreting bearing faults. S.Prabhakar et al [136] uses the Discrete Wavelet Transforms DWT for vibration signals, from ball bearings having single and multiple point defects on IRF, ORF and the combination faults that have been considered for

analysis. P.W. Tse [108] the experiment results demonstrated that Fast Fourier Transforms FFT with Envelope Detection ED can be used as a diagnostic tool for bearing faults, especially for outer race defects. However, the identification of inner race and roller defects could be very difficult. However, to diagnose the faults of inner race and roller, the tool of WA is found easier for the machine operator to interpret the analyzed results.

K.Mori et al [74] utilizes a wavelet based method for prediction of spalling in a ball bearing from vibration signal. Also, mentions that DWT is a sensitive index of the impulsive responses. J.Zarei, and J.Poshtan [70] Wavelet Packets WPA are used as a powerful diagnostic method for the detection of incipient bearing failures via stator current analysis but also states that diagnosis for inner race damages is very difficult. A. Choudhary & N. Tandon [2] developed a theoretical model to obtain vibration response due to localized defect under radial load conditions. Also, mentions that the component at defect frequency for an ORF defect is much higher than an IRF defect.

T.Williams et al [143] discusses the traditional vibration metrics such as rms, peak value, kurtosis and crest factor. The Adaptive Linear Enhancer (ALE) and High Frequency Resonance Technique (HFRT) are also introduced. It concludes that HFRT and ALE have proven to be effective in monitoring bearing condition with incipient damages. Acoustic Emission (AE) is a good method to detect the outer race failures.

Finally, before exhausting all the techniques some reflection is made on the statistical analysis methods, which according to some researchers in the field of condition monitoring classify as a traditional way of detecting faults.

W.J. Wang et al [151] compares the performance of nonlinear dynamics and Higher Order Statistics (HOS) in machine condition monitoring and fault diagnosis with particular regard to the correlation dimension and bispectra. But further concludes that correlation dimension do not present detailed information about non linear mode coupling on a frequency by frequency basis and the Gaussian noise contained in the signal can be suppressed in the bispectra. H.R.Martin, and F. Honarvar [49] looks at variations of the statistical moment analysis method that show potential for damage detection at a much earlier stage. R.B.W Heng and M.J.M. Nor [114] suggest application of sound pressure and vibration signals to detect the presence of defects in a rolling element bearing using a statistical analysis method. N. Tandon, and A. Choudhary [99] a review of vibration and acoustic measurement methods for the detection of defects in rolling element bearings is discussed. D.Dyer, and R.M.

Stewart [28] suggests statistical parameter kurtosis, that remains constant for an undamaged bearing irrespective of load and speed, yet changes with damage. The extent of damage can be assessed from the distribution of this statistical parameter in selected frequency ranges. S. Nandi and H. A. Toliyat [133] presents a brief review of bearing, stator, rotor and eccentricity related faults and their diagnosis has been discussed. P. Chen et al [100] proposes the fault diagnosis for plant machinery in an unsteady operating condition using Instantaneous Power Spectrum IPS and Genetic Programming but further stated that the parameters obtained cannot be used to precisely detect faults in unsteady operating conditions. M.J. Devaney, and L. Eren [91] encourages the current monitoring to detect and underline the bearing faults in an Induction Machine.

This research work defines the relation of incipient bearing failure due to the inner race fault in terms of its vibration signal. The FFT is found to be a most vital part of condition. This study has a clear picture of how the graph changes according to four load conditions.

7.2 Time Domain Representation of the Acquired Data

The process describes the acquisition of the vibration signal which is stored in an Excel file. This research work shows a thorough investigation of an inner race fault with four load conditions.

Time Domain Signal: Figures 7.2, 7.3, 7.4 and 7.5 depict the time domain representation for the first 500 samples (i.e. depicted on a 0 to 0.8 ms scale) that have been selected from a total 50000 of acquired samples. Four load conditions are considered and an increase in magnitudes of vibration level is seen as the load increases.

No Load

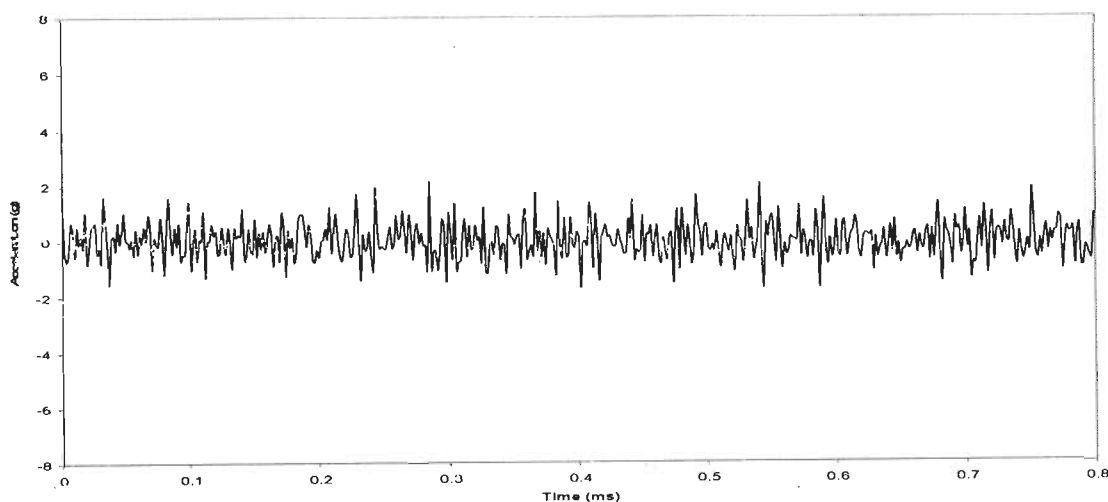


Figure 7.2: Vibration signal for inner race fault at no load.

Slight Load

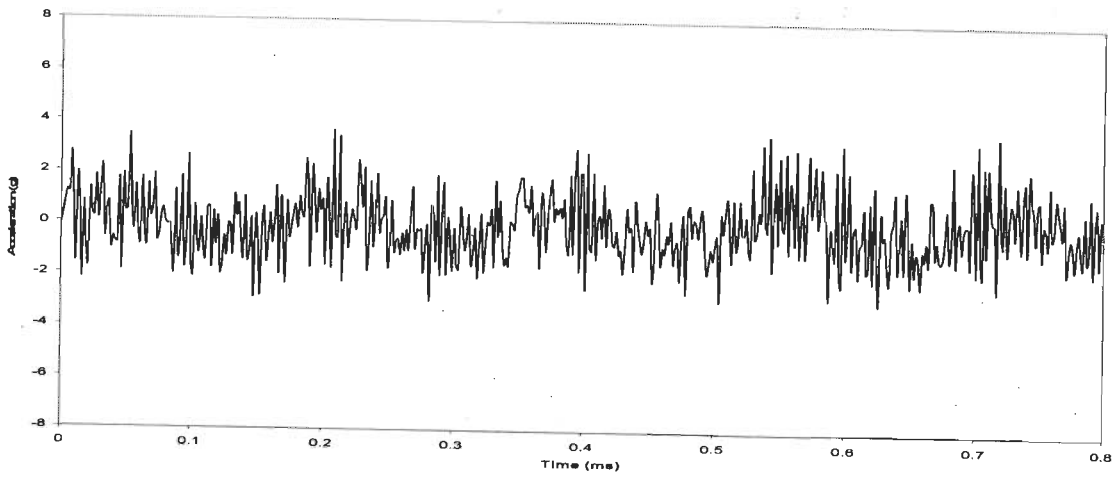


Figure 7.3: Vibration signal for inner race fault at slight load.

Half Load

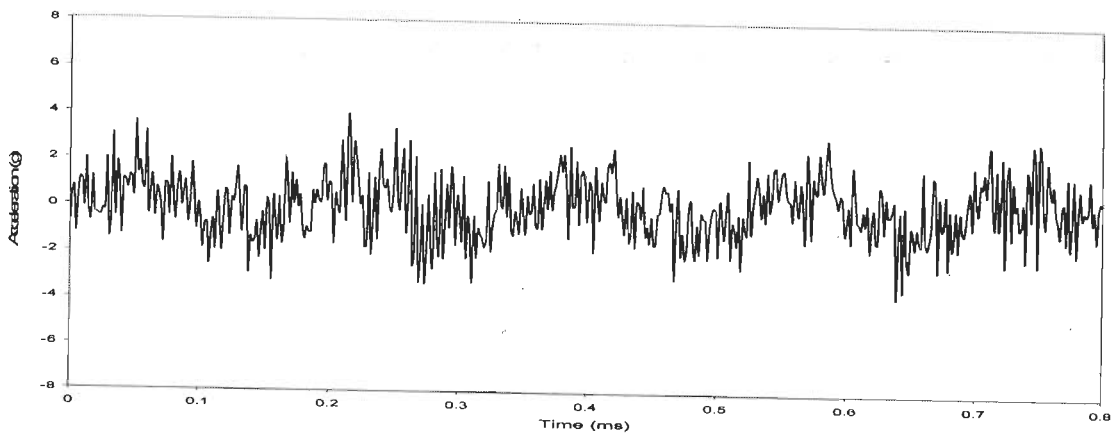


Figure 7.4: Vibration signal for inner race fault at half load.

Three Quarter Load

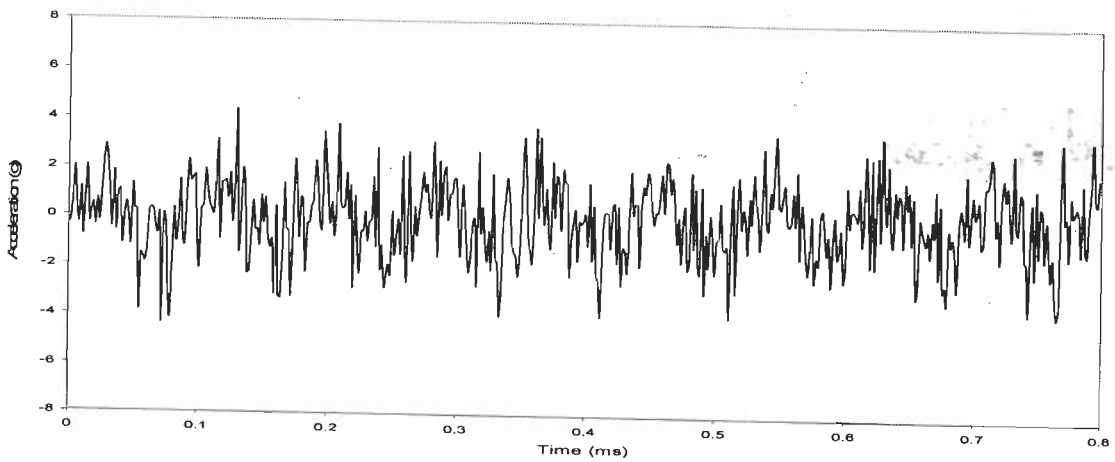


Figure 7.5: Vibration signal for inner race fault at three quarter load.

As the magnitudes increases implies, that the variations has also increased. This is reflected on the statistical parameter which is sensitive to these variation responses.

7.3 Statistical Analysis of the Acquired Data

In general, the statistical analysis can be divided into statistical parameter and statistical inferences.

7.3.1 Statistical Parameter:

H.Yang et al [52] defines the statistical parameter as the detection parameter and states that they are not generally used in diagnosing faults where, it categorically states that variance implies vibration energy level and kurtosis gives the peak distribution. H.R.Martin, and F. Honarvar [49] highlights the skewness and kurtosis with a healthy bearing, having values of kurtosis in the range of 3.0 to 3.5. R.B.W Heng.,and M.J.M. Nor [114] considers an additional parameter the crest factor and relates that, statistical parameters are affected by the shaft speed. T.Williams et al [143] utilizes the rms, peak value, kurtosis and crest factor. N. Tandon, and A. Choudhary [99] a review paper discusses the rms level, crest factor, probability distribution function and kurtosis with this parameter, which is mentioned as the most effective. D.Dyer, and R.M. Stewart [28] an important observation on kurtosis is mentioned that it remains constant for an undamaged bearing irrespective of load and speed, yet changes with damage.

In a broad sense statistical parameter can be divided into Measure of Central Tendency - MCT, Measure of Variability MV and Measure of Dispersion- MD, discussed in chapter 3. Here, the statistical parameters for four load conditions for an incipient fault for which, the time signal is shown in Figures 7.2, 7.3, 7.4 and 7.5 for no load, slight load, half load and three quarter loading respectively are presented. This is shown in Table 7.1 and 7.2, which represents a comparative view of the statistical parameters for the different load condition as well as for healthy (fault free) and inner race fault respectively.

Table 7.1: Statistical Parameters for four load conditions for a Healthy Machine (Fault Free).

| PARAMETERS | HEALTHY (FAULT FREE) | | | |
|--------------|----------------------|-------------|-----------|--------------------|
| | No Load | Slight Load | Half Load | Three Quarter Load |
| Units | | | | |
| Mean (g) MCT | -0.003 | -0.005 | -0.004 | -0.005 |

| | | | | |
|--------------------------------------|--------|--------|--------|--------|
| Standard Error (g) MV | 0.002 | 0.002 | 0.003 | 0.003 |
| Median (g) MCT | 0.000 | -0.044 | -0.015 | -0.029 |
| Mode (g) MCT | -0.034 | -0.210 | -0.269 | -0.229 |
| Standard Deviation (g) MV | 0.385 | 0.534 | 0.603 | 0.614 |
| Sample Variance (g ²) MV | 0.148 | 0.285 | 0.364 | 0.377 |
| Kurtosis MD | 2.957 | 3.494 | 3.344 | 3.474 |
| Skewness MD | -0.016 | 0.177 | 0.057 | 0.086 |
| Range (g) MV | 3.364 | 3.662 | 4.346 | 4.243 |
| Minimum (g) | -1.719 | -1.816 | -2.114 | -2.173 |
| Maximum (g) | 1.646 | 1.846 | 2.231 | 2.070 |
| Confidence Interval (95.0%) (g) | 0.003 | 0.005 | 0.005 | 0.005 |

Table 7.2: Statistical Parameter for four load condition for an inner race fault.

| PARAMETERS | INNER RACE FAULT | | | | |
|--------------------------------------|------------------|-------------|-----------|---------------|---------|
| | No Load | Slight Load | Half Load | Three Load | Quarter |
| Units | | | | | |
| Mean (g) MCT | -0.007 | -0.003 | -0.008 | | -0.005 |
| Standard Error (g) MV | 0.003 | 0.006 | 0.007 | | 0.007 |
| Median (g) MCT | -0.010 | -0.039 | -0.039 | | 0.024 |
| Mode (g) MCT | 0.107 | 0.308 | -0.278 | | 0.688 |
| Standard Deviation (g) MV | 0.721 | 1.387 | 1.460 | | 1.517 |
| Sample Variance (g ²) MV | 0.519 | 1.922 | 2.132 | | 2.300 |
| Kurtosis MD | 3.063 | 2.956 | 3.030 | | 2.847 |
| Skewness MD | 0.015 | 0.112 | 0.074 | | -0.078 |
| Range (g) MV | 6.382 | 11.138 | 12.881 | | 12.368 |

| | | | | |
|---------------------------------|--------|--------|--------|--------|
| Minimum (g) | -3.198 | -5.840 | -6.621 | -6.479 |
| Maximum (g) | 3.184 | 5.298 | 6.260 | 5.889 |
| Confidence Interval (95.0%) (g) | 0.006 | 0.012 | 0.013 | 0.013 |

In present work, a number of statistical parameters are found, for a given operating condition, to arrive at fault diagnosis. These parameters are given in Table 7.1 for a motor with healthy bearings and in Table 7.2 for load end bearing with inner race fault. Four loading conditions of the machine are considered: No Load, Slight Load, Half Load and Three Quarter Load.

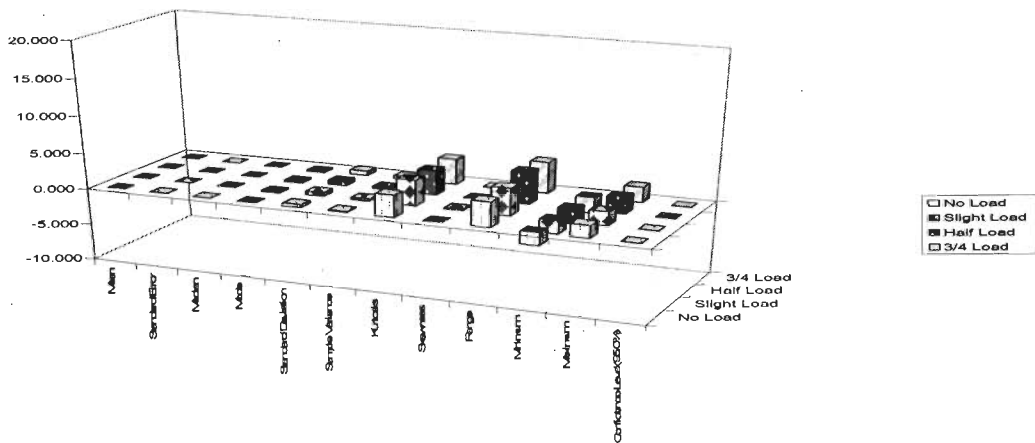


Figure 7.6: A 3-D plot showing the behaviour of statistical parameters at four load condition for Healthy Machine

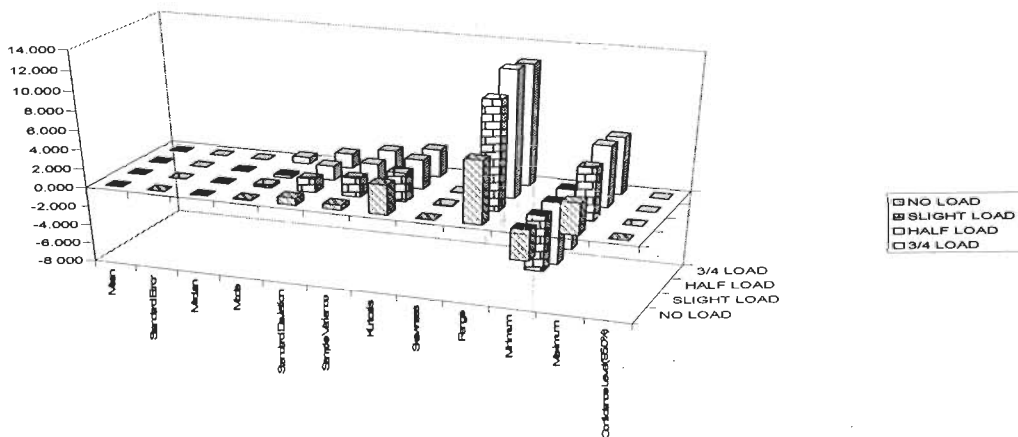


Figure 7.7: A 3-D plot showing the behaviour of statistical parameters at four load conditions for inner race fault.

The statistical parameters in Table 7.1 and 7.2 are plotted for the four load conditions as shown in Figure 7.6 and Figure 7.7 for a healthy machine and for IRF respectively; a 3-D plot indicates that the central tendency remains constant, the measure of variability shows variation and the measure of dispersion remains fairly constant for the four load conditions. This indicates that only measure of variability is important in identifying incipient bearing fault, originating in inner race. It further compares the parameters with a healthy machine.

7.3.2 Statistical Inferences

Statistical parameters are derived from the time domain vibration signal and the statistical inference is further extended by calculating the probability distribution function and cumulative distribution function. H.R.Martin, and F. Honarvar [49] states that as the interface between two surfaces in motion begins to breakdown, the shape of the PDF changes and tends to become more peaky. R.B.W Heng, and M.J.M. Nor [114] condemns the beta function parameters for both sound and vibration signals. N. Tandon, and A. Choudary [99] quotes that the probability density of acceleration of a bearing in good condition has a Gaussian distribution, whereas a damaged bearing results in non Gaussian distribution with dominant tails. D.Dyer, and R.M. Stewart [28] states that the extent of damage can be assessed from the distribution of the statistical parameter in selected frequency ranges. This research work determines the PDF and CDF for the four load conditions.

Thus the results of this research work shows that the vibration signals are Gaussian in nature, irrespective of healthy and non healthy conditions.

Probability Density Function:

The statistical inference can be derived from the probability density function which is represented as the Gaussian distribution function and is given by the equation refer to chapter 3.

$$f(x) = (1/\sigma\sqrt{2\pi}) \exp(-1/2)(x - m/\sigma)^2$$

No Load

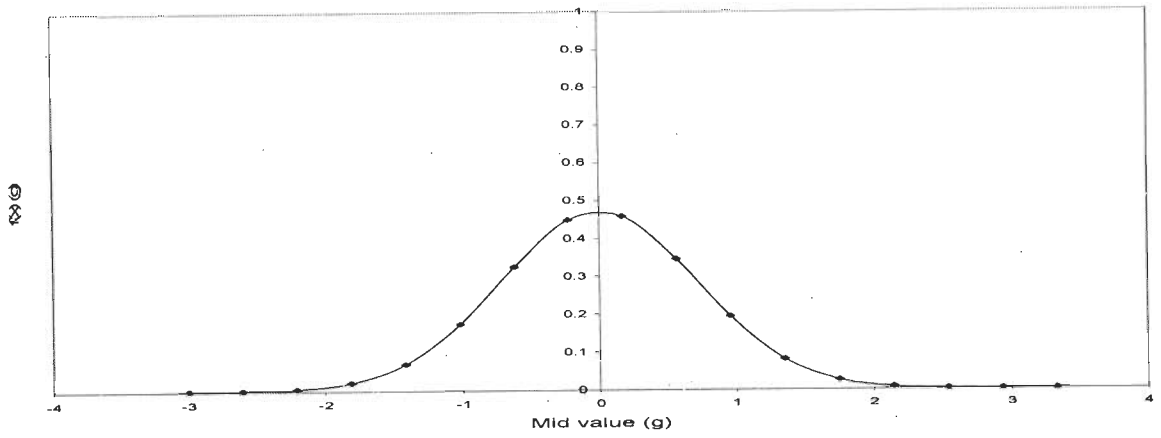


Figure 7.8: The probability density function at no load condition for inner race fault.

Slight Load:

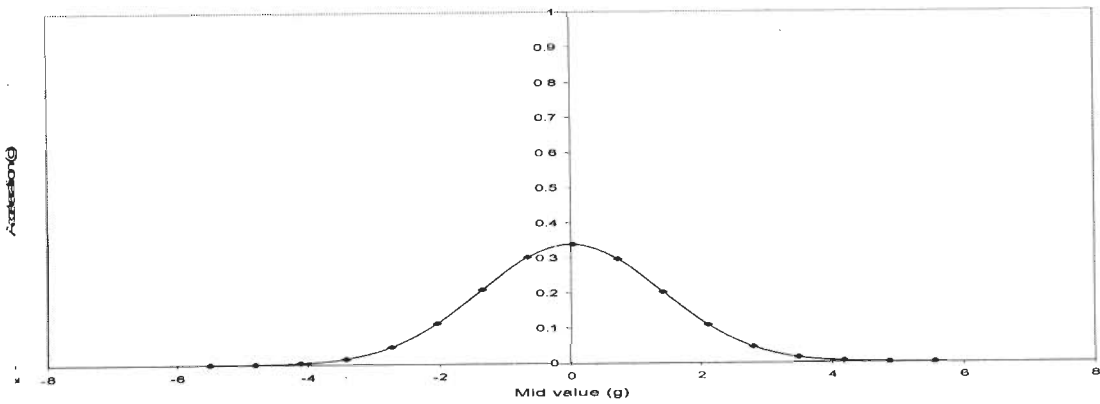


Figure 7.9: The probability density function at slight load condition for inner race fault.

Half Load:

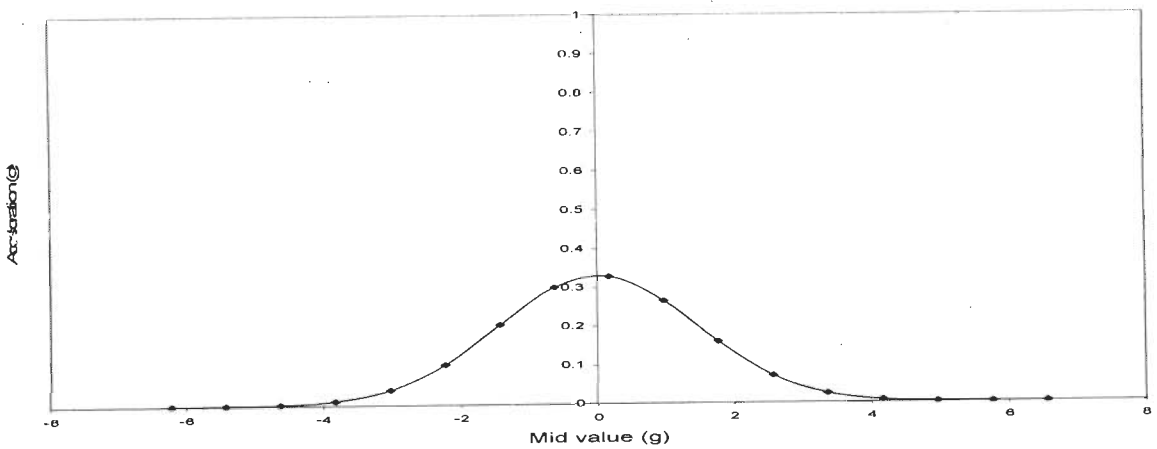


Figure 7.10: The probability density function at half load condition for inner race fault.

Three Quarter Load:

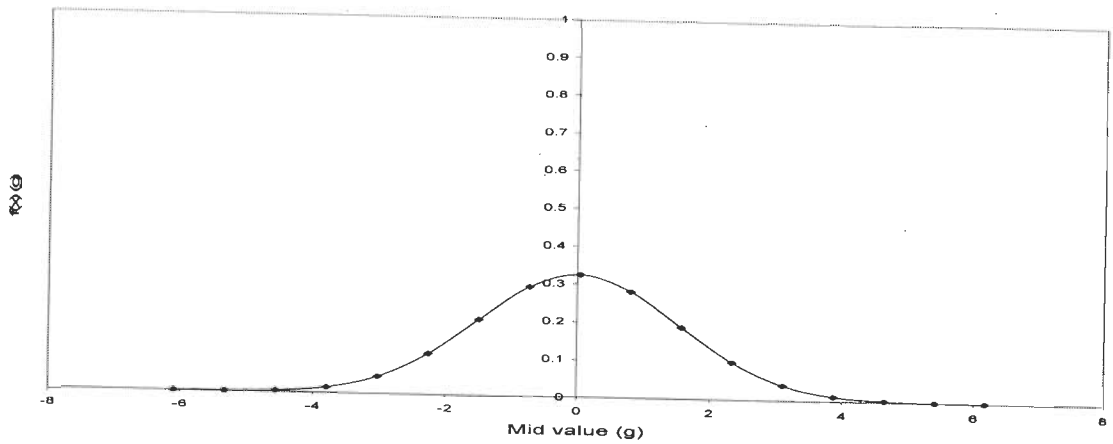


Figure 7.11: The probability density function at three quarter load condition for inner race fault.

Table 7.3: The practical value of magnitudes of the maximum value of PDF obtained for four different load conditions for inner race fault.

| Probability Density Function | | |
|------------------------------|------------|----------------|
| Load Conditions | x-axis (g) | y-axis maximum |
| No Load | 0 | 0.4567g |
| Slight Load | 0 | 0.3387g |
| Half Load | 0 | 0.3270g |
| Three Quarter Load | 0 | 0.3238g |

From, Table 7.3 the magnitudes of the PDF function decreases gradually with load. The data was further validated by chi square test which shows that chi square estimated at 8 degree of freedom and 5% of significance level is 15.51 and the chi values obtained are 3.22, 3.640, 3.614 and 5.705 for no load, slight load, half load and three quarter load respectively. This proves that for inner race fault at different load conditions for an incipient fault has a Gaussian distribution.

Cumulative Distribution Function

The cumulative distribution function having the equation $F(X) = \int f(x)dx$ is explained in chapter 3.

The probability density function was calculated for 50000 samples and the cumulative distribution is evaluated for these values of probability density function.

This research work gives a new concept of looking at the behaviour of variations by calculating the cumulative distribution function of the vibration signal. Again, the four different kinds of load conditions namely, No Load, Slight Load, Half Load and Full Load of an inner race fault were evaluated.

No Load

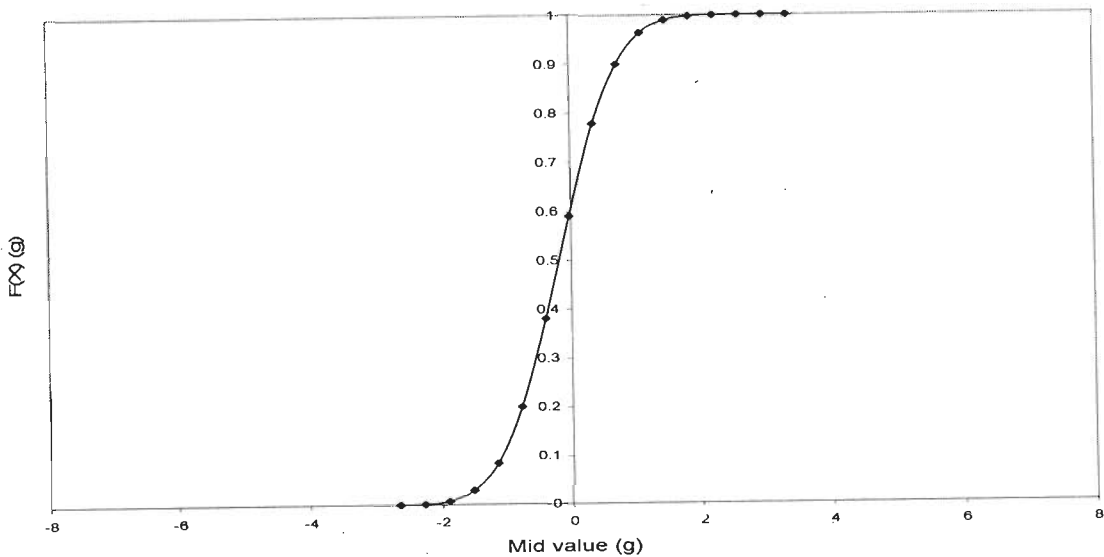


Figure 7.12: The cumulative distribution function at no load condition for inner race fault.

Slight Load

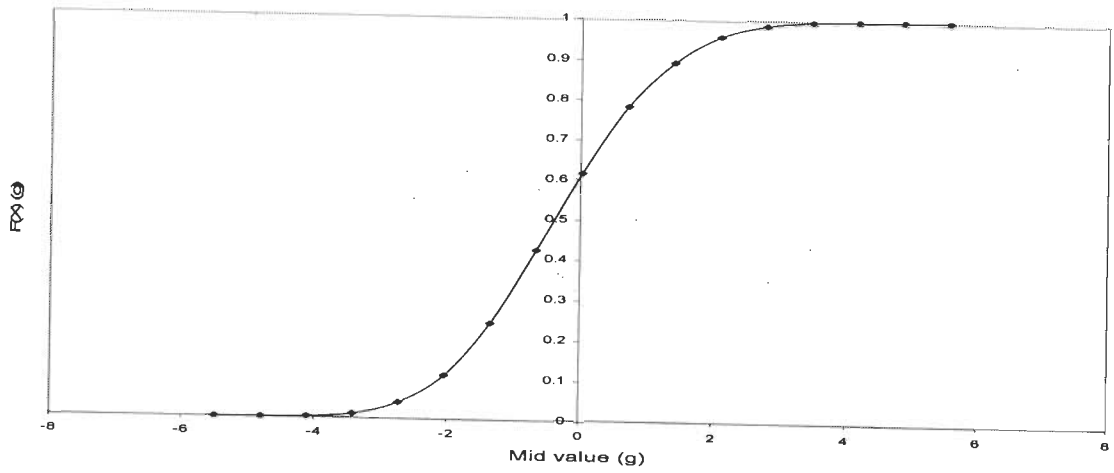


Figure 7.13: The cumulative distribution function at slight load condition for inner race fault.
Half Load

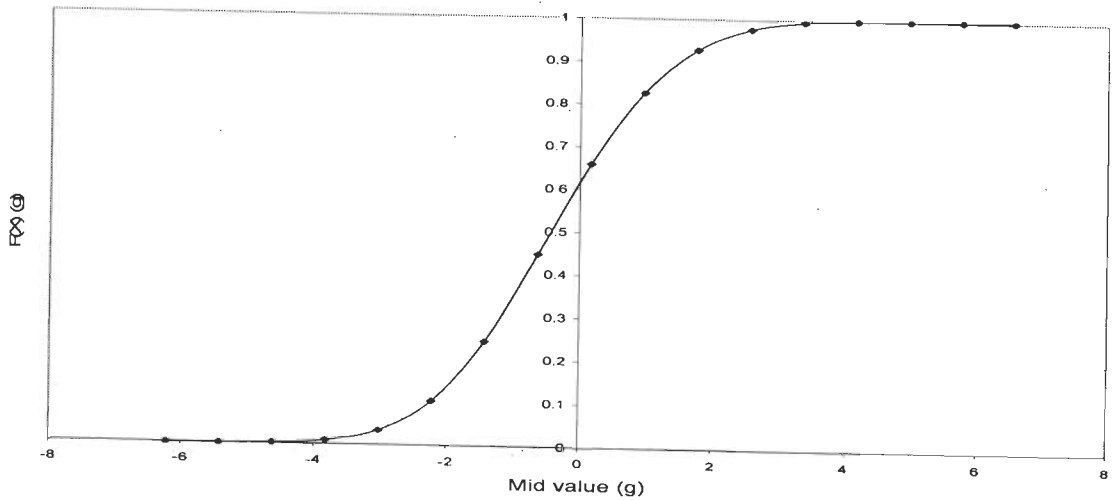


Figure 7.14: The cumulative distribution function at half load condition for inner race fault.
Three Quarter Load:

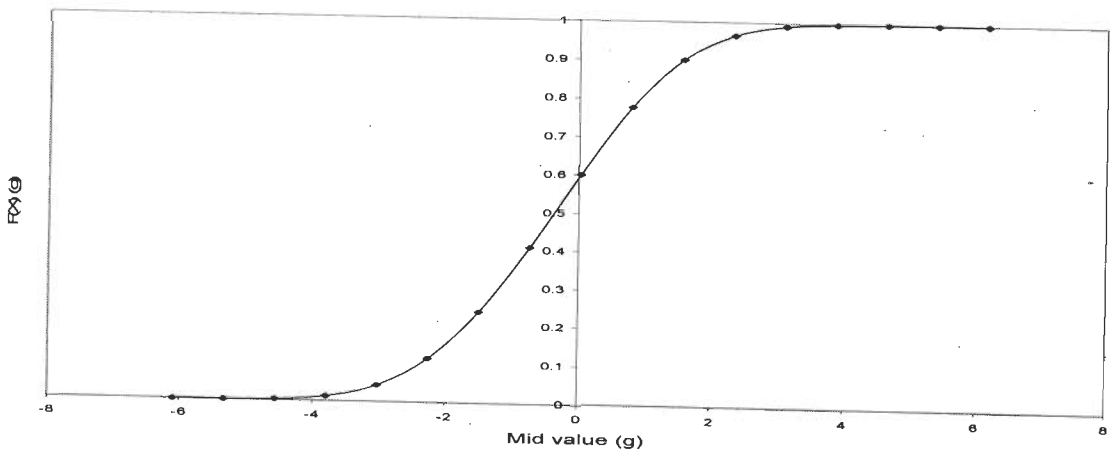


Figure 7.15: The cumulative distribution function at three quarter load condition for inner race fault.

From Figures 7.12, 7.13, 7.14, and 7.15 it can be seen that at 10% and 90% of Probability ($\mu - 1.645\sigma < x < \mu + 1.645\sigma$) have the acceleration levels that are given by the g-values. At no load it ranges from (-1.022g to 0.60g), at slight load it ranges from (-2.042g to 1.41g), at half load it ranges from (-2.22g to 1.7634g) and finally at three quarter load it ranges from (-2.26g to 1.571g) respectively.

7.4 Frequency Domain Representation

The STFT is calculated to confirm that the position of peaks of the frequencies do tally with the theoretical frequencies expected. A peak at the characteristic fault frequency clearly indicates that a fault is captured at an incipient stage.

I.E Alguindigue et al [54] state that when a machine is operating properly, vibration is small and constant. However, when a fault develops and some of the dynamic processes in the machine change, the vibration spectrum also changes. Furthermore, each time a rolling element passes over a defect, an impulse of vibration is generated. These impulses are related to fault and severity. X.Lou and K.A.Loparo [156] proceeds by examining the magnitude of the vibration data under operating conditions with severe bearing faults. It is possible to distinguish the normal data from different types of fault data. However, this is not always applicable because the signal morphology that results from a fault changes over time as the fault progresses from initiation to failure. Thus, some faults will be undetectable until failure is imminent. S.Prabhakar et al [136] observes that an IRF impulse does not appear in the lower levels because of their high frequency nature. P.W. Tse et al [108] mention that the FFT based method is difficult to detect the impacts. A. Choudhary and N. Tandon [2] specifically treats IRF, stating that the amplitudes of sidebands are not symmetrically distributed about the defect frequency. The amplitude of the sidebands at frequency higher than the defect frequency are comparatively larger. S.A. McInerny, and Y.Dai [127] says that vibrations measured on a bearing are dominated by high level imbalance and misalignment components, and include random vibrations associated with friction and other sources.

This research work shows frequency spectrum of vibration data for the inner race fault. The calculated characteristic frequencies for inner race fault of the bearing NBC-6308 (7 balls) is 103.3Hz as seen in chapter 3. These Calculated Frequencies should be dominant according to the fault considered. The prevalent frequencies are calculated and the harmonics of each individual frequency do exist on the severity and intensity of the fault. The resolution

that was considered, to obtain the result below was 0.625Hz. As the resolution becomes high, the peaks become more distinguished and can be easily classified. These frequency values may drift between (+/-) 5Hz in practical data due to variations in supply frequencies. The four load conditions are as follows:

No Load

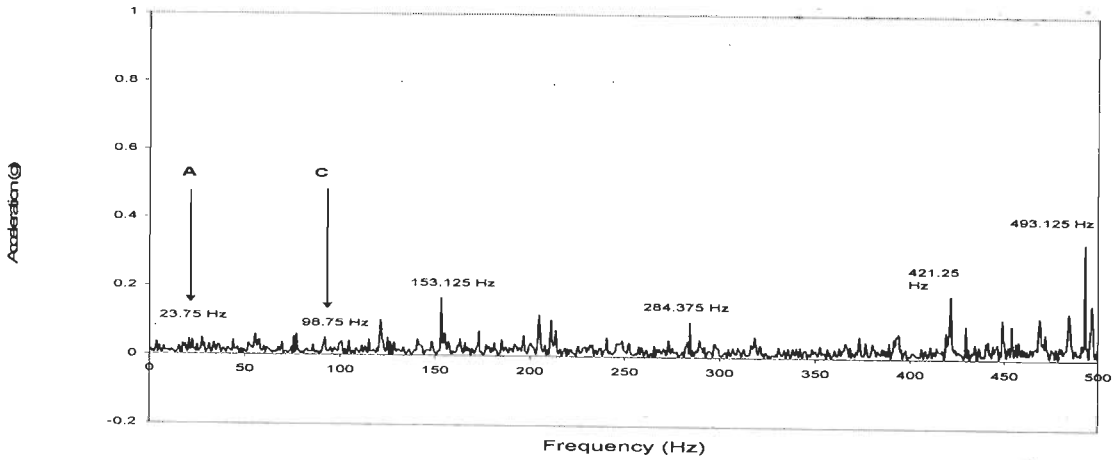


Figure 7.16: The FFT for no load condition for inner race fault.

Slight load

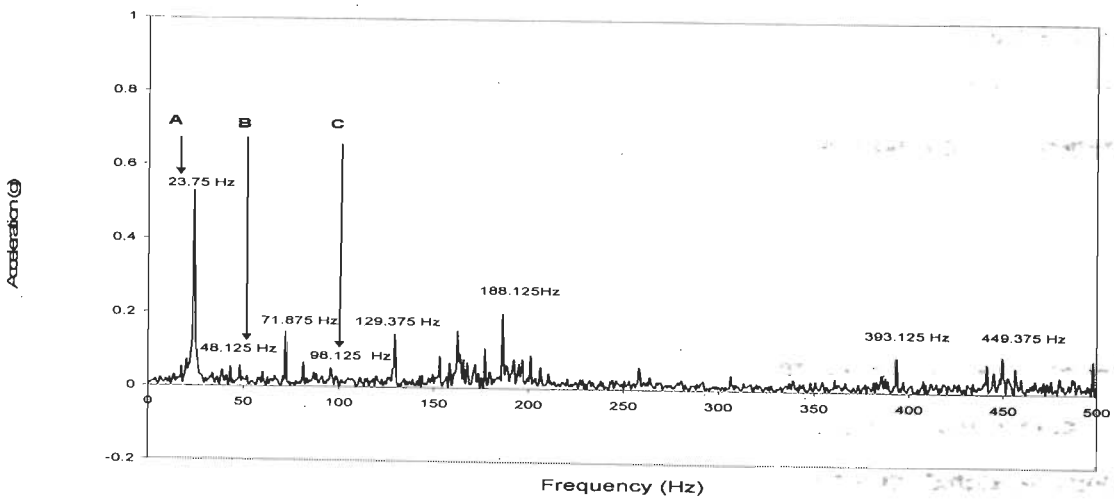


Figure 7.17: The FFT for slight load condition for inner race fault.

Half Load

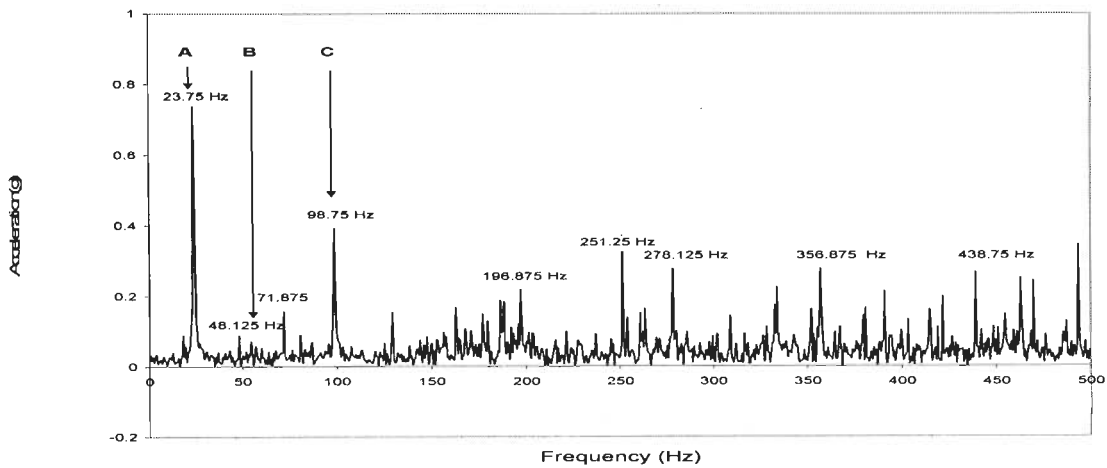


Figure 7.18: The FFT for slight load condition for inner race fault.

Three Quarter Load

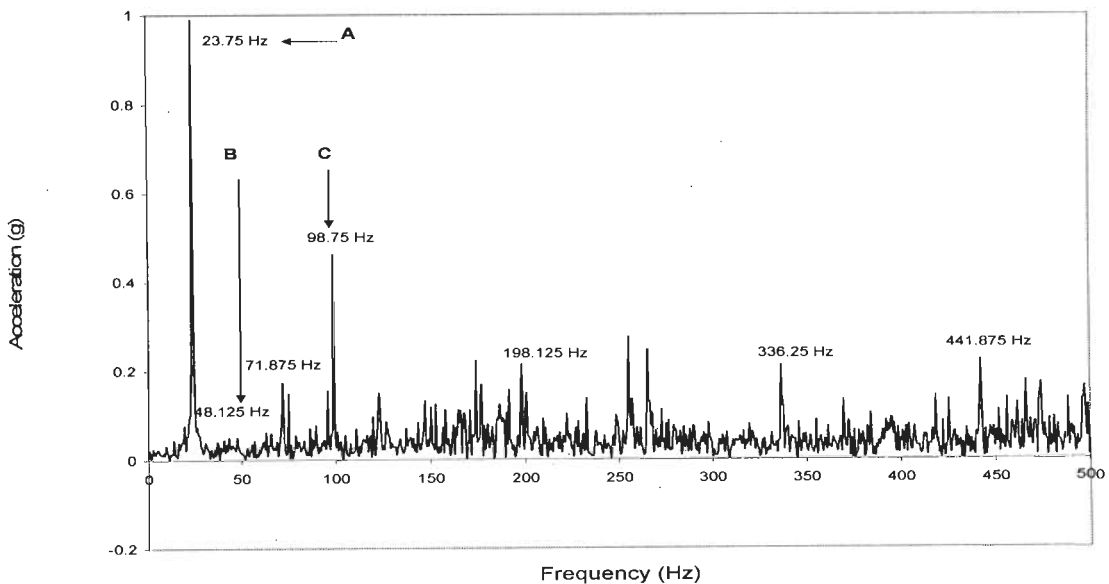


Figure 7.19: The FFT for three quarter load condition for inner race fault.

From Figures 7.16, 7.17, 7.18 and 7.19 the significant frequencies of interest are given as A,B,C. Where the bearing characteristic frequency (BCF) obtained from the vibration data is given as,

A-Rotational frequency

B-Ball spin frequency

C-Inner Race frequency

“A” is at 23.75 Hz which as mentioned is the rotational frequency; “B” is at 48.75Hz which is

the ball spin frequency.

Table 7.4: The practical value of magnitudes of the peaks obtained for four different load conditions.

| Load Condition | Practical Value Obtained | Magnitudes of These Peaks |
|--------------------|--------------------------|---------------------------|
| No Load | 98.75 Hz | 0.0116g |
| Slight Load | 98.75 Hz | 0.0758g |
| Half Load | 98.75 Hz | 0.3905g |
| Three Quarter Load | 98.75 Hz | 0.4626g |

Meanwhile from Figures 7.16, 7.17, 7.18 and 7.19 it can be seen that a peak has erupted at 98.75Hz which signifies an inner race fault and as the load increases the peak increases. Table 7.4 shows the magnitudes obtained at the fault frequency. It is of practical interest that as the load increases the fault frequency magnitude at “c” rises.

7.5 Discussion:

- (i) **Time Signal:** The vibration data signal is depicted in Figures 7.2, 7.3, 7.4 and 7.5. It can be seen that as the load increases the variation on the time domain signal increases. The no load time signal has the least variation in the vibration signal for and IRF.
- (ii) **Statistical Parameter:** Researchers have defined statistical parameters which is a very important criteria, since these are divided into central tendency, measure of variability and measure of dispersion which is discussed as below

Measure of Central tendency (MCT)

In Tables 7.1 and 7.2, it can be seen that the values are zero or very close to zero indicating an almost symmetric distribution. An excerpt from Tables 7.1 and 7.2 is depicted in the Table 7.5 below

Table 7.5: Measure of Central tendency (MCT)

| MCT | Comparing Inner Race Fault (IRF) and Healthy MCT | | | |
|------------|--|--------------------|--------------------|--------------------|
| | No Load | Slight Load | Half Load | Three Quarter Load |
| Units | | | | |
| Mean (g) | -0.007 (-0.003) | -0.003 (-0.005) | -0.008 (-0.004) | -0.005 (-0.005) |
| Median (g) | -0.010 (0.000) | -0.039 (-0.044) | -0.039 (-0.015) | 0.024 (-0.029) |

| | | | | |
|-----------------|-----------------|-----------------|-----------------|-----------------|
| Mode (g) | 0.107 | 0.308 | -0.278 | 0.688 |
| | (-0.034) | (-0.210) | (-0.269) | (-0.229) |

Data for a healthy machine is in parenthesis. For a three quarter load the median has a value of 0.024g for inner race fault and it tends to be -0.029g for healthy machine. Meanwhile, for the same load condition the value of mode is 0.688g for inner race fault and -0.229g for healthy machine.

Measure of variability (MV)

Measure of variability in terms of statistical parameter is represented by range, sample variance and standard deviation. An excerpt from Tables 7.1 and 7.2 is depicted in the Table 7.6 below

Table 7.6: Measure of variability (MV)

| MV | Comparing Inner Race Fault (IRF) and Healthy- MV | | | |
|--|--|-----------------|-----------------|--------------------|
| | No Load | Slight Load | Half Load | Three Quarter Load |
| Standard Error (g) | 0.003 | 0.006 | 0.007 | 0.007 |
| | (0.002) | (0.002) | (0.003) | (0.003) |
| Standard Deviation (g) | 0.721 | 1.387 | 1.460 | 1.517 |
| | (0.385) | (0.534) | (0.603) | (0.614) |
| Sample Variance (g²) | 0.519 | 1.922 | 2.132 | 2.300 |
| | (0.148) | (0.285) | (0.364) | (0.377) |
| Range (g) | 6.382 | 11.138 | 12.881 | 12.368 |
| | (3.364) | (3.662) | (4.346) | (4.243) |
| Minimum (g) | -3.198 | -5.840 | -6.621 | -6.479 |
| | (-1.719) | (-1.816) | (-2.114) | (-2.173) |

| | | | | |
|--------------------|----------------|----------------|----------------|----------------|
| Maximum (g) | 3.184 | 5.298 | 6.260 | 5.889 |
| | (1.646) | (1.846) | (2.231) | (2.070) |

The range has the value of 6.382g for an IRF no load condition and 3.364g for inner race fault and fault free condition respectively. Similarly, the range for three quarter loading is 12.368g for inner race fault and 4.243g for a healthy machine.

It was mentioned that as the load increases the variation increases. This can be seen in Table 7.6. The maximum and minimum values are showing the degree of the spread of the data. It has also been observed in this study that as the load increases measure of variability has significant changes at Incipient Bearing Fault.

Measure of Dispersion (MD)

Measure of dispersion is given by the kurtosis and skewness since the fault is at an incipient stage. The kurtosis and skewness remain approximately close to 3 to 3.5 and zero respectively. The maximum and minimum values are showing the degree of the spread of the data.

Table 7.7: Comparison of MD

| MD | Comparing Inner Race Fault (IRF) and Healthy MD | | | |
|-----------------|---|--------------------------------|--------------------------------|---------------------------------|
| | No Load | Slight Load | Half Load | Three Quarter Load |
| Kurtosis | 3.063 (2.957) | 2.956 (3.494) | 3.030 (3.344) | 2.847 (3.474) |
| Skewness | 0.015 (-0.016) | 0.112 (0.177) | 0.074 (0.057) | -0.078 (0.086) |

The measure of dispersion MD has no significant change for an inner race fault at an incipient stage.

The above discussion shows that the most vital measure at an incipient stage is the measure of variability.

This shows that as the machine is loaded, a clear indication of the fault condition can be seen.

d) **Probability Distribution Function (PDF):** The PDF was calculated and Table 7.3 shows a overview of these results for four load condition. As the load is increased the magnitudes fall and the PDF spreads on a wider range which can be seen in the results. This implies that measure of variation has increased which is clearly shown in Table 7.7. This research work clearly indicates a vibration signal is not only Gaussian but even if damage occurs the distribution will be Gaussian only the PDF magnitudes will fall.

e) **Cumulative Distribution Function (CDF):** Here, CDF has been evaluated on vibration data at various loads. Figures 7.12, 7.13, 7.14 and 7.15 show the CDF and the variations from No load, slight load, half load and three quarter load respectively.

iii) **Frequency Domain Representation:** The Bearing Characteristic Frequency (BCF) was calculated and this value was found to be 103Hz, whereas the practical value obtained from these results is 98.75Hz. These are depicted in Figures 7.16, 7.17, 7.18 and 7.19. Table 7.5 summarizes the peaks obtained and the respective magnitudes obtained. It can be seen that as the load increases the magnitudes of peaks also increases.

This research work clearly indicates that as the load conditions increase the magnitude of the peaks do increase.

7.6 Trend of IRF with Load Variations

Figure 7.20 shows the PDF of the four waveforms at the No load, slight load, half load and three quarter load condition for a Healthy (Fault Free). Figure 7.21 shows the PDF of the four waveforms at the No load, slight load, half load and three quarter load condition for an Inner Race Fault. Figure 7.23 shows the CDF of the four waveforms at the No load, slight load, half load and three quarter load condition for a Healthy (Fault Free) and Figure 7.24 shows the CDF of the four waveforms at the No load, slight load, half load and three quarter load condition for an Outer Race Fault.

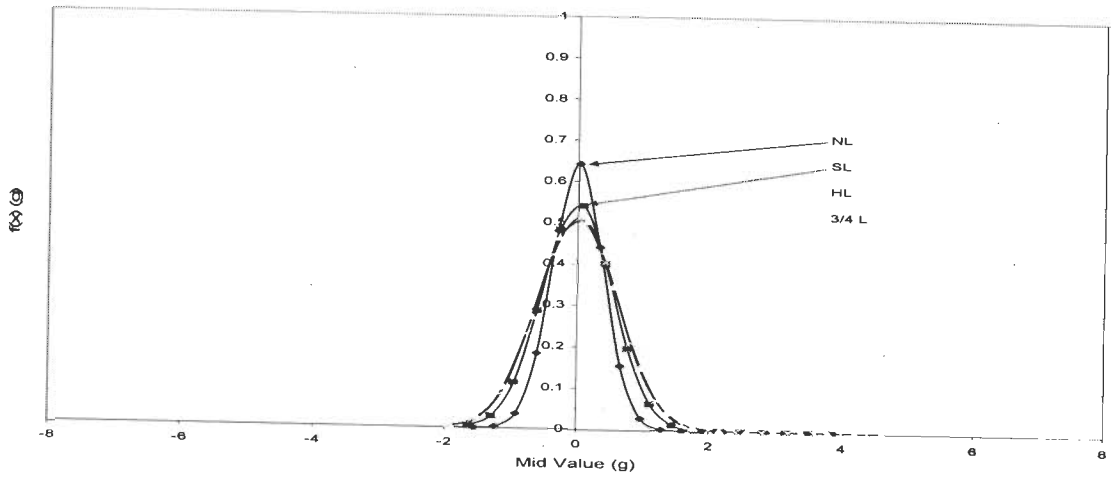


Figure 7.20: PDF of Healthy at four load condition

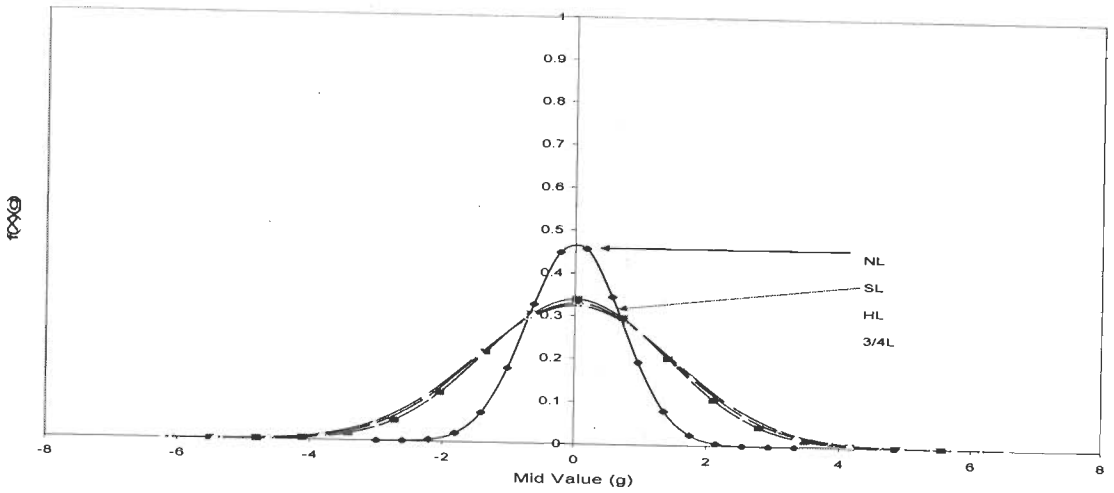


Figure 7.21: PDF of Inner race fault at four load condition

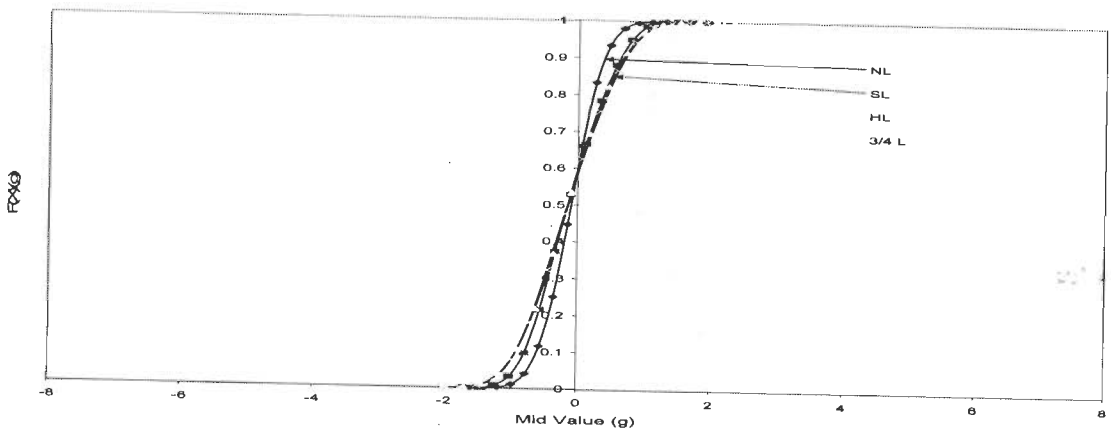


Figure 7.22: CDF of Healthy at four load condition

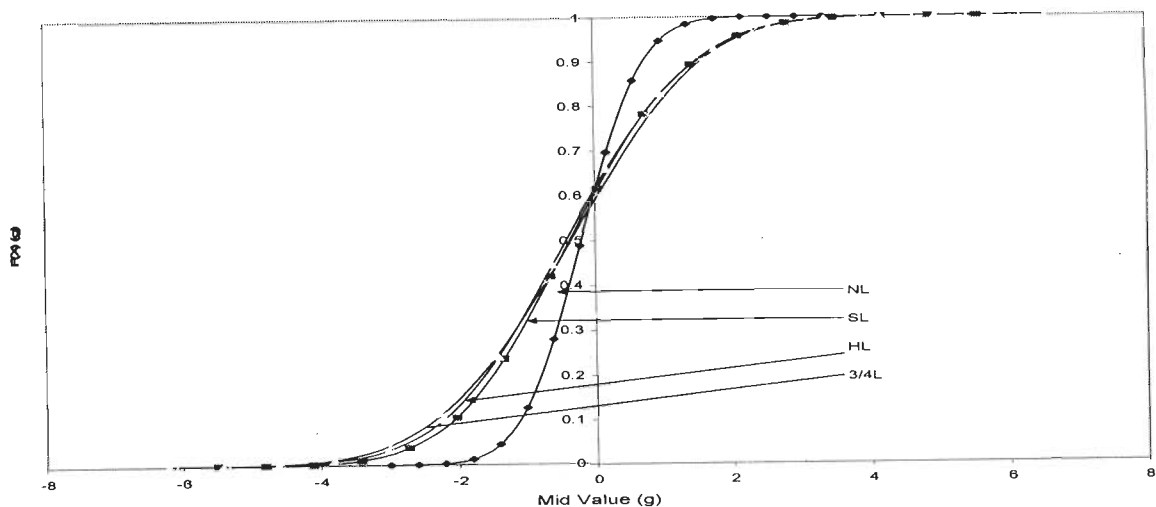


Figure 7.23: CDF of Inner race fault at four load condition

The above Figures 7.20 and 7.22 depicts the PDF and CDF responses of the healthy machine responding to the four load conditions. The graph changes due to the loading and the PDF spreads significantly for a three quarter load but is still less compared to inner race fault. Similarly, Figures 7.21 and 7.23 depicts the PDF and CDF responses of the inner race fault responding to the four load conditions the PDF spreads as the fault traverses from no load to three quarter load and they are reflected in the CDF where the largest slope is found for three quarter loading.

7.7 Conclusion

This research work categorically states the four load conditions of a 7.5 kW prime mover with an inner race fault and it can be inferred that;

- 1) As the load increases the amount of variation increases. This is further confirmed by calculating the statistical parameters.
- 2) It has also been observed that changes in the measure of central tendency and dispersion are consistent at an incipient stage as indicated, but a crucial measure is the variability which changes.
- 3) As the load increases, an increase in standard deviation, sample variance and range is observed.
- 4) It also gives an important view that as load increases the probability density function decreases but the FFT fault peak magnitude increases.

- 5) The cumulative distribution shows the probability variability of the signal. As the load increases the range increases and the graph is not sharp.
- 6) It has been observed in this study of IRF that as the load conditions increases at Incipient Bearing Failure, the data still results in a Gaussian distribution. This research work concludes that data remains normally distributed irrespective of healthy or faulty condition.
- 7) Lastly, the overview shows the load condition derived for both Healthy and inner race fault which gives a comparative measure of the variability.

Conclusions

This chapter highlights the objectives and achievements of this work and lists a few suggestions for future work.

8.1 Introduction

In this work a new approach is introduced for fault diagnosis of bearing faults of rotating electrical machines. Only Ball bearing type of bearings have been considered. A series of experiments have been performed on a 7.5 kW cage induction motor to obtain vibration signal, in acceleration parameter, through a piezo electric accelerometer with a magnetic base mounted on the bearing cap of the load-end bearing. During these investigations, three conditions of bearings are considered: when the bearing (a) is healthy (fault free) (b) has a fault in outer race (ORF) and (c) has a fault in inner race (IRF). The objective of this work is to successfully diagnose the fault at a very early stage which is termed as incipient stage. Accordingly the bearings with minor dents in outer/inner race, and not those with severe damage, have been used for investigations.

The vibration signal is subjected to chitest to demonstrate that the data is Gaussian not only for healthy bearing but for those with incipient faults as well. This has been a key factor in the analysis leading to diagnosis.

A set of time domain parameters are calculated from the vibration signal under different conditions of bearing and compared to establish the changes when the bearing just transits from healthy mode to faulty mode. The findings are confirmed using frequency domain analysis as well.

The above study is done when the motor is run under load. Four settings of load have been considered: (a) no load (b) slight load (c) half full load and (d) Three Quarter full load.

8.2 Overview of Results and Conclusion

An introduction is given in chapter 1 to FDEM and an intensive literature review that suggests that researchers have applied numerous techniques in the fault detection of electrical machines but up till now no technique have been perfected. This research work establishes not only the behavioural pattern of the signal but the way the vibration data behaves to the changes of the load conditions at incipient stage. This intensive literature review suggests that the researchers have segregated the parameters for fault detection. This research work focuses on all the parameters and their respective changes at an incipient stage and the contribution to the detection of faults. The data acquisition DAQ is discussed in chapter 2 which is in accordance to the experiments executed in the laboratory. This research work recommends that sampling frequency, the data length and eventually the resolution is of utmost importance in FDEM. The analysis technique is highlighted in chapter 3 where the careful handling of sampling frequency, length of the data and resolution is extended to the analysis of the signals. This results in obtaining a frequency spectrum or FFT that could detect the peaks of the faulty bearing. Moreover, it is emphasized that statistical analysis in tandem with time domain signal analysis becomes a powerful tool for fault detection at incipient stage. The behaviour of the vibration data is considered in chapter 4 by implementing the Non Parametric test that is the chi square test which again is the major contribution and proves that the data remains Gaussian when the induction machine enters into incipient fault mode. The behavioural pattern of the vibration data indicates that it remains Gaussian for

- a) all load conditions if driven at rated value
- b) at an incipient stage a slight introduction of fault affects the statistical values which becomes indicative of FDEM but it does not traverse to the extent of it being Non Gaussian.

A comparative study of a fault free, outer race fault and inner race fault is done in chapter 5. The analysis technique used is the time waveform representation, the statistical techniques, involving both the parameters and the inferences. The FFT that reassures that the fault is an outer and inner race fault which are the major contributors of faults in the bearing world. This study suggests how the fault when developed at an incipient stage is indicated in the signal analysis. The ORF is examined in details in chapter 6. Four load conditions are considered. A major observation is that as the FFT peak increases with the load condition and the PDF decreases simultaneously and hence this shows that they are inversely proportional

which can be related to frequency and time which clarifies the findings. The IRF is studied in chapter 7 and this had similar behavioural pattern as for the ORF except that the peaks of the FFT had shifted by $\pm 5\text{Hz}$. A similar observation is found that as the load increases the FFT distinctive peak increases in magnitude and PDF decreases for an incipient fault.

In all the cases for a single point defect the data remains Gaussian. It might have a tendency of being non Gaussian for distributed fault but this need to be studied.

8.3 A Comparison of all the Statistical Parameter and Reference to Fault Free, ORF and IRF

A contribution of this research work is the consideration of all statistical parameter at one go and not segregating a parameter to judge the condition of the machine (for example, considering kurtosis alone as a parameter to judge the fault condition). A comparison of the time thresholds statistical parameter for each condition of fault free, ORF and IRF are considered.

8.4 Positive Points Achieved in this Research Work

- 1) This research work has been experimented, tested and verified by a total of 104 runs for a fault with each case such as no load having 26 runs. Each run had 50000 data points.
- 2) Other Analysis Techniques becomes of less significance provided the fault has been detected by the time and frequency domain and hence this research work suggests that time signal supported by statistical techniques as a powerful tool for FDEM.
- 3) The vibration data was validated to be Gaussian for an incipient stage under four load conditions for healthy, outer race and inner race fault.
- 4) The DAQ and the signal analysis techniques maintain same sampling frequency and a large data points were considered. The resolution was obtained at 0.625Hz which was not done in the previous research work which provided a distinctive peak of faults in the spectrum.
- 5) Other peaks obtained at a higher side of the spectrum need to be assigned of the cause of their visibility due to imbalance, misalignment or other causes which needs to be studied, before it is allotted.

8.5 Scope for Future Work

- 1) Thresholds if incorporated on the time waveform would set alarms and this needs a study in FDEM.
- 2) The vibration data needs to be trended which is one of the aspects that could not be considered in this period of time but this needs consideration.
- 3) Other kind of bearing faults are yet to be studied. This research work considered the major contributors by ORF being 18%, 64% being the IRF fault and all the rest of the bearing faults are 18%.
- 4) ANN or any artificial Intelligence can be incorporated to trigger an onset of an alarm thus providing the detail of a fault.
- 5) Incipient stage of faults in bearing has been studied and this could be extended to distributed bearing faults.

Bibliography

- [1] A Barbour and W T Thomson, "Finite Element Analysis And On-line Current Monitoring To Diagnose Air gap Eccentricity In 3-Phase Induction Motors", IEE, EMD 97, Conference Publication, pp 1-3, No. 444, September, 1997.
- [2] A. Choudhary, and N.Tandon, "Vibration Response of Rolling Element Bearings in a Rotor Bearing System to a Local Defect Under Radial Load", Transactions of the ASME, Vol. 128, pp 252-261, 2006.
- [3] A. M. Al-Ghamd and D. Mba, "A comparative experimental study on the use of acoustic emission and vibration analysis for bearing defect identification and estimation of defect size", Elsevier Science, Mechanical Systems and Signal Processing, Vol. 20, pp.1537-1571, October 2006.
- [4] A. Murray, and J. Penman, "Extracting Useful Higher Order Features for Condition Monitoring Using Artificial Neural Networks", IEEE Transactions on Signal Processing, Vol. 45, No. 11, pp 2821-2828, November 1997.
- [5] A. Sedighi, M. Haghifam, O. P. Malik and M. Ghassemian, "High Impedance Fault Detection Based on Wavelet Transform and Statistical Pattern Recognition", IEEE Transactions on Power Delivery, Vol. 20, No. 4, pp 2414-2421, October 2005.
- [6] A. Stavrou, H. G. Sedding, and J. Penman, "Current Monitoring for Detecting Inter-Turn Short Circuits in Induction Motors", IEEE Transactions on Energy Conversion, Vol. 16, No. 1, pp 32-37, March 2001.
- [7] A.J. Hoffman and N.T. van der Merwe, "The Application of Neural Networks to Vibrational Diagnostics for Multiple Fault Conditions", Elsevier Science, Computer Standards and Interfaces Vol.24, pp 139-149, 2002.
- [8] A.Siddiqui, G.S.Yadava and B.Singh,"Identification of Three phase Induction Motor Incipient Faults using Neural Network"conference record of the IEEE International Symposium on Electrical Insulation, Indianapolis, IN USA,19-22,pp 30-34, September 2006.
- [9] A.Siddiqui, G.S.Yadava and B.Singh," A Review of Stator Fault Monitoring Techniques of Induction Motors", IEEE Transactions on Energy Conversion, Vol. 20, No. 1, pp 106-114, March 2005.
- [10] B. Liu, S.F. Ling and R. Gribonval, "Bearing failure detection using matching pursuit", Elsevier, NDT& E International Vol.35, pp 255-262, 2002.
- [11] Bo Li, M. Chow, Y. Tipsuwan and J. C. Hung, "Neural-Network-Based Motor Rolling Bearing Fault Diagnosis", IEEE Transactions on Industrial Electronics, Vol. 47, No. 5, pp 1060-1069, October 2000.
- [12] Bo Li, G. Goddu and M. Chow, "Detection of Common Motor Bearing Faults Using Frequency-Domain Vibration Signals and a Neural Network Based Approach", Proceedings of the American Control Conference Philadelphia, Pennsylvania, pp 2032-2036, June 1998.
- [13] B. Samanta and K. R. Al-Balushi, "Artificial Neural Network Based Fault

- Diagnostics of Rolling Element Bearings Using Time-Domain Features”, Elsevier Science, Mechanical Systems and Signal Processing, Vol.17, No.2, pp 317–328, 2003.
- [14] B.T. Holm-Hansen and R. X. Gao, “Vibration Analysis of a Sensor-Integrated Ball Bearing”, Transactions of the ASME, Vol. 122, pp 384-392, October 2000.
- [15] B. T. Holm-Hansen, R. X. Gao and L. Zhang, “Customized Wavelet for Bearing Defect Detection”, Transactions of the ASME, Vol. 126, pp 740-745, December 2004.
- [16] B.K.N Rao, “Handbook of Condition Monitoring, Elsevier Advanced Technology”, Oxford, 1996.
- [17] B. Raison, G. Rostaing, O. Butscher and C. Maroni, “Investigations of Algorithms for Bearing Fault Detection in Induction Drives”, pp 1696-1701, IEEE, 2002.
- [18] C. K. Mechefske and J. Mathew, “Fault Detection and Diagnosis in Low Speed Rolling Element Bearings, Part I: The Use of Parametric Spectra”, Mechanical Systems and Signal Processing, Vol.6, No.4, pp. 297-307, 1992.
- [19] C. Li, Z. Song and P. Li, “Bearing Fault Detection via Wavelet Packet Transform and Rough Set Theory, Proceedings of the 5th World Congress on Intelligent Control and Automation”, Hangzhou, P.R. China, pp 1663-1666, June 15-19, 2004.
- [20] C.J. Li and S.Y. Li, “Acoustic Emission Analysis for Bearing Condition Monitoring”, Elsevier, Vol. 85, pp 67-74, 1995.
- [21] C. M. Riley, B. K. Lin, T.G. Habetler, and G.B. Kliman, “Stator Current Harmonics and Their Causal Vibrations: A Preliminary Investigation of Sensorless Vibration Monitoring Applications”, IEEE Transactions on Industry Applications, Vol. 35, No. 1, pp 94-99, January/February 1999.
- [22] C.M. Riley, B. K. Lin, T. G. Habetler, and R. R. Schoen, “A Method for Sensorless On-Line Vibration Monitoring of Induction Machines”, IEEE, Transactions on Industry Applications, Vol. 34, No. 6, pp 1240-1245, November/December, 1998.
- [23] C. T. Kowalski and T. Orłowska-Kowalska, “Neural Networks Application for Induction Motor Faults Diagnosis, Mathematics and Computers in Simulation”, Vol.63, pp 435-448, 2003.
- [24] C. Wang and J. C. S. Lai, “Vibration Analysis of an Induction Motor”, Journal of Sound and Vibration Vol.224, No.4, pp. 733-756, 1999.
- [25] D. Ho and R. B. Randall, “Optimisation of Bearing Diagnostic Techniques Using Simulated and Actual Bearing Fault Signals”, Mechanical Systems and Signal Processing, Vol.14, No. 5, pp 763-788, 2000.
- [26] D. Stegemann, W. Reimche, U. Sudmersen, O. Pietsch, Y. Liu, “Monitoring and Vibrational Diagnostic of Rotating Machinery in Power Plants, Power Station Maintenance: Profitability Through Reliability”, 30 March – 1 April, Conference Publication No. 452, IEE, 1998.
- [27] D. Chanda, N. K. Kishore, and A. K. Sinha, “A Wavelet Multiresolution-Based Analysis for Location of the Point of Strike of a Lightning Overvoltage on a Transmission Line”, IEEE Transactions on Power Delivery, Vol. 19, No. 4, pp 1727-1733, October 2004.

- [28] D.Dyer, and R.M. Stewart, "Detection of Rolling Element Bearings Damage by Statistical Vibration Analysis", ASME, Journal of Mechanical Design, Vol. 100, pp 229-235, 1978.
- [29] F. Briz, M. W. Degner, A. B. Diez, and J.M.Guerrero, "Online Diagnostics in Inverter-Fed Induction Machines Using High-Frequency Signal Injection", IEEE Transactions on Industry Applications, Vol. 40, No. 4, pp 1153-1161, July/August, 2004.
- [30] F. C. Trutt, J. Sottile, and J. L. Kohler, "Online Condition Monitoring of Induction Motors", IEEE, Transactions on Industry Applications, Vol. 38, No. 6, pp. 1627-1632, November/December, 2002.
- [31] F.Filippetti, G. Franceschini, C. Tassoni, and Peter Vas, "AI Techniques in Induction Machines Diagnosis Including the Speed Ripple Effect", IEEE, Transactions on Industry Applications, Vol. 34, No. 1, pp 98-108, January/February, 1998.
- [32] F. Filippetti, G. Franceschini, and C. Tassoni, "Neural Networks Aided On-Line Diagnostics of Induction Motor Rotor Faults", IEEE Transactions on Industry Applications, Vol. 31. No. 4, pp 892-899, July/August, 1995.
- [33] F. K. Choy, J. Zhou, M. J. Braun and L. Wang, "Vibration Monitoring and Damage Quantification of Faulty Ball Bearings", Transactions of the ASME, Vol. 127, pp 776-783, October 2005.
- [34] F. Wan, Q. Xu and S. Li, "Vibration Analysis of Cracked Rotor Sliding Bearing System with Rotor-Stator Rubbing by Harmonic Wavelet Transform", Elsevier, Journal of Sound and Vibration, Vol271, pp 507-518, 2004.
- [35] F.F. Costa, L.A.L. de Almeida, S.R. Naidu, E. R. Braga-Filho and R. N. C. Alves, "Improving the Signal Data Acquisition in Condition Monitoring of Electrical Machines", IEEE Instrumentation and Measurement Technology Conference Vail, CO, USA. Pp 20-22, May 2003.
- [36] G.Dalpiatz and A. Rivola, "Condition Monitoring and Diagnostics in Automatic Machines: Comparison of Vibration Analysis Techniques", Mechanical Systems and Signal Processing, pp 53-73, 1997.
- [37] G.G. Yen, and K.Lin, "Wavelet Packet Feature Extraction for Vibration Monitoring", IEEE Transactions on Industrial Electronics, Vol. 47, No. 3, pp 650-667, June, 2000.
- [38] G. Goddu, B. Li, Chow and J C. Hung, "Motor Bearing Fault Diagnosis by a Fundamental Frequency Amplitude Based Fuzzy Decision System", IEEE, pp 1961-1965, 1998.
- [39] G. H. Müller and C. F. Landy, "A Novel Method to Detect Broken Rotor Bars in Squirrel Cage Induction Motors When Interbar Currents are Present", IEEE Transactions on Energy Conversion, Vol. 18, No. 1, pp 71-79, March 2003.
- [40] G Keller, and B Warrack, "Statistics for Management and Economics", 6th ed, Boston, MA: Thomson Learning, Inc; 2003.
- [41] G.Betta, C. Liguori, A. Paolillo, and A.Pietrosanto, "A DSP-Based FFT-Analyzer for the Fault Diagnosis of Rotating Machine Based on Vibration Analysis", IEEE Transactions on Instrumentation and Measurement, Vol. 51, No. 6, pp 1316-1322,

December 2002.

- [42] G.K. Singh and Saleh Al Kazzaz Sa'ad Ahmed, "Vibration Signal Analysis using Wavelet Transform for Isolation and Identification of Electrical Faults in Induction Machine", Elsevier Science, Electric Power Systems Research, Vol. 68 , pp 119-136,2004.
- [43] G.K. Singh and Saleh Al Kazzaz Sa'ad Ahmed, "Induction Machine Drive Condition Monitoring and Diagnostic Research- a Survey", Elsevier Science, Electric Power Systems Research, Vol. 64, pp 145-158, 2003.
- [44] G.S. Maruthi and K.P. Vittal, "Electrical Fault Detection in Three Phase Squirrel Cage Induction Motor by Vibration Analysis using MEMS Accelerometer", IEEE Power Electronics and Drive Systems, PEDS, pp 838-843,2005.
- [45] H. Henao, C. Demian, and G.Capolino, "A Frequency-Domain Detection of Stator Winding Faults in Induction Machines Using an External Flux Sensor", IEEE Transactions on Industry Applications, Vol. 39, No. 5, pp 1272-1279,September/October, 2003.
- [46] H. Ocak and K.A. Loparo, "A New Bearing Fault Detection and Diagnosis Scheme Based on Hidden Markov Modeling of Vibration Signals", IEEE, 2001.
- [47] H. Ocak and K.A. Loparo, "HMM-Based Fault Detection and Diagnosis Scheme for Rolling Element Bearings", Transactions of the ASME, Vol. 127, pp 299-306, August 2005.
- [48] H. Ocak and K.A. Loparo, "Estimation of the running speed and bearing defect frequencies of an induction motor from vibration data", Elsevier Science, Mechanical Systems and Signal Processing, April,2003.
- [49] H R Martin, and F Honarvar, "Application of statistical moment to bearing failure detection", *Applied Acoustics*, Vol. 44, pp. 67-77, 1995.
- [50] H. Guldemir, "Detection of Airgap Eccentricity Using Line Current Spectrum of Induction Motors", Elsevier Science, Electric Power Systems Research Vol. 64 pp 109-117, 2003.
- [51] H.Nejjari and M. E.H. Benbouzid, "Monitoring and Diagnosis of Induction Motors Electrical Faults Using a Current Park's Vector Pattern Learning Approach", IEEE Transactions on Industry Applications, Vol. 36, No. 3, pp 730-735, May/June, 2000.
- [52] H. Yang, J. Mathew and L. Ma, "Fault diagnosis of rolling element bearings using basis pursuit", Elsevier, Mechanical Systems and Signal Processing Vol.19, pp 341-356, 2005.
- [53] H. Zhengjia, Z. Jiyuan, M. Yibin and M. Qingfeng, "Wavelet Transform and Multiresolution Signal Decomposition for Machinery Monitoring and Diagnosis", Proceedings of The IEEE International Conference on Industrial Technology, pp 724-727,1996
- [54] I.E. Alguindigue, A.Loskiewicz-Buczak, and R.E. Uhrig, "Monitoring and Diagnosis of Rolling Element Bearings Using Artificial Neural Networks", IEEE Transactions On Industrial Electronics, Vol. 40, No.2, pp 209-217,1993.
- [55] I. S. Cade, P. S. Keogh, and M. N. Sahinkaya, "Fault Identification in Rotor/Magnetic Bearing Systems Using Discrete Time Wavelet Coefficients",

- IEEE/ASME, Transactions on Mechatronics, Vol. 10, No. 6, pp 648-647, December, 2005.
- [56] J D Turner and L Austin, "Electrical Techniques for Monitoring the Condition of Lubrication Oil", Institute of Physics Publishing, Vol.14,pp.1794–1800 ,2003.
- [57] J P Dron,L. Rasolofondraibe,F.Bolaers and A.Pavan, "High Resolution Methods In Vibratory Analysis:Application To Ball Bearing Monitoring And Production Machine", Elsevier, International Journal Of Solids And Structures, Vol.38, pp 4293-4313, 2001.
- [58] J.Antoni and R.B. Randall, "The Spectral Kurtosis: Application to the Vibratory Surveillance and Diagnostics of Rotating Machines", Elsevier, Mechanical Systems and Signal Processing, Vol. 20 ,pp 308–331, 2006.
- [59] J. Ilonen, J.Kamarainen, T. Lindh, J.Ahola, H. Kälviäinen, and J. Partanen, "Diagnosis Tool for Motor Condition Monitoring", IEEE Transactions on Industry Applications, Vol. 41, No. 4, pp 963-971, July/August 2005.
- [60] J. L. Kohler, J. Sottile, and F. C. Trutt, "Condition Monitoring of Stator Windings in Induction Motors: Part I—Experimental Investigation of the Effective Negative-Sequence Impedance Detector", IEEE Transactions on Industry Applications, Vol. 38, No. 5, pp 1447-1453, September/October,2002.
- [61] J. Pineyro, A. Klemmow and V. Lescano, "Effectiveness of New Spectral Tools in the Anomaly Detection of Rolling Element Bearings", Journal of Alloys and Compounds Vol. 310, pp 276–279,2000.
- [62] J. R. Stack, R.G. Harley and T. G. Habetler, "An Amplitude Modulation Detector for Fault Diagnosis in Rolling Element Bearings", IEEE Transactions on Industrial Electronics, Vol. 51, No. 5, pp1097-1102, October 2004.
- [63] J. R. Stack, T. G. Habetler and R.G. Harley, "Fault-Signature Modeling and Detection of Inner-Race Bearing Faults", IEEE Transactions on Industry Applications, Vol. 42, No. 1, pp 61-68,January/February, 2006.
- [64] J. R. Stack, T. G. Habetler and R.G. Harley, "Fault Classification and Fault Signature Production for Rolling Element Bearings in Electric Machines", IEEE Transactions on Industry Applications, Vol. 40, No. 3, pp. 735-739, May/June, 2004.
- [65] J. R. Stack, T. G. Habetler and R.G. Harley, "Experimentally Generating Faults in Rolling Element Bearings via Shaft Current", IEEE Transactions on Industry Applications, Vol. 41, No. 1, pp 25-29,January/February, 2005.
- [66] J. R. Stack, T. G. Habetler and R.G. Harley, "Bearing Fault Detection via Autoregressive Stator Current Modeling", IEEE Transactions on Industry Applications, Vol. 40, No. 3, pp. 740-747, May/June, 2004.
- [67] J. R. Stack, T. G. Habetler and R.G. Harley, "Effects of Machine Speed on the Development and Detection of Rolling Element Bearing Faults", IEEE Power Electronics Letters, Vol. 1, No. 1, pp 19-21, March, 2003.
- [68] J. Shiroishi, Y. Li, S. Liang, S. Danyluk and T. Kurfess, "Vibration Analysis for Bearing Outer Race Condition Diagnostics", Journal of the Brazilian Society of Mechanical Sciences, Vol.21,No.3, Rio de Janeiro September,1999.
- [69] Jing Lin and L. QU, "Feature Extraction Based on Morlet Wavelet and its

- Application for Mechanical Fault Diagnosis”, Journal of Sound and Vibration, Vol.234, No.1, pp 135-148,2000.
- [70] J.Zarei, and J.Poshtan, “Bearing Fault Detection Using Wavelet Packet Transform of Induction Motor Stator Current”, Elsevier, Tribology International, Vol.40, pp 763–769, 2007.
- [71] K Gilman. A Random Vibration Primer-Part 1, Newsletter, Lansmont, Field to lab. Available from: <http://www.lansmont.com/NewsLetters/HTML%5C96-02-p3.HTM> [last cited on 2009 Feb 25].
- [72] K Gilman, “A Random Vibration Primer-Part 2”, Newsletter, Lansmont, Field to lab. Available from: <http://www.lansmont.com/NewsLetters/HTML%5C96-02-p3.HTM> [last cited on 2009 Feb 25].
- [73] K. Kim, and A. G. Parlos, “Induction Motor Fault Diagnosis Based on Neuropredictors and Wavelet Signal Processing”, IEEE/ASME, Transactions on Mechatronics, Vol. 7, No. 2, pp 201-219, June 2002.
- [74] K Mori, N. Kasashima, T.Yoshioka, and Y. Ueno, “Prediction of Spalling on a Ball Bearing by Applying the Discrete Wavelet Transform to Vibration Signals”, WEAR, Vol. 195, pp 162-168, 1996.
- [75] K. Shibata, A. Takahashi and T. Shirai, “Fault Diagnosis of Rotating Machinery Through Visualisation of Sound Signals”, Mechanical Systems and Signal Processing Vol.14, No.2, pp.229-241, 2000.
- [76] K.Siwiek, S. Osowski and T. Markiewicz, “Support Vector Machine for Fault Diagnosis in Electrical Circuits”, NORSIG, IEEE, pp. 342-345, 2006.
- [77] L. E. Atlas, G. D. Bernard, and S. B.Narayanan, “Applications of Time-Frequency Analysis to Signals from Manufacturing and Machine Monitoring Sensors”, Proceedings of the IEEE, Vol. 84, NO. 9, pp 1319-1329, September1996.
- [78] L.Eren and M.J. Devaney, “Bearing Damage Detection via Wavelet Packet Decomposition of the Stator Current”, IEEE, Transactions on Instrumentation and Measurement, Vol. 53, No. 2, pp 431-436, April 2004.
- [79] L.Eren, A. Karahoca and M.J. Devaney, “Neural Network Based Motor Bearing Fault Detection”, IMTC, Instrumentation and Measurement Technology Conference, Camo, Italy,IEEE,18-20 May, 2004.
- [80] L.Eren and M.J. Devaney, “Motor Bearing Damage Detection Via Wavelet Analysis of the Starting Current Transient”, IEEE, Instrumentation and Measurement Technology Conference, Budapest, Hungary May 21-23,2001.
- [81] L. M. Rogers, “Detection of Incipient Damage in Large Rolling Element Bearings”, Advanced Materials Research, Trans Tech Publications, Switzerland, Vol. 13-14, pp. 37-44, 2006.
- [82] L R Kadiyali, editor,“Traffic engineering and transport Planning”, 7th ed, Delhi: Khanna Publications; pp. 87-170, 2000.
- [83] M.Bodruzzaman, S.S.Devgan, K.D.Mach and C.Clay, “High Resolution Estimation And Online Monitoring Of Natural Frequency Of Aircraft Structure Specimen Under Random Vibration”, pp 468-474, IEEE, 1994.
- [84] M.E.H.Benbouzid, H.Nejjari, R.Beguenane, M.Vieira, “Induction Motor Asymmetrical Faults Detection Using Advanced Signal Processing Techniques”,

- IEEE Transactions On Energy Conversion, Vol.14, No. 2, pp 147-152, June 1999.
- [85] M.E.H. Benbouzid, "Bibliography on Induction Motors Faults Detection and Diagnosis", IEEE Transactions on Energy Conversion, Vol. 14, No. 4, pp 1065-1074, December, 1999.
- [86] M. E. H, Benbouzid, M.Vieira, and C. Theys, "Induction Motors Faults Detection and Localization Using Stator Current Advanced Signal Processing Techniques", IEEE, Transactions on Power Electronics, Vol. 14, No. 1, pp 14-22, January 1999.
- [87] M. E. H, Benbouzid and G. B. Kliman, "What Stator Current Processing-Based Technique to Use for Induction Motor Rotor Faults Diagnosis", IEEE Transactions on Energy Conversion, Vol. 18, No. 2, pp 238-244, June 2003.
- [88] M. Kalkat, S. Yildirim and I. Uzmay, "Rotor Dynamics Analysis of Rotating Machine Systems Using Artificial Neural Networks", Taylor and Francis, International Journal of Rotating Machinery, Vol.9, pp 255-262, 2003.
- [89] M. F. White, "Simulation and Analysis of Machinery Fault Signals", Journal of Sound and Vibration, Vol.93 No.1, pp 95-116, 1984.
- [90] M.Haji, and H.A. Toliyat, "Pattern Recognition—A Technique for Induction Machines Rotor Broken Bar Detection", IEEE Transactions on Energy Conversion, Vol. 16, No. 4, pp 312-317, December 2001.
- [91] M.J. Devaney, and L. Eren, "Detecting Motor Bearing Faults", IEEE Instrumentation and Measurement Magazine, pp. 30-35, 2004.
- [92] M. Xu and T. Alford, "Motor Current Analysis and its Applications in Induction Motor Fault Diagnosis", Enteract, Motormonitor and Emonitor, Entek -IRD International corp., Enteract, 1998.
- [93] M. Bai, J. Huang, M. Hong and F. Su, "Fault diagnosis of rotating machinery using an intelligent order tracking system", Journal of Sound and Vibration, Vol. 280, pp 699-718, 2005.
- [94] M. Blddt, P. Granjon, B. Raisonts and G. Rostaing, "Models for Bearing Damage Detection in Induction Motors Using Stator Current Monitoring", IEEE Transactions on Industrial Electronics, Vol. 55, No. 4, pp 1813-1822, April 2008.
- [95] M D Negrea, "Electromagnetic Flux Monitoring For Detecting Faults In Electrical Machine", Helsinki, University of Technology, Department of Electrical and Communication Engineering, November, 2006. (Ph D. Thesis)
- [96] M.Fenger and W.T. Thomson, "Development of a Tool to Detect Faults in Induction Motors Via Current Signature Analysis", Iris Rotating Machine Conference, San Antonio, TX, pp 1 - 9, June 2002.
- [97] M L Sin, W L Soong, and N Ertugrul, "Induction machine on-line condition monitoring and fault diagnosis - A survey", Australasian Universities Power Engineering Conference (AUPEC), Christchurch, N.Z., 2003.
- [98] N.S. Vyas and D. Satishkumar, "Artificial neural network design for fault identification in a rotor-bearing system", Elsevier Science, Mechanism and Machine Theory, Vol.36, pp.157-175, 2001.
- [99] N Tandon, and A Choudary, "A review of vibration and acoustic measurement methods for the detection of defects in rolling element bearings", Tribology

International, Vol. 32, pp. 469-80, 1999

- [100] P.Chen, M.Taniguchi, T.Toyota, and Z.He, "Fault Diagnosis Method for Machinery in Unsteady Operating Condition by Instantaneous Power Spectrum and Genetic Programming" Elsevier, Mechanical Systems and Signal Processing, Vol.19, pp 175–194, 2005.
- [101] P. D. McFadden and J. D. Smith, "Model for the Vibration Produced by a Single Point Defect in a Rolling Element Bearing", Journal of Sound and Vibration Vol. 96, No.1, pp. 69-82, 2001.
- [102] P. D. McFadden and J. D. Smith, "The Vibration Produced by Multiple Point Defects in a Rolling Element Bearing", Journal of Sound and Vibration ,Vol.98, No.2, pp 263-273, 1985.
- [103] P.Forster and C.L.Nikias, "Bearing Estimation in the Bispectrum Domain", IEEE Transactions on Signal Processing, Vol 39, No.9, pp 1994-2006, September 1991.
- [104] P. K. Dunn, "Three Tools for Interactively Visualizing Some Distribution Theory Concepts", The American Statistician, Vol. 53, No.2, May 1999.
- [105] P. Loughlin and F. Cakrak, "Conditional Moments Analysis of Transients with Application to Helicopter Fault Data", Mechanical Systems and Signal Processing, Vol. 14, No. 4, pp 511-522,2000.
- [106] P. V. Goode and M.Chow, "Using a Neural Fuzzy System to Extract Heuristic Knowledge of Incipient Faults in Induction Motors: Part 11-Application", IEEE Transactions on Industrial Electronics, Vol. 42, No. 2, pp 139-146, April, 1995.
- [107] P. Vlok, M. Wnek and M.Zygmunt, "Utilizing statistical residual life estimates of bearings to quantify the influence of preventive maintenance actions", Elsevier, Mechanical Systems and Signal Processing, Vol. 18, pp. 833–847, 2004.
- [108] P.W. Tse , Y. H. Peng, and R.Yam, "Wavelet Analysis and Envelope Detection For Rolling Element Bearing Fault Diagnosis—Their Effectiveness and Flexibilities", Journal of Vibration and Acoustics, Vol. 123, pp 303-310, 2001.
- [109] P.W. Tse, W. Yang and H.Y. Tam, "Machine Fault Diagnosis Through an Effective Exact Wavelet Analysis", Elsevier, Journal of Sound and Vibration, Vol.277, pp.1005–1024, 2004.
- [110] P.J. McCully and C.F. Landy, "Evaluation of Current and Vibration Signals for Squirrel Cage Induction Motor Condition Monitoring", EMD97 1-3, Conference Publication No. 444, pp 331-335, IEE , September 1997
- [111] P.Pillay and Z.Xu, "Labview Implementation of Speed Detection for Mains-Fed Motors Using Motor Current Signature Analysis", IEEE, Power Engineering Review, June 1998.
- [112] Q. Sun, P. Chen, D. Zhang and F. Xi, "Pattern Recognition for Automatic Machinery Fault Diagnosis", Journal of Vibration and Acoustics, Vol.126, pp 307-316, April 2004.
- [113] R.A. Gupta, S.K. Bishnoi and R. Kumar, "Sensorless Control of Switched Reluctance Motor Drive with Fuzzy Logic Based Rotor Position Estimation", International Journal of Computer Applications, Vol. 1, No.22, pp72-79, 2010.

- [114] R.B.W. Heng and M.J.M. Nor, "Statistical Analysis of Sound and Vibration Signals for Monitoring Rolling Element Bearing Condition", *Applied Acoustics*, Vol. 53, No. 3, pp 211-226, 1998.
- [115] R. J. Povinelli, M. T. Johnson, A. C. Lindgren and J. Ye, "Time Series Classification Using Gaussian Mixture Models of Reconstructed Phase Spaces", *IEEE Transactions on Knowledge and Data Engineering*, Vol. 16, No. 6, pp 779-783, June, 2004.
- [116] R.M. Tallam, T.G. Habetler and R.G. Harley, "Continual on-line Training of Neural Networks with Applications to Electric Machine Fault Diagnostics", *Proc. of Power Electronics Specialists Conference*, Vol. 4, pp 2224-2228, 2001.
- [117] R.M. Tallam, T. G. Habetler and R. G. Harley, "Stator Winding Turn-Fault Detection for Closed- Loop Induction Motor Drives", *Industry Application Conference*, IEEE, Vol. 3, pp 1553-1557, 2002.
- [118] R.M. Tallam, T.G. Habetler, R.G. Harley, D.J. Gritter and B. Burton, "Neural network based on-line stator winding turn fault detection for induction motors", *Conference, Rec. IEEE-IAS Annual Meeting*, Vol. 1, pp 375-380, October, 2000.
- [119] R.R.Schoen, B.K.Lin, T.G.Habetler, J.H.Schlag and S.Farag, "An Unsupervised, On-Line System for Induction Motor Fault Detection Using Stator Current Monitoring", *IEEE, Transactions On Industry Applications*, Vol. 31, No.6 pp 1280-1286, November/December 1995.
- [120] R.R.Schoen, T.G.Habetler, F.Kamran and R.G.Bartheld, "Motor Bearing Damage Detection Using Stator Current Monitoring", *IEEE ,Transactions On Industry Applications*, Vol.13, No.6, pp 1274-1229 ,November/December 1995.
- [121] R. Yacamini and S. C. Chang, "Noise and Vibration from Induction Machines Fed from Harmonic Sources", *IEEE Transactions on Energy Conversion*, Vol. 10, No. 2, pp286-292, June, 1995.
- [122] R. Yan, and R. X. Gao, "Complexity as a Measure for Machine Health Evaluation", *IEEE Transactions on Instrumentation and Measurement*, Vol. 53, No. 4, pp 1327-1334, August, 2004.
- [123] R. Yan, and R. X. Gao, "Approximate Entropy as a Diagnostic Tool for Machine Health Monitoring", *Elsevier, Mechanical Systems and Signal Processing*, Vol. 21, pp 824-839, 2007.
- [124] R.B. Randall, "Applications of Spectral Kurtosis in Machine Diagnostics and Prognostics", *Trans Tech Publications, Switzerland*, Vol. 293-294, pp 21-32, 2005.
- [125] S.S.Murthy, R.K.Mittal, A.Dwivedi, G.Pavitra and S.Choudhary, "Online Performance Monitoring and Testing of Electrical Equipment using Virtual Instrumentation", *PEDS, IEEE*, pp1608-1612, 2007.
- [126] S.A. Ansari and R. Baig, "A PC-Based Vibration Analyzer for Condition Monitoring of Process Machinery", *IEEE Transactions on Instrumentation and Measurement*, Vol. 47, No. 2, pp 378-383, April, 1998.
- [127] S.A. McInerny, and Y.Dai, "Basics Vibration Signal Processing for Bearing Fault Detection", *IEEE Transactions on Education*, Vol.46, pp.149-156,2003.
- [128] S.A.S. Al Kazzaz and G.K. Singh, "Experimental Investigations on Induction

Machine Condition Monitoring and Fault Diagnosis using Digital Signal Processing Techniques", Electric Power Systems Research, Vol. 65, pp 197-221, 2003.

- [129] S. A. Kazzaaz, "Intelligent Diagnostic and Monitoring of Electrical Drives", Department of Electrical Engineering, University of Roorkee, 247667(India), June, 2001. (Phd Thesis)
- [130] S. M. A. Cruz ,A. J. M. Cardoso and H. A. Toliyat, "Diagnosis of Stator, Rotor and Airgap Eccentricity Faults in Three-Phase Induction Motors Based on the Multiple Reference Frames Theory", Industry Application Conference, IEEE, Vol2. pp 1346-1557,2003.
- [131] S. Nandi ,R.M Bharadwaj .and Hamid A. Toliyat, "Mixed Eccentricity in Three Phase Induction Machines: Analysis, Simulation and Experiments", Industry Application Conference, IEEE, Vol. 3, pp 1525-1532, 2002.
- [132] S. Nandi and H. A. Toliyat,, "Novel Frequency-Domain-Based Technique to Detect Stator Interturn Faults in Induction Machines Using Stator-Induced Voltages After Switch-Off", IEEE Transactions on Industry Applications, Vol. 38, No. 1, pp 101-109, January/February, 2002.
- [133] S Nandi, and H A Toliyat, "Condition monitoring and fault diagnosis of electrical machines-A review", Proceedings of the IEEE Industry Applications Conference-33rd Annual Meeting, Vol. 1, Phoenix, USA, pp. 197-204, Oct. 1999.
- [134] S. Nandi, H.A. Toliyat, "Fault Diagnosis of Electrical Machines- A Review," Proceedings of the IEEE IEMDC'99, Seattle, WA, May 9-12, pp. 219-221, 1999.
- [135] S.Han, H.Kim and H. Bae, "Extraction of Rotating Machine Sources for Fault Diagnostics using Independent Component Analysis", IEEE, IMTC-Instrumentation and Measurement Technology Conference Ottawa, Ontario, Canada, May 17-19, 2005.
- [136] S. Prabhakar, A.R. Mohanty, and A.S Sekhar, "Application Of Discrete Wavelet Transform For Detection Of Ball Bearing Race Faults", Elsevier, Tribology International, Vol.35, pp.793-800,2002.
- [137] S.Seker, and E. Ayaz, "A Study of Condition Monitoring for Induction Motors Under Accelerated Aging Process", IEEE Power Engineering Review, pp 35-37, July 2002.
- [138] S. Thanagasundram and F.S. Schlindwein, "Autoregressive Based Diagnostics Scheme for Detection of Bearing Faults", pp 3531-3536, Proceedings of ISMA, 2006.
- [139] S. Kumaraswamy, J. Rakesh and A.K. Nalavade, "Standardization of Absolute Vibration Level and Damage Factors for Machinery Health Monitoring", Proceedings of VETOMAC-2, pp 16-18 December 2002.
- [140] S. Wadhvani, "Analysis for Fault Identification In Rotating Electrical Machines", Department of Electrical Engineering, Indian Institute of Technology, (IITR) Roorkee, 247667(India), August, 2006. (Phd Thesis)
- [141] Spin Doctor Monitoring System, 9300DB0201, 09/2002, Raleigh, NC, USA. Available from: <http://ecatalog.squared.com/techlib/docdetail.cfm?oid=090089268009416b> [last cited on 2009 Feb 25].

- [142] T.Han, B.S.Yang, W.Choi and J.Kim, "Fault diagnosis system of induction motors based on neural network and genetic algorithm using stator current signals", *International Journal of Rotating Machinery*, Hindawi, pp 1–13, 2006.
- [143] T.Williams, X. Ribadeneira, S.Billigton, and T.Kurfess, "Rolling Element Bearing Diagnostics in Run-To-Failure Lifetime Testing", *Mechanical Systems and Signal Processing*, Vol. 15, No. 5, pp 979-993, 2001.
- [144] T. Zhang, X. Guo and Z. Wang, "On the Application of Envelope-Wavelet Analysis in the Fault Diagnosis of Rolling Bearing", *Proceedings of the Fourth International Conference on Machine Learning and Cybernetics*, Guangzhou, pp 18-21, August 2005.
- [145] T.W.S Chow and G. Fei, "Three Phase Induction Machines Asymmetrical Faults Identification" Using Bispectrum, *IEEE Transactions on Energy Conversion*, Vol. 10, No. 4, pp 688-693, December 1995.
- [146] T W. S. Chow and H.Tan, "HOS-Based Nonparametric and Parametric Methodologies for Machine Fault Detection", *IEEE Transactions on Industrial Electronics*, Vol. 47, No. 5, pp 1051- 1059, October 2000.
- [147] T W. S. Chow and S.Hai, "Induction Machine Fault Diagnostic Analysis With Wavelet Technique", *IEEE Transactions on Industrial Electronics*, Vol. 51, No. 3, pp 558-568, June 2004.
- [148] U.Chong, S.Lee and C.Sohn, "Sound Monitoring System of Operating Machines in Power Plant", *Proceedings of the 7th Korea-Russia International Symposium*, pp. 298-301, KORUS 2003.
- [149] V.K.Sharma, S.S.Murthy, B.Singh, "Analysis of Switched Motor Drive under Fault Conitions", *IEEE*, pp 553-562, 1998
- [150] W.J.Wang and P.D.McFadden, "Early Detection of Gear Failure By Vibration Analysis- I. Calculation of the Time- Frequency Distribution", *Mechanical Systems and Signal Processing*, Vol. 7, No.3, pp 193-203, 1993.
- [151] W.J.Wang, Z.T.Wu and J.Chen, "Fault Identification in Rotating Machinery Using the Correlation Dimension and Bispectra", *Nonlinear Dynamics Kluwer Academic Publishers*. Printed in the Netherlands, Vol.25, pp.383–393, 2001.
- [152] W. Wang, F. Golnaraghi and F. Ismail, "Condition monitoring of multistage printing presses", *Elsevier, Journal of Sound and Vibration*, Vol. 270, pp 755–766, 2004.
- [153] W. Wang, F. Ismail, and F. Golnaraghi, "A Neuro-Fuzzy Approach to Gear System Monitoring", *IEEE Transactions on Fuzzy Systems*, Vol. 12, No. 5, pp 710-723, October, 2004.
- [154] W.Reimche, U.Südmersen, O.Pietsch, C. Scheer, and F.W. Bach, "Basics Of Vibration Monitoring For Fault Detection And Process Control", *PANNDT, Rio-Brazil* , Conference, 2003.
- [155] W.T.Thomson and R.J.Gilmore, "Motor Current Signature Analysis To Detect Faults In Induction Motor Drives-Fundamentals", *Data, Interpretation ,and Industrial Case Histories*, *Proceeding of the Thirty Second Turbomachinery Symposium*, pp145-156, 2003.
- [156] X.Lou, and K.A.Loparo, "Bearing Fault Diagnosis Based on Wavelet Transform

- and Fuzzy Inference”, Elsevier, Mechanical Systems and Signal Processing, Vol.18, pp 1077–1095, 2004.
- [157] Y.Choi and Y.Kim, “Fault detection in a ball bearing system using minimum variance cepstrum”, Measurement Science and Technology, Vol.18, pp 1433–1440, 2007.
- [158] Z. Chen, Y.He, F Chu and J Huang, “Evolutionary Strategy for Classification Problems and its Application in Fault Diagnostics”, Elsevier Science, Engineering Applications of Artificial Intelligence, Vol.16, pp 31–38,2003.
- [159] Z.K. Peng, F.L. Chu, “Application of the Wavelet Transform in Machine Condition Monitoring and Fault Diagnostics: A Review with Bibliography” ,Elsevier, Mechanical Systems and Signal Processing, Vol 18, pp 199–221, 2004.
- [160] C.H.Chen, ”Signal Processing Handbook”, Marcel Dekker, Newyork, 1988.

Published Paper/Communicated Paper

- [1] Hina A. Khwaja, S.P. Gupta and Vinod Kumar, "A Statistical Approach for Fault Diagnosis in Electrical Machines", IETE-Journal of Research, Vol. 56, No.3, pp 146-155, May-June, 2010.

- [2] Hina A. Khwaja, S.P. Gupta and Vinod Kumar, "Experimental Investigation on Outer Race Fault in Ball Bearings of Electrical Machines using Statistical Analysis", IETE-Journal of Research, Communicated (July,2010).

APPENDIX A-1

Vibration pick-up: PU series

PU-601R

| | | | |
|----------------------------------|---------------------------------------|---------------------------|------------------|
| Form | Holdings | Attaching screw | M6×6L |
| Feature | General purpose | Case material | Hard rubber |
| Response to voltage | 5.1mV/(m/s ²) (50mV/G) | Attachment cable | Cirque cord/code |
| Frequency range (±3dB) | 5~5,000Hz (screw stop) | Cable length | 1m |
| Maximum measurement acceleration | 490m/s ² (50G) | Cable protection (Option) | |
| Maximum approved acceleration | 9,800m/s ² (1000G) | Pre-amp | Built-in |
| Resonance frequency | Above 25kHz (screw stop) | Insulation | Case iso rate |
| Operating temperature limit | -10 ~ 60°C | Mass | 170g |



APPENDIX A-2

Fluke i400s High safety AC current clamp with BNC output



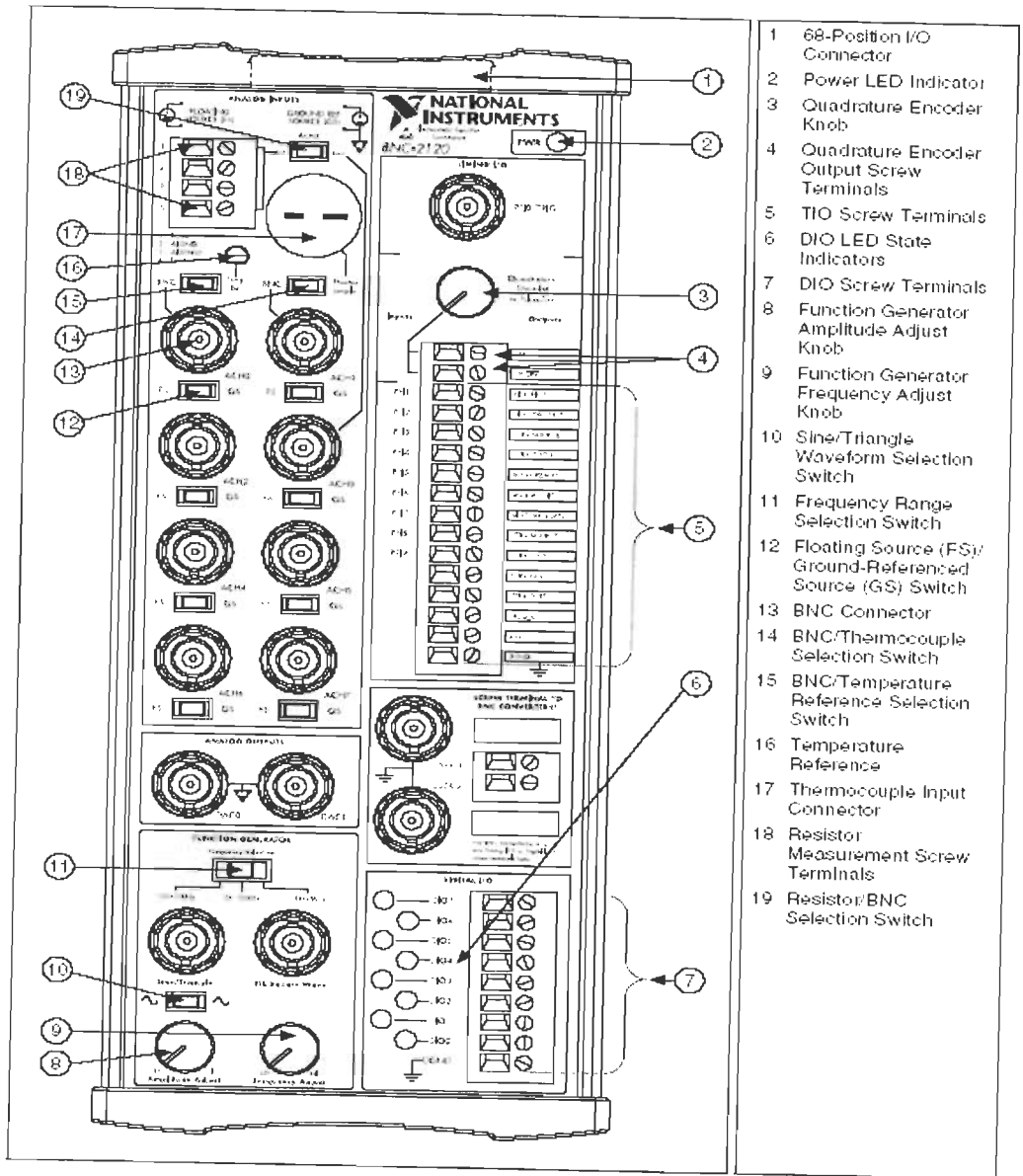
| Specifications | | |
|------------------------|---------------------------|---|
| Nominal current range: | 40 A Range 400 A Range | 0.5 A to 40 A 5 A to 400 A |
| Basic accuracy: | 40 A Range 400 A Range | 2% + 0.015 A (45-400 Hz) 2% + 0.04 A (45-400 Hz) |
| Typical Bandwidth: | 40 A Range 400 A Range | 5 Hz - 10 kHz 5 Hz - 10 kHz |
| Output level(s): | 40 A Range 400 A Range | 10 mV/A 1 mV/A |

| Safety Specifications | |
|---------------------------------|-------------------------------|
| Safety | CAT IV 600 V, CAT III, 1000 V |
| Maximum Non-Destructive Current | 1000 V AC |

FEATURES

- Companion to our scope or power quality meter to measure up to 400 A AC.
- Only current clamp available with a CAT IV 600 V / CAT III 1000 V safety rating. Specially designed to offer maximum utility in a compact shape.
- Take accurate current readings without breaking the circuit.
- Soft non-slippery over mold handle, Max. conductor Ø 32 mm
- Optional PM9081/001 BNC/Banana adapter for DMM's.
- Two ranges: 40 A & 400 A, 10 or 100 mV/Amp output.

APPENDIX A-3



BNC 2120 FRONT PANNEL

Specifications of BNC-2120

These specifications are typical at 25 ° C unless otherwise specified.

Analog Input

Number of channels (default)Eight differential
Field connections (default)Eight BNC connectors
Protection.....No additional protection provided.

Optional connections

ThermocoupleUncompensated miniature connector,
..... mates with 2-prong
..... miniature or sub-miniature connector
ResistorTwo screw terminals
Resistor measurement range 100 Ω to 1 M Ω
Resistor measurement error $\tilde{\leq} 5\%$

Power Requirement

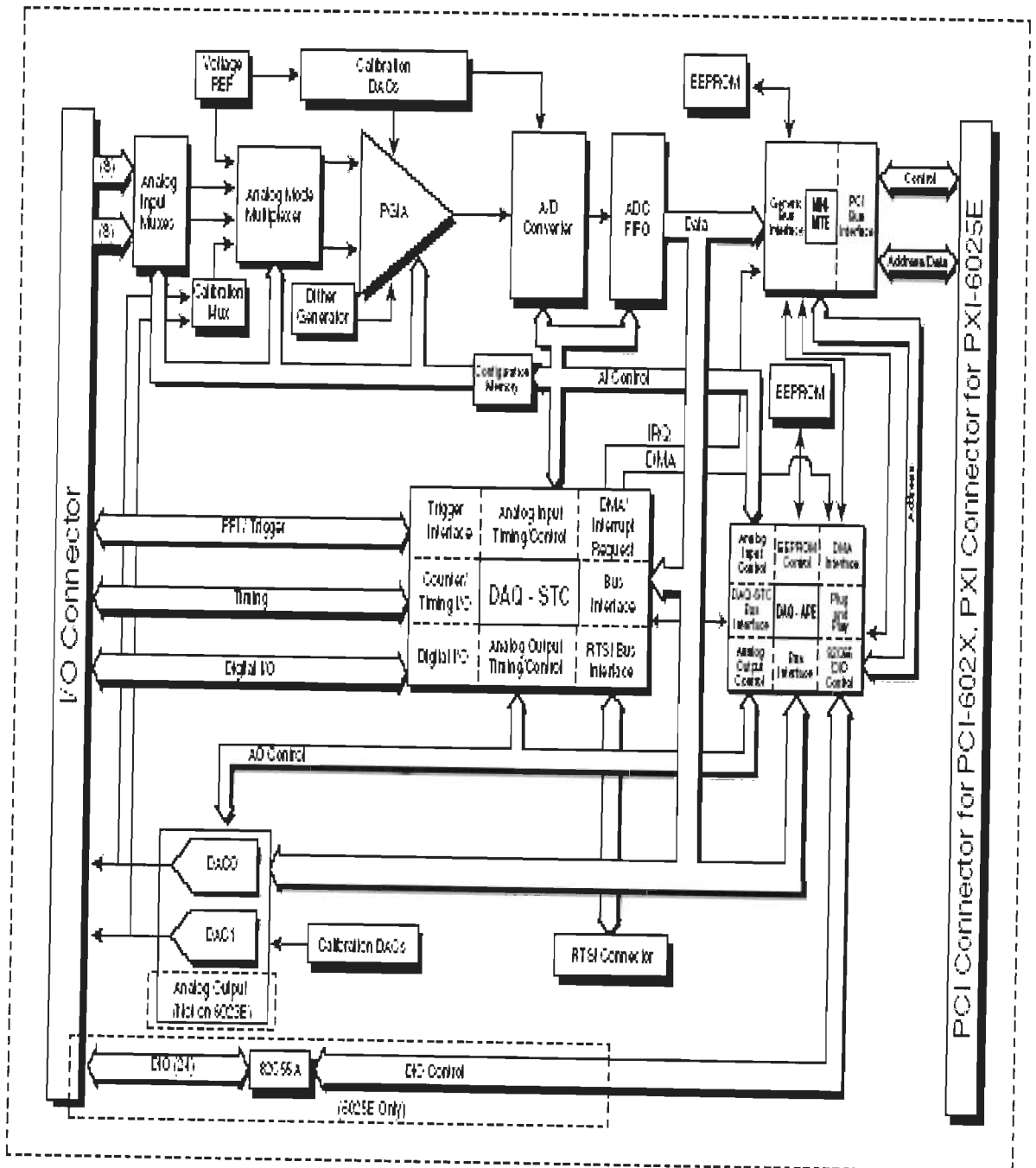
+5 VDC ($\pm 5\%$)..... 200 mA, sourced from the E Series
..... device
Power available
at +5 V screw terminal E Series power, less power
consumed . . . at +5 VDC ($\pm 5\%$)

Environment

Operating temperature..... 0 to 50 ° C
Storage temperature -55 to 125 ° C
Relative humidity..... 5 to 90% noncondensing

APPENDIX A-4

DATA ACQUISITION CARD



Block Diagram of NI 6024E

Specifications

Analog Input

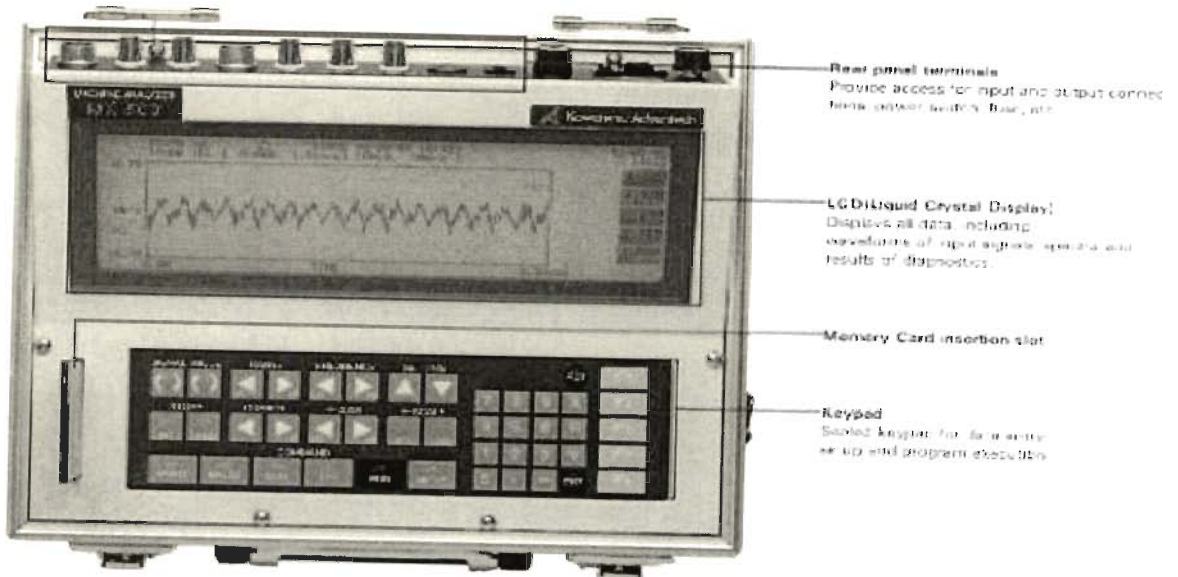
| | |
|---|--|
| Number of channels | 16 single-ended or 8 differential (software-selectable per channel) |
| Type of ADC..... | Successive approximation |
| Resolution | 12 bits, 1 in 4,096 |
| Sampling rate | 200 kS/s guaranteed |
| Input signal ranges | Bipolar only |
| Input coupling | DC |
| Max working voltage (Signal + common mode) | Each input should remain within ± 11 V of ground |

Analog Output Characteristics

| | |
|-------------------------|------------------------------|
| Number of channels..... | 2 voltage |
| Resolution..... | 12 bits, 1 in 4,096 |
| Max update rate | |
| DMA..... | 10 kHz, system dependent |
| Interrupts..... | 1 kHz, system dependent |
| Type of DAC | Double buffered, multiplying |

Digital I/O

| | |
|--|--|
| Number of channels | |
| 6025E..... | 32 input/output |
| 6023E and 6024E..... | 8 input/output |
| Compatibility | TTL/CMOS |
| Digital logic levels | |
| Input low voltage: min 0v | max 0.8v |
| Input high voltage: min 2v | max 5v |
| Input low current ($V_{in} = 0$ V) : | min (-) max -320 μ A |
| Input high current ($V_{in} = 5$ V) : | min(-) max 10 μ A |
| Power-on state | Input (High-Z), 50 k Ω pull up to +5 VDC |
| Data transfers | Programmed I/O |



Rear panel terminals
Provide access for input and output connections (power leads, etc.)

LC (Liquid Crystal) Display
Displays all data, including waveforms of input signals, spectra and results of diagnostics.

Memory Card insertion slot

Keypad
Solved keypad for basic menu set up and program execution

Features

- **On-the-spot determination of machine condition using built-in Auto-Diagnostic Software.**

The MK-500 conducts precise vibration analysis utilizing FFT's based on frequency analysis technology. With its auto-diagnostic software, the MK-500 can immediately diagnose machine condition, including causes and locations of troubled areas. The built-in field balancing software allows on-site balancing when used with the optional high speed, high accuracy LED sensor. The MK-500 also has all the standard vibrometer functions, including vibration wave patterns and vibration mode conversions through differential and integral calculations. A printed copy of available data can be obtained by using one of the optional external printers. The MK-500 combines the functions of a vibrometer, analyzer and diagnostic unit in one easy-to-use package.

- **Increased memory capacity allows multiple functions, as well as the ability to fit a multitude of applications.**

1. The 32K words of RAM enables the MK-500 to store up to 240 screen images. The stored data can be transferred to a personal computer through the standard built-in RS-232C interface. Additional screens can be stored into optional memory cards. Each card has the capacity to hold an additional 240 screens each, giving the MK-500 the ability to bring back virtually unlimited data from the field. Software is available which allows the user's personal computer to be used for filing and secondary processing of stored data.

2. In addition to the vibration input, the MK-500 has the ability to take audio and voltage signal data. The unit is equipped with a three-dimensional display to show transient memory of 32k words or spectrum changes relative to time. The MK-500 can be used as a multi-purpose analyzer including transient analysis and machine resonance measurement functions.

- **Incomparable ease of handling is accomplished by the reduced number of keys and the use of an interactive mode.**

Using the interactive mode, the next key to be pushed is indicated on the LCD screen, allowing the unit to be operated by anyone with only a minimum of training. The operator isn't required to remember complicated procedures used on conventional analyzers.

- **Extremely compact size and battery power allow the MK-500 to be used virtually anywhere**

The entire unit weighs only 5.0kg(11.02lbs) and can be carried anywhere for on-the-spot diagnostics. In addition to internal battery power, the MK-500 can utilize on-site AC or DC external power sources if available. Screens remain stored in memory even after external power is removed.

